MAXIMALLY SMOOTH TRANSITION: THE GLUSKABI RACCORDATION

A Dissertation
Presented to
The Academic Faculty

by

Deryck Yeung

In Partial Fulfillment
of the Requirements for the Degree
Doctor of Philosophy in the
Electrical and Computer Engineering

Georgia Institute of Technology
December 2011

MAXIMALLY SMOOTH TRANSITION: THE GLUSKABI RACCORDATION

Approved by:

Professor Erik I. Verriest, Advisor
Electrical and Computer Engineering
Georgia Institute of Technology

Professor Andrew F. Peterson
Electrical and Computer Engineering
Georgia Institute of Technology

Professor Magnus Egerstedt
Electrical and Computer Engineering
Georgia Institute of Technology

Professor Tom Morley
School of Mathematics
Georgia Institute of Technology

Professor Patricio A. Vela
Electrical and Computer Engineering
Georgia Institute of Technology

Date Approved: July 29, 2011

To my parents

ACKNOWLEDGEMENTS

First of all, I would like to express my deepest gratitude to my advisor, Prof. Erik I. Verriest for mentoring me in many different ways. His courses, aimed at uncovering the basic principles instead of just facts, are always an intellectual delight for me. His creativity and enthusiasm for any problem that comes his way are just astonishing to observe. His desire of avoiding fads in choosing a research problem is something I admire greatly. Finally, *aquila non captat muscas* is a phrase that I will always keep in mind! Also, I would like to thank Prof. Egerstedt, Prof. Vela, Prof. Peterson and Prof. Morley for serving on my committee.

I have made many friends in the course of my education at Georgia Tech. I thank Dwi Sianto Mansjur, a good friend that I have known for many years, for always being there for me. It was a pleasure to work with other colleagues: Florent Delmotte, Jermey Jackson, Tejas Mehta, Ganesh Sundaramoorthi, Rajbabu Velmurugan, Ted Wada.

Finally, I would like to thank Denny and Lydia for their support, patience, guidance and encouragement throughout the years. Angelique gave me many funny moments to remember when we shared an apartment some years ago. I dedicate this work to my parents for all the sacrifices they have made in order for me to have a decent education.

TABLE OF CONTENTS

LIST OF FIGURES

SUMMARY

The objective of this dissertation is to provide a framework of constructing a transitional behavior, connecting any two trajectories from a set with a particular characteristic, in such a way that the transition is as inconspicuous as possible. By this we mean that the connection is such that the characteristic behavior persists during the transition. These characteristic classes include stationary solutions, limit cycles etc. We call this framework the Gluskabi raccordation. This problem is motivated from physical applications where it is often desired to steer a system from one stationary solution or periodic orbit to another in a 'smooth' way. Examples include motion control in robotics, chemical process control and quasi-stationary processes in thermodynamics, etc.

Before discussing the Gluskabi raccordations of periodic behaviors, we first study several periodic phenomena. We start off with a study of the self-propulsion of a number of legless, toy creatures based on differential friction under periodic excitations in Chapter 2. This friction model is based on viscous friction which is predominant in a wet environment. We investigate the effects of periodic control on locomotion, and study both the harmonic and optimal periodic control of the so-called flapper. Finally, we analyze a simple prototype of a snake, the two-piece snake, under a periodic excitation.

In Chapter 3 we consider a periodic control problem involving a type of hybrid system. Specifically, we solve a control problem for a stochastic system, under the basic constraint that the feedback control signal and the observations from the system cannot use the communication channel simultaneously. Hence, two modes of operation result: 1) an observation mode where outputs from the system are transmitted

to the controller, and no inputs are sent back to the plant, 2) a control mode where the output of the plant is decoupled from the controller, but control signals are transmitted back to the plant. We seek an optimal periodic regime in a statistical steady state by switching between the observation and the control mode. For this, the optimal gains for the controller and the observer in either mode are determined. This is solved by considering the deterministic model for the second order information state (the covariances). In addition, we show that the observation mode can be reduced to a lower order model, which leads to a multi-mode multi-dimensional (M^3D) problem.

In Chapter 4 we investigate the simplest special case of the Gluskabi raccordation, namely the quasi-stationary optimal control problem. This forces us to revisit the classical terminal controller [12]. Along the way we give an alternative and *constructive* proof of the necessary conditions of optimality of the LQ problem, which further shows that there is a decomposition of the problem into two subproblems. We analyze the performance index as the control horizon increases to infinity. This problem gives a good example where the limiting operation and integration do not commute. Such a misinterpretation can lead to an apparent paradox. In this chapter we use symmetrical components (the parity operator) to shed light on the correct solution [57].

The Gluskabi raccordation is presented in Chapter 5, 6 and 7. In Chapter 5 we use several examples to introduce the concept [59] and provide two methods, the direct and indirect method, to construct the aforementioned maximally 'smooth' transitions. The direct method involves the nullspace of an operator, and the Gluskabi raccordation is obtained by minimizing the deviation away from this nullspace. On the other hand, the indirect method first maps this null space to a parameter space. By finding the 'smoothest' path in the parameter space and then reconstituting the actual trajectory from these parameters, we obtain the Gluskabi raccordation.

In Chapter 6 we consider the signal Gluskabi raccordation. This is the Gluskabi

raccordation *without* a dynamical system. We apply to general framework in Chapter 5 to construct the Gluskabi raccordation between any two periodic signals [66, 67, 68]. Detailed algorithms based on the direct method are provided. The indirect method is also considered, and it involves the dynamic phasors. Finally, we point out the connection between the direct and indirect method for the quasi-periodic raccordation.

In Chapter 7 we expand the theory of the signal raccordation in Chapter 6 to include a dynamical system. By considering the dynamics as a *hard* constraint, the behavioral modeling of dynamical system pioneered by Willems [61] provides the right framework for this extension. All results in Chapter 6 are readily extended.

Finally, in Chapter 8 we conclude and provide several directions for further research.

CHAPTER I

INTRODUCTION

Periodic control systems have been studied for a long time [4, 6] . It has been observed that periodic operations in many control processes are advantageous. In chemical reactors, for instance, periodic cycling of the reactants gives better yield than keeping the reactors in a steady state [3]. This fact is also known to farmers as they periodically switch their crops. Periodic phenomena are also prevalent in nature; human hearts beat under a regular rhythm and birds fly by periodically flapping their wings. In fact all animal locomotion are a result of some form of periodic behavior.

However, it is often necessary to change the behavior of a system from one mode to another via a sequence of quasi-stationary paths because drastic changes are not desired. This is of interest in, for instance, chemical process control, where it is often necessary to change the operating point from one periodic orbit to another as smoothly as possible. Many works have been published in chemical process control, see for instance [3, 10, 35] and references therein. It is known that there exists various periodic solutions corresponding to the optimal periodic control of chemical reactors, and the optimal solution may be unstable. In [35] the author solved the stabilization problem around various suboptimal orbits by using simple relay type of controls.

In this thesis, we will first consider several periodic phenomena. We start off with a study of self-propulsion of several legless toy creatures [58]. We assume the inertial

forces are much smaller compared to the applied forces. The induced motion of the body is entirely due to viscous friction contact with the environment. The friction coefficient depends on the body geometry, and we adopt a model where it is simply a function of the sign of the velocity. This model is not as restrictive as it may seem since in [70] it is shown that motion in dry sand can be approximately modeled as motion in fluid. The amount of work related to locomotion is vast. Of particular interest to us are [17, 21, 29, 34, 27, 41, 36, 46]. Periodic and optimal periodic control form an integral part of our investigation and [6, 18, 5] are general references in this subject.

The aforementioned friction model leads to systems that are hybrid. Roughly speaking, hybrid systems are dynamical systems that switches among a finite set of modes. Thus, they are systems that exhibit both continuous-time and discrete behavior. The origins of hybrid systems can be traced back to Witsenhausen [62], and the literature is now vast. A small sample of references for modeling and optimal control in this area include [8, 9, 26, 63, 64].

In the thesis we will also consider a switching problem involving a new class of hybrid systems, the Multi-Mode Multi-Dimensional (M^3D). The objective is to stabilize the system to a periodic steady state [65]. M^3D systems are first introduced in [56, 51], and these are hybrid systems where each mode dynamics has a different dimension. In [56] it is shown that M^3D systems arise naturally in nonlinear balancing. In [51] the optimal timing (switching) control of the M^3D systems was studied while [54] considered these systems subject to Poissionian sequencing. Finally, in [37] it is shown that M^3D systems appear naturally in the modeling of the dynamics of an

ice skater, and the optimal strides minimizing the energy expenditure were obtained herein.

Our interest in this thesis is not solely periodic control per se. Our aim is to study the transition of one predefined system's behavior to another. Specifically, we will concentrate on transitions that are 'quasi-stationary' in some extended behavioral sense. As an example, in a chemical reactor the processes are often steered from one periodic regime to another by slowly changing the reactants in order to avoid drastic changes. In other words, the transition will be made in a quasi-periodic fashion.

This study is also of interest in robotics. In [22] the authors studied an autonomous puppetry control problem under the view point of hybrid systems. Various modes were defined so that the puppet is supplied with a rich class of behaviors. However, it is necessary to enrich this class of behaviors with *transition* modes such that the transition from one periodic motion to another is as smooth as possible to mimic human motion. In recent studies of arm motions, one theory of single and multiple joint movements argues that arm motions follow a series of equilibrium postures [7], and motion is merely a transfer from one steady state to another through a quasi-static path.

Another application where the notion of quasi-static transition is of importance is the leader based coordination problem studied in [31]. The problem involves a group of robots being controlled by a smaller group of leaders, and the resulting model is a stable linear system. It is of interest to steer the configuration of the robots from one equilibrium position to another via a quasi-static path. A similar problem was also considered in [57] in addition to a paradox in the terminal controller problem.

The terminal controller problem is classical, and a discussion may be found in [12]. Algorithms and related numerical issues are expounded in [11].

Finally, we mention an application in finite time thermodynamics [1]. A Carnot cycle consists of two adiabatic and two isothermal processes, and it is in general a very slow process. Furthermore, it is the most efficient cycle for converting a given amount of thermal energy into work. However, a device based the cycle cannot be built in practice. In order to approximate the cycle an ad-hoc solution based on stepwise transitions has been studied in [1]. This naturally raises the question as to how to design smoother transitions for a quasi-static transfer. The construction presented in this thesis is relevant to this problem.

In control theory the idea of quasi-stationarity is used frequently. In [69] the authors design a controller for a linear time varying (LTV) system with unknown parameters by first treating it as linear time invariant (LTI) system at each time instant. More recently, in [48] the author studied a control technique of nonlinear systems via equilibrium paths. An equilibrium path is a quasi-stationary path that connects two different points in the equilibrium manifold. Several practical advantages were explored in the paper. In quantum mechanics, the quasi-stationary approach forms the foundation of the WKB theory in solving the Schrödinger wave equation and is closely related to the Berry phase [25].

As alluded to earlier the main theme of the thesis is to construct systematically smooth transfers for signals or trajectories of dynamical systems between elements of a particular subset of solutions (stationary solutions, limit cycles, etc). This construction is first introduced in [59]. In the following chapters we will present and

extend the theory in several directions. In addition we apply the framework to construct quasi-periodic transition between any two periodic signals and trajectories. Numerical algorithms will also be discussed.

CHAPTER II

LOCOMOTION BASED ON DIFFERENTIAL FRICTION

Animal locomotion has long been studied by many researchers. Legged locomotion is currently a vast and interdisciplinary field with many contributions from engineers, scientists and applied mathematicians [28]. Unlike legged animals, legless animals such as snakes and fish propel themselves by deforming their body accordingly to interact with the environment. Legless animals are generally more capable in moving on different types of terrains than legged animals. A snake, for example, move easily both on ground and water by using essentially the same type of locomotion. It can also climb trees by extending its body from branch to branch. In comparison, the varieties of legged locomotion seem to be rather small. Swimming is also well studied. For instance, swimming at low speed was studied in [46]. It was shown that at low Reynold's number microscopic organisms propel themselves by periodically changing their body's boundaries. Animal locomotion is the foundation of essentially all biologically inspired robots.

In this chapter, inspired by the many varieties of legless locomotion, we shall study self-propulsion of a few legless, toy creatures based on differential friction. This friction model is based on viscous friction which is predominant in wet environment. The model is not as restrictive as it may seem since in [70] it is shown that motion in dry sand can be approximately modeled as motion in fluid. In the differential friction

model the friction experienced depends on the direction of locomotion. This results in hybrid systems which are linear in the control. In our study we shall neglect the inertia of the creatures. With this assumption the problem at hand becomes a quasi-static one. This allows us to write down static kinematic equations and static relations between the forces and velocities involved. In [52] this friction model has been used to study worm-like motion and Fourier techniques have been used to investigate its periodicity. In the same spirit of the current chapter we considered an ice-skating model in [37]; the resulting model is a M^3D system and we carefully analyzed an optimal skating pattern that minimizes the energy expenditure of the skater.

In Section 2.1 we introduce the friction model used throughout this chapter. In Section 2.2 we derive the equation of motion of the flapper. In Section 2.3 we study the periodic motion of this creature. Several periodic, suboptimal locomotions will be presented. Furthermore, an optimal periodic control will be obtained. In Section 2.4 we extend the previous results to a simplified model of a snake. In Section 2.5 we conclude and present various future research directions.

2.1 Friction Model: differential friction

Scales form an integral part of many crawlers. In order to study locomotion effectively the frictional effects of these scales need to be modeled accurately. Scales come in different shapes and sizes. An approximation is shown in Figure 1.

We model the frictional effects of these scales as the friction one would experience when he/she pushes these rectangular plates raised at one end over a surface. Obviously, the friction experienced depends on the direction in which these plates are

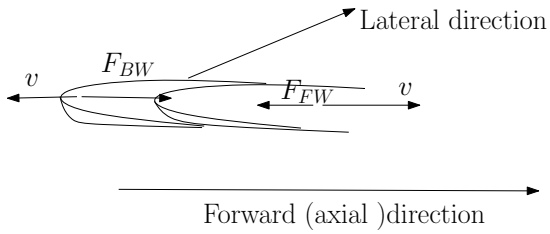

Figure 1: Differential Friction Model

being pushed. In short, the differential friction model is a friction model, where the force of friction depends on the direction of locomotion. An animal with scales as in Figure 1 experiences a friction of $F_{FW} = -\mu_{FW} v$ when the scales slide forward with a velocity v. This friction points to the backwards direction as $\mu_{FW} > 0$ is the *forward* friction coefficient. Similarly, when the scales slide backwards over its environment the total friction is $F_{BW} = -\mu_{BW} v$, where $\mu_{BW} > 0$ is the *backward* friction coefficient. The friction in the transversal or lateral direction is $F_t = -\mu_t v$, where $\mu_t > 0$ is the *transversal* friction coefficient. In the differential friction model, it is assumed that the friction coefficients satisfy the following ordering: $\mu_{BW} >> \mu_t > \mu_{FW} > 0$, where μ_{BW} is much larger than the other friction coefficients. This implies that the backwards friction F_{BW} is much larger when the scales slide backwards, which agrees with the geometry of the scales of the body. In fact, the stands in legged locomotion may be modeled by letting both friction coefficients to be infinite. Finally, as a shorthand notation, we introduce a function $\mu_A(v)$, which describes the axial friction coefficient with the positive direction shown in Figure 1. Thus,

$$\mu_a(v) = \begin{cases} \mu_{FW} & \text{if v} > 0; \\ \mu_{BW} & \text{if v} < 0. \end{cases} \tag{1}$$

2.2 Flapper

In this section we consider our first simple toy creature. Consider the flapper system in Figure 2. Two (inflexible) rods are hinged at O with the scales orientations as shown. We assume that the instantaneous velocity of the flapper aOb is directed towards the left. The half-opening angle is θ. Let $\dot{\theta} = \omega$ be the angular velocity of rod Oa. At a point P, which is a distance s away from the hinge O, the resulting linear velocity is ωs.

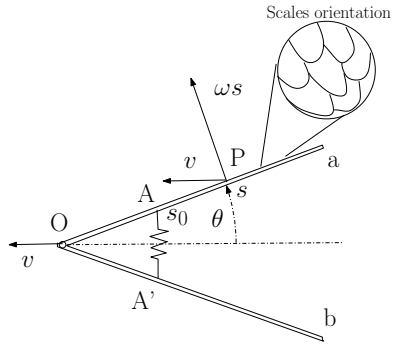

Figure 2: The Flapper

The combined velocity component in the axial and transversal direction of the section of the rod Oa at P is $v_a = v\cos\theta$ and $v_t = \omega s + v\sin\theta$. This results in an axial and transversal friction force at this point $F_a(s) = -\mu_a(v)\, v\cos\theta$ and $F_t(s) = -\mu_t\,(v\sin\theta + \omega s)$. where $\mu_a(v)$ is as defined in (1). We consider F_a positive if directed towards O. Likewise F_t is positive in counterclockwise direction.

Integrating over the total length of Oa, which is assumed to have length one, we

get the total axial and transversal force of Oa

$$\mathbf{F}_a = -\mu_a(v) v \cos\theta \tag{2}$$

$$\mathbf{F}_t = -\mu_t \left(v \sin\theta + \frac{\omega}{2} \right). \tag{3}$$

For both rods, the resulting friction forces imposed by v and ω in the x-coordinate direction is

$$\mathbf{F}_x = -\mathbf{F}_a \cos\theta - \mathbf{F}_t \sin\theta \tag{4}$$

and for rod Oa, the resulting friction force in the y-direction is $\mathbf{F}_y = -\mathbf{F}_a \sin\theta + \mathbf{F}_t \cos\theta$. Substituting (2) and (3) into (4) we find the condition for equilibrium: $\mathbf{F}_a \cos\theta + \mathbf{F}_t \sin\theta = 0$ from which $\mu_a(v)\, v \cos^2\theta + \mu_t \left(v \sin\theta + \frac{\omega}{2} \right) \sin\theta = 0$. It follows that for given ω and θ, the instantaneous velocity, neglecting inertia (equivalently, the mass of the flapper is zero), is

$$v(\omega, \theta) = -\frac{1}{2} \frac{\mu_t \omega \sin\theta}{\mu_a(v) \cos^2\theta + \mu_t \sin^2\theta} \tag{5}$$

Note that v still appears in the right hand side. However, it is clear that with $\omega > 0$, v must be negative, and vice versa. Hence

$$v(\omega, \theta) = -\frac{1}{2} \frac{\mu_t \omega \sin\theta}{\mu_a(-\omega) \cos^2\theta + \mu_t \sin^2\theta} \tag{6}$$

We note that this requires a force $\mathbf{F}$ extended by the arm A'A to counter the vertical friction $\mathbf{F}_y$ $\mathbf{F} = -\mu_a(-\omega)\, v \cos\theta \sin\theta + \mu_t \left(v \sin\theta + \frac{\omega}{2} \right) \cos\theta$. Substituting the equilibrium condition, we get $\mathbf{F} = \frac{\mu_t \mu_a(-\omega) \omega \cos\theta}{2[\mu_a(-\omega)\cos^2\theta + \mu_t \sin^2\theta]}$. The work done by this force when the rod rotates over $\mathrm{d}\theta$ is $\mathrm{d}W = \mathbf{F}\mathrm{d}y = \mathbf{F} s_0 \cos\theta\, \mathrm{d}\theta = \mathbf{F} s_0 \omega \cos\theta\, \mathrm{d}t$. Thus,

$$\mathrm{d}W = \frac{\mu_t \mu_a(-\omega) s_0 \omega^2 \cos^2\theta}{2[\mu_a(-\omega)\cos^2\theta + \mu_t \sin^2\theta]}\, \mathrm{d}t. \tag{7}$$

2.3 Periodic Regime

In this section we study the behavior of the flapper when it has a periodic steady state. Equivalently, we may assume that the variables, ω, θ, and v are periodic with period T. We denote the corresponding radial frequency as $\nu = \frac{2\pi}{T}$.

2.3.1 Similitude

Assume the applied force is such that it results in an angular velocity $\omega_1(t)$ of the flapper. What happens if we speed this up by a factor k? Let thus $\omega_k(t) = k\omega_1(kt)$. We have $\theta_1(t) = \theta_0 + \int_0^t \omega_1(\tau)\,\mathrm{d}\tau$ and $\theta_k(t) = \theta_0 + \int_0^t \omega_k(\tau)\,\mathrm{d}\tau$. Thus $\theta_k(t) = \theta_0 + k\int_0^t \omega_1(k\tau)\,\mathrm{d}\tau = \theta_0 + \int_0^{kt} \omega_1(\sigma)\,\mathrm{d}\sigma$. and $\theta_k\left(\frac{t}{k}\right) = \theta_0 + \int_0^t \omega_1(\sigma)\,\mathrm{d}\sigma = \theta_1(t)$.

It follows then from (6) also that $v(\omega_k(t), \theta_k(t)) = k\, v(\omega_1(kt), \theta_1(kt))$ Likewise, the rate of applied energy (required instantaneous power) is obtained from (7) and scales as $P(\omega_k(t), \theta_k(t)) = k^2\, P(\omega_1(kt), \theta_1(kt))$.

The distance traveled by the flapper in one period is given by the integral, assuming k is a positive integer

$$x_k\left(\frac{T}{k}\right) \;=\; \int_0^{T/k} v(\omega_k(t), \theta_k(t))\,\mathrm{d}t = x_1(T). \tag{8}$$

This is therefore independent of the frequency. The energy spent in one complete stroke is

$$\mathcal{E}_k\left(\frac{T}{k}\right) \;=\; \int_0^{T/k} P(\omega_k(t), \theta_k(t))\,\mathrm{d}t = k\mathcal{E}_1(T). \tag{9}$$

Hence to travel a total distance $x_1(T)$, we either spend one cycle at frequency ν, requiring $\mathcal{E}_1(T)$, or k cycles at a frequency $k\nu$. Hence the average velocity is $\overline{v}_k = \frac{x_k(T/k)}{T/k} = \frac{kx_1(T)}{T} = k\overline{v}_1$ and the average power is $\overline{P}_k = \frac{\mathcal{E}_k(T/k)}{T/k} = \frac{k^2\mathcal{E}_1(T)}{T} = k^2\overline{P}_1$. This

gives a quadratic model for the effective friction. Indeed, consider the simple friction model $F = -\mu_{\text{eff}} v$ A distance x is covered in x/v time units. The work done against friction is $W = |F|x$. The power is thus $P = |F|x/(x/v) = |F|v = \mu_{\text{eff}}\, v^2$. Here, we get thus

$$\mu_{\text{eff}} = \frac{\overline{P}_1}{\overline{v}_1^2} = \frac{\mathcal{E}_1/T}{x_1(T)^2/T^2} = T\frac{\mathcal{E}_1(T)}{x_1(T)}. \tag{10}$$

2.3.2 Harmonic control

In this section we do not yet consider the optimal periodic control, but let θ vary harmonically. Let $\theta(t) = \theta_0 + \omega_0 \cos \nu t$ with $\nu = 2\pi/T$. We require that $\theta_0 - \omega_0 \geq 0$ and $\theta_0 + \omega_0 \leq \frac{\pi}{2}$. Then $\omega(t) = -\omega_0 \nu \sin \nu t$, which means that we start with the flapper closing stroke, which provides the push for the creature.

We found for the period $T = 1$ and parameters $\mu_B = 1, \mu_t = 0.5$ the resulting speed (towards the left) and distance traveled in Figure 3 and Figure 4 for various values of μ_{FW}, $\mu_{FW} = 0.01$, 0.1 and 1. As expected, in the latter case there is no net motion and the most power is consumed. The required power as function of the time within one period is also shown for the same values of μ_{FW} in Figure 5.

The effective friction coefficient for the flapper is shown as function of μ_{FW} for this periodic regime with $\mu_t = 0.5$ and $\mu_{BW} = 1$ in Figure 6.

2.3.3 Optimal Periodic Regime

In this section we will study the optimal periodic control. Assume that the flapper's motion is in a periodic steady state with period T. Over one period the excursion of the flapper is $x(T) = \int_0^T v(\omega, \theta)\ dt$. We maximize the excursion in one period with the constraints that the amount of energy is fixed, i.e $W(T) = W_T$ and that the motion

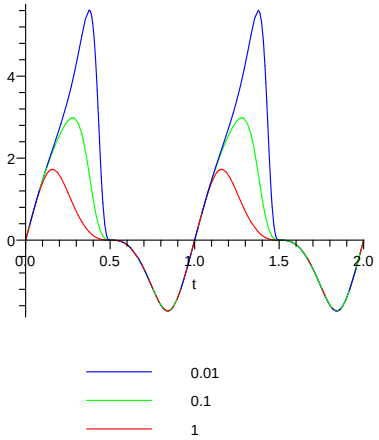

Figure 3: Speed for $\mu_{FW} = 0.01, 0.1, 1$, $\mu_B = 1$ and $\mu_t = 0.5$.

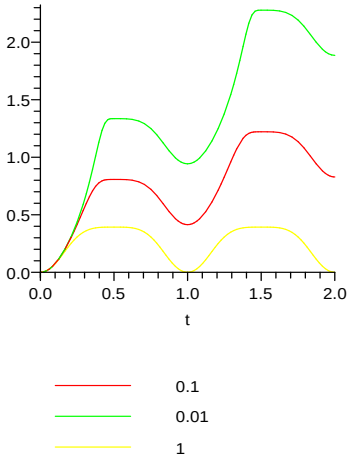

Figure 4: Distance traveled for $\mu_{FW} = 0.01, 0.1, 1$, $\mu_B = 1$ and $\mu_t = 0.5$.

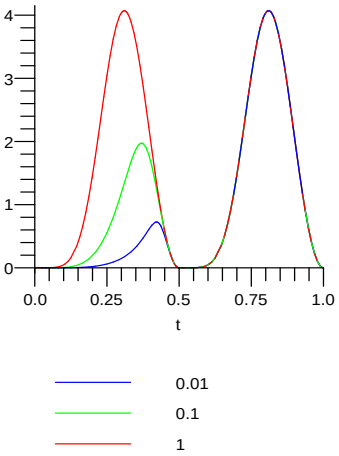

Figure 5: Power for $\mu_{FW} = 0.01, 0.1, 1$, $\mu_B = 1$ and $\mu_t = 0.5$.

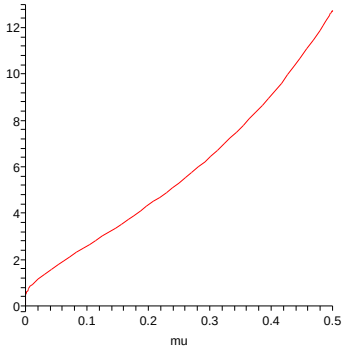

Figure 6: Effective friction coefficient.

is periodic: $\theta(0) = \theta_0 = \theta(T)$. Let θ_0 be arbitrary in $[0, \pi/2]$. The extended state equations are $\dot{\theta} = \omega$, $\dot{W} = \frac{\mu_t \mu(-\omega) s_0 \omega^2 \cos^2\theta}{2[\mu_a(-\omega)\cos^2\theta + \mu_t \sin^2\theta]}$. The control input is ω. From (6) the Hamiltonian is

$$H = \frac{1}{2}\frac{\mu_t \omega \sin\theta}{\mu_a(-\omega)\cos^2\theta + \mu_t \sin^2\theta} + \lambda_\theta \omega + \lambda_W \frac{\mu_t \mu_a(-\omega) s_0 \omega^2 \cos^2\theta}{2[\mu_a(-\omega)\cos^2\theta + \mu_t \sin^2\theta]}.$$

Since the function $\mu_a(-\omega)$ is not differentiable the Pontryagin Maximum Principle [12] needs to be used. The Hamiltonian is bi-modal and it is quadratic in ω for $\omega > 0$ and $\omega < 0$. Therefore, the optimality condition for $\omega > 0$, the backward moving stroke, is $\omega_{BW} = \frac{-\mu_t \sin\theta - 2\lambda_\theta[\mu_{BW}\cos^2\theta + \mu_t \sin^2\theta]}{2\lambda_W \mu_t \mu_{BW} s_0 \cos^2\theta} > 0$. For $w < 0$, the forward moving stroke, is $\omega_{FW} = \frac{-\mu_t \sin\theta - 2\lambda_\theta[\mu_{FW}\cos^2\theta + \mu_t \sin^2\theta]}{2\lambda_W \mu_t \mu_{FW} s_0 \cos^2\theta} < 0$, The costate equations are $\dot{\lambda}_\theta = -\frac{\partial H}{\partial \theta}$ and $\dot{\lambda}_W = -\frac{\partial H}{\partial W} = 0$.

For the simulation it is assumed that the period $T = 1$sec and the initial starting angle $\theta(0) = \pi/17$. A standard gradient descent algorithm has been implemented to find the optimal control $\omega(t)$. The results are shown in Figure 7, Figure 8, Figure 9 and Figure 10. As in Figure 10 the creature goes backwards initially when opening its flappers and moves forward when they are closed. The net effect is a forward motion due to the differential friction.

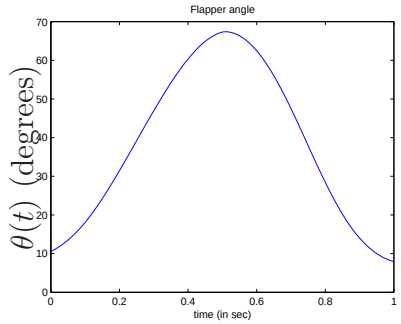

Figure 7: Flapper's angle $\theta(t)$

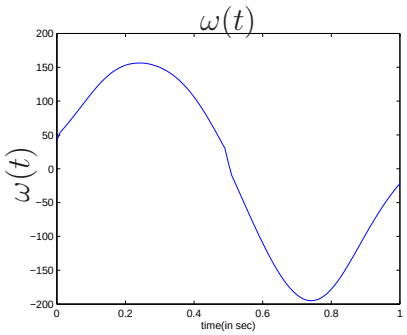

Figure 8: Angular frequency $\omega(t)$

2.4 Two-Piece snake

We extend the previous analysis to a simplified model of a snake, Figure 11. We will derive the friction forces exerted by the environment on the snake. First, consider a small piece with length dr of the snake from either the upper or lower bar, which is located at $r(t)$ with respect to a inertial reference frame with basis $\{e_x, e_y\}$, Figure 12.

According to the differential friction model (1) the friction experienced by this

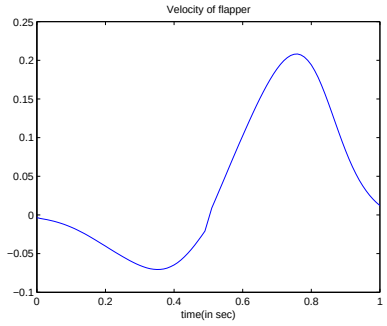

Figure 9: Velocity $v(t)$

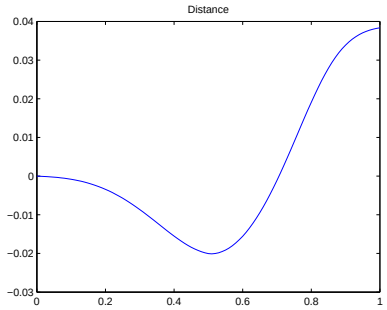

Figure 10: Distance $x(t)$

differential slab is

$$\begin{aligned} F_{B_x}(r,\beta) &= -\mu_a(\langle \dot{r}, B_x\rangle)\langle \dot{r}, B_x\rangle B_x \\ F_{B_y}(r,\beta) &= -\mu_T\langle \dot{r}, B_y\rangle B_y, \end{aligned} \tag{11}$$

where $\langle\cdot,\cdot\rangle$ denotes the inner product, $B_x = \begin{bmatrix} \cos(\beta) & \sin(\beta) \end{bmatrix}'$ is the axial direction and $B_y = \begin{bmatrix} -\sin(\beta) & \cos(\beta) \end{bmatrix}'$ is the transversal direction, both with respect to the inertial reference frame. The total x and y components of the friction force are $F_x(r,\beta) = \langle F_{B_x}, e_x\rangle + \langle F_{B_y}, e_x\rangle$, and $F_y(r,\beta) = \langle F_{B_x}, e_y\rangle + \langle F_{B_y}, e_y\rangle$, respectively. The virtual work due to virtual displacements in the x and y direction of the differential

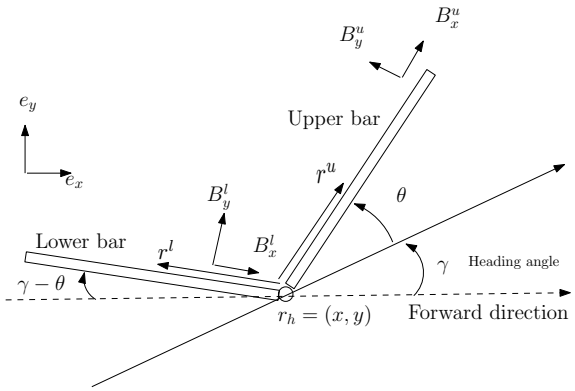

Figure 11: Two-piece snake.

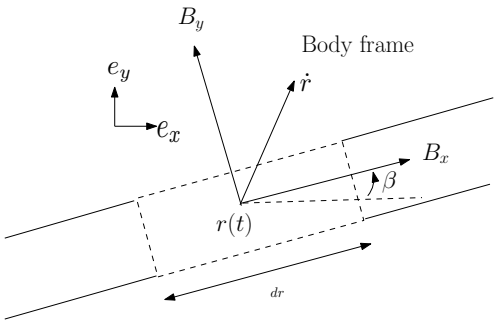

Figure 12: Differential piece of snake.

piece at r is

$$\delta W_r = F_x(r,\beta)\delta x + F_y(r,\beta)\delta y \tag{12}$$

We now proceed to derive the friction forces acting on the entire snake. Let $r_h = (x, y)$ denote the position of the hinge of the snake, Figure 11. We further assume that both links have unit length. A point $r \in [0, 1]$ units away from the hinge on the upper and lower bar is

$$r^u = r_h + rB_x^u, \tag{13}$$

$$r^l = r_h - rB_x^l, \tag{14}$$

where with respect to the inertial reference frame, $B_x^u = \begin{bmatrix} \cos(\theta+\gamma), & \sin(\theta+\gamma) \end{bmatrix}'$ and $B_x^l = \begin{bmatrix} \cos(\gamma-\theta), & \sin(\gamma-\theta) \end{bmatrix}'$, respectively. We will use the Lagrangian dynamics approach to find the generalized friction forces. Recall the Euler-Lagrange equations

$$\frac{d}{dt}\frac{\partial L}{\partial \dot{q}} - \frac{\partial L}{\partial q} = Q, \tag{15}$$

where L is the Lagrangian and Q contains the external and control forces. Let the generalized coordinates be $q = [x,\, y,\, \theta,\, \gamma]$, Figure 11. From (13) the virtual displacements at a distance r from the hinge on the *upper* bar, $\delta r^u = (\delta x_r^u, \delta y_r^u)$, due to the virtual displacements in the generalized coordinates, are

$$\delta x_r^u = \delta x - r\sin(\theta+\gamma)(\delta\theta+\delta\gamma), \tag{16}$$

$$\delta y_r^u = \delta y + r\cos(\theta+\gamma)(\delta\theta+\delta\gamma)$$

Similarly from (14), the virtual displacements on the *lower* bar are

$$\begin{aligned} \delta x_r^l &= \delta x + r\sin(\gamma-\theta)(\delta\gamma-\delta\theta), \\ \delta y_r^l &= \delta y - r\cos(\gamma-\theta)(\delta\gamma-\delta\theta) \end{aligned} \tag{17}$$

Substituting (13), (14), (16), (17) into (12), the friction forces on both the upper and lower bar r units away from the hinge r_h may be expressed

$$\begin{aligned} \delta W_r &= F_x(r^u,\theta+\gamma)\delta x_r^u + F_y(r^u,\theta+\gamma)\delta y_r^u + F_x(r^l,\gamma-\theta)\delta x_r^l + F_y(r^l,\gamma-\theta)\delta y_r^l \\ &= \Big(F_x(r^u,\theta+\gamma)+F_x(r^l,\gamma-\theta)\Big)\delta x + \Big(F_y(r^u,\theta+\gamma)+F_y(r^l,\gamma-\theta)\Big)\delta y + \\ &\quad +\Big(-F_x(r^u,\theta+\gamma)\sin(\theta+\gamma)+F_y(r^u,\theta+\gamma)\cos(\theta+\gamma) \\ &\quad -F_x(r^l,\gamma-\theta)\sin(\gamma-\theta)+F_y(r^l,\gamma-\theta)\cos(\gamma-\theta)\Big)r\delta\theta + \\ &\quad \Big(-F_x(r^u,\theta+\gamma)\sin(\theta+\gamma)+F_y(r^u,\theta+\gamma)\cos(\theta+\gamma) \\ &\quad +F_x(r^l,\gamma-\theta)\sin(\gamma-\theta)-F_y(r^l,\gamma-\theta)\cos(\gamma-\theta)\Big)r\delta\gamma, \end{aligned}$$

which is in the form

$$\delta W_r = T_x(r,\dot{x},\dot{y},q)\delta x + T_y(r,\dot{x},\dot{y},q)\delta y + +T_\theta(r,\dot{x},\dot{y},q)\delta\theta + T_\gamma(r,\dot{x},\dot{y},q)\delta\gamma. \tag{18}$$

Integrating the previous expression (18) over $[0,1]$, we obtain the total virtual work of the external friction forces on the *entire* snake. Indeed, the integral is

$$\begin{aligned} \delta W &= \underbrace{\int_0^1 T_x(r,\dot{x},\dot{y},q)dr}_{F_x^t(\dot{x},\dot{y},q)}\ \delta x + \underbrace{\int_0^1 T_y(r,\dot{x},\dot{y},q)dr}_{F_y^t(\dot{x},\dot{y},q)}\ \delta y \\ &+ \underbrace{\int_0^1 T_\theta(r,\dot{x},\dot{y},q)dr}_{F_\theta^t(\dot{x},\dot{y},q)}\ \delta\theta + \underbrace{\int_0^1 T_\gamma(r,\dot{x},\dot{y},q)dr}_{F_\gamma^t(\dot{x},\dot{y},q)}\ \delta\gamma, \end{aligned}$$

from which we can easily identify the total generalized friction forces, $F_x^t(\dot{x},\dot{y},q)$, $F_y^t(\dot{x},\dot{y},q)$, $F_\theta^t(\dot{x},\dot{y},q)$ and $F_\gamma^t(\dot{x},\dot{y},q)$.

The applied control is the torque F_c around the hinge. The external generalized force Q in (15) is

$$Q{=}[F_x^t(\dot{x},\dot{y},q), F_y^t(\dot{x},\dot{y},q), F_\theta^t(\dot{x},\dot{y},q){+}F_c, F_\gamma^t(\dot{x},\dot{y},q)]' \tag{19}$$

We further assume that the snake is in a quasi-periodic state and the inertia is small. This allows us to set the left hand side of (15) to zero, because the Lagrangian is linear in mass. Then (19) can be rewritten in the form

$$A(\dot{x},\dot{y},q)\dot{q} = [0,0,F_c,0]', \tag{20}$$

where

$$A(\dot{x},\dot{y},q) = \begin{bmatrix} A_{x1} & A_{y1} & A_{\theta 1} & A_{\gamma 1} \\ A_{x2} & A_{y2} & A_{\theta 2} & A_{\gamma 2} \\ A_{x3} & A_{y3} & A_{\theta 3} & A_{\gamma 3} \\ A_{x4} & A_{y4} & A_{\theta 4} & A_{\gamma 4} \end{bmatrix}, \tag{21}$$

The exact expressions of the matrix components are given Appendix A. The determinant of $A(\dot{x},\dot{y},q)$ can be shown to be

$$\det A(\dot{x},\dot{y},q) = a\cos(\theta)^4 - a\cos(\theta)^2 + \frac{2\mu_T^2}{9}(g_u+g_l), \tag{22}$$

where g_u, g_l are defined in (274) and $a = -\frac{\mu_T^2}{9}(\mu_T^2 - 4(g_u+g_l)\mu_T + 16g_ug_l)$. It is obvious that, since $-\frac{\pi}{2} \le \theta \le \frac{\pi}{2}$, (22) is quadratic in $\cos(\theta)^2$ over the interval $[0,1]$. The extremum of (22) is at $\cos(\theta)^2 = 1/2$ and at this value (22) is $\frac{\mu_T^2}{36}(\mu_T^2 + 4(g_l + g_u) + 16g_lg_u) > 0$ by the positivity of each term. Furthermore, if $\cos^2\theta = 0$ or 1 (

i.e., $\theta = \pm\frac{\pi}{2}$ or $\theta = 0$), then (22) is $\frac{2\mu_T^2}{9}(g_u + g_l) > 0$ by the definition of $\mu_a(\cdot)$. Thus, (22) is always positive in the interval $-\frac{\pi}{2} \leq \theta \leq \frac{\pi}{2}$, regardless of the sign of a. Thus $A(\dot{x}, \dot{y}, q)$ is invertible over this interval. Hence, (20) can be written

$$\dot{q} = \frac{b(\dot{x}, \dot{y}, q)}{\det A(\dot{x}, \dot{y}, q)} Fc, \tag{23}$$

where $b(\dot{x}, \dot{y}, q)$ is the third column of the adjugate matrix, Adj $A(\dot{x}, \dot{y}, q)$.

Due to the bi-modal nature of $\mu_a(\cdot)$ the system (23) is hybrid and from the previous equations it appears that the system has at least 4 modes. However, it can shown that

$$\frac{\langle \dot{r}^u, B_x^u \rangle}{\langle \dot{r}^l, B_x^l \rangle} \quad = \quad -\frac{4g_l + \mu_T \tan^2\theta}{4g_u + \mu_T \tan^2\theta}, \tag{24}$$

by using the first two components of (23). Thus, the velocities on both the upper and lower link along the axial directions, at a distance r away from the hinge, have opposite sign. This further implies that when the upper link is gliding forward, the lower link is sliding backwards and vice versa.

We now proceed to compute the work imparted by the snake. From (11) the total friction forces *on* the snake at both the upper and lower link, at a distance r from the hinge r_h, are $F_{tot}^u(r) = F_{B_x}(r^u, \theta + \gamma) + F_{B_y}(r^u, \theta + \gamma)$ and $F_{tot}^l(r) = F_{B_x}(r^l, -\theta + \gamma) + F_{B_y}(r^l, -\theta + \gamma)$, respectively. The total work at r is

$$W_{tot}(r) \quad = \quad F_{tot}^u(r)\frac{dr^h}{dt}dt + F_{tot}^l(r)\frac{dr^l}{dt}dt.$$

After dividing the previous expression by dt and integrating over $[0, 1]$, we obtain the power consumed *by* the snake is

$$\frac{dW_{tot}}{dt} = -\Big(\int_0^1 F_{tot}^u(r)\frac{dr^h}{dt}dr\Big) \; - \Big(\int_0^1 F_{tot}^l(r)\frac{dr^l}{dr}\Big). \tag{25}$$

To simulate the snake we assume the input torque is $F_c(t) = 20\cos t$. The starting angles are $\theta(0) = 0$ and $\gamma(0) = -0.35$. The simulation duration is over one period $T = 2\pi$. (Figure 13). The forward direction is to the right. As in the flapper the two-piece snake slides backwards initially and then forward. The locomotion is inefficient as seen in the figure. The total distance traveled sideways is almost four times the forward motion. This is due to the overly simplified model. If additional links are added, this sideways motion will decrease substantially. Notice that when the torque is positive (counter clockwise) the snake moves in the negative y-direction, and vice verse for clockwise torque. This is in accordance with our intuition because of the tangential (to the body) friction. It is also shown by experimentation that sideways motion is decreased when the tangential coefficient μ_T is increased (for rounded scales).

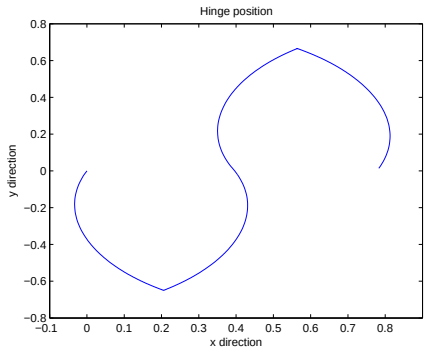

Figure 13: Hinge position $r_h(t)$.

2.5 Extensions and conclusions

Previous discussions can be extended to other robotic devices. One could offset two flappers to obtain a tortoise Figure 15. In this case the flapper angles θ_1 and θ_2 have

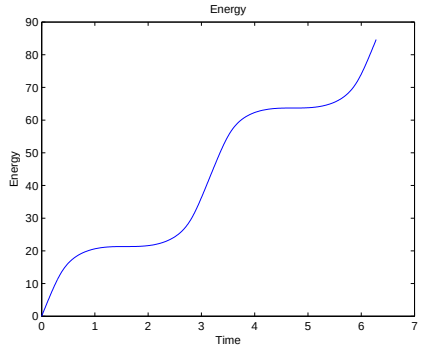

Figure 14: Energy expended snake .

opposite phases to accommodate locomotion.

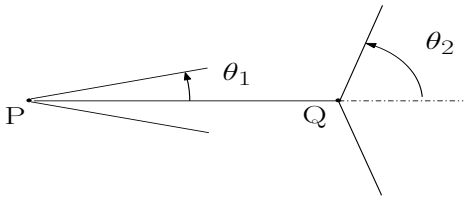

Figure 15: Tortoise

In this chapter we introduced the differential friction model which was used throughout to study locomotion. The model allows us to model the stands in legged locomotion by letting the friction coefficients to be infinite. As a result of this model the equations of motions obtained are of hybrid nature which are linear in the control. In our study we have neglected inertia of the creatures considered. This allowed us to obtain static relations between the forces and velocities for our creatures. This is not particularly restrictive since it is long known that acceleration is only a means to an end when it comes to locomotion [17]. Furthermore, we have studied the locomotive behavior under periodic steady state assumption. Suboptimal periodic controls as well as an optimal periodic control problem were considered.

CHAPTER III

A STOCHASTIC APPROACH TO OPTIMAL SWITCHING BETWEEN CONTROL AND OBSERVATION

In many real world applications control and observation happen simultaneously: output of a plant is continuously monitored while at the same time an observer-controller produces a feedback signal to modify the plant dynamics. However, there also many control problems where the process of control and observation need to be separated in time due to physical restrictions.

A remote system e.g a robotic vehicle may receive control signal from a distant controller. Due to power constraint (e.g solar cells or batteries) the robot is restricted either to probe the communication channel with the controller for new control instructions or to steer itself based on previous information already received from the controller. Only one of these two operations can take place at a time. Another instance of this temporal separation happens in chemical reactor control. More specifically, in Plug Flow Reactors or Piston Flow Reactors (PFR) several reagents are pumped through a series of pipes each with its own temperature to control the concentrations of each substance. As the reagents proceed through the PFR chemical reactions occur. At discrete instants a sample of the reaction product is analyzed for its composition with a mass- spectrometer (gas chromatograph). Based on this

observation the temperature controls are adjusted [60], [19].

In all these examples there is a clear periodic temporal separation between the control mode and the observation mode of the systems. It is obvious that the requisite periodic switching between these two modes prevents us from having a steady state in the strict classical sense. What one hopes to achieve is a periodic steady state by switching between these two modes. If this periodic steady state is possible it is also of interest to know when the optimal switching needs to occur. The problem just mentioned requires us to resort to the theory switched dynamical system.

Traditional switched dynamical systems are often modeled as a differential inclusion

$$\dot{x}(t) \in \{f_a((x(t), u(t))\}_{a \in A}$$

where A is a index set, $x \in \mathbb{R}^n$, $u(t) \in \mathbb{R}^k$ and $\{f_a : \mathbb{R}^{n+k} \to \mathbb{R}^n\}_{a \in A}$ is a collection of functions. The optimal control problem of this class of systems where the control variable consists of a set of switching times and a control input $u(t)$ has been studied in for example, [8] and [26]. In all these studies, the dimension of the state x is assumed to be the same at each switching time. Recently this restriction was removed [51]. In this paper a class of switched dynamical systems, the Multi-Mode Multi-Dimensional system (M^3D) has been explored. These M^3D systems are switched systems characterized by modes with state space of different dimensions. Several types of switching are mentioned and the necessary conditions of the optimal switching (timing) control are also presented therein.

In this chapter we study a periodic mode switching problem for a linear time

invariant system where the results fit nicely into this M^3D setting. The problem is related to periodic control problems. Periodic control problems have been studied in, for example, [32] and [18]. Application to chemical processes is explored in [23] to obtain chemical pseudo-steady state. In these papers a periodic control is assumed. In our approach, however, we periodically switch between two modes: an observation mode and a control mode to accomplish a periodic steady state. Second order information provides here a deterministic state model for the stochastic state (information state) of the system. An approximation leads here to a M^3D model. This chapter is organized as follows: in Section 3.1 the problem is set up, in Section 3.2 M^3D systems are reviewed. In Section 3.3 we provide a numerical simulation to illustrate the key points. Conclusions and comments are presented in Section 3.4.

3.1 System modeling

Consider a continuous, stochastic linear time invariant plant for which control and observation must be separated in time. The system is assumed to be of order n and follows the dynamics

$$\begin{aligned} \dot{x} &= Ax + bu + gw \\ y &= cx + v \end{aligned}$$

where w and v are zero mean, uncorrelated white noise signals modelling the actuator and sensor noise. The actuator and sensor have variances R and Q, respectively. (see Figure (16)) In what follows we shall only be concerned with the stabilization of the plant. Therefore, to avoid pathological cases, we will assume from the onset that the pair (A, c) is observable and (A, b) reachable.

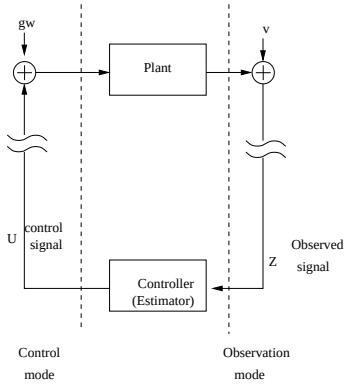

Figure 16: Optimal switching between control and observation

We describe the two modes of operation: during an *observation* mode the controller receives information $z = y$ only and the plant is not being controlled due to the assumption that control and observation need to separated in time. One may think of a single communication channel between plant and controller with data transfer restricted to one direction at a time. The system equations are now

$$\begin{aligned} \dot{x} &= Ax + gw \\ z &= cx + v \end{aligned}$$

The control station runs an estimator for this system with gain ℓ. This simulator obeys

$$\dot{\hat{x}} = A\hat{x} + \ell(z - c\hat{x})$$

Note: if a remote control problem is modelled then channel noise needs to be taken into account. The observed signal is then $z = y + \tilde{y}$ where $\tilde{y}$ is the channel noise with variance, say, Ω. The ideas are similar for plant dynamics replaced by a more realistic model. In this paper, however, we solely look at LTI systems.

In the *control* mode the station transmits u, obtained by operating on the available

information at the controller. In this mode the plant output is disconnected from the simulator. The plant then follows

$$\dot{x} = Ax + gw + bu$$

with the control input being given by the dynamic feedback

$$u = -k\hat{x}$$

where the simulated state, $\hat{x}$ evolves according to

$$\dot{\hat{x}} = A\hat{x} - bk\hat{x}.$$

Note again that if a communication channel is involved between the plant and the controller the feedback signal needs to be $u = -k\hat{x} + \tilde{u}$ where $\tilde{u}$ is again the channel noise.

We can now introduce a binary mode signal, m, with $m = 1$ denoting the observation mode and $m = 0$ the control mode. Thus, the combined state equations may be written as

$$\begin{aligned} \dot{x} &= Ax + (1-m)(bu) + gw \\ z &= m(cx + v) \end{aligned}$$

It is assumed that the station performs deterministic calculations to obtain $u(t)$ from the past information $\{z(\theta)|\theta < t\}$ fast and error free.

3.1.1 Stochastic Analysis: information state model

In this section we study the stochastic properties of the system mentioned in the previous section. In the observation mode, we have $m = 1$, and the plant and

estimator equations reduce to

$$\begin{aligned}\dot{x} &= Ax + gw \\ \dot{\hat{x}} &= (A - \ell c)\hat{x} + \ell c x + \ell v\end{aligned}$$

Define now the state estimation error $\tilde{x} = x - \hat{x}$, then alternatively we may write the combined state and error dynamics as

$$\frac{d}{dt}\begin{bmatrix} x \\ \tilde{x} \end{bmatrix} = \begin{bmatrix} A & 0 \\ 0 & A - \ell c \end{bmatrix}\begin{bmatrix} x \\ \tilde{x} \end{bmatrix} + \begin{bmatrix} gw \\ gw - \ell v \end{bmatrix}.$$

Define further the covariance matrix, the information state, to be

$$\text{Cov}\begin{bmatrix} x \\ \tilde{x} \end{bmatrix} = \begin{bmatrix} \Pi & X \\ X' & P \end{bmatrix},$$

then it satisfies the following one-way decoupled equations

$$\begin{aligned}\dot{\Pi} &= A\Pi + \Pi A' + gQg' \\ \dot{P} &= (A - \ell c)P + P(A - \ell c)' + gQg' + \ell R\ell' \\ \dot{X} &= AX + X(A - \ell c)' + gQg'.\end{aligned}$$

Similarly, during the control mode, with $m = 0$, the state and estimator dynamics are

$$\begin{aligned}\dot{x} &= Ax - bk\hat{x} + gw \\ \dot{\hat{x}} &= (A - bk)\hat{x}.\end{aligned}$$

The combined dynamics is now,

$$\frac{d}{dt}\begin{bmatrix} x \\ \tilde{x} \end{bmatrix} = \begin{bmatrix} A - bk & bk \\ 0 & A \end{bmatrix}\begin{bmatrix} x \\ \tilde{x} \end{bmatrix} + \begin{bmatrix} gw \\ gw \end{bmatrix}.$$

In the control mode the covariance equations are one-way coupled

$$\begin{aligned}
\dot{\Pi} &= (A-bk)\Pi + \Pi(A-bk)' + bkX' + Xk'b' + gQg' \\
\dot{P} &= AP + PA' + gQg' \\
\dot{X} &= (A-bk)X + bkP + XA' + gQg'.
\end{aligned}$$

Notice that during the observation mode all the covariance equations are decoupled while during the control mode the error variance P drives the cross-covariance X which in turn drives the plant covariance Π. Clearly, in the observation mode the plant state covariance diverges, while in the control mode the estimation error covariance blows up. Consider now a stochastic control with as objective the minimization of the final state covariance $\Pi(T)$. We may also want to penalize $\Pi(t)$ during the interval $[0,T]$. Generally in optimal control problem, the input energy is also penalized. Therefore, the energy of input $u = k\hat{x}$ needs to be considered as well. The average energy of this input is $\mathbf{E}(uu') = k\Sigma(t)k'$ where $\Sigma = \mathbf{E}(\hat{x}\hat{x}')$ Taking all these into account we form the cost functional

$$J = Tr\Big\{\Pi(T)\Big\} + \int_0^T \rho\, Tr\Big\{\Pi(t)\Big\} + k\Sigma(t)k'\,dt. \tag{26}$$

for some weighting constant ρ. The control variables are now the gains k and ℓ, which may be time varying. In addition we switch between observation and control mode at the instants τ_i. If a cost of $\alpha_{\rm obs}$ per time unit is attached to observation and the duration of this mode is $(\tau_{i-1} - \tau_i)$ then the cost of an observation mode is $\alpha_{\rm obs}(\tau_{i-1} - \tau_i)$. Similarly, a control mode costs $\alpha_{\rm ctr}(\tau_{i-1} - \tau_i)$ in such an interval. In the interval $[0,T]$ this amounts to a cost of $(\alpha_{\rm obs} - \alpha_{\rm ctr})m(t)$ where $m(t)$ is the binary

mode signal as defined before. Thus, this term can be added to the integrand in the performance index to include to the cost of each mode. It may also be reasonable to associate a cost with the switching itself. If each switch costs an amount γ, then we may add the term $\gamma|\dot{m}(t)|$ to the integrand. Since $\dot{m}$ is zero except at the switching instants where a Dirac δ is contributed. Regularization methods as explained in [50] can be used.

Recall that the covariance equations are all decoupled during the observation mode. Thus in the observation mode the equations for Π and P are self sufficient and X is not needed. However, in the control mode P drives X which in turn drives Π. Therefore, all three equations are needed during the control mode. A reduced model may be given by deleting X in the observation mode and initializing (replacing) at the onset of the control mode the X dynamics with the solution to $\Pi = XP^{-1}X'$ e.g. by taking a square root $X = \Pi^{1/2}P^{T/2}$ or the geometric mean between Π and P^{-1}. Hence the reduced information model involves the (matrix) state $[\Pi, P]'$ in the observation mode and the state $[\Pi, P, X']'$ in the control mode. In summary: the observation mode of the reduced problem is governed by

$$\begin{aligned} \dot{\Pi} &= A\Pi + \Pi A' + gQg' \\ \dot{P} &= (A - \ell c)P + P(A - \ell c)' + gQg' + \ell R\ell', \end{aligned} \tag{27}$$

and the control mode consists of

$$\begin{aligned} \dot{\Pi} &= (A - bk)\Pi + \Pi(A - bk)' + bkX' + Xk'b' + gQg' \\ \dot{P} &= AP + PA' + gQg' \\ \dot{X} &= (A - bk)X + bkP + XA' + gQg'. \end{aligned} \tag{28}$$

When switching from an observation mode to a control mode the mode changes according to the nonlinear transition

$$[\Pi, P]_{\text{obs}} \to [\Pi, P, P^{1/2}\Pi^{T/2}]_{\text{ctr}} \tag{29}$$

Similarly, for a transition from a control mode to an observation mode the mode transition follows

$$[\Pi, P, X]_{\text{ctr}} \to [\Pi, P]_{\text{obs}}.$$

The performance index to be minimized is (26). Due to the symmetry, the system dimensions are respectively $n(n+1)$ and $n(2n+1)$ in the observation and the control mode.

3.2 Multi-Mode Multi-Dimensional Systems

To solve the proposed optimization problem we need to resort to the so-called Multi-Mode Multi-Dimensional systems which is first introduced in [51]. MMMD systems form a class of hybrid systems where the number of states may change at each switching time. To simplify notation we assume a fixed sequence of controlled vector fields, $\dot{X}_i = f_i(X_i, U_i)$, where $f_i : \mathbb{R}^{n_i \times m_i} \times \mathbb{R}^c \to \mathbb{R}^{n_i \times m_i}$, for $i = 1, \ldots, N$. Here, X_i is a matrix of size $n_i \times m_i$ and U_i a vector of size c which is assumed to be fixed throughout. Furthermore, the switches between different modes are time-driven and that there are $N-1$ switches,$\overline{\tau} = [\tau_1, \ldots, \tau_{N-1}]$ with $\tau_0 = 0$ and $\tau_N = T$. At each switching instant $\tau_i,\ i = 1, \ldots, N-1$, the state changes according to $X_{i+1}(\tau_i^+) = F_{i+1,i}\big(X_i(\tau_i^-)\big)$ where each $F_{i+1,i} : \mathbb{R}^{n_i \times m_i} \to \mathbb{R}^{n_{i+1} \times m_{i+1}}$ is a continuously differentiable transition function.

Several state transitions such as energy limited transition and pseudo continuity transition are possible and we refer the reader to [51] for details.

3.2.1 Optimality conditions for Multi-Mode Multi-Dimensional System

In this section the necessary conditions for the M^3D system are derived below. The derivation here differs from [51] in the fact that 1: nonlinear transitions are used, 2: the dynamical systems are matrix differential equations of matrices. The latter condition forces the re-derivation because tensor products need to be used in the transitions as shown below. For the rest the derivation is similar to [51].

The performance index (P. I)

$$J = \int_0^T L(X, U)\, dt + \Phi(X(T)) \tag{30}$$

which expands into

$$J = \sum_{i=1}^{N} \int_{\tau_{i-1}}^{\tau_i} L_i(X_i, U_i)\, dt + \Phi_N(X_N(T)). \tag{31}$$

where a mode occurs in the interval $[\tau_{i-1}, \tau_i)$. Define the Hamiltionian in $[\tau_{i-1}, \tau_i)$

$$H_i(X_i, U_i, \lambda_i) = L_i(X_i, U_i) + Tr\{\lambda_i f(X_i, U_i)\}. \tag{32}$$

where λ_i is a $m_i \times n_i$ matrix Lagrange multiplier.

Theorem:

A MMMD system minimizes the performance index J in (31), with fixed initial time ($\tau_0 = 0$) and terminal time ($\tau_N = T$) if the switching times τ_i, $i = 1, \ldots, N-1$ are chosen to solve the following:

Euler-Lagrange Equations:

$$\dot{\lambda}_i = -\frac{\partial H_i}{\partial X_i} \tag{33}$$

with $\tau_{i-1} < t < \tau_i,\ i = 1, \ldots, N,$

Boundary Conditions:

$$\lambda_N(T^-) \ = \ \left(\frac{\partial \Phi}{\partial X_N}\right) \tag{34}$$

$$\lambda_i^{kl}(\tau_i^-) = Tr\Big[\lambda_{i+1}(\tau_i^+)\big[\frac{\partial F_{i+1,i}}{\partial X}\big]_{kl}\Big] \tag{35}$$

for $1 \leq k \leq m_i$, $1 \leq l \leq n_i$ and $1 \leq n \leq N$, where

$$\Big[\frac{\partial F_{i+1,i}}{\partial X}\Big]_{kl} = \begin{bmatrix} \frac{\partial F_{i+1,i}^{11}}{\partial X_{lk}} & \cdots & \frac{\partial F_{i+1,i}^{1 m_{i+1}}}{\partial X_{lk}} \\ \vdots & \frac{\partial F_{i+1,i}^{ij}}{\partial X_{lk}} & \vdots \\ \frac{\partial F_{i+1,i}^{n_{i+1}1}}{\partial X_{lk}} & \cdots & \frac{\partial F_{i+1,i}^{n_{i+1} m_{i+1}}}{\partial X_{lk}} \end{bmatrix}$$

Optimality Conditions:

$$H_i(\tau_i^-) = H_{i+1}(\tau_i^+) \tag{36}$$

Proof. Since each state transitions satisfy $X_{i+1}(\tau_i^+) = F_{i+1,i}(X_i(\tau_i^-))$, we adjoin the state constraints to the P.I by using a set of matrix Lagrange multipliers μ_i where the dimension is $m_{i+1} \times n_{i+1}$ for $i = 1, \ldots, N-1$. The adjoint P.I is

$$\begin{aligned} J_0 \ &= \ \Phi_N(X_N(T)) + \sum_{i=1}^{N-1} Tr\Big[\mu_i[X_{i+1}(\tau_i^+) - \\ &- \ F_{i+1,i}(X_i(\tau_i^-))]\Big] + \sum_{i=1}^{N} \int_{\tau_{i-1}^+}^{\tau_i^-} L_i(X_i, U_i) + \\ &+ \ Tr\big[\lambda_i(f_i(X_i, U_i) - \dot{X}_i)\big]\ dt \end{aligned}$$

Following similar arguments as in [51] we obtain the variation after perturbing the

final state, the switching times, inputs and states in each mode

$$\begin{aligned}\delta J = & Tr\Big[\left(\frac{\partial \Phi_N}{\partial X_N(T)} - \lambda_N(\tau_N^-)\right)\eta_N(T)\Big] + \sum_{i=1}^{N-1} A_i\theta_i + \\ & + \sum_{i=1}^{N-1} Tr\left[\Big[\mu_i + \lambda_{i+1}(\tau_i^+)\Big]\eta_{i+1}(\tau_i^+)\right] - \\ & - \sum_{i=1}^{N-1}\sum_{k=1}^{m_i}\sum_{l=1}^{n_i}\left(\lambda_i^{kl}(\tau_i^-) + \dots\right. \\ & + \left.\left\{\sum_{r=1}^{m_{i+1}}\sum_{s=1}^{n_{i+1}} \mu_i^{rs}\big[\frac{\partial F_{i+1,i}}{\partial X}\big]_{kl}^{sr}\right\}\right)\eta_i^{lk}(\tau_i^-) + \\ & + \sum_{i=1}^{N}\int_{\tau_{i-1}^+}^{\tau_i^-}\left(\frac{\partial H_i}{\partial U_i}\nu_i + Tr\Big[\Big(\dot\lambda_i + \frac{\partial H_i}{\partial X_i}(X_i,u_i,\lambda_i)\Big)\eta_i\Big]\right)dt\end{aligned}$$

where

$$\begin{aligned}A_i = & L_i(X_i,U_i)\big|_{\tau_i^-} - L_{i+1}(X_{i+1},U_{i+1})\big|_{\tau_i^+} + \\ & + \sum_{k=1}^{m_{i+1}}\sum_{l=1}^{n_{i+1}}\mu_i^{kl}(\tau_i^+)\left[\dot X_{i+1}^{lk}(\tau_i^+) - \right. \\ & - \left.\sum_{r=1}^{m_i}\sum_{s=1}^{n_i}\big[\frac{\partial F_{i+1,i}}{\partial X}\big]_{rs}^{lk}\dot X_i^{sr}(\tau_i^-)\right]\end{aligned}$$

By choosing the Lagrange multiplier λ_i appropriately and after some manipulations the necessary conditions are readily obtained.

■

3.2.2 Square root transition

As required in the necessary condition (35) the derivative of the transition function needs to be taken. The transition from a observation mode to a control mode involves the products of two square root matrices (29).Since matrix square roots of a positive definite symmetric matrix P are in general not unique we settle for the unique positive definite symmetric square root $R = R' > 0$ with $P = R^2$. With this, the derivative of

R with respect to P is well defined. We now compute this derivative. First consider the matrix derivative $\frac{dR^2}{dP} = \frac{dP}{dP}$. The components of the RHS are

$$\begin{aligned}\left[\frac{dP}{dP}\right]^{ij}_{\alpha\beta} &= \frac{dP_{ij}}{dP_{\beta\alpha}} \\ &= \delta_{i\beta}\delta_{j\alpha}\end{aligned}$$

where $1 \leq \alpha, \beta \leq n$ and $1 \leq i, j \leq n$.

Similarly,

$$\left[\frac{dR^2}{dP}\right]^{ij}_{\alpha\beta} = \left[\left[\frac{dR}{dP}\right]_{\alpha\beta} R\right]_{ij} + \left[R\left[\frac{dR}{dP}\right]_{\alpha\beta}\right]_{ij}$$

where

$$\left[\frac{dR}{dP}\right]_{\alpha\beta} = \begin{bmatrix} \left[\frac{\partial R}{\partial P}\right]^{11}_{\alpha\beta} & \cdots & \left[\frac{\partial R}{\partial P}\right]^{1n}_{\alpha\beta} \\ \vdots & \left[\frac{\partial R}{\partial P}\right]^{ij}_{\alpha\beta} & \vdots \\ \left[\frac{\partial R}{\partial P}\right]^{n1}_{\alpha\beta} & \cdots & \left[\frac{\partial R}{\partial P}\right]^{nn}_{\alpha\beta} \end{bmatrix}$$

for fixed α and β.

Hence, the matrix square root $\frac{dR}{dP}$ satisfies the following Lyapunov-like equation.

$$\left[\frac{dR}{dP}\right]_{\alpha\beta} R + R\left[\frac{dR}{dP}\right]_{\alpha\beta} = M_{\beta,\alpha} \tag{37}$$

where

$$M_{\beta,\alpha} = \begin{bmatrix} 0 & \cdots & 0 \\ \vdots & \delta_{i\beta}\delta_{j\alpha} & \vdots \\ 0 & \cdots & 0 \end{bmatrix}$$

From (37)

$$\big((I \otimes R) + (R \otimes I)\big)\ vec\left[\frac{dR}{dP}\right]_{\alpha\beta} = vec\ M_{\beta,\alpha}$$

.Since R is positive definite the eigenvalues for $(I \otimes R) + (R \otimes I)$ is also positive. Thus, $vec\Big[\frac{dR}{dP}\Big]_{\alpha\beta}$ can be solved for by

$$vec\Big[\frac{dR}{dP}\Big]_{\alpha\beta} = \Big((I \otimes R) + (R \otimes I)\Big)^{-1} vec\ M_{\beta,\alpha}$$

Consistency with the scalar case is evident.

3.3 Examples

In this section we study an example. The information states (28) and (29) have the dynamics. During an observation mode the Hamiltonian H_o is

$$\begin{aligned}\mathbf{H}_o = \rho\, Tr\big[\Pi(t)\big] + k'\Sigma(t)k + Tr\big[\lambda_\Pi\Big(A\Pi + \Pi A' + gQg'\Big)\big] \\ +\quad Tr\big[\lambda_p\Big((A-\ell c)P + P(A-\ell c)' + gQg' + \ell R\ell'\Big)\big]\end{aligned}$$

The input gradient is $\frac{\partial \mathbf{H}_0}{\partial \ell} = -2cP\lambda_P + 2Rl'\lambda_P$, while the co-states are

$$\begin{aligned}-\frac{d}{dt}\lambda_\Pi &= \rho I + \lambda_\Pi A + A'\lambda_\Pi \\ -\frac{d}{dt}\lambda_P &= \lambda_P(A - lc) + (A - lc)'\lambda_P\end{aligned}$$

Similarly, during a control mode the Hamiltonian H_c is

$$\begin{aligned}\mathbf{H}_c = \rho\, Tr\big[\Pi(t)\big] + k'\Sigma(t)k + Tr\big[\lambda_P\Big(AP + PA' + gQg'\Big)\big] \\ + Tr\big[\lambda_\Pi\Big((A-bk')\Pi + \Pi(A-bk')' + bk'X' + Xkb' + gQg'\Big)\big] \\ + Tr\big[\lambda_X\Big((A-bk')X + bk'P + XA' + gQg'\Big)\big]\end{aligned}$$

while the input gradient is

$$\frac{\partial \mathbf{H}_c}{\partial k} = 2k'\Sigma - 2b'\lambda_\Pi\Pi + 2b'\lambda_\Pi X - b'\lambda_X' X' + b'\lambda_X' P$$

where $\Sigma = \Pi - X' - X + P$. The co-states are

$$\begin{aligned}
-\frac{d}{dt}\lambda_\Pi &= \rho I + kk' + \lambda_\Pi(A - bk') + (A - bk')'\lambda_\Pi \\
-\frac{d}{dt}\lambda_P &= kk' + \lambda_P A + A'\lambda_P + \lambda_X bk' \\
-\frac{d}{dt}\lambda_X &= -2kk' + 2kb'\lambda_\Pi + \lambda_X A + A'\lambda_X - \lambda_X bk'
\end{aligned}$$

It is desired to obtain a pseudo-steady state by switching between an observation mode and a control mode. Obviously, this is a periodic problem and we therefore look at a period of T second. Assume a minimal system (A, b, c) with the performance index (26) which is minimized over $l(t)$, $k(t)$ and a switching time τ_1. In this periodic setting the functions $l(t)$ and $k(t)$ can be periodically extended to obtain the full solution. We assume an observation mode precedes a control mode in the simulation.

For a numerical example assume the noises have unit variance: $R = Q = 1$, $T = 1$ and the system parameters are $a = 1$, $b = 1$, $c = 1$ and $g = 1$. A gradient descent algorithm with a fixed step size is implemented for the simulation. Since the input is discontinuous at the switching time it needs to be taken care of at the boundary as the algorithm iterates. When the switching time is changed due to the switching time gradient the support of one the inputs increases, while the other support decreases. For the longer support the boundary from the previous run gets extended until the new switching time while for the shorter input a piece of the same length is removed.

The conceptual algorithm is as follows:

Step 1: Guess initial conditions for switching time τ_1, $\ell(t)$, $k(t)$, $\Pi(0)$ and $P(0)$.

Step 2: Run information states forward and co-states backwards.

Step 3: Update τ_1, $\ell(t)$, $k(t)$.

Step 4: Correct boundaries of $\ell(t)$, $k(t)$ around the new switching time τ_1.

Step 5: Repeat Step 2.

The initial guess for the switching time is $\tau_1 = \frac{T}{2} = 0.5$ sec. It converges to 0.566 sec. The information states in the resulting optimal periodic regime are shown in Figure (18) for one period ($T = 1$).

The algorithm above is also applied to a second order system with

$$A = \begin{bmatrix} 0.5 & 3 \\ 0 & 0.2 \end{bmatrix}, \; b = \begin{bmatrix} 0 \\ 1 \end{bmatrix}, \; c = \begin{bmatrix} 1 & 1 \end{bmatrix}$$

Since the number of information states is 8 in the observation mode and 12 in the control mode the graph of the information states is omitted. The feedback gain $l(t)$ and the control $k(t)$, however, are shown in Figure (20). The optimal gains are relatively complex. In practice a piecewise linear approximation could be used to lower implementation complexity with negligible increase of the cost function. This is feasible because near optimality the cost function is insensitive to small variations. Since a regular gradient descent algorithm with fixed step size is used it is obvious that the algorithm is slow and will spiral around a local minimum. An improvement could be made by introducing a variable step size algorithm such as the Armijo step size [2].

3.4 Conclusion

We have seen that many real world applications are constrained to switch periodically between observation and control. Examples are one way communication of a remote vehicle and Plug Flow Reactors in chemical processing. This paper explored this

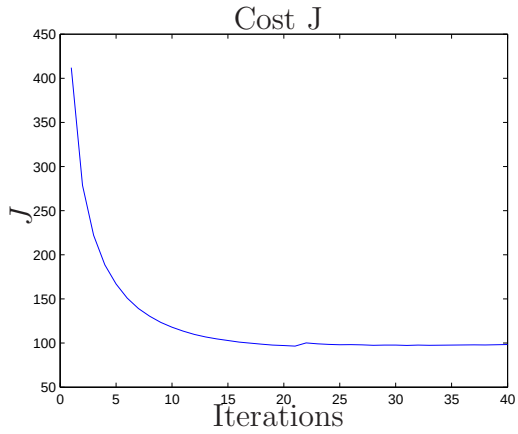

Figure 17: Cost J for scalar system

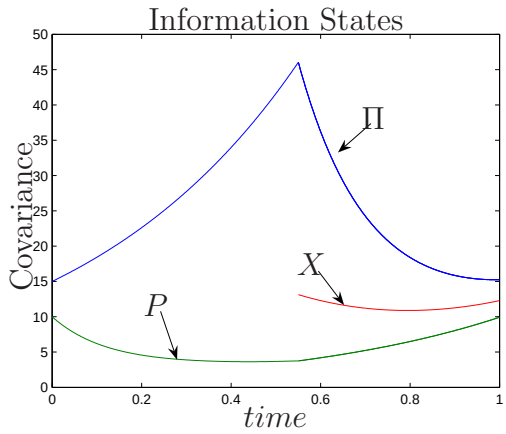

Figure 18: Information states for scalar system

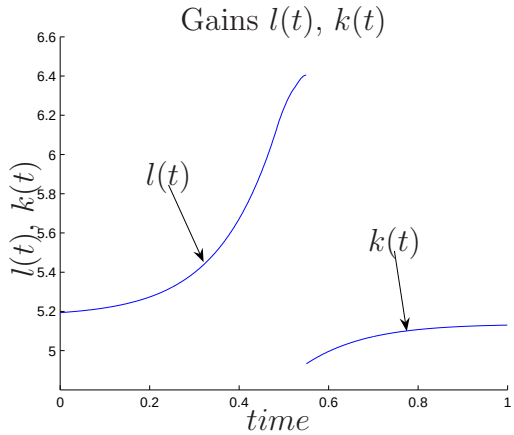

Figure 19: Gains $l(t)$ and $k(t)$ for scalar system

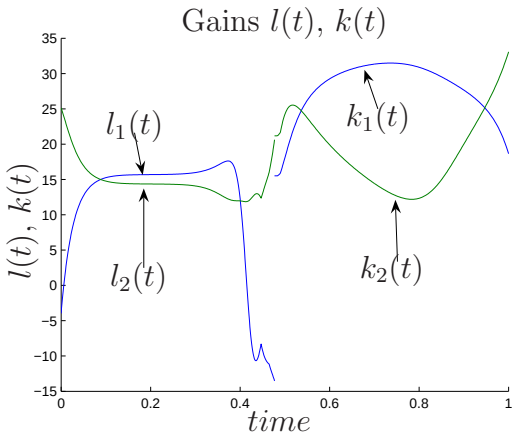

Figure 20: Gains $l(t)$ and $k(t)$ for second order system

switching problem by casting it into a M^3D setting where the information states of the system are used instead of the true plant-observer dynamics. By periodically switching between an observation mode and a control mode we obtain a periodic steady state. Furthermore, a numerical example was given to illustrate this.

Whereas in this paper we have assumed that the period of the M^3D system was fixed, the optimal period is easily determined. This is achieved either experimentally, (i.e., by running the basic optimal control algorithm for different periods), or by solving the optimal control problem analytically and implementing the additional degree of freedom in the gradient search.

CHAPTER IV

PARITY IN LQ CONTROL: THE INFINITE TIME LIMIT FOR TERMINAL CONTROL

As a preparation for the upcoming discussion of the Gluskabi raccordation in the next chapters we revisit the classical terminal controller expounded in, for instance, [12], in this chapter. We provide a constructive proof of the optimality condition, which is derived in [12] in an ad-hoc fashion. Furthermore, we discuss the limiting case $T \to \infty$ for the terminal controller and show that there exists a decomposition of the terminal controller into two subproblems.

4.0.1 Terminal Controller

The terminal controller apecialized to a linear system is the following optimization:

$$\begin{aligned} \min_{u} \quad & \int_0^T x'Px + \rho u^2 \, dt \\ \text{subject to:} \quad & \dot{x} = Ax + bu, \;\; x(0) = x_0, \, x(T) = x_f, \end{aligned} \tag{38}$$

where P is a $n \times n$ positive semi-definite matrix: $P \succeq 0$, ρ is positive: $\rho > 0$; A and b are $n \times n$ and $n \times 1$ matrices, respectively.

For this problem to be well posed, it is required that the system in (38) to be reachable. That means that the reachability gramian,

$$\mathcal{R}_T = \int_0^T \Phi(0,t) b b' \Phi'(0,t) \, dt, \tag{39}$$

needs to be invertible, where $\Phi(t,\tau) = \exp A(t-\tau)$ is the state transition matrix of (38). An equivalent condition for the invertibility of (39) is that the *reachability* matrix,

$$\mathcal{R}(A,b) = \left[\begin{array}{cccc} b & Ab & \dots & A^{n-1}b \end{array} \right], \tag{40}$$

has full rank.

The solution to the terminal controller is also well known (cf. [12] Section 5.3) and involves the Hamiltonian system

$$\left[\begin{array}{c} \dot{x} \\ \dot{\lambda} \end{array} \right] = \underbrace{\left[\begin{array}{cc} A & -\frac{1}{\rho}bb' \\ -P & -A \end{array} \right]}_{\mathbf{H}} \left[\begin{array}{c} x \\ \lambda \end{array} \right], \tag{41}$$

where λ is the costate equation, and $\mathbf{H}$ is the Hamiltonian matrix. The solution to (41) is

$$\left[\begin{array}{c} x(t) \\ \lambda(t) \end{array} \right] = e^{\mathbf{H}(t-T)} \left[\begin{array}{c} x(T) \\ \lambda(T) \end{array} \right], \tag{42}$$

where $\lambda(T) = \nu$ needs to be determined from the given boundary conditions $x(0) = x_0$ and $x(T) = x_f$. Since numerical properties of the state transition matrix are unattractive [12], the *sweep method* has been developed to solve (42).

The sweep method *postulates* that the costate equation $\lambda(t)$ and the boundary conditions, $\psi = x_f$ and $\lambda(T) = \nu$, satisfy the following two equations:

$$\lambda(t) = S(t)x(t) + R(t)\nu \tag{43}$$

$$\psi = U(t)x(t) + Q(t)\nu \tag{44}$$

To satisfy the boundary conditions, it is required that $S(T) = 0$, $R(T) = I$, $U(T) = I$ and $Q(T) = 0$, respectively. These equations are subsequently substituted into (41) to obtain the Riccati equation

$$\dot{S} + SA + A'S + P - \frac{Sbb'S}{\rho} = 0 \tag{45}$$

and

$$\dot{R} + (A' - \frac{Sbb'}{\rho})R = 0. \tag{46}$$

With the process of back-substitution, it is required that

$$U(t) = R'(t) \tag{47}$$

to maintain consistency.

In the following section, we will give a different proof of the sweep method by explicitly *constructing* the Ricatti equation from the state transition matrix (42). With this constructive proof, we remove the assumptions (43) and (44) made in [12].

In many practical situations it is often desired to keep a stationary system close to a reference point with acceptable control over a long period of time. This is essentially equivalent to the LQ problem in (38) with $T \to \infty$ and *without* the final state constraint. The boundedness of this limit is guaranteed if the system is reachable. This is the same reachability condition (40) as required for the terminal controller problem. The reachability condition alone is not enough to guarantee the asymptotic solution to be stable. To ensure this stability, it is further required that the system is observable. For the optimal control problem in (38), this additional observability

requirement is equivalent to

$$\text{rank } \mathcal{O}(c, A) = \text{rank} \left[\begin{array}{cccc} c' & A'c' & \dots & (A')^{n-1}c' \end{array} \right]' = n, \tag{48}$$

where $c = P^{T/2}$. The matrix $\mathcal{O}(c, A)$ is called the *observability* matrix.

If $P = 0$, then the LQ problem in (38) reduces to the *minimum energy problem*. The optimal control for this problem [12] is

$$u_{opt}(t, T, x_0) = \frac{\rho}{2}[x_f - \Phi(T, 0)x_i]' \mathcal{R}_T^{-1} [x_f - \Phi(T, 0)x_i]. \tag{49}$$

It is obvious in (49) that the optimal control diverges as $T \to 0$ since the reachability gramian approaches a singular matrix. Thus, as the control becomes faster, it is also becoming more "violent" because the inverse of a nearly singular matrix has unbounded norm. In [45] the divergence rate of the optimal control (49) for a *multi-input* linear time-invariant system is found to be

$$||R_T|| \sim \gamma T^{-K+1/2}, \ T \to 0, \tag{50}$$

where K is the smallest integer such that

$$\text{rank} \left[\begin{array}{cccc} B & AB & \dots & A^K B \end{array} \right] = n, \tag{51}$$

and $x_0 \neq 0$. The read-in matrix B is now a $n \times m$ matrix. By duality a similar result holds for the observability matrix.

4.1 A constructive proof

In the following, we will derive equations (43), (44), (45) and (46) *without* postulating (43) and (44). Our proof is constructive, and the sweep method is put on a equal footing with the transition matrix method.

First, we partition the transition matrix (42) into

$$e^{\mathbf{H}(t-T)} = \begin{bmatrix} \Phi^o_{11}(t,T) & \Phi^o_{12}(t,T) \\ \Phi^o_{21}(t,T) & \Phi^o_{22}(t,T) \end{bmatrix} = \Phi^o(t,T). \tag{52}$$

The final state, $x(T) = x_f$, can readily be solved for:

$$x_f = {\Phi^o_{11}}^{-1}(t,T)\left(x(t) - \Phi^o_{12}(t,T)\lambda(T)\right). \tag{53}$$

After substituting this equation into the second row of (42), we obtain for the costate equation,

$$\lambda(t) = \underbrace{\Phi^o_{21}(t,T){\Phi^o_{11}}^{-1}(t,T)}_{S(t)}x(t) + \underbrace{\left(\Phi^o_{22}(t,T) - \Phi^o_{21}(t,T){\Phi^o_{11}}^{-1}(t,T)\Phi^o_{12}(t,T)\right)}_{R(t)}\nu \tag{54}$$

Thus, we obtain (43) by construction, which is *postulated* in [12]. In summary,

$$S(t) = \Phi^o_{21}(t,T){\Phi^o_{11}}^{-1}(t,T), \tag{55}$$

$$R(t) = \Phi^o_{22}(t,T) - \Phi^o_{21}(t,T){\Phi^o_{11}}^{-1}(t,T)\Phi^o_{12}(t,T). \tag{56}$$

It is clear from (52) that $\Phi^o_{11}(T,T) = \Phi^o_{22}(T,T) = I$ and $\Phi^o_{12}(T,T) = \Phi^o_{21}(T,T) = 0$. Hence,

$$S(T) = 0 \quad \text{and} \quad R(T) = I, \tag{57}$$

which are the desired boundary conditions. Differentiating λ in (54) and substituting the state and costate equations in (41) readily shows the requisite nullity for all t of

$$\left[\dot{S} + SA + A'S + P - S\frac{bb'}{\rho}S\right]x + \left[\dot{R} + A'R - S\frac{bb'}{\rho}R\right]\nu.$$

Since this must be true for all x and ν, the coefficient matrices must vanish. Therefore,

we obtain the matrix differential equations,

$$\dot{S} + SA + A'S + P - \frac{1}{\rho} Sbb'S = 0, \quad S(T) = 0, \tag{58}$$

$$\dot{R} + \left[A - \frac{1}{\rho} bb'S \right]' R = 0, \quad R(T) = I. \tag{59}$$

Substituting (54) into (41), the state equation becomes

$$\dot{x} \;\; = \;\; \left[A - \frac{1}{\rho} bb'S \right] x - \frac{1}{\rho} bb'R\nu. \tag{60}$$

Letting $\Phi(t, \tau)$ be the transition matrix of the time variant closed loop matrix $A - \frac{1}{\rho} bb'S$, the solution to (60) is

$$x(t) = \Phi(t, 0)x_i - \int_0^t \Phi(t, \tau) \frac{bb'}{\rho} R(\tau)\nu \, d\tau. \tag{61}$$

Recall that the transition matrix satisfies

$$\frac{\partial}{\partial t}\Phi(t, \tau) = \left[A - \frac{1}{\rho} bb'S \right] \Phi(t, \tau), \quad \Phi(t, t) = I,$$

and that the problem has the constraints $x(0) = x_i$ and $x(T) = x_f$. After setting

$$\Omega(t) = - \int_0^t \Phi(t, \tau) \frac{bb'}{\rho} R(\tau) \, d\tau, \tag{62}$$

the previous equation (61) gives

$$x(t) = \Phi(t, 0)x_i + \Omega(t)\nu. \tag{63}$$

Evaluating at $t = T$, we get as a special case

$$x_f = x(T) = \Phi(T, 0)x_i + \Omega(T)\nu. \tag{64}$$

From this we get in turn

$$\Omega(T)^{-1}[x_f - \Phi(T, 0)x_i] = \nu, \tag{65}$$

provided that $\Omega(T)$ is invertible. It follows from (59) that

$$-\dot{R}'(t) = R'(t)\left[A - \frac{1}{\rho}bb'S(t)\right], \quad R'(T) = I. \tag{66}$$

By the uniqueness of the solution of differential equations, this implies that

$$R'(t) = \Phi(T,t). \tag{67}$$

In light of (56), the time varying closed loop transition matrix $\Phi(T,t)$, which does not have an explicit closed form solution in general, can simply be expressed in terms of the sub-matrices of the exponential of the Hamiltonian matrix **H**. This matrix exponential can always be obtained by, for example, taking the Laplace transform of **H**. Exploiting the semi-group property of the transition matrix, we get

$$\Omega(t) \;=\; -\Phi(t,T)\int_0^t \Phi(T,\tau)\frac{bb'}{\rho}\Phi'(T,\tau)\,d\tau \tag{68}$$

and

$$\Omega(T) = -\int_0^T \Phi(T,\tau)\frac{bb'}{\rho}\Phi'(T,\tau)\,d\tau. \tag{69}$$

This is the negative of the reachability gramian of the closed loop system. Hence, $\Omega(T)$ is nonsingular if the original system (A,b) is reachable.

Finally, we derive from (63)

$$x_i = \Phi^{-1}(t,0)[x(t) - \Omega(t)\nu],$$

and from (64)

$$x_f \;=\; \Phi(T,t)x(t) + [\Omega(T) - \Phi(T,t)\Omega(t)]\nu.$$

This is of the form

$$x_f = \Psi(t)x(t) + \Lambda(t)\nu, \tag{70}$$

where $\Psi(t) = \Phi(T,t)$ and

$$\begin{aligned}\Lambda(t) &= [\Omega(T) - \Phi(T,t)\Omega(t)] \\ &= -\int_t^T \Phi(T,\tau)\frac{bb'}{\rho}\Phi'(T,\tau)\,d\tau.\end{aligned}$$

In [12] the form in (70) is *postulated*; the differential equations for $\Psi(t)$ and $\Lambda(t)$ are derived by the differentiation of the *postulated* equations (43) and (44) with appropriate substitutions. In the previous derivations, however, they are obtained by *construction*, which is more elegant.

4.1.1 Optimal Performance Index

With the substitutions of (43), (65), (67) and the optimality condition into (61), we obtain

$$\dot{x} = Ax - \frac{bb'}{\rho}\left(S(t)x + \Phi'(T,t)\Omega^{-1}(T)[x_f - \Phi(T,0)x_i]\right),$$

which has solution

$$x(t) = \Phi(t,0)x_i - \int_0^t \Phi(t,\tau)\frac{bb'}{\rho}\Phi(t,\tau)'\,d\tau\Phi'(T,t)\Omega^{-1}(T)(x_f - \Phi(T,0)x_i).$$

After the substitution of the previous result into the performance index and some manipulations, we derive

$$J = x_i'S(0)x_i - x_f'S(T)x_f + [x_f' - x_i'\Phi'(T,0)]\,[-\Omega^{-1}(T)]\,[x_f - \Phi(T,0)x_i].$$

By using the boundary condition $S(T) = 0$ in (57), the well-known (e.g., see [12]) equation for the performance index is

$$J = \frac{1}{2}\left(x_i'S(0)x_i + [x_f' - x_i'\Phi'(T,0)]\,[-\Omega^{-1}(T)]\,[x_f - \Phi(T,0)x_i]\right). \tag{71}$$

4.1.2 Invariance in terminal controller problem

With the substitution of (65) into (70), we obtain, after some rearrangements,

$$x(t) = [\Phi(t,T) - \Phi(t,T)\Lambda(t)\Omega^{-1}(T)]x_f + \Phi(t,T)\Lambda(t)\Omega^{-1}(T)\Phi(T,0)x_i. \quad (72)$$

Similarly, after substituting (72) and (65) into (54), we obtain for the costate

$$\begin{aligned}\lambda(t) &= \Big[S(t)\Phi(t,T)[I - \Lambda(t)\Omega^{-1}(T)] + \Phi'(T,t)\Omega^{-1}(T)\Big]x_f + \\ &+ \Big[S(t)\Phi(t,T)\Lambda(t)\Omega^{-1}(T)\Phi(T,0) - \Phi'(T,t)\Omega^{-1}(T)\Phi(T,0)\Big]x_i, \quad (73)\end{aligned}$$

and for the control

$$\begin{aligned}u(t) &= -\frac{1}{\rho}b'\Big[S(t)\Phi(t,T)[I - \Lambda(t)\Omega^{-1}(T)] + \Phi'(T,t)\Omega^{-1}(T)\Big]x_f + \\ &- \frac{1}{\rho}b'\Big[S(t)\Phi(t,T)\Lambda(t)\Omega^{-1}(T)\Phi(T,0) - \Phi'(T,t)\Omega^{-1}(T)\Phi(T,0)\Big]x_i. \quad (74)\end{aligned}$$

It is clear from (72), (73) and (74) that the state, costate and control are linear in x_i and x_f. Therefore, if the initial and final states are scaled by a real number α, the optimal performance index (71) will be scaled by α^2. We summarize this in the following proposition.

Proposition 4.1.1. *If J^* is the optimal performance index of the terminal controller with initial and final states x_i and x_f, respectively, then the optimal performance index J^*_α corresponding to the same problem, but with both x_i and x_f scaled by α, is $J^*_\alpha = \alpha^2 J^*$.*

4.1.3 Interpretation and decomposition

It is well known that, if the final state is free, the solution to the regulator problem with initial condition x_i has an associated minimal cost $J = \frac{1}{2}x_i'S(0)x_i$. In this

problem one is only interested in minimizing J and not in reaching a desired final state. In addition, since there is no (quadratic) weight on the final state, $S(0)$ is given by the solution at $t = 0$ of the Riccati equation

$$-\dot{S} = A'S + SA + P - S\frac{bb'}{\rho}S, \quad S(T) = 0.$$

Clearly, this is exactly the first term in (71).

Consider now the closed loop system

$$\dot{x} = \left(A - \frac{bb'}{\rho}S\right)x + bu_{\text{ext}}, \tag{75}$$

obtained from the optimal regulator problem. Suppose we want to select the external control u_{ext}, which drives the state from x_i at $t = 0$ to x_f at $t = T$, and has minimal energy $J_u = \frac{1}{2}\int_0^T u_{\text{ext}}^2\, dt$. Then it is also well known that this minimal energy is given by $\frac{1}{2}[x_f' - x_i'\Phi'(T,0)]\,[\mathcal{R}_T]^{-1}\,[x_f - \Phi(T,0)x_i]$, where $\mathcal{R}_T$ is the reachability gramian of the closed loop system,

$$\mathcal{R}_T = \int_0^T \Phi(T,\tau)bb'\Phi'(T,\tau)\, d\tau.$$

Since $-\Omega(T) = \frac{1}{\rho}\mathcal{R}_T$ from (69), we conclude that the second term in (71) is the cost associated with the external input necessary for reaching the desired final state with the closed loop system (75).

4.1.3.1 Superposition and Interference

Obviously, the previous two subproblems are intermingled in the terminal controller problem. In summary, we consider the following problems **P1** and **P2**, respectively:

P1: Starting from the initial condition x_i and with a free endpoint, choose the

control u_1 in the system $\dot{x}_1 = Ax_1 + bu_1$ to minimize the performance index $J_1 = \frac{1}{2}\int_0^T [x_1' P x_1 + \rho u_1^2]\, dt$.

P2: Starting from the zero initial state, choose the control u_2 of minimal energy $\mathcal{E}_{u_2} = \frac{\rho}{2}\int_0^T u_2^2\, dt$ in the closed loop system $\dot{x}_2 = (A - \frac{bb'}{\rho}S)x_2 + bu_2$, which reaches the final state $x_f - \Phi(T,0)x_i$.

P1 has solution

$$\dot{x}_1 = (A - \frac{bb'}{\rho}S)x_1, \quad x_1(0) = x_i \tag{76}$$

because $u_1 = -\frac{1}{\rho}b'Sx_1$. The performance index is $J_1 = \frac{1}{2}x_i' S(0) x_i$. Similarly, **P2** has solution

$$\dot{x}_2 = (A - \frac{bb'}{\rho}S)x_2 + bb'\Phi'(T,t)\mathcal{R}_T^{-1}[x_f - \Phi(T,0)x_i] \tag{77}$$

with $x_2(0) = 0$ and gives the input energy

$$\mathcal{E}_{u_2} = \frac{\rho}{2}[x_f - \Phi(T,0)x_i]'\, \mathcal{R}_T^{-1}\, [x_f - \Phi(T,0)x_i],$$

where $\mathcal{R}_T = \int_0^T \Phi(T,t)bb'\Phi'(T,t)\, dt$ is the reachability gramian.

Define now a new state variable $x = x_1 + x_2$, then

$$\dot{x} = (A - \frac{bb'}{\rho}S)x + bb'\Phi'(T,t)\mathcal{R}_T^{-1}[x_f - \Phi(T,0)x_i] \tag{78}$$

from (252) and (77), and the boundary conditions are $x(0) = x_i$, $x(T) = x_f$, respectively. From the uniqueness theorem of ordinary differential equations (ODE), this state equation with its boundary conditions has exactly the same solution as the terminal controller problem because $\mathcal{R}_T = -\rho\Omega(T)$.

The performance index for the combined problem is the "superposition" of x_1 and x_2, where $u = u_1 + u_2 - \frac{b'S}{\rho}x_2$ is the total input to the open-loop system $\dot{x} = Ax + bu$.

Thus,

$$J = \frac{1}{2}\int_0^T (x_1' + x_2')P(x_1 + x_2) + \rho u^2\, dt. \tag{79}$$

By expanding (79) and using the results above, this implies a "correlation-like" identity

$$\rho\int_0^T u_1 u_2\, dt = \int_0^T [x_1', u_1]\begin{bmatrix} P & -Sb \\ -b'S & \rho \end{bmatrix}\begin{bmatrix} x_2 \\ u_2 \end{bmatrix} dt, \tag{80}$$

which has the interpretation of an "interference".

4.1.4 Infinite Time LQ problem

In this section, we will study the asymptotic behavior of the terminal controller problem. Recall from the introduction that for the *terminal controller* to be well posed, it is required that the system is reachable. We will show, through an example, that more conditions are needed for the asymptotic terminal controller to be meaningful.

4.1.4.1 An illustrative Example

Consider the one dimensional system, $\dot{x} = u$. It is desired to

$$\min_u J_T = \int_0^T \rho u^2\, dt,$$

subjected to $x(0) = x_0$ and $x(T) = x_f$. This is, in fact, a minimum energy problem. The Hamiltonian matrix is

$$\mathbf{H} = \begin{bmatrix} 0 & -\frac{1}{\rho} \\ 0 & 0 \end{bmatrix},$$

which has two zero eigenvalues at the origin. Obviously, this system is not observable because the pair $\mathcal{O}(P^{1/2}, A) = 0$, where $P = 0$. The system is, however, reachable. The reachability grammian (39) is $W(0,T) = \int_0^T d\sigma = T$ because the transition

matrix is $\Phi(t,\tau) = 1$. The optimal input (49) is $u(t) = -\frac{1}{T}(x_0 - x_f)$, and the state is $x(t) = -\frac{1}{T}(x_0 - x_f)t + x_0$. The optimal cost easily follows:

$$J_T = \int_0^T \rho \frac{1}{T^2}(x_0 - x_f)^2 \, dt = \rho \frac{1}{T}(x_0 - x_f)^2.$$

Therefore, $\lim_{T\to\infty} J_T = 0$. This implies that there is no energy expended in transferring from x_i to x_f! Notice, however, that

$$\int_0^T x^2(t) \, dt \;\; = \;\; \frac{(x_0 - x_f)^2 T}{3} - \frac{(x_0 - x_f)x_0 T}{2} + x_0^2 T,$$

and $\lim_{T\to\infty} \int_0^T x^2(t) \, dt = \infty$. The energy in the state variable x is unbounded even though the optimal cost is zero! To avoid the energy of the state to become unbounded as $T \to \infty$, the additional requirement is that the system be observable. The idea is that, by requiring observability, the influence of the state will be present in the performance index. Thus, the infinite time *terminal controller* problem requires the same conditions as the *regulator* problem for it to be well posed.

Remark 4.1.1. *It is instructive to investigate what truly happens with the state and input in the previous example. For a fixed horizon* $[0, T]$ *the state is a straight line starting from* x_0 *and ending in* x_f*, and the input is a horizontal line scaled by* $\frac{1}{T}$*. As* $T \to \infty$ *the state* $x(t)$ *approaches a horizontal line* $x(t) = x_0$ *and the input approaches* $u(t) \equiv 0$*. In other words, when the horizon or* T *is increases, all final states* x_f *looks essentially the same as the initial state* x_0*. Therefore, there is no input needed for the transfer (*$u(t) \equiv 0$*). This is consistent with the interpretation that the transfer is quasi-static. Indeed, as* T *get larger and larger, the transfer is slower. In the limit it appears that the system stays at the initial state* x_0 *because there is a infinite transfer time.*

In the following, we exploit the decomposition of the terminal controller problem into its symmetric components. This will allow us to obtain the optimal performance index in terms of the state, costate variables and its boundary conditions, which will be essential in the infinite terminal controller problem. To prepare for the decomposition, we will first prove two important lemma's.

Let $\mathbf{H}$ be the Hamiltonian matrix and $\lambda \in \mathtt{spec}\,\mathbf{H}$, the spectrum of $\mathbf{H}$. Define

$$\cosh(\mathbf{H}) = \frac{1}{2}\left(e^{\mathbf{H}} + e^{-\mathbf{H}}\right) \quad \text{and} \quad \sinh(\mathbf{H}) = \frac{1}{2}\left(e^{\mathbf{H}} - e^{-\mathbf{H}}\right). \tag{81}$$

Lemma 4.1.1. $\sinh \mathbf{H}$ *is invertible if and only if* $\lambda \neq j\pi k$, $k \in \mathbb{Z}$.

Proof. To prove necessity, we assume $\sinh \mathbf{H}$ is not invertible and $\lambda \neq j\pi k$. Then there exists a $x \neq 0$ such that $(\sinh \mathbf{H})x = 0$. This implies that $(\exp -\mathbf{H})(\exp 2\mathbf{H} - I)x = 0$. Thus, $(\exp 2\mathbf{H})x = x$. Since $\lambda \in \mathtt{spec}\,\mathbf{H}$, $\mathrm{e}^{2\lambda}$ is the eigenvalue of $\exp 2\mathbf{H}$. Hence, $\mathrm{e}^{2\lambda} = 1 = \mathrm{e}^{\mathrm{j}2\pi\mathrm{k}}$. This implies $\lambda = j\pi k$, which is a contradiction. Therefore, we have shown that if $\lambda \neq j\pi k$, $\sinh \mathbf{H}$ is invertible.

To prove sufficiency, we assume that $\sinh \mathbf{H}$ is invertible and want to show that $\lambda \neq j\pi k$. Let (λ, x) be an eigen-pair of $\mathbf{H}$. Then $\mathrm{e}^{\mathbf{H}}\mathrm{x} = \mathrm{e}^{\lambda}\mathrm{x}$ and $\mathrm{e}^{-\mathbf{H}}\mathrm{x} = \mathrm{e}^{-\lambda}\mathrm{x}$. Therefore, $\sinh \mathbf{H}\, x = \frac{1}{2}(\mathrm{e}^{\mathbf{H}} - \mathrm{e}^{-\mathbf{H}})\mathrm{x} = \frac{1}{2}(\mathrm{e}^{\lambda} - \mathrm{e}^{-\lambda})\mathrm{x} = \sinh \lambda \mathrm{x}$. In other words, $\sinh \lambda \in \mathtt{spec}\ \sinh \mathbf{H}$. Thus, $\sinh \lambda \neq 0$ because $\sinh \mathbf{H}$ is invertible. That implies $\lambda \neq j\pi k$ because $\mathrm{e}^{-\lambda}(\mathrm{e}^{2\lambda} - 1) \neq 0$. ∎

A similar argument as in the previous lemma will proof the following.

Lemma 4.1.2. $\cosh \mathbf{H}$ *is invertible if and only if* $\lambda \neq j(\frac{\pi}{2} + \pi k)$, $k \in \mathbb{Z}$.

We also need a property of the Hamiltonian matrix $\mathbf{H}$. From [33, p.139] the following is known.

Lemma 4.1.3. $\mathbf{H}$ *has eigenvalues with zero real part if and only if they are also eigenvalues of the unobservable and/or unreachable part of* (A, b, c).

Hence, we have the following for a minimal realization:

Lemma 4.1.4. *If* (A, b, c) *is minimal (i.e.* (A, b) *is reachable and* (c, A) *is observable), then* $\mathbf{H}$ *has no eigenvalues on the imaginary axis.*

Combining the previous three lemma's, we obtain the following proposition.

Proposition 4.1.2. *If* (A, b, c) *is minimal, then* $\sinh(\mathbf{H}t)$ *and* $\cosh(\mathbf{H}t)$ *are invertible for all* $t \neq 0$.

Observe that from lemma (4.1.3) that $\mathbf{H}$ might still be invertible as long as the eigenvalues on the imaginary axis are not unobservable and/or unreachable.

4.1.5 Symmetrization

In this section, we decompose the LQ problem into its symmetric components. For notational simplicity, we shall time-shift the optimal control problem to the symmetric interval $[-T/2, T/2]$ and refer to this LQ problem as the *Symmetrical LQ Problem*. We assume that the system is both reachable and observable for the infinite LQ problem to be meaningful.

We introduce the operators $\mathbf{D}$ for differentiation with respect to time and $\mathbf{R}$ for the *parity* operator, i.e., $\mathbf{R}x(t) = x(-t)$. These operators anti-commute,

$$\mathbf{DR} = -\mathbf{RD}.$$

For simplicity, let $[\ x \quad \lambda\ ]' = \eta$, and note that $\mathbf{D}\eta = \mathbf{H}\eta$ and $\mathbf{DR}\eta = -\mathbf{RD}\eta = -\mathbf{HR}\eta$.

We introduce further the odd and even operators:

$$\mathcal{O} = \frac{1}{2}(\mathbf{I} - \mathbf{R}) \text{ and } \mathcal{E} = \frac{1}{2}(\mathbf{I} + \mathbf{R}).$$

Then

$$\begin{aligned} \mathbf{D}\mathcal{E}\eta &= \frac{1}{2}(\mathbf{D} + \mathbf{DR})\eta \\ &= \frac{1}{2}\mathbf{H}(\mathbf{I} - \mathbf{R})\eta \\ &= \mathbf{H}\mathcal{O}\eta \\ \mathbf{D}\mathcal{O}\eta &= \mathbf{H}\mathcal{E}\eta, \end{aligned}$$

and thus both $\mathcal{E}\eta$ and $\mathcal{O}\eta$ are solutions to the second order equation $(\mathbf{D}^2 - \mathbf{H}^2)\xi = 0$. The general solution to the above second order system is

$$\eta = \cosh \mathbf{H}t\, C_1 + \sinh \mathbf{H}t\, C_2.$$

However, let us not forget that the solution for $\mathcal{E}\eta$ and $\mathcal{O}\eta$ must respectively be even and odd. Hence,

$$\mathcal{E}\eta = \cosh \mathbf{H}t \ \ \mathcal{E}\eta_0 \text{ and } \mathcal{O}\eta = \sinh \mathbf{H}t \ \ \mathcal{O}\eta_0.$$

Since

$$\mathcal{E}\eta(\frac{T}{2}) = \cosh \mathbf{H}\frac{T}{2} \ \ \mathcal{E}\eta_0 \text{ and } \mathcal{O}\eta(\frac{T}{2}) = \sinh \mathbf{H}\frac{T}{2} \ \ \mathcal{O}\eta_0,$$

we get

$$\begin{aligned} \mathcal{E}\eta_t &= \cosh \mathbf{H}t \ \left[\cosh\left(\mathbf{H}\frac{T}{2}\right)\right]^{-1} \ \mathcal{E}\eta_{T/2}, \\ \mathcal{O}\eta_t &= \sinh \mathbf{H}t \ \left[\sinh\left(\mathbf{H}\frac{T}{2}\right)\right]^{-1} \ \mathcal{O}\eta_{T/2}. \end{aligned}$$

These inverses exist because of theorem (4.1.2). Finally, the initial and final conditions of the states, but not of the costates, are specified. These can, however, be eliminated from the equation relating $\mathcal{E}\eta$ to $\mathcal{O}\eta$. Indeed,

$$\mathbf{D}\mathcal{E}\eta = \mathbf{H}\sinh\mathbf{H}t\ \cosh^{-1}\mathbf{H}\frac{T}{2}\ \mathcal{E}\eta,$$

and this is equal to

$$\mathbf{H}\mathcal{O}\eta = \mathbf{H}\sinh\mathbf{H}t\ \sinh^{-1}\mathbf{H}\frac{T}{2}\ \mathcal{O}\eta.$$

This necessitates, therefore, the relation

$$\cosh^{-1}\left(\mathbf{H}\frac{T}{2}\right)\ \mathcal{E}\eta_{\frac{T}{2}} = \sinh^{-1}\left(\mathbf{H}\frac{T}{2}\right)\ \mathcal{O}\eta_{\frac{T}{2}}.$$

Equivalently,

$$\sinh\left(\mathbf{H}\frac{T}{2}\right)\ \begin{bmatrix} x_f + x_i \\ \lambda_f + \lambda_i \end{bmatrix} = \cosh\left(\mathbf{H}\frac{T}{2}\right)\ \begin{bmatrix} x_f - x_i \\ \lambda_f - \lambda_i \end{bmatrix}.$$

We summarize now:

Theorem 4.1.1. *The symmetrical optimal LQ control problem for a transfer from initial state x_i to a final state x_f has the solution*

$$\sinh\left(\mathbf{H}\frac{T}{2}\right)\ \begin{bmatrix} \mathcal{O}x(t) \\ \mathcal{O}\lambda(t) \end{bmatrix} = \sinh\left(\mathbf{H}t\right)\ \begin{bmatrix} \frac{1}{2}(x_f - x_i) \\ \frac{1}{2}(\lambda_f - \lambda_i) \end{bmatrix}, \tag{82}$$

$$\cosh\left(\mathbf{H}\frac{T}{2}\right)\ \begin{bmatrix} \mathcal{E}x(t) \\ \mathcal{E}\lambda(t) \end{bmatrix} = \cosh\left(\mathbf{H}t\right)\ \begin{bmatrix} \frac{1}{2}(x_f + x_i) \\ \frac{1}{2}(\lambda_f + \lambda_i) \end{bmatrix}, \tag{83}$$

with the constraint

$$\sinh\left(\mathbf{H}\frac{T}{2}\right)\ \begin{bmatrix} x_f + x_i \\ \lambda_f + \lambda_i \end{bmatrix} = \cosh\left(\mathbf{H}\frac{T}{2}\right)\ \begin{bmatrix} x_f - x_i \\ \lambda_f - \lambda_i \end{bmatrix}. \tag{84}$$

It is clear from the previous theorem that as $T \to \infty$, while t being kept finite i.e., $t < T/2$, both the state and costate, hence the control, converge to zero. However, this does not imply that the performance index converges to zero as we shall discover in the next section.

First, we prove a useful result, which aids the computation of the hyperbolic matrix functions.

Theorem 4.1.2. *The* cosh *and* sinh *transition matrices may be computed in the Laplace domain as*

$$\cosh \mathbf{H}t = \mathcal{L}^{-1}\left\{s(s^2\mathbf{I} - \mathbf{H}^2)^{-1}\right\} \tag{85}$$

$$\sinh \mathbf{H}t = \mathcal{L}^{-1}\left\{\mathbf{H}(s^2\mathbf{I} - \mathbf{H}^2)^{-1}\right\} \tag{86}$$

Proof. We prove the formula for sinh. The cosh formula is analogous.

$$\begin{aligned}
\sinh \mathbf{H}t &= \frac{1}{2}\mathcal{L}^{-1}\left[(sI - \mathbf{H})^{-1} - (sI + \mathbf{H})^{-1}\right] \\
&= \mathcal{L}^{-1}\left[\mathbf{H}(sI - \mathbf{H})^{-1}(sI + \mathbf{H})^{-1}\right] \\
&= \mathcal{L}^{-1}\left[\mathbf{H}(s^2I - \mathbf{H}^2)^{-1}\right]
\end{aligned}$$

Alternatively, the formula can also be proven from Dunford's Integral Theorem. ∎

The optimal control, being equal to $u(t) = -\frac{1}{\rho}b'\lambda$, can also be expressed in terms of the odd and even parts of the costate vector. This is shown in the following section.

4.1.6 Performance Index

The performance index follows from

$$\begin{aligned} J &= \frac{1}{2}\int_{-T/2}^{T/2} \xi'(t)Q\xi(t)\,dt, \\ &= \frac{1}{2}\int_{0}^{T/2} \left[\xi'(t)\mathbf{R}'Q\mathbf{R}\xi(t) + \xi'(t)Q\xi(t)\right]\,dt, \end{aligned}$$

where $\mathbf{R}'$ is assumed to act to the left and

$$Q = \begin{bmatrix} P & 0 \\ 0 & \rho \end{bmatrix}.$$

Note also that

$$\begin{aligned} \xi'\mathbf{R}'Q\mathbf{R}\xi + \xi'Q\xi &= \frac{1}{2}\left(\xi'(\mathbf{I}+\mathbf{R})'Q(\mathbf{I}+\mathbf{R})\xi + \xi'(\mathbf{I}-\mathbf{R})'Q(\mathbf{I}-\mathbf{R})\xi\right) \\ &= 2\left(\xi'\mathcal{E}'Q\mathcal{E}\xi + \xi'\mathcal{O}'Q\mathcal{O}\xi\right), \end{aligned}$$

and this yields then

$$J = \int_0^{T/2} (\mathcal{E}\xi)'Q(\mathcal{E}\xi)\,dt + \int_0^{T/2} (\mathcal{O}\xi)'Q(\mathcal{O}\xi)\,dt.$$

The advantage of this form is that the boundary conditions now involve both the initial and the final states, x_i and x_f, respectively. Specifically, with $\mathcal{O}u = \frac{1}{\rho}b'\mathcal{O}\lambda$ and $\mathcal{E}u = \frac{1}{\rho}b'\mathcal{E}\lambda$, we get

$$\xi'Q\xi = [x', u'] \begin{bmatrix} P & 0 \\ 0 & \rho \end{bmatrix} \begin{bmatrix} x \\ u \end{bmatrix} = [x', \lambda'] \begin{bmatrix} P & 0 \\ 0 & \frac{1}{\rho}bb' \end{bmatrix} \begin{bmatrix} x \\ \lambda \end{bmatrix},$$

and thus

$$J = \int_0^{T/2} [(\mathcal{E}x)'P(\mathcal{E}x) + \frac{1}{\rho}(\mathcal{E}\lambda)'bb'(\mathcal{E}\lambda)]\,dt + \int_0^{T/2} [(\mathcal{O}x)'P(\mathcal{O}x) + \frac{1}{\rho}(\mathcal{O}\lambda)'bb'(\mathcal{O}\lambda)]\,dt.$$

We summarize the previous analysis in the following theorem:

Theorem 4.1.3. *The optimal performance index, J, equals*

$$J = \frac{1}{4}[x_f' + x_i', \lambda_f' + \lambda_i'] \left[\cosh\left(\mathbf{H}'\frac{T}{2}\right)\right]^{-1} \mathbf{Ch}(T) \left[\cosh\left(\mathbf{H}\frac{T}{2}\right)\right]^{-1} \begin{bmatrix} x_f + x_i \\ \lambda_f + \lambda_i \end{bmatrix} +$$

$$+ \quad \frac{1}{4}[x_f' - x_i', \lambda_f' - \lambda_i'] \left[\sinh\left(\mathbf{H}'\frac{T}{2}\right)\right]^{-1} \mathbf{Sh}(T) \left[\sinh\left(\mathbf{H}\frac{T}{2}\right)\right]^{-1} \begin{bmatrix} x_f - x_i \\ \lambda_f - \lambda_i \end{bmatrix},$$

where the sinh- and cosh- integrals are defined by

$$\mathbf{Sh}(T) = \int_0^{T/2} \sinh(\mathbf{H}'t) \begin{bmatrix} P & \\ & \frac{1}{\rho}bb' \end{bmatrix} \sinh(\mathbf{H}t)\, dt$$

$$\mathbf{Ch}(T) = \int_0^{T/2} \cosh(\mathbf{H}'t) \begin{bmatrix} P & \\ & \frac{1}{\rho}bb' \end{bmatrix} \cosh(\mathbf{H}t)\, dt$$

Whereas the integrals **Sh** and **Ch** diverge as $T \to \infty$, the products

$$\left[\cosh\left(\mathbf{H}'\frac{T}{2}\right)\right]^{-1} \mathbf{Ch}(T) \left[\cosh\left(\mathbf{H}\frac{T}{2}\right)\right]^{-1}$$

and

$$\left[\sinh\left(\mathbf{H}'\frac{T}{2}\right)\right]^{-1} \mathbf{Sh}(T) \left[\sinh\left(\mathbf{H}\frac{T}{2}\right)\right]^{-1}$$

remain bounded as shown in appendix B.

We summarize the previous analysis in the theorem below.

Theorem 4.1.4. *The terminal controller which is also observable has a finite and nonzero optimal performance index as $T \to \infty$.*

4.1.7 Interpretation of infinite time LQ-problem.

In this section, we discuss the solution for the *infinite* LQ problem. It is clear that, for the optimal performance index to be bounded, both the control and the state should

converge to zero over an infinite time interval. Indeed, if either the state or the control does not converge to zero over an unbounded interval, then there exists a real number $c > 0$ such that either $x'Px > c > 0$ or $\rho u^2 > c > 0$ over an infinite interval. This implies the optimal performance index over the infinite interval is unbounded. This contradicts the boundedness of the optimal performance index. This may seem contradictory: if both the state and the control are zero over an infinite interval, then there could *not* be a state transfer from x_i to x_f! The truth is that the input brings the state from x_i to the zero at $t = -\infty$ as fast as possible. Both the state and the control stay at zero for a very long time until the input brings the state back to x_f at $t = \infty$.

Another way to see this is to compactify the infinite time axis into a circle. The input drives the state to zero at one end, where the state and input become increasingly more violent as T increases. In general, as T increases, both the control and

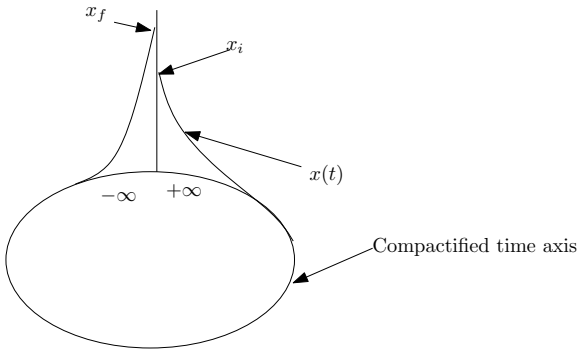

Figure 21: Compactified time interval for infinite LQ problem

the state become more "violent" at $t = -T/2$ and $t = T/2$ as shown in the examples below.

4.1.8 Examples

4.1.8.1 Example 1: Infinite time terminal controller.

We solve the two point boundary value problem associated with the control of the system $\dot{x} = x + u$ with the performance index $J_T = \frac{1}{2}\int_{-T/2}^{T/2}(x^2 + \rho u^2)\,dt$.

Introducing a new parameter $\omega = \sqrt{\frac{1+\rho}{\rho}}$, one easily finds the optimal trajectory $x(t)$:

$$x(t) = \frac{\left[-e^{1/2\,\omega\,(T+2\,t)} + e^{-1/2\,\omega\,(T+2\,t)}\right] x_f + \left[-e^{-1/2\,\omega\,(2\,t-T)} + e^{1/2\,\omega\,(2\,t-T)}\right] x_i}{-e^{\omega\,T} + e^{-\omega\,T}}.$$

Its even and odd parts are

$$\begin{aligned}\mathcal{E}x(t) &= \frac{1}{2}\,\frac{e^{-\omega\,t}x_i + e^{\omega\,t}x_f + e^{\omega\,t}x_i + e^{-\omega\,t}x_f}{e^{-1/2\,\omega\,T} + e^{1/2\,\omega\,T}},\\ \mathcal{O}x(t) &= -\frac{1}{2}\,\frac{-e^{\omega\,t}x_i + e^{\omega\,t}x_f - e^{-\omega\,t}x_f + e^{-\omega\,t}x_i}{e^{-1/2\,\omega\,T} - e^{1/2\,\omega\,T}},\end{aligned}$$

respectively. Figure (22) shows a plot of these functions.

After introducing a relative time $\tau = \frac{2t}{T}$ and setting $\frac{\omega T}{2} = \kappa$, we have

$$\mathcal{E}x(\tau) = \frac{1}{2}\,\frac{(x_i + x_f)\cosh(\kappa\,\tau)}{\cosh(\kappa)} \quad \text{and} \quad \mathcal{O}x(\tau) = \frac{1}{2}\,\frac{(x_f - x_i)\sinh(\kappa\,\tau)}{\sinh(\kappa)}$$

in the interval $\tau \in (0, 1)$. The performance index at the optimum evaluates to

$$J_T = \frac{1}{2}\frac{N(x_i, x_f, \omega, T)}{(\omega^2 - 1)\sinh(\omega\,T)}, \tag{87}$$

where the numerator N is

$$\begin{aligned}N(x_i, x_f, \omega, T) &= \left({x_i}^2 + {x_f}^2\right)\cosh(\omega\,T)\,\omega - \sinh(\omega\,T)\left({x_f}^2 - {x_i}^2\right) - 2\,x_i\,x_f\,\omega.\\ &= \left((x_f - x_i)\cosh(\frac{\omega T}{2}) - (x_f + x_i)\sinh(\frac{\omega T}{2})\right)^2.\end{aligned}$$

Clearly, in the limit $T \to \infty$ both $\mathcal{E}x$ and $\mathcal{O}x$ tend to zero while the performance index converges to the nonzero value

$$J_\infty = \frac{1}{2}\frac{(x_i{}^2 + x_f{}^2)\,\omega - (x_f{}^2 - x_i{}^2)}{(\omega^2 - 1)}. \tag{88}$$

Figure (23) shows the optimal solution $x(t)$ for various values of T. The time axis has been normalized to aid comparison. It is clear that the transfer at both ends become more aggressive as the horizon increases.

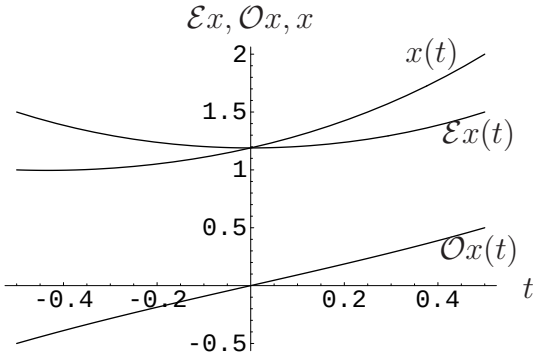

Figure 22: Example 1: Terminal controller with $x_i = 1, x_f = 2$ for $T = 1$

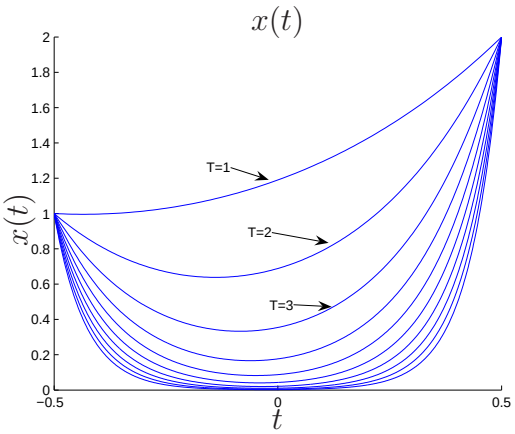

Figure 23: Example 1: Comparison of $x(t)$ for various T

4.1.8.2 Example 2: Quasi-static transfer

In this section, we consider a quasi-static transfer problem. It involves the transfer from one equilibrium (u_i, x_i) to another equilibrium (u_f, x_f) for the stable system

$$\dot{x} = -x + u. \tag{89}$$

The equilibria consist of the line $x = u$. The objective is to minimize the performance index

$$J_T = \frac{1}{2}\int_{-T/2}^{T/2} \dot{x}^2 + \rho \dot{u}^2 \, dt, \tag{90}$$

which is a measure of non-stationarity. As shown in Figure (24), the pair (u, x) converges to the line $x = u$ as $T \to \infty$. We turn this problem in the standard LQ

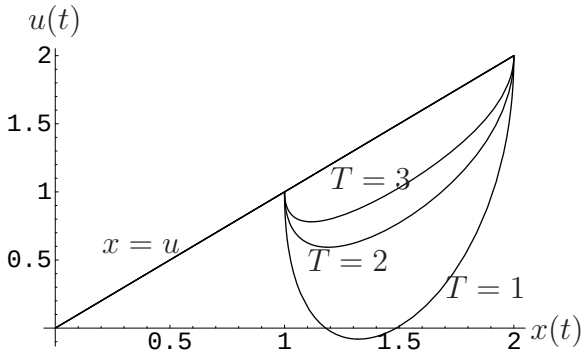

Figure 24: Quasi-static transfer: $x_i = 1, x_f = 2$ for $T = 1, T = 2, T = 3$

form by extending the state equation (89) to

$$\frac{d}{dt}\begin{bmatrix} x \\ u \end{bmatrix} = \begin{bmatrix} -1 & 1 \\ 0 & 0 \end{bmatrix}\begin{bmatrix} x \\ u \end{bmatrix} + \begin{bmatrix} 0 \\ 1 \end{bmatrix} v. \tag{91}$$

The performance index in (89) becomes $J_T = \frac{1}{2}\int_{-T/2}^{T/2} || - x + u||^2 + \rho v^2 \, dt$. The Hamiltonian is $H = \frac{1}{2}\rho v^2 + \frac{1}{2}|| - x + u||^2 + \lambda_x'(-x+u) + \lambda_u v$. The Hamiltonian system

is

$$\frac{d}{dt}\left[\begin{array}{c} x \\ u \\ \hline \lambda_x \\ \lambda_u \end{array}\right] = \underbrace{\left[\begin{array}{cc|cc} -1 & 1 & 0 & 0 \\ 0 & 0 & 0 & -\frac{1}{\rho} \\ \hline -1 & 1 & 1 & 0 \\ 1 & -1 & -1 & 0 \end{array}\right]}_{\mathbf{H}} \left[\begin{array}{c} x \\ u \\ \hline \lambda_x \\ \lambda_u \end{array}\right] \tag{92}$$

with the boundary condition

$$\left[\begin{array}{cc|cc} x' & u & \lambda_x' & \lambda_u \end{array}\right]'_{t=\frac{T}{2}} = \left[\begin{array}{cc|cc} x_f' & u_f & \nu_x & \nu_u \end{array}\right]', \tag{93}$$

where ν_x and ν_u are parameters to be determined. Let the transition matrix of (92) be partitioned into

$$\Phi(t,\tau) = \left[\begin{array}{cc} \Phi_{11}(t,\tau) & \Phi_{12}(t,\tau) \\ \Phi_{21}(t,\tau) & \Phi_{22}(t,\tau) \end{array}\right]. \tag{94}$$

Then from (92) and (93) the unknown parameters ν_x and ν_u are

$$\left[\begin{array}{c} \nu_x \\ \nu_u \end{array}\right] = \Phi_{12}^{-1}\left(\frac{T}{2}, -\frac{T}{2}\right)\left[\left[\begin{array}{c} x_f \\ u_f \end{array}\right] - \Phi_{11}\left(\frac{T}{2}, -\frac{T}{2}\right)\left[\begin{array}{c} x_i \\ u_i \end{array}\right]\right] \tag{95}$$

The characteristic polynomial of the Hamiltonian matrix $\mathbf{H}$ is

$$a(s) = \det(sI - \mathbf{H}) = s^2(s^2 - 1 - \frac{1}{\rho}). \tag{96}$$

It has two zeros at the origin of the complex plane and $s = \pm\sqrt{1+\frac{1}{\rho}}$. The zero eigenvalues at the origin imply that the extended state system (91) is not minimal from lemma (4.1.4). Indeed, for this problem the system is not observable because any shift in the state variable $x(t)$ by a constant will be differentiated away in the

performance index (90). Therefore, it is not guaranteed that the infinite time limit of this quasi-static transfer problem will produce a bounded state $x(t)$.

After a tedious computation one could in fact show that the optimal cost J_T in (90) with $r = 1$ is

$$J_T = \frac{2}{T - \sqrt{2}\tanh\frac{T}{\sqrt{2}}}. \tag{97}$$

which decays monotonically to zero as $T \to 0$. This justifies our intuition that less effort is needed for a quasi-stationary process as the control horizon increases.

The technique in the quasi-static transfer problem has been successfully applied in [31] to solve a leader based coordination problem: the autonomous sheep herding problem. The problem involves the movement of a group of herding dogs in order to maneuver the herd in the desired way. It is shown in [31] that the dynamics is $\dot{x} = Ax + bu$, and the performance index is

$$J = \frac{1}{2}\int_0^T \dot{x}'P\dot{x} + \dot{u}'Q\dot{u}\ dt, \tag{98}$$

which is equivalent to the previous quasi-static problem.

4.2 Quasi-stationary LQ problem

In this section we take a more in-depth look at the quasi-stationary problem. By introducing $\dot{u} = v$ in (98) we obtain a standard LQ problem

$$J_T = \int_0^T ||\dot{x}||^2 + \rho v^2\ dt \tag{99}$$

subject to the dynamics

$$\begin{aligned} \dot{x} &= Ax + bu \\ \dot{u} &= v, \end{aligned} \tag{100}$$

while retaining static boundary conditions $(x,u)_i$ and $(x,u)_f$ on the subspace $Ax + bu = 0$, where A is Hurwitz.

Denote

$$\tilde{A} = \begin{bmatrix} A & b \\ 0 & 0 \end{bmatrix}, \tag{101}$$

the state transition matrix of (100) is

$$e^{\tilde{A}t} = \begin{bmatrix} e^{At} & \frac{(e^{At}-I)A^{-1}b}{t} \\ 0 & t \end{bmatrix}.$$

This is easily obtained by observing that $\tilde{A}^k = \begin{bmatrix} A^k & A^{k-1}b \\ 0 & 0 \end{bmatrix}$ and that the $(1,2)$ element of the expansion $I + \tilde{A}t + \tilde{A}^2\frac{t^2}{2!} + \tilde{A}^3\frac{t^3}{3!} + \dots$ is

$$\begin{aligned} \left[e^{\tilde{A}t}\right]_{(1,2)} &= b + Ab\frac{t}{2!} + A^2b\frac{t^2}{3!} + \dots \\ &= \left(-I + I + At + A^2\frac{t^2}{2!} + A^3\frac{t^3}{3!} + \dots\right)\frac{A^{-1}b}{t} \\ &= \frac{1}{t}\left(e^{At} - I\right)A^{-1}b \end{aligned}$$

Proposition 4.2.1. *If (A,B) is reachable, then the system in (100) is also reachable.*

Proof. If (A,B) is reachable, then

$$\operatorname{rank}\left[\begin{array}{c|c} sI - A & b \end{array}\right] = n,$$

for all $s \in \mathbb{C}$ from the PBH test. This implies that

$$\operatorname{rank}\left[\begin{array}{cc|c} sI - A & b & 0 \\ 0 & s & 1 \end{array}\right] = n + 1, \tag{102}$$

for all $s \in \mathbb{C}$. From the PBH test again, the system in (100) is reachable. ∎

In the simple scalar example in the previous section we saw that the optimal cost J_T in (97) decays to zero. This is in general the case for any n dimensional systems. Observe that J_T is invariant when x and u are shifted by a constant. This shows that the state (x, u) is not observable in J_T. We have the following for the optimal cost J_T.

Proposition 4.2.2. *The optimal cost J_T in* (99) *decays to zero as $T \to 0$.*

Proof. We construct a sub-optimal solution satisfying the boundary conditions such that $J_T \to 0$ as $T \to \infty$; the optimal solution, therefore, will decay to zero as well.

For simplicity of notation we will assume that $z = (x, u) \in \mathbb{R}^n$and that (100) has been transformed to the reachable canonical form without loss of generality;

$$\dot{z}(t) = \begin{bmatrix} -a_1 & -a_2 & -a_3 & \dots & -a_n \\ 1 & & & & \\ & 1 & & & \\ & & & 1 & 0 \end{bmatrix} z(t) + \begin{bmatrix} 1 \\ 0 \\ \vdots \\ 0 \end{bmatrix} u(t),\ t \in [0, 1]\,.$$

Since $z_i = (x_i, u_i), z_f = (x_f, u_f) \in \mathbb{R}^n$ are given and $2n$ boundary conditions need to be satisfied, we set the n^{th} component of z

$$z_n(t) \;=\; p_{2n-1}t^{2n-1} + p_{2n-2}t^{2n-2} + \ldots + p_1 t + p_0,\ t \in [0, 1].$$

From the dynamics we obtain

$$\begin{aligned} \dot{z}_n(t) &= z_{n-1}(t), \\ &= (2n-1)p_{2n-1}t^{2n-2} + (2n-2)p_{2n-2}t^{2n-3} + \ldots + 2p_2 t + p_1, \end{aligned}$$

$$
\begin{aligned}
\dot{z}_{n-1}(t) &= z_{n-2}(t) \\
&= (2n-1)(2n-2)p_{2n-1}t^{2n-3} + (2n-3)(2n-2)p_{2n-2}t^{2n-4} + \ldots + 2p_2, \\
&\vdots \\
\dot{z}_{n-(k-1)}(t) &= z_{n-k}(t) \\
&= (2n-1)(2n-2)\ldots(2n-k)p_{2n-1}t^{2n-1-k} \\
&\quad +(2n-2)(2n-3)\ldots(2n-1-k)p_{2n-2}t^{2n-2-k} + \ldots + k!p_k,
\end{aligned}
$$

for $k = 1, \ldots, n-1$, $t \in [0,1]$. Clearly, $z_n(0) = p_0$, $\dot{z}_n(0) = z_{n-1}(0) = p_1$, $\ddot{z}_n(0) = z_{n-2}(0) = 2p_2, \ldots$ etc. The first p_i, $i = 1, \ldots, n$ are easily found this way. Evaluating the previous set of equations at $t = 1$, we obtain n equations in the remaining n unknowns, which can be used to solve for the remaining coefficients.

We introduce a change of variable $t \to \frac{t}{T}$ we obtain a set of polynomials defined over $t \in [0, T]$:

$$
\begin{aligned}
z_n\left(\frac{t}{T}\right) &= p_{2n-1}\left(\frac{t}{T}\right)^{2n-1} + p_{2n-2}\left(\frac{t}{T}\right)^{2n-2} + \ldots + p_1\frac{t}{T} + p_0, \\
\dot{z}_n\left(\frac{t}{T}\right) &= z_{n-1}\left(\frac{t}{T}\right), \\
&= (2n-1)p_{2n-1}\frac{t^{2n-2}}{T^{2n-1}} + (2n-2)p_{2n-2}\frac{t^{2n-3}}{T^{2n-2}} + \ldots + 2p_2\frac{t}{T^2} + p_1\frac{1}{T}, \\
\dot{z}_{n-1}\left(\frac{t}{T}\right) &= z_{n-2}\left(\frac{t}{T}\right) \\
&= (2n-2)(2n-1)p_{2n-1}\frac{t^{2n-3}}{T^{2n-1}} + (2n-3)(2n-2)p_{2n-2}\frac{t^{2n-4}}{T^{2n-2}} + \ldots \\
&\quad +2p_2\frac{1}{T^2}, \\
&\vdots
\end{aligned}
$$

$$\begin{aligned}
\dot{z}_{n-(k-1)}\left(\frac{t}{T}\right) &= z_{n-k}\left(\frac{t}{T}\right) \\
&= (2n-1)(2n-2)\dots(2n-k)p_{2n-1}\frac{t^{2n-1-k}}{T^{2n-1}} \\
&\quad +(2n-2)(2n-3)\dots(2n-1-k)p_{2n-2}\frac{t^{2n-2-k}}{T^{2n-2}}+\dots+k!p_k\frac{1}{T^k},
\end{aligned}$$

for $k = 1, \dots, n-1$. In other words

$$\dot{z}_{n-r}\left(\frac{t}{T}\right) = \sum_{k=r+1}^{2n-1} \alpha_k^r \frac{t^{k-(r+1)}}{T^k},\ r = 0, \dots, n-1,$$

where the exact form of the coefficients α_k^r are not important for our purpose. Observe

$$\begin{aligned}
\int_0^T \frac{t^{s-(p+1)}}{T^s}\frac{t^{q-(r+1)}}{T^q} &= \int_0^T \frac{t^{s+q-(p+r+2)}}{T^{s+q}}dt, \\
&= \begin{cases} \frac{1}{s+q-(p+r+2)}T^{-(p+r+1)}, & s+q-(p+r+2)\neq 0 \\ T^{1-(s+q)}, & else \end{cases}
\end{aligned}$$

for $p, r = 0, \dots, n-1$, $s = p+1, \dots, 2n-1$, $q = r+1, \dots, 2n-1$, and since the first term in the performance index in (99) is a linear combination of the these terms, the integral $\int_0^T \|\dot{z}(t)\|^2\, dt$ decays to zero at a rate of $\frac{1}{T}$.

Taking the first derivative of the first equation in the dynamics we see that $\dot{u}$ is also a linear combination of the terms considered before and thus, decays to zero as $T \to \infty$. ∎

Proposition 4.2.3. *The performance index of the minimum energy control problem decays to zero as the horizon approaches infinity.*

Proof. Since $\inf \int_0^T \|\dot{u}(t)\|_R^2 dt \leq \int_0^T \|\dot{u}(t)\|_R^2 dt \leq \int_0^T \|\dot{x}(t)\|_P^2 + \|\dot{u}\|_R^2 dt$, we obtain $\inf \int_0^T \|\dot{u}(t)\|_R^2 dt \leq \inf \int_0^T \|\dot{x}(t)\|_P^2 + \|\dot{u}\|_R^2 dt$. ∎

The previous analysis begs the question as to why the optimal cost in the infinite time terminal controller (88) is bounded away from zero while that of the quasi-stationary problem decays to zero as $T \to \infty$. The answer lies in the observability of the state x in the performance indices. In the terminal controller the energy of any x enters J_T while any constant x will not contribute to the cost of the quasi-stationary problem. Observe that the suboptimal solution in the previous proposition approach a straight line with zero slope as $T \to \infty$.

The optimal control for the quasi-static problem cannot be obtained via the symmetrization method, because the zero eigenvalue of $\tilde{A}$ is unobservable in (99). This is easily seen from the PBH test applied to $\tilde{A}$ and $c = [A \;\; b]$:

$$\left[\begin{array}{cc} sI - A & -b \\ 0 & s \\ \hline A & b \end{array}\right].$$

For $s = 0$ the rank of the previous matrix fails to be $n+1$. From 4.1.3 the Hamiltonian matrix $\mathbf{H}$ is not invertible; and $\cosh(\mathbf{H}\frac{T}{2})(\ \sinh(\mathbf{H}\frac{T}{2}))$ are not invertible which is needed in the symmetrization method. To circumvent this problem we may replace $\tilde{A}$ in (101) with

$$\tilde{A}_\epsilon = \tilde{A} = \left[\begin{array}{cc} A & b \\ 0 & \epsilon \end{array}\right],$$

where $\epsilon > 0$ is small. The matrix

$$\left[\begin{array}{cc} sI - A & -b \\ 0 & s - \epsilon \\ \hline A & b \end{array}\right].$$

always has rank equal to $n+1$. If $s \neq \epsilon$, then the first $n+1$ rows are independent. If $s = \epsilon$, this matrix may be transformed into

$$\left[\begin{array}{cc} \epsilon I & 0 \\ 0 & 0 \\ \hline A & b \end{array}\right],$$

which has $n+1$ independent rows as $b \neq 0$. The pair $\left(\tilde{A}_\epsilon,\ [0_{1\times n},\ 1]'\right)$ is still reachable. With this modification we may now proceed to find the optimal control u_ϵ and state x_ϵ. Subsequently, by letting $\epsilon \to 0$ we obtain the desired x and u.

CHAPTER V

GLUSKABI RACCORDATION: AN INTRODUCTION

In this chapter we begin with the main theme in this thesis. The problem we consider involves the connection of two trajectories from a set with particular behavior. The objective is to make such a transition as inconspicuous as possible, in that such characteristic behavior should persist during the transition. Such particular behaviors classes can be stationary solutions, limit cycles, or more general classes. Specifically, assume a set $\mathcal{X}$, consisting of persistent behaviors defined over $\mathbb{R}$, is given.The objective is to connect two elements x_i and x_f in $\mathcal{X}$ with a 'smooth' path y such that $x_i(t) = y(t)$, $t \leq 0$ and $x_f(t) = y(t)$, $t \geq 1$. By a 'smooth' path we mean a path that locally resembles a member of a particular behavioral set $\mathcal{X}$. Therefore, it 'persists' in its behavior.

Why is such a construction of interest? One theory of articulated movements argues that arm motions follow a series of equilibrium postures [7], and motion is merely a transfer from one steady state to another through a quasi-static path. In our language, $\mathcal{X}$ is the set consisting of all equilibrium postures, and arm motion is a 'smooth' trajectory connecting two elements in $\mathcal{X}$. Quasi-static transitions in thermodynamics show the same flavor. In locomotion one is often interested in gait transitions. Golubitsky [24] studied the transition gaits of horses, which exhibit even more interesting transition behaviors.

The generation of 'smooth' trajectories is further of interest in certain robotics applications. In [22] the authors studied an autonomous puppetry control problem under the view point of hybrid systems. Various modes were defined so that the puppet is supplied with a rich class of behaviors. However, it is necessary to enrich this class of behaviors with *transition* modes such that the transition from one periodic motion to another is as smooth as possible to mimic human motion.

Finally, we mention an application in finite time thermodynamics [1]. A Carnot cycle consists of two adiabatic and two isothermal processes, and it is in general a very slow process. Furthermore, it is the most efficient cycle for converting a given amount of thermal energy into work. However, a device based the cycle cannot be built in practice. In order to approximate the cycle an ad-hoc solution based on stepwise transitions has been studied in [1]. This naturally raises the question as to how to design smoother transitions for a quasi-static transfer.

The framework of constructing 'smooth' or maximally pleasing trajectories will be called the Gluskabi raccordation. Raccordation comes from the French word 'raccorder' which means literally 'to connect'. The notion stems from a problem in civil engineering, where for instance two planes have to be connected by some smooth, easily constructed surface. A case in point is the connection of a vertical canal wall to a gently sloping river bank, by a maximally pleasing surface. If one considers maximally pleasing here to mean easily constructed, then such a raccordation is given by a piece of a hyperbolic paraboloid. This is a regular surface in the sense that through each point there are two straight lines lying completely in the surface. This means that one can simply construct a framework from straight beams and pour concrete

over it. Another example of a raccordation is found in hydraulics, where it is known as the coupling of two pipes of different diameter in such a way that minimal hydraulic potential is lost by the flow [59].

Gluskabi, on the other hand, is a mythical culture hero, and 'transformer' of the Wabanaki people. According to the myth, Gluskabi made himself from dust, and he has the ability to transform animals [47]. In our context he is the 'transformer' between elements in a smaller set (the set of stationary solutions, limit cycles etc) while the transition does not belong to this set.

To clarify what we mean by 'transforming things' let us first consider a simple example. Specifically, we will construct the Gluskabi raccordation of two second order polynomials. We will present two methods; the first method involves the kernel while the second method involves the image of an operator.

5.0.1 Polynomial raccordation: the direct method

Let $\mathbb{R}_3[t]$ be the set of 2^{nd} order polynomials of the form $p(t) = a_0 + a_1 t + a_2 t^2$. Any 2^{nd} order polynomial $p(t)$ satisfies

$$\mathcal{O}p = \mathbf{D}^3 p = 0.$$

Thus, $\mathbb{R}_3[t]$ is the kernel of $\mathcal{O}$.

The Gluskabi raccordation seeks a new polynomial, not necessarily in $\mathbb{R}_3[t]$, connecting two polynomials, p_i and p_f in $\mathbb{R}_3[t]$, that is as 'close' to $\mathbb{R}_3[t]$ as possible. A *direct* approach is to seek a p that minimizes the 'deviation' from $\mathbb{R}_3[t]$; this deviation

being the norm of the 'equation error':

$$\min_{p} \int_{-\infty}^{\infty} \| \left(\mathcal{O}p\right)(t)\|^2 dt = \int_{-\infty}^{\infty} \| \left(\mathbf{D}^3 p\right)(t)\|^2 \, dt$$
$$\text{subject to } p(t) = p_i(t), t \leq 0, \;\; p(t) = p_f(t), \; t \geq 1, \; p_i, p_f \in \mathbb{R}_3[t]. \qquad (103)$$

Let $\mathbf{D}^3 p = u$, $x_1 = p$, $x_2 = \dot{x}_1$, $x_3 = \dot{x}_2$ and $\mathcal{T} = [0, 1]$, we may transcribe the problem into the standard LQ form

$$\min_{u} \int_{0}^{1} \|u\|^2 \, dt \qquad (104)$$

with the dynamics

$$\frac{d}{dt} \begin{bmatrix} x_1 \\ x_2 \\ x_3 \end{bmatrix} = \begin{bmatrix} 0 & 1 & 0 \\ 0 & 0 & 1 \\ 0 & 0 & 0 \end{bmatrix} \begin{bmatrix} x_1 \\ x_2 \\ x_3 \end{bmatrix} + \begin{bmatrix} 0 \\ 0 \\ 1 \end{bmatrix} u$$

and the boundary conditions

$$x(0^-) = \begin{bmatrix} p_i(0^-) \\ \dot{p}_i(0^-) \\ \ddot{p}_i(0^-) \end{bmatrix} = \begin{bmatrix} p_i^0 \\ p_i^1 \\ 2p_i^2 \end{bmatrix} \text{ and } x(1) = \begin{bmatrix} p_f(1) \\ \dot{p}_f(1) \\ \ddot{p}_f(1) \end{bmatrix} = \begin{bmatrix} p_f^0 + p_f^1 + p_f^2 \\ 2p_f^2 + p_f^1 \\ 2p_f^2, \end{bmatrix},$$

where $p_i(t) = p_i^2 t^2 + p_i^1 t + p_i^0$ and $p_f(t) = p_f^2 t^2 + p_f^1 t + p_f^0$. This is a standard terminal controller problem [12]. Observe that an impulse at $t = 0^-$ steering $x(t)$ from $x(0)$ at $t = 0^-$ to $x(1)$ at $t = 0^+$ is not an optimal solution since causes (103) to be unbounded.

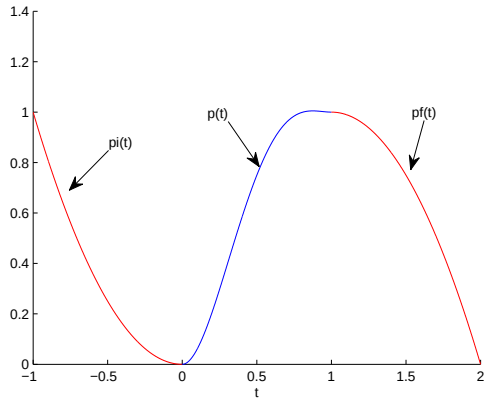

Figure 25: The Gluskabi raccordation of $R_3[t]$: direct method

From the standard LQ solution we obtain the raccordation

$$\begin{aligned} p(t) &= x_1(t) = p_0^i + p_1^i t + p_2^i t^2 + a_2 + a_3 t^3 + a_4 t^4 \qquad (105) \\ a_2 &= -3(p_2^i - p_2^f) - 6(p_1^i - p_1^f) - 10(p_0^i - p_0^f) \\ a_3 &= 3(p_2^i - p_2^f) + 8(p_1^i - p_1^f) + 15(p_0^i - p_0^f) \\ a_4 &= -(p_2^i - p_2^f) - 3(p_1^i - p_1^f) - 6(p_0^i - p_0^f). \end{aligned}$$

As an example, let us connect $p_i(t) = t^2$ to $p_f(t) = 2t - t^2$. Substituting the parameters into (105), we obtain the raccordation polynomial

$$p(t) = 7t^2 - 10t^3 + 4t^4,\ t \in [0,1]\,, \qquad (106)$$

that is 'closest' to $\mathbb{R}[t]$ in the sense of (103). Observe that the raccordation polynomial $p(t), t \in [0,1]$ is of degree 4. In Figure 25, the raccordation $p(t)$, $t \in [0,1]$ connecting $p_i(t)$, $t \in [-1,0]\,,$ and $p_f(t)$, $t \in [1,2]$ is shown.

Remark 5.0.1. *Observe that any $p \in \mathbb{R}_3[t]$ is also in the kernel of the operator $\mathcal{O} = q(\mathbf{D})\mathbf{D}^3$, where $q(\mathbf{D})$ is any polynomial in $\mathbf{D}$. However, $\mathbb{R}_3[t]$ is the null space*

of the minimal *degree polynomial* $\mathcal{O} = \mathbf{D}^3$. *We, therefore, call the representation of* $\mathbb{R}_3[t]$ *the* minimal *kernel representation of* $\mathcal{O} = \mathbf{D}^3$.

5.0.2 Polynomial raccordation: the indirect method

We now consider a different method of connecting two polynomials. A second order polynomial, $p(t) = a_0 + a_1 t + a_2 t^2 \in \mathbb{R}_3[t]$ or, equivalently, the null space of the operator $\mathcal{O} = \mathbf{D}^3$, may be parameterized by its coefficients:

$$\begin{aligned} \phi : \mathbb{R}_3[t] &\rightarrow \mathbb{R}^3 : \\ p(t) = a_0 + a_1 t + a_2 t^2 &\rightarrow [a_0, a_1, a_2] = \theta \end{aligned}$$

Thus, we associate a second order polynomial with a point in $\mathbb{R}^3$. Given two polynomials $p_{i,f} = p_2^{i,f} t^2 + p_1^{i,f} t + p_0^{i,f}$ with their coefficients $\theta^{i,f} = (p_0^{i,f}, p_1^{i,f}, p_2^{i,f}) \in \mathbb{R}^3$, what is now an appropriate measure of smoothness? The straight line with a uniform speed, $\theta^*(\alpha) = \theta^i(1-\alpha) + \theta^f \alpha$, $\alpha \in \mathcal{T} = [0, 1]$, clearly may be considered the smoothest path joining the two sets of parameters. In fact it can easily be shown that this solution minimizes the energy of the path

$$\int_{\mathcal{T}} \left\| \frac{d\theta}{dt} \right\|_{\Theta}^2 dt. \tag{107}$$

However, this line also minimizes the distance:

$$\int_{\mathcal{T}} \left\| \frac{d\theta}{dt} \right\|_{\Theta} dt. \tag{108}$$

In Riemannian geometry a geodesic is defined as a path along which the velocity is constant; *locally* this is the shortest distance solution [38] (*globally*, this is not the case. Take, for instance, two points that are not antipodal on a great circle of a

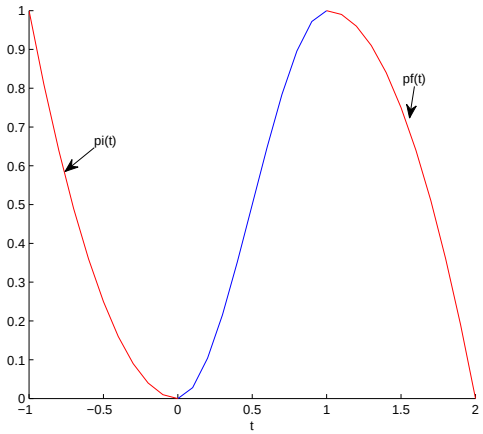

Figure 26: The Gluskabi raccordation of $R_3[t]$: indirect method

sphere). The straight line solution induces, for each α, a second order polynomial

$$\begin{aligned} x(t,\theta(\alpha)) &= \phi^{-1}(\theta^*(\alpha)) = \theta_0^*(\alpha) + \theta_1^*(\alpha)t + \theta_2^*(\alpha)t^2 \qquad (109) \\ &= (p_0^i(1-\alpha) + p_0^f\alpha) + (p_1^i(1-\alpha) + p_1^f\alpha)t + (p_2^i(1-\alpha) + p_2^f\alpha)t^2 \end{aligned}$$

in $\mathbb{R}_3[t]$. The raccordation polynomial is defined to be

$$p(t) = x(t,\theta(\alpha))|_{\alpha=t},\ t \in [0,1] \qquad (110)$$

which is itself a polynomial of degree 3 instead of degree 2.

In Figure 26 we show $p_i(t) = t^2, t \in [-1,0]$ and $p_f(t) = 2t - t^2,\ t \in [-1,0]$ while the raccordation (110) is

$$p(t) = 3t^2 - 2t^3,\ t \in [0,1]. \qquad (111)$$

In Figure 27 we show the family $x(t,\theta(\alpha))$ and the projection $p(t) = x(t,\theta(\alpha))|_{\alpha=t}$.

Remark 5.0.2. *Observe that* (109) *is function of two independent variables. In fact it is a homotopy. Recall a homotopy of two continuous functions* $p_i, p_f,\ T \to S$ *is a continuous function* $H : T \times [0,1] \to Y$ *such that* $H(t,0) = p_i(t)$ *and* $H(t,1) = p_f(t)$.

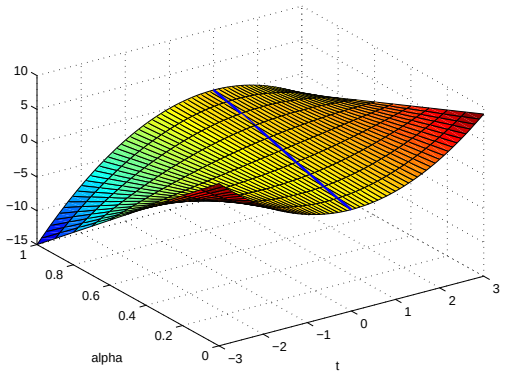

Figure 27: The Gluskabi raccordation of $R_3[t]$: indirect method

Remark 5.0.3. *Observe that the raccordations in* (106) *and* (111) *are different. These methods produces different raccordations in general.*

5.1 General Framework

In the following we will extract the main ingredients from the previous two constructions. We will only consider the Gluskabi raccordation problem *without* constraint in the current and following chapter. We call this the signal Gluskabi raccordation. In Chapter 7, we will extend the framework to include a dynamical system. It turns out the extension is readily made if we consider the dynamics as a hard constraint.

5.1.1 Direct method

Let T denote the time axis and $\mathcal{W}$ the signal space. Then $\mathcal{V} = \mathcal{W}^T$ denotes the set of all maps from T to $\mathcal{W}$. Let $\mathcal{X} \subset \mathcal{V}$ denote the set for which the Gluskabi raccordation is sought. We assume that there exists an operator $\mathcal{O} : \mathcal{V} \to \mathcal{V}$ such that

$$\begin{aligned} \mathcal{X} &= \ker \mathcal{O} \\ &= \{x \in \mathcal{V} | \mathcal{O}x = 0\}. \end{aligned} \tag{112}$$

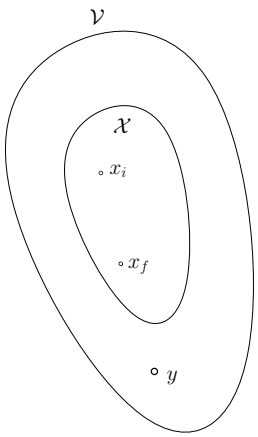

Figure 28: The Gluskabi raccordation problem.

Obviously,

$$\int_{-\infty}^{\infty} \| \left(\mathcal{O}x\right)(t)\|_{\mathcal{W}}^2 dt = 0. \tag{113}$$

for any $x \in \mathcal{X}$.

The Glucabi raccordation based on the direct method is the minimization problem:

$$\begin{aligned} &\inf_{y\in\mathcal{V}} \frac{1}{2}\int_{-\infty}^{\infty} \| \left(\mathcal{O}y\right)(t)\|_{\mathcal{W}}^2 dt \text{ subject to} \\ &y(t) = x_i(t),\, t \leq 0,\ y(t) = x_f(t),\, t \geq 1 \end{aligned} \tag{114}$$

for some x_i, $x_f \in \mathcal{X}$.

Let $\widehat{\mathcal{O}} : \mathcal{V} \to \mathcal{V}$ be an operator and define a new operator $\widetilde{\mathcal{O}} = \widehat{\mathcal{O}}\mathcal{O}$. If $0 \in \ker \widetilde{\mathcal{O}}$, then the kernel of $\widetilde{\mathcal{O}}$ clearly contains $\ker \mathcal{O}$ and, therefore, $\mathcal{X} \subset \ker \widetilde{\mathcal{O}}$. The representation of $\mathcal{X}$ as the kernel of an operator $\mathcal{O}$ in (112) is thus minimal in the sense that if $\mathcal{X}$ is contained in $\ker \mathcal{O}$, there does not exist another operator $\overline{\mathcal{O}}$, whose kernel is strictly in $\ker \mathcal{O}$. We call the representation of $\mathcal{X}$ in (112) the *minimal kernel representation* of $\mathcal{X}$.

Remark 5.1.1. *If $\mathcal{X} = \mathbb{R}_3[t]$ and $\mathcal{O} = \mathbf{D}^3$, then we recover the Gluskabi raccordation of two second order polynomial in Section 5.0.1.*

5.1.2 Indirect method

As indicated in the polynomial raccordation example, an alternative method of constructing the raccordation involves first parameterizing $\mathcal{X} = \ker \mathcal{O}$. The raccordation is subsequently reconstituted by mapping the 'smoothest' path in the parameter space to the original space $\mathcal{V}$.

Formally, we postulate that there exists a function $\phi : \mathcal{X} \to \Theta$ that parameterizes all of $\mathcal{X}$ onto a parameter space Θ. As this parameterizes all of $\mathcal{X}$ we call this representation the *maximal image representation* of $\mathcal{X}$. The Gluskabi raccordation with the maximal image representation of $\mathcal{X}$ involves the following steps:

1. Parameterization of $\mathcal{X}$: Let $x \in \mathcal{X}$ be parameterized by a global parameter

$$\phi : \mathcal{X} \to \Theta$$

   such that the map ϕ is bijective: (1) injection: $\phi(x_1) = \phi(x_2)$ implies $x_1 = x_2$, (2) surjection: if $\theta \in \Theta$, then there exists a $x \in \mathcal{X}$ such that $\phi(x) = \theta$.

2. Local characterization of $\mathcal{X}$: Let $x \in \mathcal{X}$, then there is a continuum of maps $\phi_\alpha^{loc} : \mathcal{X} \to \theta$, such that the following invariance holds:

$$x \in \mathcal{X} \to \phi_\alpha^{loc}(x) \equiv \phi(x), \forall \alpha \in \mathbb{R}. \tag{115}$$

3. Extension of $\mathcal{X}$: We extend the set $\mathcal{X}$ to a set $\mathcal{Y}$, $\mathcal{X} \subset \mathcal{Y}$ such that

   (a) If $\phi_\alpha^{loc}(y) = \theta \in \Theta, \forall \alpha \in \mathbb{R}$, then $y \in \mathcal{X}$ and $\phi(y) = \theta$.

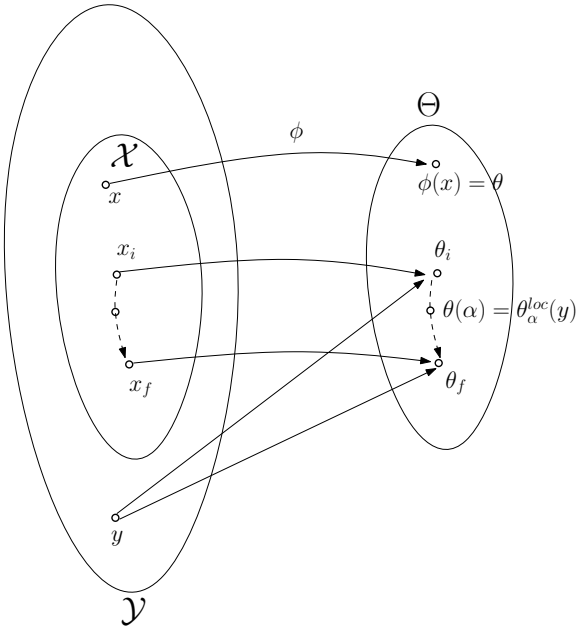

Figure 29: The Gluskabi raccordation problem.

(b) If $y \in \mathcal{Y}\backslash\mathcal{X}$, then $\phi_\alpha^{loc}(y) = \theta(\alpha)$, where $\frac{d\theta(\alpha)}{d\alpha} \neq 0$ in the sense of Fréchet.

4. Reconstruction: Let $x_i, x_f \in \mathcal{X}$. We construct a $y \in \mathcal{Y}$ such that

$$\begin{aligned} \phi_\alpha^{loc}(y) &= \theta_i, \text{ for } \alpha < 0, \text{ where } \theta_i = \phi(x_i) \\ \phi_\alpha^{loc}(y) &= \theta_f, \text{ for } \alpha > 1, \text{where } \theta_f = \phi(x_f) \end{aligned}$$

$\phi_\alpha^{loc}(y) = \theta(\alpha)$ for $\alpha \in \mathcal{T} = [0,\, 1]$, where $\theta(\alpha)$, $\alpha \in \mathcal{T}$ is as 'smooth' as possible.

In other words,

$$\begin{aligned} y(t) &= x_i(t),\, t \leq 0, \\ y(t) &= x_f(t),\, t \geq 1, \\ y(t) &= x(t;\alpha)|_{\alpha=t} = \phi^{-1}\theta(\alpha))|_{t=\alpha},\, \alpha \in \mathcal{T} \end{aligned} \tag{116}$$

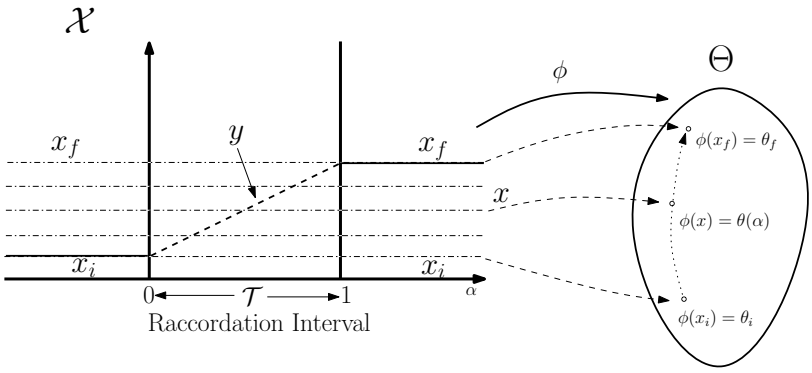

Figure 30: The Gluskabi raccordation

5.1.3 Non-uniqueness in parameterization

Consider a simple example where the raccordation of two constants is sought. Clearly, $\mathcal{X}$ consists of all constant *functions*. There are many ways to parameterize $\mathcal{X}$. Consider two such parameterizations where the parameter spaces coincide: $\phi_k : \mathcal{X} \to \Theta_k = \mathbb{R}$, $k = 1, 2$: $\phi_1(g) = \sigma_0 g = g(0)$ and $\phi_2(g) = (\sigma_0 g)^3 = g(0)^3$. Since $\mathbb{R}$ is one dimensional the smoothest path connecting two elements in the parameter space Θ is the straight line with constant derivative. The corresponding raccordations connecting two constant functions in $\mathcal{X}$ are constructed by (116), where the map $\phi_k^{-1}\theta_k(\alpha))$, $k = 1, 2$ is

$$\begin{aligned} \phi_1^{-1}\theta_1(\alpha) &= g_i(0)(1-\alpha) + g_f(1)\alpha, \\ \phi_2^{-1}\theta_2(\alpha) &= \left(g_i^3(0)(1-\alpha) + g_f^3(1)\alpha\right)^{\frac{1}{3}} \alpha \in [0,1]. \end{aligned}$$

Clearly, the raccordations are different.

Observe that since $\mathcal{Y}$ is a function space, $x \in \mathcal{Y}$ is a function of t and the parameter $\theta \in \Theta$, or explicitly $x(t, \theta)$. Let

$$d_{\mathcal{Y}}(x, y) = \|x - y\|_{\mathcal{Y}} = \left(\int_{\mathcal{T}} \|x(t) - y(t)\|^2 dt\right)^{\frac{1}{2}} \tag{117}$$

be a metric on $\mathcal{Y}$. The metric space $(\mathcal{Y}, d)$ induces a Riemanian metric d_Θ on the parameter space Θ:

$$\begin{aligned} d_{\mathcal{Y}}(x, x+dx) &= \|dx\|_{\mathcal{Y}} \\ &= \sqrt{\int_{\mathcal{T}} d\theta' \frac{\partial x'(t,\theta)}{\partial \theta} \frac{\partial x(t,\theta)}{\partial \theta} d\theta \, dt} \\ &= \sqrt{d\theta' \int_{\mathcal{T}} \frac{\partial x'(t,\theta)}{\partial \theta} \frac{\partial x(t,\theta)}{\partial \theta} dt \; d\theta} \\ &= \sqrt{d\theta' G(\theta) d\theta} \qquad (118) \\ &= d_\Theta(\theta, \theta + d\theta) \\ &= \|d\theta\|_\Theta . \end{aligned}$$

Hence, the geodesic of the path $\theta(\alpha)$, $\alpha \in \mathcal{I}$, connecting their parameters $\theta_i = \phi(x_i) \in \Theta$, $i = 0, 1$ where $x_i \in \mathcal{Y}$, $i = 0, 1$ is the minimum of

$$\int_{\mathcal{I}} \|dx\|_{\mathcal{Y}} \, d\alpha = \int_{\mathcal{I}} \|d\theta\|_\Theta \, d\alpha \qquad (119)$$

As noted before, the trajectory minimizing the energy of the path

$$\int_{\mathcal{I}} \left\| \frac{d\theta}{d\alpha} \right\|_\Theta^2 d\alpha \qquad (120)$$

also minimizes the distance. However, this produces in addition the 'smoothest' trajectory and it also simplifies the computations tremendously.

Let $\phi_i : \mathcal{X} \to \Theta$, $i = 0, 1$ be two parameterizations of $\mathcal{X}$ into the parameter space Θ, then it is clear from (118) and (119) that the arclength and energy are the same for these parameterizations. The only difference lies in the measure (or the Riemannian metric) of the differential element. This, however, does not imply that the respective raccordations coincide since they are constructed by mapping the geodesic solution back to the function space $\mathcal{Y}$ via ϕ^{-1} in (116).

5.1.4 Quasi-harmonic raccordation

In order to further elucidate the construction via the indirect method we will consider the raccordation of two harmonics.

Let $\mathcal{X}$ denote the set consisting of all complex exponents of the form $Me^{j\omega t}, t \in \mathbb{R}, M \in \mathbb{C}$ with a fixed frequency ω:

$$\mathcal{X} = \{Me^{j\omega t},\, t \in \mathbb{R},\, M \in \mathbb{C}\} \tag{121}$$

We seek to connect two phasors in this set in a quasi-harmonic fashion.

The quasi-harmonic transition will be of the form $u(t) = M(t)e^{j\omega t},\, t \in \mathcal{T}$, whence

$$\frac{|\dot{u}|}{|u|} = \frac{\left|\dot{M} + j\omega\right|}{|M|} \leq \frac{\left|\dot{M}\right|}{|M|} + \omega.$$

In order for $u(t)$ to be quasi-harmonic with frequency ω we impose $\frac{\left|\dot{M}\right|}{|M|} \ll \omega$. Since each phasor in $\mathcal{X}$ is parameterized by $M \in \mathbb{C}$ we may set the parameter space $\Theta = \mathbb{C}$ and express x explicitly to denote the dependence on M.

Introduce the norm on $\mathcal{Y}$

$$\|x\|_{\mathcal{Y}}^2 = \frac{1}{T}\int_0^T \|x\|^2\, dt \tag{122}$$

which induces the metric

$$d_{\mathcal{Y}}(x, y) = \|x - y\|_{\mathcal{Y}} = \left(\frac{1}{T}\int_0^T \|x(t, M_1) - y(t, M_2)\|^2\, dt\right)^{\frac{1}{2}} \tag{123}$$

for $x, y \in \mathcal{Y}$.

Since M is complex we let $M = Re^{j\phi}, R > 0$, then $dx = e^{j\omega t}dM = (dRe^{j\phi} +$

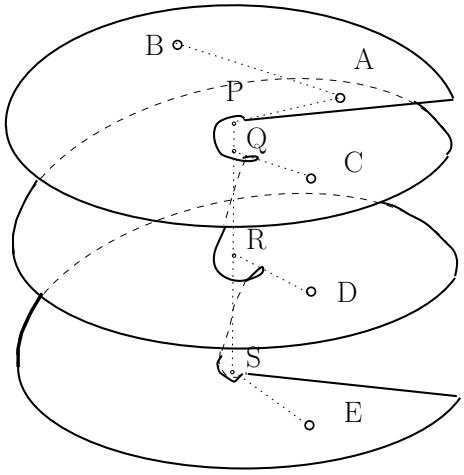

Figure 31: Geodesics

$jRe^{j\phi}d\phi)e^{j\omega t}$. From (123)

$$\begin{aligned} d^2_{\mathcal{Y}}(x, x+dx) &= \|dx\|^2_{\mathcal{Y}} \\ &= \int_0^T \|(dRe^{j\phi} + jRe^{j\phi}d\phi)\|^2\, dt \\ &= dR^2 + R^2 d^2\phi - 2Re\{jRdRd\phi\} \\ &= dR^2 + R^2 d^2\phi. \end{aligned}$$

The raccordation is the minimum of (120):

$$\min \frac{1}{2} \int_{\mathcal{I}} \left(\frac{dR}{d\alpha}\right)^2 + R^2 \left(\frac{d\phi}{d\alpha}\right)^2 d\alpha \tag{124}$$

We may proceed to find the necessary conditions of optimality and the resulting equations are not easily solved for. However, observe that the metric is just an expression in polar coordinates and this is not the regular $\mathbb{R}^2$ or the complex plane $\mathbb{C}$ as an angle α and its counterparts at $\alpha + 2\pi k, k \in \mathbb{Z}$ cannot be identified. We identify the previous with a infinite screw plane. (31).

Since the space is Euclidean, we infer that geodesics are straight lines and that the straight line with uniform speed minimizes (124). If the initial and final parameter

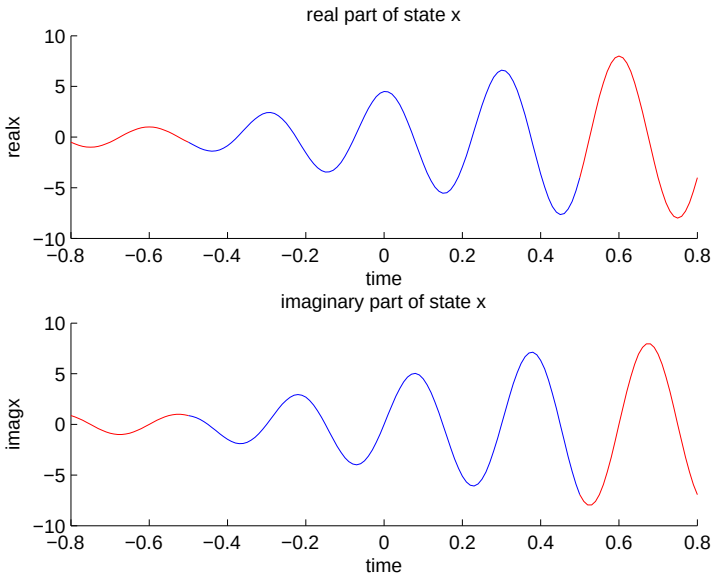

Figure 32: Image representation: phase plane. (Red curves indicate initial and final harmonic.)

lie on the same screw sheet, then the straight line connecting them is the solution to (124).(e.g., the straight line AB) However, if they lie on two different sheets, then the path must first approach and rotate around the origin and extend to the final parameter.(e.g., the path APQC.)

For $M_i = 1$, $M_f = 8$ and $T = 0.3$ the raccordation is shown in Figure 32 and Figure 33. In this example both M_i and M_f lie on the same sheet of the screw in Figure 31. We now consider an example where M_i and M_f reside on two different screw sheets. Let $M_i = e^{j\pi/3}$ and$M_f = 3e^{j8\pi/3}$. As indicated by the screw identification, the geodesic in the parameter space has to approach the origin. This causes the magnitude of the raccordation to pinch to zero as shown in Figure 35 and Figure 36. The geodesic then rotates around the origin through an angle of $7\pi/3$ extends towards M_f. The 'kink' in Figure 37 is caused by this rotation.

Figure 33: Image representation: real and imaginary part of x

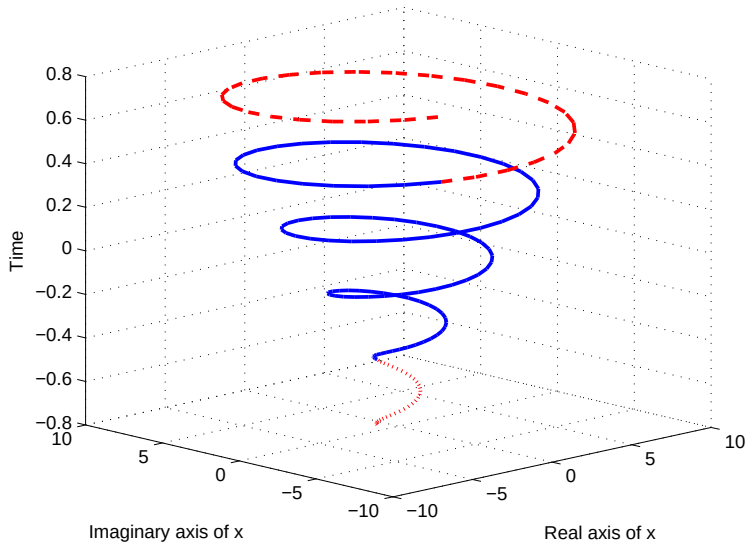

Figure 34: Image representation: phase plane

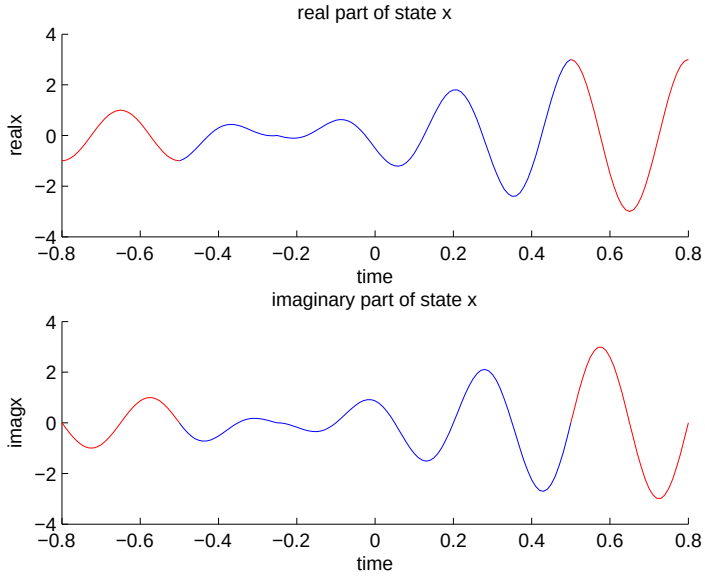

Figure 35: Real and imaginary parts

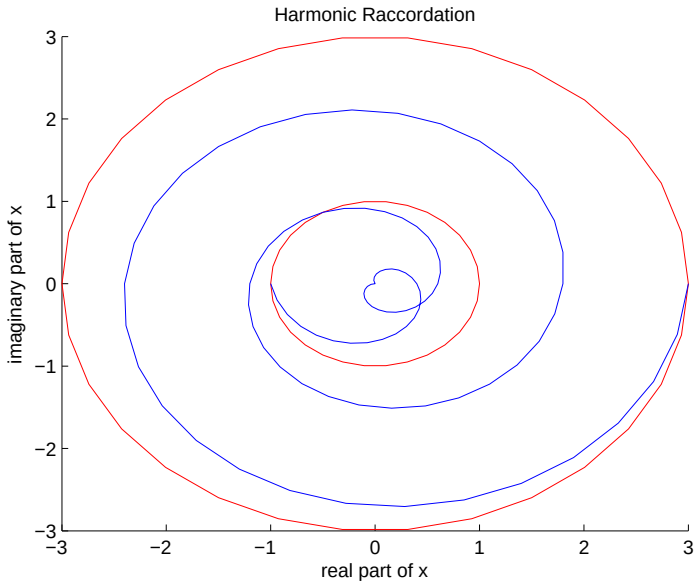

Figure 36: Phase plane

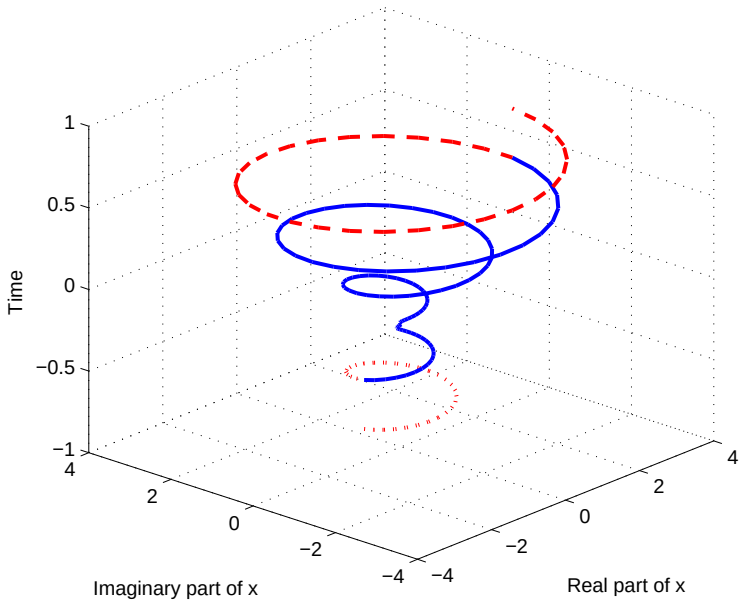

Figure 37: Real and imaginary parts

5.1.4.1 Frequency raccordation

The previous raccordation is of the amplitude modulation type. As an immediate extension we consider the frequency ω as a parameter and seek the corresponding raccordation. Let $\mathcal{X}$ be the class of phasors: $X = \{Me^{j\omega t+\phi}, \theta = (M, \omega, \phi) \in \mathbb{R}^+ \times \mathbb{R} \times \mathbb{R} = \Theta, t \in \mathbb{R}\}$, where the raccordation between $x_k(t, M_k, \omega_k, \phi_k) = M_k e^{j\omega_k t+\phi_k}$, $k = 0, 1$ is sought.With this parameterization the differential element dx due to changes in the parameters is

$$dx = e^{j(\omega t+\phi)}dM + jtMe^{j\omega t}d\omega + jMe^{j(\omega t+\phi)}d\phi,$$

whence the arc length measure is

$$\|dx\|^2 = dM^2 + M^2 \begin{bmatrix} d\theta & d\omega \end{bmatrix} \begin{bmatrix} 1 & \frac{1}{2} \\ \frac{1}{2} & \frac{1}{3} \end{bmatrix} \begin{bmatrix} d\theta \\ d\omega \end{bmatrix} \tag{125}$$

for $\mathcal{T} = [0, 1]$.

Instead of solving (120) immediately, we first consider a simpler problem with the arclength measure

$$dx^2 = dM^2 + M^2(d\omega^2 + d\theta^2) \tag{126}$$

(120) is now

$$\begin{aligned} \min J &= \frac{1}{2}\int_0^1 u_1^2 + M^2(u_2^2 + u_3^2)\, dt \qquad (127)\\ \dot{M} &= u_1 \\ \dot{\omega} &= u_2 \\ \dot{\theta} &= u_3 \end{aligned}$$

The Hamiltonian is $H = u_1^2 + M^2(u_2^2 + u_3^2) + \lambda_M u_1 + \lambda_\omega u_2 + \lambda_\theta u_3$,and the optimality conditions imply

$$-u_1 = \lambda_M \tag{128}$$

$$-M^2 u_2 = \lambda_\omega \tag{129}$$

$$-M^2 u_3 = \lambda_\theta \tag{130}$$

The costates equations are

$$-M(u_2^2 + u_3^2) = \dot{\lambda}_M \tag{131}$$

$$0 = \dot{\lambda}_\omega \tag{132}$$

$$0 = \dot{\lambda}_\theta \tag{133}$$

Therefore, $\lambda_\omega = c_1$ and $\lambda_\theta = c_2$, where c_1 and c_2 are two constants. From (128) and (129), $\frac{u_2}{u_3} = \frac{\lambda_\omega}{\lambda_\theta}$, from which we conclude that u_2 is proportional to u_3; $ku_2 = u_3 (k =$

$\frac{\lambda_\theta}{\lambda_\omega}$). Eliminating u_3 from (127) we obtain the optimization problem in the previous section with M scaled by a factor of $1+k^2$. Straight line solutions involving M and ω with uniform speed are optimal. Once this is found we may use the proportionality $u_3 = ku_2$ to find u_3. If $k > 1$ then θ rotates faster on the the infinite screw representation, while the opposite is true when $k < 1$.

Since the original arc length measure (125) may be obtained from (126) by a linear transformation of the coordinates, straight lines with uniform speed also minimize (120) with the arc length measure (125).

5.1.4.2 Direct method

The raccordations in the previous section are based on the indirect method. It is also of interest to investigate the direct method. Any element $x \in \mathcal{X}$satisfies $\mathcal{O}x = (\mathbf{D} - j\omega)x = 0$, $\omega = \frac{2\pi}{T}$. Hence, the kernel representation of $\mathcal{X}$ in (112) is the null space of $\mathcal{O} = (\mathbf{D} - j\omega)$.

Denote the initial and final phasor by $x_{i,f}(t) = M_{i,f}e^{j\omega t}$, $M_i \in \mathbb{C}$, respectively. For this example the raccordation interval is $\mathcal{T} = \left[-\frac{1}{2}, \frac{1}{2}\right]$ instead of the usual unit interval. After introducing a change of variable we have

$$\dot{x} = j\omega x + u. \tag{134}$$

The raccordation problem specializes to the following:

$$\begin{aligned} &\min_{y\in\mathcal{Y}} \frac{1}{2}\int_{\mathcal{T}} \|u\|^2 \text{ subject to} \\ &y(t) = x_i(t),\ t \le -\frac{1}{2},\ \ y(t) = x_f(t),\ t \ge \frac{1}{2},\ x_{i,f} \in \mathcal{X}. \end{aligned} \tag{135}$$

From the necessary conditions of optimality derived in Appendix (C) we obtain for

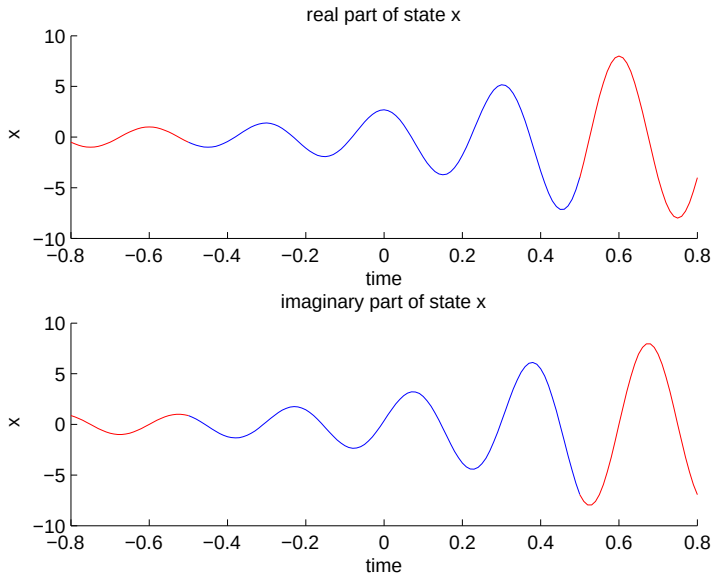

Figure 38: Kernel representation of phasor raccordation: real and Imaginary part of x

the complex Hamiltonian system

$$\begin{bmatrix} \dot{x} \\ \dot{\lambda} \end{bmatrix} = \begin{bmatrix} j\omega\mathbf{I} & -\mathbf{I} \\ 0 & -j\omega\mathbf{I} \end{bmatrix} \begin{bmatrix} x \\ \lambda \end{bmatrix} \tag{136}$$

with the boundary conditions

$$x_i\left(-\frac{1}{2}\right) = M_i e^{-j\omega\frac{1}{2}} \text{ and } x_f\left(\frac{1}{2}\right) = M_f e^{j\omega\frac{1}{2}}$$

This is the complexified classical terminal controller. An example is simulated based on the gradient descent algorithm. The initial and final orbit are $x_i(t) = 1e^{j\omega t}$ and $x_f(t) = 8e^{j\omega t}$, respectively, where $\omega = \frac{2\pi}{T}, T = 0.3$.

In Figure 38 the real and imaginary part of the quasi-harmonic x The red curves denote the initial and final phasor, while the blue part shows the quasi-harmonic transition. In Figure 39, the phasor raccordation is shown on the complex plane. It is clear the the phasor smoothly changes from the inner to the outer circle. u is shown

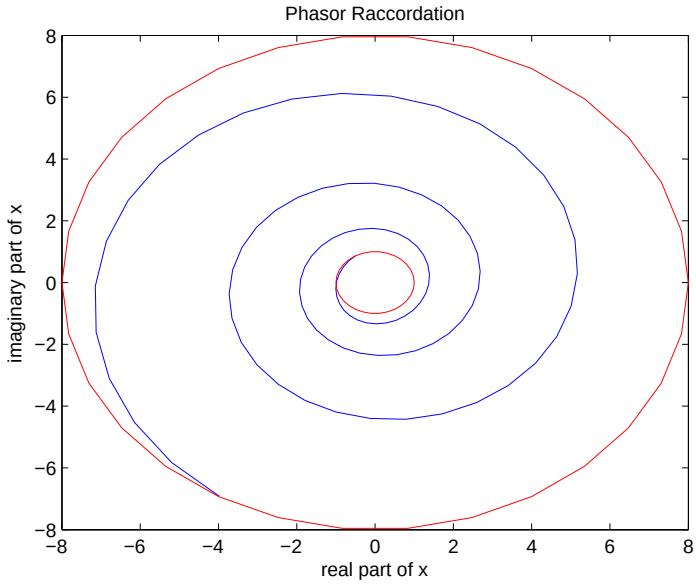

Figure 39: Kernel representation of phasor raccordation: evolution of x

in Figure 41.

5.1.5 Frequency raccordation

We present the frequency raccordation based on the kernel representation in this section. Let $\mathcal{X}$ denote the set of all harmonic signals of the form $Me^{j\omega t}$, then for any $x \neq 0$, $\frac{\dot{x}}{x} = j\omega$ and $\frac{d}{dt}\left(\frac{\dot{x}}{x}\right) = 0$ for all ω. Observe that the set in (121) is a subset $\mathcal{X}$. To minimize the non-constancy of the frequency between the transition we pose the following problem:

$$\min \int_0^1 |\mathcal{O}x|^2 = \int_0^1 \left| \frac{d}{dt}\left(\frac{\dot{x}}{x}\right) \right|^2 dt. \tag{137}$$

In order to solve this we introduce the change of variable

$$\dot{x} = xu \tag{138}$$

$$\dot{u} = v. \tag{139}$$

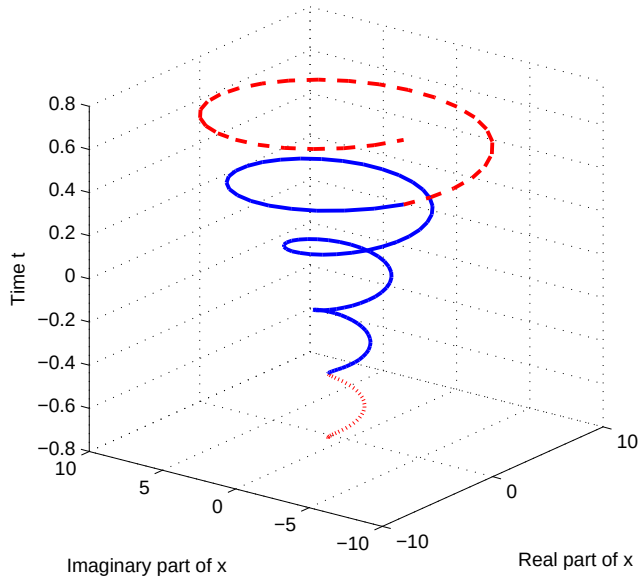

Figure 40: Kernel representation of phasor raccordation: evolution of x

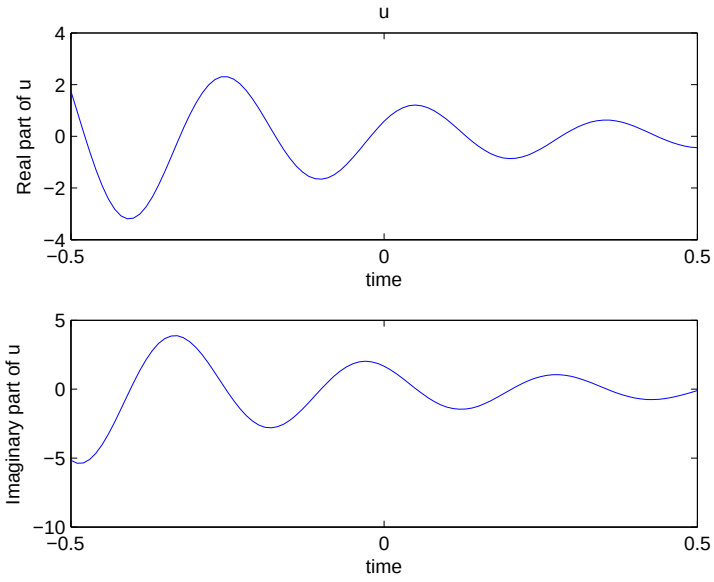

Figure 41: Kernel representation of phasor raccordation: real and imaginary part of u

and hence (137) is

$$\int_0^1 \|u\|^2 \, dt \tag{140}$$

with the boundary conditions $x(t) = Ae^{j\omega_0 t}$, $t \leq 0$ and $x(t) = Be^{j\omega_1 t}$, $t \geq 1$.

Proposition 5.1.1. *The optimality condition of (140) is*

$$v = -\lambda_u,$$

where

$$\dot{\lambda}_x = -\lambda_x u^*, \tag{141}$$

$$\dot{\lambda}_u = -\lambda_x x^*, . \tag{142}$$

$\nu_x = \lambda_x(1)$ *and* $\nu_u = \lambda_u(1)$ *are chosen such that the final state constraints are met.*

Proof. Since all functions are complex we adjoin their adjoints to keep the performance index real,:

$$\begin{aligned} J_0 = {} & \nu_x^*(x(1) - x_f) + \nu_u^*(u(1) - u_f) + (x(1) - x_f)^*\nu_x + (u(1) - u_f)^*\nu_u + \\ & \int_0^1 v^*v + \lambda_x^*(ux - \dot{x}) + (ux - \dot{x})^*\lambda_x + \lambda_u^*(v - \dot{u}) + (v - \dot{u})^*\lambda_u. \end{aligned}$$

We perturb $v \to v + \epsilon\tilde{v}$, $u \to u + \epsilon\tilde{u}$ and $x \to x + \epsilon\tilde{x}$ and after keeping the first order terms we obtain

$$\begin{aligned} J_\epsilon = {} & \nu_x^*(x(1) - x_f + \epsilon\tilde{x}(1)) + \nu_u^*(u(1) - u_f + \epsilon\tilde{u}(1)) \\ + {} & (x(1) - x_f + \epsilon\tilde{x}(1))^*\nu_x + (u(1) - u_f + \epsilon\tilde{u}(1))^*\nu_u + \\ + {} & \int_0^1 v^*v + \epsilon\left(\tilde{v}^*v + v^*\tilde{v}\right) + \lambda_x^*\left(ux - \dot{x} + \epsilon(\tilde{u}x + u\tilde{x} - \dot{\tilde{x}})\right) + \\ + {} & \left(ux - \dot{x} + \epsilon(\tilde{u}x + u\tilde{x} - \dot{\tilde{x}})\right)^*\lambda_x \\ + {} & \lambda_u^*\left(v - \dot{u} + \epsilon\left(\tilde{v} - \dot{\tilde{u}}\right)\right) + \left(v - \dot{u} + \epsilon\left(\tilde{v} - \dot{\tilde{u}}\right)\right)^*\lambda_u \, dt \end{aligned}$$

The Fréchet derivative is

$$\begin{aligned}\delta J &= (\nu_x - \lambda_x(1))^* \tilde{x}(1) + (\nu_x - \lambda_x(1)) \tilde{x}^*(1) + (\nu_u - \lambda_u(1))^* \tilde{u}(1) + (\nu_u - \lambda_u(1)) \tilde{u}^*(1) \\ &+ \int_0^1 (v + \lambda_u)^* \tilde{v} + (v + \lambda_u) \tilde{v}^* + \left(\lambda_x x^* + \dot{\lambda}_u\right)^* \tilde{u} + \left(\lambda_x x^* + \dot{\lambda}_u\right) \tilde{u}^* \\ &+ \left(\lambda_x u^* + \dot{\lambda}_x\right)^* \tilde{x} + \left(\lambda_x u^* + \dot{\lambda}_x\right) \tilde{x}^*\end{aligned}$$

We *choose*

$$\begin{aligned}\dot{\lambda}_x &= -\lambda_x u^*, \\ \dot{\lambda}_u &= -\lambda_x x^*,\end{aligned}$$

$\nu_x = \lambda_x(1)$ and $\nu_u = \lambda_u(1)$ are chosen such that the final state constraints are met. The optimality condition is, therefore,

$$v = -\lambda_u.$$

■

From (141) and (138) we obtain $\frac{\dot{x}}{x} = -\frac{\dot{\lambda}_x^*}{\lambda_x^*}$, which has solution $x(t) = \frac{k}{\lambda_x^*(t)}$ for some constant k. Therefore, from (142) and the stationary condition

$$x^* \lambda_x = -\dot{\lambda}_u = k^* = \dot{v} = \ddot{u}$$

Thus, $u(t)$ is a second order polynomial in t with complex coefficients; $u(t) = c_2 t^2 + c_1 t + c_0$. In light of (141) $\lambda_x(t) = \lambda_x(0) e^{-\int_0^t u^*(\tau) d\tau} = p_0 e^{-(p_3 t^3 + p_2 t^2 + p_1 t)}$. Hence, $x(t) = \frac{k}{\lambda_x^*(t)} = k_0 e^{(k_3 t^3 + k_2 t^2 + k_1 t)}$.

Since $\frac{\dot{x}(t)}{x(t)} = u(t)$, we have $u(0) = \frac{\dot{x}(0)}{x(0)} = j\omega_0$ and $u(1) = \frac{\dot{x}(1)}{x(1)} = j\omega_1$. The raccordation is $\frac{\dot{x}(t)}{x(t)} = u(t) = (3k_3 t^2 + 2k_2 t + k_1)$ and therefore, $k_1 = j\omega_0$.

Evaluating $x(t)$ at $t = 0$ and $t = 1$, we obtain $x(0) = A = k_0$ and and $x(1) = Be^{j\omega_1} = Ae^{(k_3+k_2+k_1)}$. Hence, $k_3 + k_2 = \ln\frac{B}{A} + j(\omega_1 - \omega_0)$. Also, $\frac{\dot{x}(1)}{x(1)} = (3k_3 + 2k_2 + j\omega_0) = u(1) = j\omega_1$.

We have the system

$$\begin{bmatrix} 1 & 1 \\ 2 & 3 \end{bmatrix} \begin{bmatrix} k_2 \\ k_3 \end{bmatrix} = \begin{bmatrix} \ln\frac{B}{A} + j(\omega_1 - \omega_0) \\ j(\omega_1 - \omega_0) \end{bmatrix}$$

and hence

$$\begin{aligned} \begin{bmatrix} k_2 \\ k_3 \end{bmatrix} &= \begin{bmatrix} 3 & -1 \\ -2 & 1 \end{bmatrix} \begin{bmatrix} \ln\frac{B}{A} + j(\omega_1 - \omega_0) \\ j(\omega_1 - \omega_0) \end{bmatrix} \\ &= \begin{bmatrix} 3\ln\frac{B}{A} + 2j(\omega_1 - \omega_0) \\ -2\ln\frac{B}{A} - j(\omega_1 - \omega_0). \end{bmatrix} \end{aligned}$$

Substituting these into $x(t)$

$$\begin{aligned} x(t) &= Ae^{\left(-2\ln\frac{B}{A} - j(\omega_1-\omega_0)\right)t^3} e^{\left(3\ln\frac{B}{A} + 2j(\omega_1-\omega_0)\right)t^2} e^{j\omega_0 t} \\ &= A\left(\frac{B}{A}\right)^{-2t^3+3t^2} e^{-j(\omega_1-\omega_0)t^3 + 2j(\omega_1-\omega_0)t^2 + j\omega_0 t}. \end{aligned}$$

A simple computation shows that $\dot{x}(0) = j\omega_0 A$ and $\dot{x}(1) = j\omega_1 Be^{j\omega_1}$. In other words, the derivatives are matched at the boundaries.

Figure (42) shows an example of the frequency raccordation. The initial and final harmonics are $x(t) = 2e^{\omega_0 t}$, $\omega_0 = \frac{2\pi}{0.1}$, $t \leq 0$ and $x(t) = 2.5e^{\omega_1 t}$, $\omega_1 = \frac{2\pi}{0.15}$, $t \geq 1$, respectively.

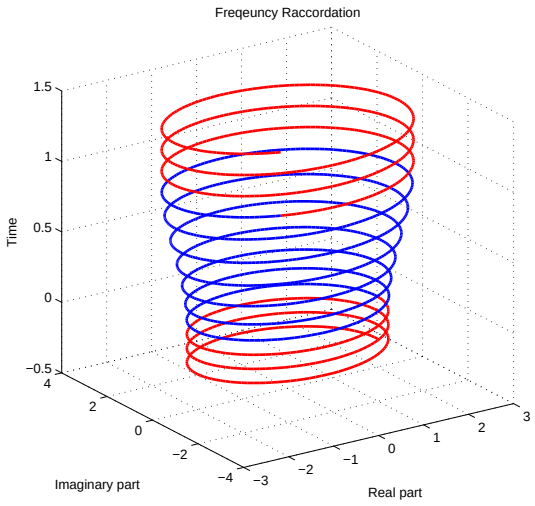

Figure 42: Harmonic frequency raccordation $x(t)$

CHAPTER VI

SIGNAL GLUSKABI RACCORDATION

In this chapter we delve further into the Gluskabi raccordation presented in the previous chapter. In Chapter 5 we explored the construction via several examples; it is based on two methods: the direct and indirect method which in turn relate to the kernel and image representations, respectively.

In this chapter we extend the method to quasi-periodic raccordation. That is the Gluskabi raccordation between two periodic signals. We will investigate two cases. In the first case the periodic signals have the same periods while in the second case the periods are different. The current chapter may be considered a stepping stone to the next where the Gluskabi raccordation with dynamics is considered. Indeed, dynamics only adds a hard constraint on the behavior, but conceptually amounts to the same framework.

In addition we present detailed derivations of all the algorithms used to compute the raccordations. All algorithms developed in this chapter are readily modified to accommodate for the necessary changes in the dynamic case.

6.1 Quasi-periodic raccordation I

6.1.1 Direct method

Let $\mathcal{X}$ denote the set of periodic behaviors with period T. The quasi-periodic raccordation seeks a 'smooth' transition that connects two trajectories x_0 and x_1 in $\mathcal{X}$.

Define the operator $\mathcal{O} = \mathbf{I} - \mathcal{T}_T$ we immediately see that $\mathcal{X} = \ker \mathcal{O}$. Specializing (114) to this case, we obtain the following optimization problem:

$$\min_x J_0 = \frac{1}{2}\int_0^{1+T} ||x(t) - x(t-T)||_R^2 \, dt \, \text{subject to}$$
$$x(t) = x_0(t),\, t \leq 0 \text{ and } x(t) = x_1(t),\, t \geq 1, \tag{143}$$

where both the initial and final orbits are T periodic: $x_i(t) = x_i(t-T)$, $i = 0, 1$, $\forall t \in \mathbb{R}$ and $T << 1$. We first introduce a change of variable

$$x(t) = x(t-T) + u(t),\, t \in [0, 1+T]\,. \tag{144}$$

to transform the problem into a more familiar form. The $T-$periodicity of $x_1(t)$, $t \in [1, \infty)$ implies that the final constraint is $x_1(t)$, $t \in [1, 1+T]$. The optimization problem in itself does not seem very interesting. However, it is a part of a larger problem considered in the next chapter. Furthermore, we will use this problem to elucidate the derivation of the gradient descent algorithm that we will used repeatedly in the sequel.

In order to derive the necessary conditions of optimality and an algorithm, we first compute the Fréchet derivative of x at an arbitrary point $s \in [1, 1+T]$. To this end, let

$$J_k^s = e_k' x(s),\, s \in [1, 1+T], \tag{145}$$

subject to (144) where e_k is the k^{th} unit vector. Adjoin (144) to (145)

$$J_k^s = \int_0^{1+T} \lambda_k^{s\prime} \left(x(t) - x(t-T) - u(t)\right) \, dt + e_k' x(s).$$

and after letting $x(t) \to x(t) + \epsilon\eta(t)$ and $u(t) \to u(t) + \epsilon v(t)$, we obtain the Frèchet derivative

$$\begin{aligned} \delta J_k^s &= e_k'\eta(s) + \int_0^{1+T} \lambda_k^{s\prime}(t)\left(\eta(t) - \eta(t-T) - v(t)\right) dt \qquad (146) \\ &= e_k'\eta(s) - \int_{-T}^{0} \lambda_k^{s\prime}(t+T)\eta(t)dt + \int_0^1 \left(\lambda_k^{s\prime}(t) - \lambda_k^{s\prime}(t+T)\right)\eta(t)dt + \\ &+ \int_1^{1+T} \lambda_k^{s\prime}(t)\eta(t)dt - \int_0^{1+T} \lambda_k^{s\prime}(t)v(t)dt \end{aligned}$$

This shows that $\eta(s)$ has to be explicitly calculated which is not desirable. In order to avoid this we average $x(t)$ in a neighborhood of s:

$$J_k^s = \frac{1}{\Delta}\int_s^{s+\Delta} e_k' x(t)dt. \qquad (147)$$

If $\Delta \to 0$, then $J_k^s \to e_k' x(s)$. With this approximation we obtain the following:

Proposition 6.1.1. *The Fréchet derivative of (147) is*

$$\delta J_k^s = -\int_0^{1+T} \lambda_k^{s\prime}(t)\delta u(t)dt, \qquad (148)$$

where

$$\begin{aligned} \lambda_k^s(t) &= \lambda_k^s(t+T),\ t \in [0,1] \qquad (149) \\ \lambda_k^s(t) &= -\frac{1}{\Delta}e_k = -e_k\Pi^\Delta(t-s),\ t \in [1, 1+T], \end{aligned}$$

and

$$\Pi^\Delta(t) = \begin{cases} \frac{1}{\Delta}, & t \in [0,\Delta], \\ 0 & \textit{else}, \end{cases}.$$

is an approximation of the Dirac delta function.

Proof. It is easily shown that

$$\begin{aligned}\delta J_k^s &= -\int_{-T}^{0} \lambda_k^{s\prime}(t+T)\eta(t)dt + \int_0^1 \left(\lambda_k^{s\prime}(t) - \lambda_k^{s\prime}(t+T)\right)' \eta(t)dt + \\ &+ \int_s^{s+\Delta} \left(\frac{1}{\Delta} e_k' + \lambda_k^{s\prime}(t)\right) \eta(t)dt + \int_1^s \lambda_k^{s\prime}(t)\eta(t)dt + \\ &+ \int_{s+\Delta}^{1+T} \lambda_k^{s\prime}(t)\eta(t)dt - \int_0^{1+T} \lambda_k^{s\prime}(t)v(t)dt.\end{aligned}$$

We *choose*

$$\begin{aligned}\lambda_k^s(t) &= \lambda_k^s(t+T),\ t \in [0,1] \\ \lambda_k^s(t) &= -\frac{1}{\Delta} e_k = -e_k \Pi^{\Delta}(t-s),\ t \in [1, 1+T]\end{aligned}$$

and the desired result follows. ∎

(149) shows that λ_k^s is a sequence of Π^{Δ}. Indeed, let $\lfloor \frac{s}{T} \rfloor = m$, then there will be $m+1$ copies of Π^{Δ} in the interval $[0, 1+T]$ for s. From (149) we have

$$\lambda_k^s(t) = -\sum_{r=0}^{m} e_k \Pi^{\Delta}(t + rT - s). \tag{150}$$

and, therefore,

$$\delta J_k^s = \int_0^{1+T} \sum_{r=0}^{m_i} e_k' \Pi^{\Delta}(t + rT - s)\delta u(t),\ k = 1, \ldots, n.$$

This clearly shows that δu is sampled at the intervals $[s - rT, s + \Delta - rT)$, $r = 0, \ldots, m_i$. As $\Delta \to 0$, $\lambda_k^s(t)$ approaches a sequence of Dirac delta functions with a period of T.

Now that the influence of the boundary mismatch is found, we proceed to compute the Fréchet derivative of the original problem (143) in the *absence* of the boundary condition. Indeed, let

$$\min_u J_v = \frac{1}{2} \int_0^{1+T} \|u\|_R^2 \, dt \tag{151}$$

where u satisfies (144) and x is assumed free in $[1, 1+T]$. The optimal solution is clearly $u(t) \equiv 0$, however, the explicit form of the Fréchet derivative is needed.

Proposition 6.1.2. *The Fréchet derivative of (151) is*

$$\delta J_v = \int_0^{1+T} u'(t) R \delta u(t)\, dt. \tag{152}$$

Proof. Adjoin (144) to (151) and retain the first order terms we obtain

$$\begin{aligned} \delta J_v &= \int_0^{1+T} (Ru(t) - \lambda(t))' v(t)\, dt + \int_0^1 (\lambda(t) - \lambda(t+T))' \eta(t) dt \\ &+ \int_1^{1+T} \lambda'(t)\eta(t) dt \end{aligned} \tag{153}$$

By *choosing* $\lambda = 0, t \in [1, 1+T]$ and hence, $\lambda(t) \equiv 0$, $t \in [0, 1+T]$, we obtain (152).

■

Recall that the constraint in (143) is a function x defined over $\mathcal{I} = [1, 1+T]$. With the previous results we may now consider a simpler version. Indeed, first discretize the interval $\mathcal{I}$ via $s_i = s_0 + i\Delta$, $i = 0, \ldots, N$ with $s_0 = 1$ and $s_N \leq 1+T$; the constraints $x(s_i)$, $i = 0, \ldots, N$ with its corresponding $\delta J_k^{s_i}$ form now a finite set which is simpler to handle than the original problem.

Consider now the following Fréchet derivative of this approximation:

$$\delta J_v + \sum_{i=0}^{N} \sum_{k=1}^{n} \nu_k^{s_i} \delta J_k^{s_i} = \int_0^{1+T} \left(Ru(t) - \sum_{i=0}^{N} \sum_{k=1}^{n} \nu_k^{s_i} \lambda_k^{s_i}(t) \right)' \delta u(t) dt, \tag{154}$$

where $\nu_k^{s_i}$, $i = 1, \ldots, N$, $k = 1, \ldots, n$ are yet to be determined.

If

$$\delta u(t) = -\left(Ru(t) - \sum_{i=0}^{N} \sum_{k=1}^{n} \nu_k^{s_i} \lambda_k^{s_i}(t) \right), \tag{155}$$

then (154) is negative and improving, hence not optimal, unless

$$u(t) - \sum_{i=0}^{N} \sum_{k=1}^{n} \nu_k^{s_i} \lambda_k^{s_i}(t) \equiv 0. \tag{156}$$

With this choice of δu the variation $e_k' \delta x(s_i)$ may be obtained by substituting (155) into (148). Indeed, in matrix notation

$$\delta \mathbf{J}_j = \mathbf{U}_j - \mathbf{\Lambda}_j \boldsymbol{\nu}_j,\ j = 1, \ldots, n, \tag{157}$$

where

$$\delta \mathbf{J}_j = \begin{bmatrix} \delta J_j^{s_0}, \\ \delta J_j^{s_1}, \\ \vdots \\ \delta J_j^{s_N} \end{bmatrix}, \mathbf{U}_j = \begin{bmatrix} \int_0^{1+T} \lambda_j^{s_0\prime}(t) \left(Ru(t)\right) dt, \\ \int_0^{1+T} \lambda_j^{s_1\prime}(t) \left(Ru(t)\right) dt \\ \vdots \\ \int_0^{1+T} \lambda_j^{s_N\prime}(t) \left(Ru(t)\right) dt \end{bmatrix}, \boldsymbol{\nu}_j = \begin{bmatrix} \nu_j^{s_0}, \\ \nu_j^{s_1}, \\ \vdots \\ \nu_j^{s_N} \end{bmatrix}$$

and

$$[\mathbf{\Lambda}_j]_{li} = \int_0^{1+T} \lambda_j^{s_l\prime}(t) \lambda_j^{s_i}(t) dt.$$

Since $\int_0^{1+T} \lambda_j^{s_l\prime}(t) \lambda_k^{s_i}(t) dt = 0$ unless $j = k$, all the terms with $j \neq k$ do not enter the problem. It is also clear from (150) that $\mathbf{\Lambda}_j$ is diagonal and invertible, whence

$$\boldsymbol{\nu}_j = \mathbf{\Lambda}_j^{-1} \left(\mathbf{U}_j - \delta \mathbf{J}_j\right),\ j = 1, \ldots, n,$$

For $\delta \mathbf{J}_j = 0$ the final state constraints are satisfied and (154) is negative, hence not optimal, unless (156) holds. In light of (155) and (149), we might equivalently redefine the costate equations

$$\begin{aligned} \hat{\lambda}(t) &= \hat{\lambda}(t+T),\ t \in [0,1] \\ \hat{\lambda}(t) &= -\sum_{i=0}^{N} \nu^{s_i} \Pi^{\Delta}(t - s_i),\ t \in [1, 1+T], \end{aligned} \tag{158}$$

where $[\nu^{s_i}]_k = \nu_k^{s_i}$ and the corresponding gradient of (155) is

$$\delta u(t) = -\left(Ru(t) - \hat{\lambda}(t)\right). \tag{159}$$

We may now summarize the previous computations in the following proposition.

Proposition 6.1.3. *Let $x(s_i) = x_f(s_i)$, $1 \leq s_i \leq 1+T$, $i = 1, \ldots, N$. The necessary conditions of optimality of*

$$\min_u J_0 = \frac{1}{2}\int_0^{1+T} \|u\|_R^2 \, dt,$$

where $x(t) = x(t-T) + u(t)$, may be obtained by adjoining $\sum_{i=0}^{N} \nu^{s_i\prime}(x(s_i) - x_f(s_i))$ to J_0. Indeed, the stationary condition is

$$u(t) = R^{-1}\lambda(t),$$

where the costate $\lambda(t)$ satisfies

$$\begin{aligned} \lambda(t) &= \lambda(t+T),\ t \in [0,1] \\ \lambda(t) &= -\sum_{i=0}^{N} \nu^{s_i} \Pi^{\Delta}(t - s_i),\ t \in [1, 1+T], \end{aligned}$$

ν^{s_i}, $i = 1, \ldots, N$ are chosen such that the final state constraints are satisfied.

6.1.2 A gradient descent algorithm

The computations in the previous section allow us to derive a gradient descent algorithm. Although the optimal solution may by obtained tediously by hand as the costate equations in (170) are rather simple, the algorithm presented below will be a part of a larger algorithm needed to calculate the raccordation problem with dynamical constraint. The algorithms are based on [11, 12] and may be interpreted as

seeking discrete step sizes δu such that (152) subject to (148) is minimized. However, (152) is linear in δu and a minimum does not exist. To create a minimum we instead minimize

$$\begin{aligned} \delta\overline{J} &= \delta J_v + \int_0^{1+T} \frac{\|\delta u\|^2}{2k_1}\, dt \\ &= \int_0^{1+T} u' R\delta u + \frac{\|\delta u\|^2}{2k_1}\, dt \end{aligned} \tag{160}$$

with the constraints (148). Adjoin this via the Lagrange multipliers $\nu_k^{s_i}$,

$$\delta\overline{J} = \int_0^{1+T} u' R\delta u + \frac{\|\delta u\|^2}{2k_1}\, dt + \sum_{i=0}^{N}\sum_{k=1}^{n} \nu_k^{s_i} \left(- \int_0^{1+T} \lambda_k^{s_i\prime}(t)\delta u dt - \delta J_k^{s_i} \right) \tag{161}$$

and after neglecting changes in the coefficients the second variation is

$$\delta^2\overline{J} = \int_0^{1+T} \left(u' R + \frac{\delta' u}{k_1} - \sum_{i=0}^{N}\sum_{k=1}^{n} \nu_k^{s_i} \lambda_k^{s_i\prime}(t) \right) dt\, \delta(\delta u).$$

The minimum is attained if

$$\delta u(t) = -k_1 \left(Ru(t) - \sum_{i=0}^{N}\sum_{k=1}^{n} \nu_k^{s_i} \lambda_k^{s_i}(t) \right). \tag{162}$$

Observe that this is exactly (155) scaled by a step size parameter k_1. After substituting this into (148), we obtain a scaled version of (157),

$$\delta\mathbf{J}_j = k_1 \left(\mathbf{U}_j - \mathbf{\Lambda}_j \boldsymbol{\nu}_j \right),\ j = 1, \ldots, n,$$

whence

$$\boldsymbol{\nu}_j = \mathbf{\Lambda}_j^{-1} \left(\mathbf{U}_j - \frac{1}{k_1}\delta\mathbf{J}_j \right),\ j = 1, \ldots, n.$$

Substitute this into (162)

$$\begin{aligned}\delta u(t) &= -k_1\left(Ru(t) - \sum_{k=1}^{n}\boldsymbol{\lambda}_k(t)\boldsymbol{\nu}_k\right)\\ &= -k_1\left(Ru(t) - \sum_{k=1}^{n}\boldsymbol{\lambda}_k(t)\boldsymbol{\Lambda}_k^{-1}\left(\mathbf{U}_k - \frac{1}{k_1}\delta\mathbf{J}_k\right)\right),\\ &= -k_1\left(Ru(t) - \sum_{k=1}^{n}\boldsymbol{\lambda}_k(t)\boldsymbol{\Lambda}_k^{-1}\mathbf{U}_k\right) - \sum_{k=1}^{n}\boldsymbol{\lambda}_k(t)\boldsymbol{\Lambda}_k^{-1}\delta\mathbf{J}_k', \qquad (163)\end{aligned}$$

where

$$\boldsymbol{\lambda}_k(t) = \begin{bmatrix} | & | & & | \\ \lambda_k^{s_0} & \lambda_k^{s_1} & \dots & \lambda_k^{s_N} \\ | & | & & | \end{bmatrix}.$$

It is important to observe that the gradient consists of two parts; the second term is the gradient due to the boundary mismatch. We may now summarize the algorithm in the following.

Algorithm 6.1.1. *Let $I = [0, 1+T]$ be the simulation interval, dt the discretization time step, $x(t) = x_0(t), t \in [-T, 0]$ and $x(t) = x_f(t), t \in [1, 1+T]$. Denote $s_0 = 1$, $s_i = s_0 + idt$, $i = 0, \dots, N$.*

1. *Guess a input $u(t)$, $t \in [0, 1+T]$.*

2. *Compute $x(t) = x(t-T) + u(t)$, $t \in [0, 1+T]$.*

3. *Costate equations*

$$\begin{aligned}\lambda_k^{s_i}(t) &= \lambda_k^{s_i}(t+T),\ t \in [0,1]\\ \lambda_k^{s_i}(t) &= -e_k\Pi^{\Delta}(t - s_i),\ t \in [1, 1+T]\,, \qquad (164)\end{aligned}$$

for $i = 0, \dots, N$ and $k = 1, \dots, n$.

4. *Compute the boundary mismatch:* $\Delta x(s_l) = x(s_l) - x_f(s_l)$, $l = 0, \ldots, N$, *and* $\delta J_k^{s_l} = e_k' \delta x(s_l)$, $l = 0, \ldots, N$ *and* $\delta x(s_l) = -k_2 \Delta x(s_l)$, $0 < k_2 \leq 1$.

5. *Compute* (163).

6. *Update* u *by* $u_{new}(t) = u(t) + \delta u(t)$.

7. *Repeat step 2 with the new input* $u_{new}(t)$.

Some care needs to be exercised in choosing the parameter $k_1 \geq 0$ and $k_2 \geq 0$. In the first few iterations one may set $k_1 = 0$ and k_2 a small positive number; in light of (163) this implies that the gradient δu only improves the input in the direction of decreasing the boundary mismatch. Subsequently, one may gradually increase k_2 to one until a satisfactory candidate is found. Finally, k_1 may be increased from zero to improve the input in the other direction.

Example 6.1.1. *Since there are as many state variable* x *as inputs* u *in* (144)*, we will consider a scalar example. We set* $x_0(t) = \sin(\omega t)$, $t \in (-\infty, 0]$,$x_1(t) = 3\sin(\omega t)$, $t \in (1, \infty]$, $\omega = \frac{2\pi}{T}$, $T = 0.1$. x *is shown in Figure 43 while the magnitude of* δu *is shown in Figure 44.*

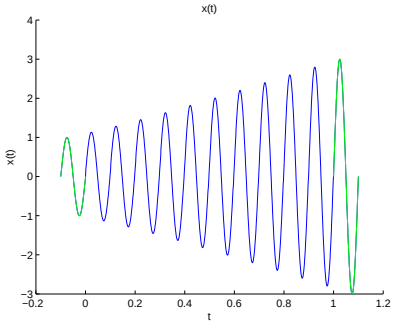

Figure 43: $x(t)$

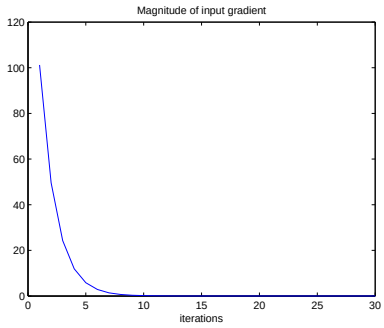

Figure 44: Magnitude of δu

6.1.3 An overview of the algorithm

The previous algorithm serves as a prototype for the problems considered in the following chapters,we therefore extract the main ingredients of the derivations that will be needed in the sequel.

Recall that the main problems involves the minimization of a functional subject to 1) a dynamical constraint and 2) a set of final state constraints. A high level view of the algorithm consists of the following four parts:

Algorithm 6.1.2. *(Gradient descent algorithm)*

1. *Compute the Frèchet derivative of the final state constraint (cf. (148)) and denote this by δJ_f.*

2. *Compute the Frèchet derivative of the original optimal control problem* without *the final state constraint (cf. (152)) and denote this by δJ_v.*

3. *Since both Frèchet derivatives, δJ_v and δJ_f, are linear in δu, we pose the optimization problem* (161) *to limit the size of δu and to create a minimum; the Frèchet derivative of the final state is adjoint to J_v via a Lagrange multiplier ν.*

Finally, compute the corresponding gradient δu, which is a function of ν.

4. *Eliminate δu from the Frèchet derivatives δJ_f using the expression in the previous step. Solve for ν under the assumption of the reachability of the dynamical system.*

   Substitute ν into δu obtained in the previous step. The final δu consists, in general, of two parts: one involves the final state variation and the other, multiplied by the step size parameter k_1, is the variation of the input in the absence of the final state constraint (cf. (163)). The remark of the choice of k_1 and k_2 is applicable in general.

6.1.3.1 The continuous case: $\Delta \to 0$

Recall that the algorithm in the previous section is based on the discretization of the time axis to obtain a finite set of final state constraints. We now return to the original problem. Observe first that $\Delta \to 0$ or, equivalently, $\frac{T}{\Delta} = N \to \infty$, $\Pi^{\Delta}(t) \to \delta(t)$. In light of the costate $\lambda_k^{s_i}$ in (149), which is a function of two variables, we introduce the notation $\lambda(t, s)$. Letting $\Delta \to 0$ in (147) and (149),respectively, we obtain

$$J_k(s) = e_k' x(s)$$

and the costate

$$\begin{aligned} \lambda_k(t, s) &= \lambda_k(t + T, s),\ t \in [0, 1] \qquad (165) \\ \lambda_k(t, s) &= -e_k \delta(t - s),\ t, s \in [1, 1 + T]\,. \end{aligned}$$

The Frèchet derivative of $\delta J_k(s)$ in (148) is

$$\delta J_k(s) = e_k' \delta x(s) = -\int_0^{1+T} \lambda_k'(t, s) \delta u(t) dt. \qquad (166)$$

Consider now the continuous analogue of (154) by adjoining $\delta J_k(s)$ via the scalar functions $\nu_k(s)$, $s \in [1, 1+T], k = 1, \ldots, n$:

$$\begin{aligned} & \delta J_v + \int_1^{1+T} \sum_{k=1}^{n} \nu_k(s) \delta J_k(s) ds \\ = & \int_0^{1+T} u'(t) R \delta u(t) dt - \int_1^{1+T} \sum_{k=1}^{n} \nu_k(s) \left(\int_0^{1+T} \lambda_k'(t,s) \delta u(t) dt \right) ds \\ = & \int_0^{1+T} \left(Ru(t) - \sum_{k=1}^{n} \int_1^{1+T} \nu_k(s) \lambda_k(t,s) ds \right)' \delta u(t) dt \end{aligned} \tag{167}$$

If

$$\delta u(t) = - \left(Ru(t) - \sum_{k=1}^{n} \int_1^{1+T} \nu_k(s) \lambda_k(t,s) ds \right), \; t \in [0, 1+T], \tag{168}$$

then (167) is negative, hence improving, unless it is zero and the constraints are satisfied: $\delta J_k(s) \equiv 0$, $s \in [1, 1+T]$, $k = 1, \ldots, n$. To obtain the Frèchet derivative of the final state constraint we substitute (168) into (166)

$$\begin{aligned} \delta J_k(s) &= \int_0^{1+T} \lambda_k'(t,s) \left(Ru(t) - \sum_{j=1}^{n} \int_1^{1+T} \nu_j(r) \lambda_j(t,r) dr \right) dt, \qquad (169) \\ &= \int_0^{1+T} \underbrace{\lambda_k'(t,s) Ru(t) dt}_{\Gamma_k(s)} - \sum_{j=1}^{n} \int_1^{1+T} \nu_j(r) \underbrace{\int_0^{1+T} \lambda_k'(t,s) \lambda_j(t,r) dt}_{\Lambda_{kj}(s,r)} dr. \end{aligned}$$

In matrix notation

$$\begin{aligned} \delta J(s) &= \Gamma(s) - \int_1^{1+T} \Lambda(s,r) \nu(r) dr, \\ &= \Gamma(s) - G\nu(s), \end{aligned}$$

which is the continuous analogue of (157). This is a Fredholm integral equation of the first type. Since G is invertible, the unknown function $\nu(s)$, $s \in [1, 1+T]$ can be explicitly solved for via

$$\nu(s) = G^{-1} \left(\Gamma - \delta J \right)(s), \; s \in [1, 1+T].$$

Observe from the costate equation (165) that for a fixed $s \in [1, 1+T]$

$$\lambda_k(t,s) = -\sum_{l=0}^{\lfloor \frac{s}{T} \rfloor} e_k \delta(t+lT-s),$$

and the integral in (168)

$$\begin{aligned}
\int_1^{1+T} \nu_k(s)\lambda_k(t,s)ds &= -\int_1^{1+T} \nu_k(s) \sum_{l=0}^{\lfloor \frac{s}{T} \rfloor} e_k \delta(t+lT-s)ds \\
&= -\int_1^{1+T} \sum_{l=0}^{\lfloor \frac{s}{T} \rfloor} \nu_k(t+lT) e_k \delta(t+lT-s)ds \\
&= -\nu_k(t+lT)e_k
\end{aligned}$$

for $1 \leq t+lT \leq 1+T$ or $1-lT \leq t \leq 1+(1-l)T$, $l = 0, \ldots, \lfloor \frac{s}{T} \rfloor$. Thus, $\nu_k(t)$, $t \in [1, 1+T]$ is extended to the interval $[0,1]$ by shifting it to the left an integer number of T. We may thus redefine the costate (165):

$$\begin{aligned}
\lambda(t) &= \lambda(t+T),\, t \in (0,1)\,, \\
\lambda(t) &= -\nu(t),\, t \in [1, 1+T]\,. \qquad (170)
\end{aligned}$$

The corresponding gradient in (168)

$$\delta u(t) = -\left(Ru(t) - \lambda(t)\right),\, t \in [0, 1+T]\,, \qquad (171)$$

We summarize the previous computations in the following proposition.

Proposition 6.1.4. *The necessary conditions of optimality of* (143) *are obtained by adjoining* $\int_1^{1+T_1} \nu(t)(x(t) - x_1(t))dt$ *to* J_0. *Indeed, the optimal* $u(t)$ *satisfies* $u(t) = R^{-1}\lambda(t)$, $t \in [0, 1+T]$, *where* $\lambda(t)$ *satisfies (170). The unknown* $\nu(t)$ *needs to chosen such that the final constraint is met.*

Proof. After adjoining (144) and the final state constraint via two Lagrange multipliers $\lambda(t)$ and $\nu(t)$ to J_0, we obtain

$$\begin{aligned} J_0 &= \frac{1}{2}\int_0^{1+T} \|u(t)\|_R^2 + \lambda'(t)(x(t) - x(t-T) - u(t))\,dt + \\ &\quad \int_1^{1+T} \nu'(t)(x(t) - x_1(t))\,dt. \end{aligned} \tag{172}$$

We will justify the way the final state constraint is adjoint in Section 6.1.2. Letting $x(t) \to x(t) + \epsilon\eta(t)$ and $u(t) \to u(t) + \epsilon v(t)$, we further obtain

$$\begin{aligned} J_\epsilon = &\frac{1}{2}\int_0^{1+T} \|u(t) + \epsilon v(t)\|_R^2 + \lambda'(t)\left(x(t) - x(t-T) - u(t)\right) + \\ &+\epsilon\lambda'(t)\left(\eta(t) - \eta(t-T) - v(t)\right)\,dt \\ &+ \int_1^{1+T} \nu'(t)(x(t) - x_1(t) + \epsilon\eta(t))\,dt. \end{aligned}$$

Therefore, the Fréchet derivative is

$$\begin{aligned} \delta J &= \lim_{\epsilon\to 0} \frac{J_\epsilon - J_0}{\epsilon} \\ &= \int_0^{1+T} u'(t)Rv(t) + \lambda'(t)\left(\eta(t) - \eta(t-T) - v(t)\right)\,dt \\ &\quad + \int_1^{1+T} \nu'(t)\eta(t)\,dt \\ &= \int_0^{1+T} (Ru(t) - \lambda(t))'\,v(t)\,dt - \int_{-T}^{0} \lambda'(t+T)\eta(t)\,dt \\ &\quad + \int_0^{1} (\lambda(t) - \lambda(t+T))'\,\eta(t)\,dt + \\ &\quad \int_1^{1+T} (\nu(t) + \lambda(t))'\,\eta(t)\,dt \end{aligned}$$

Since $x(t)$ is given in $[-T, 0]$, $\eta(t) = 0$, $t \in [-T, 0]$ and in order to avoid computing η we *choose*

$$\begin{aligned} \lambda(t) &= \lambda(t+T),\, t \in (0,1)\,, \\ \lambda(t) &= -\nu(t),\, t \in [1, 1+T] \end{aligned}$$

which is (170). The Frèchet derivative is

$$\delta J = \int_0^{1+T} \left(Ru(t) - \lambda(t)\right)' \delta u(t)\, dt$$

and the stationary condition implies that

$$u(t) = R^{-1}\lambda(t),\, t \in [0, 1+T]\,.$$

■

6.1.4 Indirect method

We now reconsider the quasi-periodic raccordation based on the indirect method. As we will be dealing with T-periodic functions we first review the notion of dynamic phasors.

6.1.4.1 Dynamic Phasors

In this section we review the notion of dynamic phasors. We follow the notation in [49, 16].

Let $x \in L_2[t, t-T] = \left\{x | \int_{t-T}^{t} \|x(t)\|^2 dt < \infty\right\}$ and the sliding Fourier coefficients are defined as

$$\begin{aligned} \langle x \rangle_k (t) &= \frac{1}{T} \int_{t-T}^{t} x(\tau) e^{-jk\omega\tau}\, d\tau & (173) \\ &= \frac{1}{T} \int_{-T}^{0} x(t+\tau) e^{-jk\omega(t+\tau)}\, d\tau. & (174) \end{aligned}$$

After taking the derivative with respect to t, we obtain

$$\frac{d}{dt} \langle x \rangle_k (t) = \langle \dot{x} \rangle_k - jk\omega \langle x \rangle_k (t),\, k \in \mathbb{Z}. \quad (175)$$

Observe that this relationship relates the time domain dynamics of $x(t)$ to that of $\{\langle x\rangle_k(t)\}_{k=-\infty}^{\infty}$, the dynamics of the Fourier coefficients. Another useful relationship between x and $\dot{x}$ may be obtained by integrating (174) by parts;

$$\langle x\rangle_k(t) = \frac{1}{jk\omega}\left(\frac{1}{T}\left(x(t-T)-x(t)\right)e^{-jk\omega t} + \langle \dot{x}\rangle_k(t)\right) \tag{176}$$

for $k \neq 0$. The first term comes from the discontinuity of $x(t-T)$ and $x(t)$ in the periodic extension of $x(\tau)$, $\tau \in (t-T, t]$. This results in a Dirac distribution in the classical Fourier analysis. Eliminating $\langle x\rangle_k$from (175) using (176), we obtain

$$\frac{d}{dt}\langle x\rangle_k(t) = \frac{1}{T}\left(x(t)-x(t-T)\right)e^{-jk\omega t},\ k \neq 0 \tag{177}$$

From (175) it is clear that for $k = 0$

$$\begin{aligned}\frac{d}{dt}\langle x\rangle_0(t) &= \langle \dot{x}\rangle_0 \\ &= \frac{1}{T}\int_{-T}^{0}\dot{x}(t+\tau)\,d\tau \\ &= \frac{1}{T}\left(x(t)-x(t-T)\right)\end{aligned}$$

Hence,

$$\frac{d}{dt}\langle x\rangle_k(t) = \frac{1}{T}(x(t)-x(t-T))e^{-jk\omega t},\ k \in \mathbb{Z}. \tag{178}$$

This shows that the dynamics of the Fourier coefficients $\{\langle x\rangle_k(t)\}_{k=-\infty}^{\infty}$ is controlled by the discontinuity of x at the boundaries of the sliding window $(t-T, t]$. The steady state of the dynamics of $\langle x\rangle$ consists of all $T-$periodic orbits (if they exist) since $\frac{d}{dt}\langle x\rangle_k(t) = 0$, $k \in \mathbb{Z}$ if and only if $x(t-T) = x(t), \forall t \in \mathbb{R}$.

6.1.4.2 Fourier synthesis

In this section we discuss the issue of synthesis from the dynamic phasors. From (176) the Fourier coefficients reconstitute a signal $\hat{x}(\tau)$, $\tau \in (t-T, t]$:

$$\begin{aligned}
\hat{x}_t(\tau) &= \langle x \rangle_0 (t) + \sum_{k \neq 0} \langle x \rangle_k (t) e^{j\omega k \tau}, \ \tau \in (t-T, t] \\
&= \langle x \rangle_0 (t) + \sum_{k \neq 0} \frac{1}{jk\omega} \langle \dot{x} \rangle_k (t) e^{j\omega k \tau} + \sum_{k \neq 0} \frac{1}{jk\omega} \frac{1}{T} \left(x(t-T) - x(t) \right) e^{jk\omega(\tau - t)} \\
&= \langle x \rangle_0 (t) + \sum_{k \neq 0} \frac{1}{jk\omega} \langle \dot{x} \rangle_k (t) e^{j\omega k \tau} - \sum_{k \neq 0} \frac{1}{jk\omega} \frac{d}{dt} \langle x \rangle_k (t) e^{jk\omega\tau} \\
&= x_t^r(\tau) + x_t^s(\tau), \qquad (179)
\end{aligned}$$

where

$$\begin{aligned}
x_t^r(\tau) &= \langle x \rangle_0 (t) + \sum_{k} \frac{1}{j\omega k} \langle \dot{x} \rangle_k (t) e^{jk\omega\tau} \\
x_t^s(\tau) &= \sum_{k \neq 0} \frac{1}{jk\omega} \frac{1}{T} \left(x(t-T) - x(t) \right) e^{jk\omega(\tau - t)} \\
&= \frac{1}{T} \left(x(t-T) - x(t) \right) \sum_{k \neq 0} \frac{1}{jk\omega} e^{jk\omega(\tau - t)}
\end{aligned}$$

Observe that $x_t^r(\tau)$ is the reconstitution of the regular (continuous) part of x while $x_t^s(\tau)$ is the reconstitution of the impulsive part; this impulsive part is caused by the discontinuity of x at t or, equivalently, at $t-T$ as the domain of the synthesis is the circle $\mathbb{R}/\mathbb{Z}T$, where t and $t-T$ are identified. $x_t^s(\tau)$ converges to a straight line with 'slope' $\frac{1}{T}\left(x(t-T) - x(t)\right)$ on $(t-T, t]$ in the L_2 sense. In hindsight the previous decomposition is rather obvious; $x(t)$, $t \in (t-T, t]$, may be written as the sum of a straight line connecting $x(t-T)$ and $x(t)$ with a slope $\frac{1}{T}\left(x(t-T) - x(t)\right)$ and a function that is continuous at $t-T$ and t, where $t-T$ and t are identified.

The following facts are obvious: (1) $x_t^s(t - \frac{T}{2}) = 0$; (2) $\tau = t, t-T$, $x_t^s(\tau) = 0$ as the

Fourier series converges to the average of a discontinuity. This implies that $\hat{x}(\tau)|_{\tau=t}$ will have an error of $\left\| \frac{x(t-T)-x(t)}{2T} \right\|$ from the original signal $x(t)$; thus, $\hat{x}(\tau)|_{\tau=t} \neq x(t)$ in general. After a change of variable $\tau \to \tau + t$ in the synthesis

$$\hat{x}(\tau) = \sum_{k=-\infty}^{\infty} x_k(t) e^{jk\omega\tau},\ t - T \leq \tau \leq t, \tag{180}$$

we obtain

$$\hat{x}(t+\tau) = \sum_{k=-\infty}^{\infty} \langle x \rangle_k (t) e^{jk\omega(t+\tau)},\ -T \leq \tau \leq 0,$$

which shows that $\langle x \rangle_k (t)$ for *all* $k \in \mathbb{Z}$ are the the Fourier coefficients of the history of the trajectory $x(t)$ in $(t-T, t]$.

We now consider the periodic raccordation in Section 6.1.1 using the indirect method in Section 5.1.2. Recall that $\mathcal{O} = \mathcal{T}_T - \mathbf{I}$ and $\mathcal{X} = \ker \mathcal{O}$, and since each $x \in \mathcal{X}$ is $T-$ periodic, we parameterize $\mathcal{X}$ (assuming each x satisfies the usual regularity assumptions of Fourier analysis) via the Fourier coefficients $\langle x \rangle_k = \frac{1}{T} \int_0^T x(\tau) e^{jk\omega\tau}\, d\tau$. This constitutes the global map ϕ in the framework of Section 5.1.2. Let the local map be the sliding Fourier expansion (173), then the indirect method reduces to

$$\min_{\{\langle x \rangle_k\}_{k \in \mathbb{Z}}} \int_0^1 \sum_{k=-\infty}^{\infty} \left\| \frac{d \langle x \rangle_k (t)}{dt} \right\|_{R_k}^2 dt,\ R_k \succ 0, \tag{181}$$

subject to $\langle x \rangle_k (t) = \langle x_i \rangle_k$, $t \in (-\infty, 0]$ and $\langle x \rangle_k (t) = \langle x_f \rangle_k$, $t \in [1, \infty)$, $k \in \mathbb{Z}$, where x_i and x_f are two $T-$periodic orbits for which the raccordation is sought. The solution is $\langle x \rangle_k (t) = \langle x \rangle_k (0)(1-t) + \langle x \rangle_k (1) t$, $t \in [0, 1]$.

In light of the discussions in Section 6.1.4.1, $\frac{d\langle x \rangle_k (t)}{dt} \equiv 0$, $t \in (-\infty, 0] \cup [1+T, \infty)$. Hence, the raccordation has the interpretation of connecting two trajectories in a quasi-stationary fashion since it minimizes the change in its parameters, the Fourier

coefficients. By introducing a change of variable: $\frac{d\langle x\rangle_k(t)}{dt} = \langle u\rangle_k(t)$, we recognize this as a infinite dimensional LQ terminal controller problem. The dynamics of $\langle x\rangle_k(t)$ are decoupled and thus may be solved individually for each $k \in \mathbb{Z}$.

It is of interest to know how the kernel method is related to the image method for both the signal and dynamic raccordation. This is summarized in the following proposition.

Proposition 6.1.5. *If x minimizes the direct method in* (143) *and* $\sum_{k=-\infty}^{\infty} R_k = R$, *then $\langle x\rangle_k(t)$, $k \in \mathbb{Z}$ minimize the indirect method in* (181).

Proof. From (178)

$$\int_I \sum_{k=-\infty}^{\infty} \left|\left| \frac{d}{dt} \langle x\rangle_k(t) \right|\right|_{R_k}^2 dt = \frac{1}{T^2} \int_I ||x(t) - x(t-T)||_R^2 \, dt$$

and the result follows immediately. ∎

The previous proposition is reminiscent of the discussions in Section 5.1.3 (cf. (118)), where it was argued that the minimum in the parameter space Θ also minimizes the change in the function space $\mathcal{Y}$. In this present context the parameterization is given by the Fourier series representation, the Fourier coefficients being the parameters. The minimum of the change of the parameters also minimizes the non-periodicity in the function space.

Although proposition (6.1.5) shows that the kernel and image methods are closely related, these two methods, nevertheless, produce different trajectories in general. Observe that the solutions to (181) are not the trajectories; they are the Fourier coefficients of the trajectories. We synthesize the trajectories via (179) and obtain

$\hat{w}_t(\tau) = (\hat{x}_t(\tau), \hat{u}_t(\tau))\,,\ \tau \in (t-T, t]$, which is a function of two parameters. A time domain behavior may be obtained by evaluating $\hat{w}_t(\tau)$ at $\tau = t$. This, however, will create an error between w and $\hat{w}_t(\tau)|_{\tau=t}$; the error has a magnitude equal to the average of the discontinuity of w at t and $t-T$ as remarked in Section (6.1.4.2). It is more appropriate to synthesize w at the mid point: $w(t) = \hat{w}_t(\tau)|_{\tau=t-\frac{T}{2}}$ as the impulsive part will not contribute to the synthesis.

6.2 Quasi-periodic raccordation II

The Gluskabi raccordations in the previous sections are all in the form of *amplitude* modulation; we connect two signals with a common period T by changing the amplitudes only. This raises the question as to how one would modify the previous approach to connect two periodic signals with different periods.

6.2.1 Direct method

Recall that (143) attempts to minimize the deviations in the amplitude only. In order to penalize the periodicity in the kernel method we adjoin the term $\int_0^{1+T_1} \left\|\dot{T}(t)\right\|^2 dt$ to (143):

$$\min_{x,T} J_0 = \frac{1}{2}\int_0^{1+T_1} ||x(t) - x(t-T(t))||_R^2 + \left\|\dot{T}(t)\right\|^2 dt$$

After introducing a change of variable as in (144) the dynamics is

$$x(t) = x(t-T(t)) + u(t) \tag{182}$$

$$\dot{T}(t) = v(t), \tag{183}$$

which is a delay system with time varying delay; u and v are now the inputs. It is argued in [53, 55] that such systems exhibit a causal behavior only if $1-\dot{T} = 1-v > 0$.

This, in turn, causes another problem as a minimum might not exist when the control parameter is constrained in an open set (we can only infimize in this case). Therefore, we reformulate the problem:

$$\min_{u,v} \int_0^{1+T_1} \|u(t)\|^2 + \rho\|v(t)\|^2 \, dt, \tag{184}$$

subject to the dynamics in (182) and (183) with $v \leq 1 - \epsilon,$ for some small $\epsilon > 0$. The boundary conditions are $T(t) = T_0$, $x(t) = x_0(t)$, $t < 0,$ and $T(t) = T_1$, $x(t) = x_1(t)$, $t > 1$. Since the optimal solution in (182) involves the variation in the argument of x, we now seek a suboptimal solution. Observe that $T(t) \in \mathbb{R}$, which is one dimensional, hence the straight line

$$T(t) = \begin{cases} T_0, & t < 0 \\ T_0(1-t) + T_1 t, & t \in [0,1] \\ T_1, & t > 1 \end{cases} \tag{185}$$

minimizes the second term in (184), assuming that $\dot{T} = T_1 - T_0 < 1 - \epsilon$, $\epsilon > 0$. This is, in general, the case as we require $T_0, T_1 << 1$ for a quasi-stationary transition in the Gluskabi raccordation.

Finally, a suboptimal solution to the quasi-periodic raccordation in (182) is as follows:

$$\begin{aligned} \min_u J_0 &= \int_0^{1+T_1} \|u(t)\|_R^2 \, dt \text{ subject to} \\ x(t) &= x(t - T(t)) + u(t), \\ x_0(t) &= x_0(t - T_0),\ t \leq 0, \\ x_1(t) &= x_1(t + T_1),\ t \geq 1, \end{aligned} \tag{186}$$

with $T(t)$ in (185).

Using similar technique as in (143) the optimality conditions are readily obtained:

Proposition 6.2.1. *The stationary condition of the optimization problem in* (186) *is*

$$u(t) = R^{-1}\lambda(t),\ t \in [0, 1+T_1]. \tag{187}$$

where the costate equations satisfy

$$\begin{aligned} \lambda(\tau) &= \frac{1}{1-\dot{T}}\lambda\left(\frac{\tau+T_0}{1-\dot{T}}\right),\ \tau \in [0, 1-T_1), \\ \lambda(t) &= \lambda(t+T_1),\ t \in [1-T_1, 1), \\ \lambda(t) &= -\nu(t),\ t \in [1, 1+T_1]. \end{aligned} \tag{188}$$

The unknown function $\nu(t)$ is chosen such that the final state constraints are met.

Proof. Adjoin the final constraint and the dynamics via ν and λ, respectively, to the performance index

$$J_0 = \frac{1}{2}\int_0^{1+T_1} \|u(t)\|_R^2 + \lambda'(x(t) - x(t-T(t)) - u(t))dt + \int_1^{1+T_1} \nu'(t)(x(t) - x_1(t))dt \tag{189}$$

Perturbing J_0 via $u \to u + \epsilon v$ and $x \to x + \epsilon\eta$ the Frechet derivative is

$$\begin{aligned} \delta J &= \int_0^{1+T_1} (Ru(t) - \lambda(t))'v(t)\,dt + \int_0^{1+T_1} \lambda'(t)\eta(t) - \lambda'(t)\eta(t-T(t))\,dt + \\ &+ \int_1^{1+T_1} \nu'(t)\eta(t)\,dt \end{aligned} \tag{190}$$

With the change of variable $\tau = t - T(t) = (1-\dot{T})t - T_0$, $t \in [0,1]$ and $\tau = t - T_1$, $t \in [1, 1+T_1]$ the third term simplifies to

$$\begin{aligned} & \int_0^{1+T_1} \lambda'(t)\eta(t-T(t))dt \\ = & \int_0^1 \lambda'(t)\eta(t-T(t))dt + \int_1^{1+T_1} \lambda'(t)\eta(t-T_1)dt \\ = & \frac{1}{1-\dot{T}}\int_{-T_0}^{1-T_1} \lambda'\left(\frac{\tau+T_0}{1-\dot{T}}\right)\eta(\tau)d\tau + \int_{1-T_1}^1 \lambda'(\tau+T_1)\eta(\tau)d\tau. \end{aligned}$$

$$\begin{aligned}\delta J &= \int_0^{1+T_1} (Ru(t) - \lambda(t))' v(t)\, dt + \int_0^{1-T_1} \left(\lambda(\tau) - \frac{1}{1-\dot{T}}\lambda\left(\frac{\tau+T_0}{1-\dot{T}}\right)\right)' \eta(\tau) d\tau \\ &+ \int_{1-T_1}^{1} \left(\lambda(\tau) - \lambda\left(\tau + T_1\right)\right)' \eta(\tau)\tau + \int_1^{1+T_1} \left(\lambda(\tau) + \nu(\tau)\right)' \eta(\tau) d\tau\end{aligned} \tag{191}$$

We *choose*

$$\begin{aligned}\lambda(\tau) &= \frac{1}{1-\dot{T}}\lambda\left(\frac{\tau+T_0}{1-\dot{T}}\right),\ \tau \in [0, 1-T_1] \\ \lambda(t) &= \lambda(t+T_1),\ t \in [1-T_1, 1] \\ \lambda(t) &= -\nu(t),\ t \in [1, 1+T_1].\end{aligned}$$

and the stationary condition is

$$u(t) = R^{-1}\lambda(t),\ t \in [0, 1+T_1]$$

Hence, the closed loop system is

$$x(t) = x(t - T(t)) + \lambda(t) \tag{192}$$

■

Remark 6.2.1. *If $\dot{T} = 0$, equivalently, $T_0 = T_1$ we recover* (170)*.*

In order to see that the previous scheme achieves the desired frequency modulation we will consider a special case of (186). Indeed, (186)) is minimal if $u(t) \equiv 0$ or equivalently, $x(t) = x(t - T(t))$. We now construct an x such that the final state constraint is also satisfied. Denote $g(t) = t - T(t)$ and let $g(t_1) = 0$, $g(t_2) = t_1$, $g(t_3) =$

$t_2, \ldots, g(t_n) = t_{n-1}$. It is easily shown that

$$t_n = \sum_{k=1}^{n} \frac{T_0}{(1-\dot{T})^k}. \tag{193}$$

Choose T_0, T_1 and some positive integer N such that $\frac{T_0}{(1-\dot{T})^N} = T_1$ $t_N = \sum_{k=1}^{N-1} \frac{T_0}{(1-\dot{T})^k} +$ $T_1 = 1$, then we may explicitly compute $x(t) = x(t - T(t))$, $t \in (0, 1 + T_1]$ for a given T_0 periodic $x_0(t)$. Let the initial condition be $x(t) = x_0(t)$, $t \in [-T_0, 0]$ and

$$\begin{aligned}
x(t) &= x_0(t - T(t)) = x_0(g(t)),\ t \in (0, t_1] \\
x(t) &= = x_0(g \circ g(t)),\ t \in (t_1, t_2] \\
&\vdots \\
x(t) &= x_0(g^N(t)),\ t \in (t_{N-1}, t_N] = (1 - T_1, 1] \\
x(t) &= x_0(g^N(t - T_1)),\ t \in (1, 1 + T_1].
\end{aligned}$$

If the final state constraint is

$$x_1(t) = x_0(g^{N+1}(t)), t \in (1, 1 + T_1], \tag{194}$$

then all necessary conditions optimality are satisfied and this x is optimal. The idea is to squash (or extend depending on T_0 and T_1) and shift the initial condition x_0 to fit in the intervals $(t_k, t_{k+1}]$, $k = 1$, $k = 1, \ldots, N$. (see Figure 45) Observe that

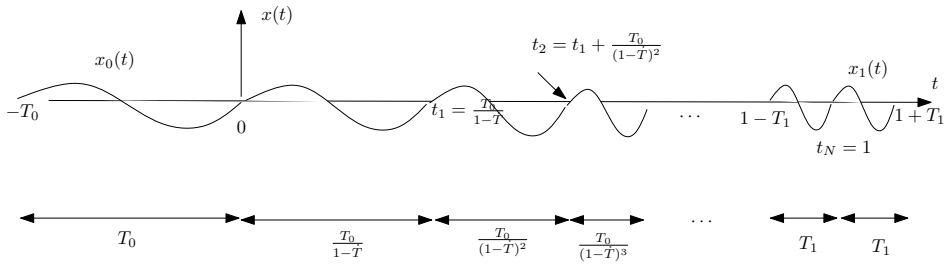

Figure 45: $\dot{T} = (T_1 - T_0) < 0$

x exhibits a frequency modulation (FM). However, for arbitrary T_0 and T_1 $x(t)$ has both FM and AM behavior. If $T_0 = T_1 = T$, then the x is constructed by patching only shifted versions of x_0; no scaling of the function is necessary. This is exactly the case in (143).

6.2.2 Gradient descent algorithm

In this section we derive a gradient descent algorithm based on the technique developed in the previous sections. A technical difficulty, however, arises in a direct extension of previous ideas. Specifically, let dt be the quantization step size of the time axis; $t = kdt$, $k \in \mathbb{Z}$ and the corresponding discretization of $T(t)$ is $T(t) = \dot{T}kdt + T_0$. However, this needs to be quantized to a integer to express the delay in integer *samples*, and in turn introduces an error Δ or $T(t) = \hat{T}(t) + \Delta(t)$, where $\hat{T}(t)$ is the quantized value of $T(t)$. The quantized dynamics is

$$\begin{aligned} x(kdt) &= x(kdt - (\hat{T}(kdt) + \Delta(kdt))) + u(kdt) \\ &\approx x(kdt - \hat{T}(kdt)) - \dot{x}(kdt - \hat{T}(kdt))\Delta(kdt) + u(kdt). \end{aligned}$$

The error Δ is amplified by the hight-pass filter characteristic of the differentiation operation. In order to avoid this we regularize the problem by adding the term $\int_0^{1+T_1} \left\| \frac{d}{dt} \left(x(t) - x(t - T(t)) \right) \right\|^2$. This way the quantization error will be filtered out when x is obtained by integrating $\dot{x}$ since integration is a low-pass process.

We thus reformulate the problem:

$$\min_u J_0 = \frac{1}{2} \int_0^{1+T_1} \|x(t) - x(t - T(t))\|_P^2 + \|u(t)\|_R^2 \, dt \tag{195}$$

subject to

$$\dot{x}(t) = \begin{cases} (1-\dot{T})\dot{x}(t-T(t)) + u(t), & t \in [0,1) \\ \dot{x}(t-T_1) + u(t), & t \in [1, 1+T_1] \end{cases} \tag{196}$$

and $x(t) = x_f(t)$, $t \in [1, 1+T_1]$.

In order to derive a gradient descent algorithm for (195) we first compute the Frèchet derivative of the boundary constraint.

Proposition 6.2.2. *Let $s \in [1, 1+T_1]$ and $J_k^s = e_k' x(s)$. Then*

$$\delta J_k^s = \int_0^{1+T_1} \lambda_k^{s\prime}(t)\delta u(t)dt, \tag{197}$$

where $\forall s \in [1, 1+T_1]$

$$\begin{aligned} \dot{\lambda}_k^s(t) &= \dot{\lambda}_k^s\left(\frac{t+T_0}{1-\dot{T}}\right), t \in [0, 1-T_1), \\ \dot{\lambda}_k^s(t) &= \dot{\lambda}_k^s(t+T_1), t \in [1-T_1, 1), \\ \dot{\lambda}_k^s(t) &= 0, t \in [1, 1+T_1), t \neq s. \end{aligned}$$

The boundary conditions for $s \in (1, 1+T_1)$ are

$$\begin{aligned} \lambda_k^s(1^- - T_1) &= \lambda_k^s(1^+ - T_1) + (1-\dot{T})\lambda_k^s(1^-) - \lambda_k^s(1^+) \\ \lambda_k^s(s^-) &= e_k + \lambda_k^s(s^+) \\ \lambda_k^s(1^-) &= \lambda_k^s(1+T_1) + \lambda_k^s(1^+) \\ \lambda_k^s(1+T_1) &= 0, \\ \lambda_k^s(1^-) &= \lambda_k^s(1^+), \end{aligned}$$

while for $s = 1$

$$\begin{aligned}
\lambda_k^s(1^-) &= e_k + \lambda_k^s(1^+) + \lambda_k^s(1+T_1), \\
\lambda_k^s(1+T_1) &= 0, \\
\lambda_k^{s\prime}(1^- - T_1) &= \lambda_k^{s\prime}(1^+ - T_1) + (1-\dot{T})\lambda_k^{s\prime}(1^-) - \lambda_k^{s\prime}(1^+),
\end{aligned}$$

and for $s = 1 + T_1$

$$\begin{aligned}
\lambda_k^s(1^-) &= \lambda_k^s(1^+) + \lambda_k^s(1+T_1) \\
\lambda_k^s(1+T_1) &= e_k \\
\lambda_k^{s\prime}(1^- - T_1) &= \lambda_k^{s\prime}(1^+ - T_1) + (1-\dot{T})\lambda_k^{s\prime}(1^-) - \lambda_k^{s\prime}(1^+).
\end{aligned}$$

Proof. See Proof (E.1) in Appendix E. ∎

The boundary conditions for $s \in (1, 1+T_1)$ imply the continuity of λ_k^s at $t = 1$; it is also easily seen that $\lambda_k^s(s^+) = 0$ and, hence, $\lambda_k^s(s^-) = e_k$. Furthermore, since $\lambda_k^s(1^-) = \lambda_k^s(1^+) = \lambda_k^s(s^-) = e_k$ we have that $\lambda_k^s(1^- - T_1) = \lambda_k^s(1^+ - T_1) - \dot{T}\lambda_k^s(s^-) = \lambda_k^s(1^+ - T_1) - \dot{T}e_k$. In other words the derivative $\lambda_k^s(t)$, $t \in [1, 1+T_1]$ contains impulses at $t = s$ and $t = 1 - T_1$ $\dot{\lambda}_k^s(t) = -e_k\delta(t-s) + \dot{T}e_k\delta(t-(1-T_1))$, $t \in [1, 1+T_1]$. The last three costates equations'propagate' the impulses backwards towards $t = 0$ forming a impulse train with a non-uniform spacing between them.

For $s = 1$, $\lambda_k^s(1+T_1) = \lambda_k^s(1^+) = 0$ and thus $\lambda_k^s(1^-) = e_k$, and $\lambda_k^s(1^- - T_1) = \lambda_k^s(1^+ - T_1) + (1-\dot{T})\lambda_k^s(s^-) = \lambda_k^s(1^+ - T_1) + (1-\dot{T})e_k$. Subsequently, we have $\dot{\lambda}_k^s(t) = -e_k\delta(t-s) - (1-\dot{T})e_k\delta(t-(1-T_1))$, $t \in [1, 1+T_1]$.

Finally, for $s = 1 + T_1$ we have $\lambda_k^s(t) \equiv e_k$, $t \in [1^+, 1 + T_1]$. Hence, $\lambda_k^s(1^-) = \lambda_k^s(1^+) + e_k$, $\lambda_k^s(1^-) = 2e_k$ and, subsequently, $\lambda_k^s(1^- - T_1) = \lambda_k^s(1^+ - T_1) + (1 - 2\dot{T})\lambda_k^s(s^-) = \lambda_k^s(1^+ - T_1) + (1 - 2\dot{T})e_k$. Therefore, $\dot{\lambda}_k^s(t) = -e_k\delta(t-1) - (1 - 2\dot{T})e_k\delta(t - (1 - T_1))$, $t \in [1, 1 + T_1]$.

We now proceed to consider the Fréchet derivative of (195) *without* the final state constraints. To conform to the notations in the algorithm (6.1.2) we will denote the performance index in (195) by J_v.

Proposition 6.2.3. *The Fréchet derivative of* (195) without *the final state constraints is*

$$\delta J_v = \int_0^{1+T_1} \left(u'(t)R + {\lambda_v}'(t)\right) \delta u(t) dt, \tag{198}$$

where

$$\begin{aligned}
\dot{\lambda}_v'(t) &= -\left(x(t) - x(t - T(t)) - \frac{1}{1-\dot{T}}\left(x\left(\frac{t+T_0}{1-\dot{T}}\right) - x(t)\right)\right)' P + \\
&\quad \dot{\lambda_v}'\left(\frac{t+T_0}{1-\dot{T}}\right),\ t \in [0, 1 - T_1), \\
\dot{\lambda}_v'(t) &= -\left(2x(t) - x(t - T(t)) - x(t + T_1)\right)' P + \dot{\lambda}_v'(t + T_1),\ t \in [1 - T_1, 1), \\
\dot{\lambda}_v'(t) &= -(x(t) - x(t - T_1))' P,\ t \in [1, 1 + T_1).
\end{aligned}$$

The boundary conditions are $\lambda_v(1 + T_1) = 0$, ${\lambda_v}'(1^-) = {\lambda_v}'(1^+) + \lambda_v(1 + T_1)$ *and* $-\lambda_v'(1^- - T_1) + \lambda_v'(1^+ - T_1) + (1 - \dot{T}){\lambda_v}'(1^-) - {\lambda_v}'(1^+) = 0$.

Proof. See Proof (E.2) in Appendix E. ∎

As in Algorithm (6.1.1) we discretize the final section $x(t) = x_f(t)$, $t \in [1, 1 + T_1]$ by setting $s_0 = 1$, $s_i = s_0 + idt$, $i = 0, \ldots, N$ where dt is the time step.

Algorithm 6.2.1. *Let $I = [0, 1 + T_1]$ be the simulation interval and $x(t) = x_0(t), t \in [-T_0, 0]$.*

1. *Guess an input $u(t)$, $t \in [0, 1 + T_1]$.*

2. *Compute the dynamics (196) forward for $t \in [0, 1 + T_1]$.*

3. *Compute the costate equations λ_k^s, for $s = s_i, i = 0, \ldots, N$ in Proposition (6.2.2).*

4. *Compute λ_v in Proposition (6.2.3) with $\lambda_v(1 + T_1) = 0$.*

5. *Compute the boundary mismatch: $\Delta x(s_l) = x(s_l) - x_f(s_l)$, $l = 0, \ldots, N$.Set $\delta J_k^{s_l} = e_k' \delta x(s_l)$, $l = 0, \ldots, N$, where $\delta x(s_l) = -k_2 \Delta x(s_l)$, $0 < k_2 \leq 1$. Form the following:*

$$\begin{aligned}
\delta \boldsymbol{J}_j &= \left[\begin{array}{cccc} \delta J_j^{s_0}, & \delta J_j^{s_1}, & \ldots, & \delta J_j^{s_N} \end{array} \right]', \qquad (199) \\
\boldsymbol{U}_j &= \left[\begin{array}{cccc} \int_0^{1+T} \lambda_j^{s_0\prime}(t) \left(Ru(t) + \lambda_v(t) \right) dt, & \ldots, & \int_0^{1+T} \lambda_j^{s_N\prime}(t) \left(Ru(t) + \lambda_v(t) \right) dt \end{array} \right]', \\
\boldsymbol{\Lambda}_j &= \left[\begin{array}{cccc} \lambda_j^{00}, & \lambda_j^{10}, & \ldots, & \lambda_j^{N0} \\ \lambda_j^{01}, & \lambda_j^{11}, & \ldots, & \lambda_j^{N1} \\ \vdots & & \ddots & \\ \lambda_j^{0N}, & \lambda_j^{1N}, & \ldots, & \lambda_j^{NN}, \end{array} \right], \lambda_j^{li} = \int_0^{1+T} \lambda_j^{s_l\prime}(t) \lambda_j^{s_i}(t) dt
\end{aligned}$$

6. *Compute the input gradient:*

$$\delta u(t) = -k_1 \left(\left(Ru(t) + \lambda_v(t) \right) - \sum_{k=1}^{n} \boldsymbol{U}_k' \boldsymbol{\Lambda}_k^{-1} \boldsymbol{\lambda}_k(t) \right) + \sum_{k=1}^{n} \delta \boldsymbol{J}_k' \boldsymbol{\Lambda}_k^{-1} \boldsymbol{\lambda}_k(t), \quad (200)$$

where

$$\boldsymbol{\lambda}_k(t) = \left[\begin{array}{cccc} \lambda_k^{s_0}(t), & \lambda_k^{s_1}(t), & \ldots, & \lambda_k^{s_N}(t) \end{array} \right]'$$

7. *Update* u *by* $u_{new}(t) = u(t) + \delta u(t)$.

8. *Repeat step 2 with the new input* $u_{new}(t)$.

The derivation of the previous algorithm can be found in Proof E.3 in Appendix E.

Example 6.2.1. *As an example of the previous algorithm we construct the raccordation of the sinusoids* $\sin(\frac{2\pi}{T_i}t)$, $i = 0, 1$, *where* $T_0 = 0.1$ *and* $T_1 = 0.3$. *Figure (46) shows the raccordation* $x(t)$ *while Figure (47) shows the magnitude of the gradient.*

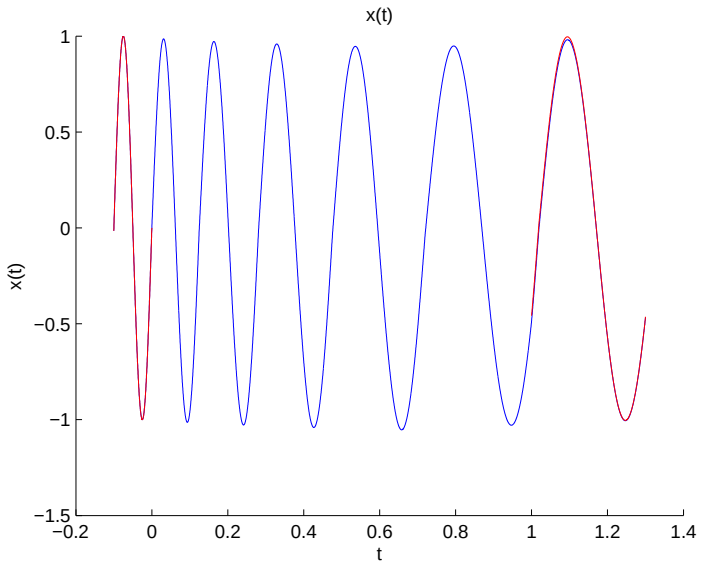

Figure 46: $x(t)$

6.2.2.1 The continuous case: $\Delta \to 0$

The previous algorithm is constructed, as in Section 6.1.3.1, by first approximating the final section $x_f(t)$ in $\mathcal{I} = [1, 1 + T_1]$ with a finite set by discretizing $\mathcal{I}$. We now turn our attention to the original problem.

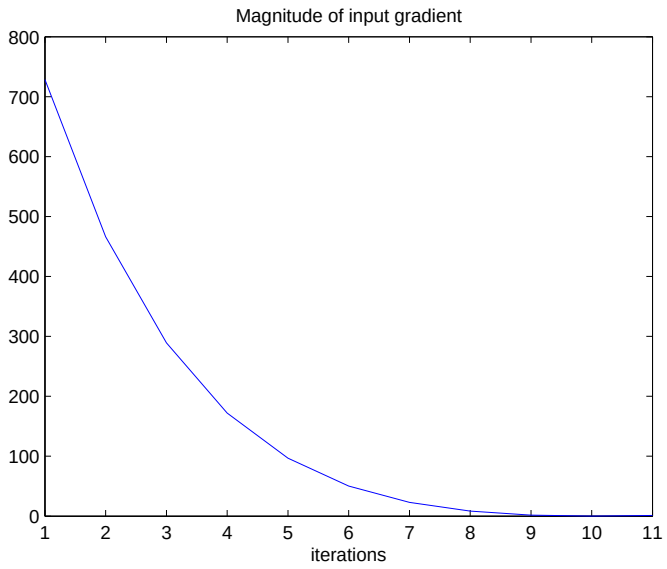

Figure 47: Magnitude of input gradient δu

As before let us introduce a change of notation in Proposition (6.2.2): $J_k^s \to J_k(s)$ and $\lambda^s(t) \to \lambda(t,s)$ Adjoin $\delta J_k(s)$ via the scalar functions $\nu_k(s)$, $s \in [1, 1+T], k = 1, \ldots, n$ to δJ_v:

$$\begin{aligned} & \delta J_v + \int_1^{1+T} \sum_{k=1}^{n} \nu_k(s) \delta J_k(s) ds \\ = & \int_0^{1+T_1} \left(u'(t)R + {\lambda_v}'(t)\right) \delta u(t) dt + \int_1^{1+T} \sum_{k=1}^{n} \nu_k(s) \left(\int_0^{1+T} \lambda_k'(t,s) \delta u(t) dt \right) ds \\ = & \int_0^{1+T} \left(Ru(t) + \lambda_v(t) + \sum_{k=1}^{n} \int_1^{1+T} \nu_k(s) \lambda_k(t,s) ds \right)' \delta u(t) dt \end{aligned} \tag{201}$$

If

$$\delta u(t) = -\left(Ru(t) + \lambda_v(t) + \sum_{k=1}^{n} \int_1^{1+T} \nu_k(s) \lambda_k(t,s) ds \right), \; t \in [0, 1+T_1], \tag{202}$$

then (201) is negative, hence improving, unless the integrand is zero and, in addition, the constraints are satisfied: $\delta J_k(s) \equiv 0$, $s \in [1, 1+T]$, $k = 1, \ldots, n$. To obtain the

Frèchet derivative of the final state constraint we substitute (202) into (197)

$$\begin{aligned}\delta J_k(s) &= \int_0^{1+T} \lambda_k'(t,s)\left(Ru(t)+\lambda_v(t)+\sum_{j=1}^{n}\int_1^{1+T}\nu_j(r)\lambda_j(t,r)dr\right)dt \qquad (203)\\ &= \underbrace{\int_0^{1+T}\lambda_k'(t,s)\left(Ru(t)+\lambda_v(t)\right)dt}_{U_k(s)}+\sum_{j=1}^{n}\int_1^{1+T}\nu_j(r)\underbrace{\int_0^{1+T}\lambda_k'(t,s)\lambda_j(t,r)dt}_{\Lambda_{kj}(s,r)}dr,\end{aligned}$$

and in matrix notation

$$\begin{aligned}\delta J(s) &= U(s)+\int_1^{1+T}\Lambda(s,r)\nu(r)dr,\\ &= U(s)+G\nu(s).\end{aligned}$$

If G is invertible, the unknown function $\nu(s)$, $s\in[1,1+T]$ can be explicitly solved for via

$$\nu(s)=G^{-1}\left(U+\delta J\right)(s).$$

Denote the integral term in (202)

$$\hat{\lambda}(t)=\sum_{k=1}^{n}\int_1^{1+T}\nu_k(s)\lambda_k(t,s)ds.$$

In light of the discussion after Proposition (6.2.2)

$$\begin{aligned}\frac{d\hat{\lambda}(t)}{dt} &= \sum_{k=1}^{n}\int_1^{1+T}\nu_k(s)\frac{d\lambda_k(t,s)}{dt}ds,\\ &= \sum_{k=1}^{n}\int_1^{1+T}\nu_k(s)e_k\delta(s-t)ds,\\ &= \sum_{k=1}^{n}\nu_k(t)e_k,\end{aligned}$$

for $t\in[1,1+T_1]$. As the costate equation in Proposition (6.2.2) 'propagates' the impulse at $t=s$ towards to $t=0$, scaled versions of $\frac{d\hat{\lambda}(t)}{dt}$, $t\in[1,1+T_1]$ are replicated

to the left. In light of (202) and the linearity of costate equations in Proposition 6.2.2 and Proposition 6.2.3 we may equivalently define

$$\begin{aligned}
\dot{\lambda}'(t) &= -\left(x(t) - x(t-T(t)) - \frac{1}{1-\dot{T}}\left(x\left(\frac{t+T_0}{1-\dot{T}}\right) - x(t)\right)\right)' P + \\
&\quad \dot{\lambda}'\left(\frac{t+T_0}{1-\dot{T}}\right),\ t \in [0, 1-T_1), \qquad (204)\\
\dot{\lambda}'(t) &= -\left(2x(t) - x(t-T(t)) - x(t+T_1)\right)' P + \dot{\lambda}'(t+T_1),\ t \in [1-T_1, 1),\\
\dot{\lambda}'(t) &= -\nu(t) - (x(t) - x(t-T_1))'P,\ t \in [1, 1+T_1).
\end{aligned}$$

with the boundary conditions $\lambda(1+T_1) = \nu(1+T_1)$, $\lambda(1^-) = \nu(1^+) + \lambda(1^+) + \lambda(1+T_1)$ and $-\lambda'(1^- - T_1) + \lambda'(1^+ - T_1) + (1-\dot{T})\lambda'(1^-) - \lambda'(1^+) = 0$.

This allows us the redefine the costate equation and we summarize the previous calculations in the following proposition.

Proposition 6.2.4. *The necessary conditions of optimality of (195) are obtained by adjoining* $J_c = \int_1^{1+T_1} \nu'(t)(x(t) - x_1(t))dt + \nu'(1)(x(1) - x_1(1^+)) + \nu'(1+T_1)(x(1+T_1) - x_1(1+T_1))$ *to* J_0. *Indeed, the optimal* $u(t)$ *satisfies* $u(t) = -R^{-1}\lambda(t)$, $t \in [0, 1+T]$, *where* $\lambda(t)$ *satisfies (204). The unknown function* $\nu(t)$, $t \in [1, 1+T_1]$ *needs to chosen such that the final constraint is met.*

Proof. The result follows immediately by adjoining the Fréchet derivative of J_c,

$$\int_1^{1+T_1} \nu'(t)\eta(t)dt + \nu'(1)\eta(1) + \nu'(1+T_1)\eta(1+T_1)$$

to (296). ∎

6.2.3 Indirect method

How does one modify the indirect method in Section 6.1.4 to accommodate the quasi-peirodic raccordation of two signals of different periods? Recall that the indirect

method minimizes the change of the trajectory in Θ, $\{\langle x\rangle_k(t)\}_{k=-\infty}^{\infty}$, $\mathcal{T}=[0,1]$, connecting $\{\langle x_0\rangle_k\}_{k=-\infty}^{\infty}(t)$, $t<0$ and $\{\langle x_1\rangle_k\}_{k=-\infty}^{\infty}(t)$, $t>1$. (cf. (181))

In extending the previous method to the quasi-periodic raccordation at hand we encounter several difficulties. First of all, since the fundamental periods T_0 and T_1 of x_0 and x_1, respectively, are different in this case, it is not clear what the fundamental period T in the Fourier basis $e^{j\frac{2\pi}{T}kt}$, $k\in\mathbb{Z}$ is. If $\frac{T_0}{T_1}=\frac{p}{q}$, $p,q\in\mathbb{N}$, $q\neq 0$, is rational and coprime, then x_i, $i=0,1$ are periodic with the fundamental period $T=qT_0=pT_1$; we have reduced the indirect method to(181). The $T-$ periodicity of x_i, $i=0,1$ implies that $\frac{d}{dt}\langle x_i\rangle_k\equiv 0$, $k\in\mathbb{Z}$, $i=0,1$, and hence we may interpret this, similar to Section 6.1.4, as a quasi-stationary transition between two stationary states in the parameter space, the Hilbert Space L_2. This, unfortunately, fails if $\frac{T_0}{T_1}$is irrational.

To circumvent this impasse we may first write $\frac{T_0}{T_1}=\frac{p}{q}+r$ for some p, $q\in\mathbb{N}$, $q\neq 0$, $r\in\mathbb{R}$ with p and q coprime. With $T=qT_0$ the raccordation via the indirect method is the optimization problem:

$$\min_{\{\langle x\rangle_k\}_{k\in\mathbb{Z}}}\int_0^1\sum_{k=-\infty}^{\infty}\left\|\frac{d}{dt}\langle x\rangle_k(t)\right\|_{R_k}^2 dt,\ R_k\succ 0,\ k\in\mathbb{Z},\tag{205}$$

subject to the boundary conditions: $\langle z\rangle_k(t)=\left(\langle x_0\rangle_k(t),\frac{d}{dt}\langle x_0\rangle_k(t)\right)$, $t<0$ and $\langle z\rangle_k(t)=\left(\langle x_1\rangle_k(t),\frac{d}{dt}\langle x_1\rangle_k(t)\right)$, $t>1$ for $k\in\mathbb{Z}$. In light of (178) $\frac{d}{dt}\langle x_0\rangle_k(t)\equiv 0$, $t<0$, and $\frac{d}{dt}\langle x_1\rangle_k(t)\neq 0$, $t>1$, $k\in\mathbb{Z}$; the magnitude of $\frac{d}{dt}\langle x_1\rangle_k(t)$, however, retains the period of T_1. Unlike the raccordation in (181) the non-vanishing derivative of the Fourier coefficients of the target orbit need to be attained as well. In general it is advantageous to choose a T such that the sliding window $(t-T,t]$ contains several periods of x_1.

Finally, the raccordation is obtained by evaluating the Fourier synthesis sum at half-period delay point, $\tau = t - \frac{T}{2}$ as discussed at the end of Section 6.1.4; this way the singular part has no effect on the reconstruction.

6.3 Conclusion

In anticipating the upcoming chapter we applied the framework of the Gluskabi raccordation to the quasi-periodic raccordation *without* dynamical constraint. We considered two cases. In the first case the periodic signals have the same period while the second case involves periodic signals of two different periods. Specifically, for each case we considered both the direct and indirect method, and the relationships between these methods were explored.

For the direct method we have provided detailed derivations for the gradient descent algorithms needed to generate the Gluskabi raccordation. The main idea is to discretize the final state constraint and then decompose the optimization problem into two sub-problems. The first sub-problem is the original optimization problem in the *absence* of the final state constraints while the second sub-problem involves the computation of the Fréchet derivatives of the final state constraints. The general procedure is outlined in Algorithm 6.1.2. For the quasi-periodic raccordation between two periodic signals of two different periods the algorithm needs to be preceded by a regularization procedure in order to avoid a round-off error build-up caused by the quantization of $T(t)$.

On the other hand, the indirect method involves the notion of dynamic phasors, and the resulting dynamics evolve in the infinite dimensional parameter space, the

Hilbert space l_2. By using a basic property of the dynamic phasor we elucidated the relationship between the direct and indirect method (cf. Proposition 6.1.5).

CHAPTER VII

DYNAMIC GLUSKABI RACCORDATION

In the previous chapter we explored the signal raccordation. Specifically, this is the Gluskabi raccordation *without* dynamic constraints. In this chapter we extend the framework to the dynamic case. Recall the signal raccordation involves an operator $\mathcal{O}$, and the direct method seeks the 'smoothest' transition between any two elements, w_i, w_f, in the nullspace of $\mathcal{O}$ by minimizing the 'deviation' from ker $\mathcal{O}$ (cf. (114)):

$$\min_{w\in\mathcal{V}} \int_0^1 \|(\mathcal{O}w)(t)\|_{\mathcal{W}}^2 \, dt \text{ subject to} \tag{206}$$
$$w(t) = w_i(t),\, t \leq 0,\ w(t) = w_f(t),\, t \geq 1,\, w_i, w_f \in \ker \mathcal{O}.$$

On the other, the indirect method involves the minimization of the change of a parameterization of ker $\mathcal{O}$.

Observe that the signal raccordation does not involve a dynamical system with an input u and an output y. In other words, the raccordation w, obtained from (206) and having the same dimension as the pair (y, u), does not satisfy this dynamics in general. However, this impasse is easily circumvented by realizing that the dynamics is nothing more than a *hard* constraint on the set of all possible raccordation. Thus, the raccordation needs to be sought in the set consisting of all trajectories that satisfy the dynamics.

In order to put the dynamic raccordation on a sound footing we find the behavioral approach of modeling dynamical systems developed in [44, 61] particularly appealing.

Roughly speaking, in this approach a dynamical system is modeled as a subset $\mathcal{B}$, the behavior, of a larger set $\mathcal{V}$, the set of all possible trajectories, that is consistent with the laws describing the phenomenon of interest. Any equation describing $\mathcal{B}$ is only one of the many representations of the behavior.

The dynamic Gluskabi raccordation is of interest in various robotics applications. Specifically, it is often necessary in robotics to enrich the class of gaits with *transition* modes such that the transition from one periodic motion to another (e.g. from walking to running) is as gradual as possible to mimic natural human motion [22]. In another application [39] gaits are generated by interpolating between key poses. The framework presented in this chapter may provide a way to systematically generate truly smooth motions instead of the aforementioned interpolation technique.

7.1 The direct method

In order to extend the signal raccordation in Section 5.1.1 we will take the behavioral point of view of dynamical systems by considering them as a collection of trajectories [61]. More specifically, a dynamical system is modeled as a triple

$$\Sigma = (T, \mathcal{W}, \mathcal{B}), \tag{207}$$

where T is the time axis, $\mathcal{W}$ the signal space and $\mathcal{B}$ the behavior. $\mathcal{V} = \mathcal{W}^T$ is the set of all trajectories, and the behavior $\mathcal{B} \subset \mathcal{V}$ is the set of all *possible* trajectories that are consistent with dynamical description. Let $\mathcal{O} : \mathcal{V} \to \mathcal{V}$ be an operator, then

$$\ker \mathcal{O} \cap \mathcal{B} \subseteq \mathcal{V} \tag{208}$$

contains all trajectories of the dynamical system that are also in the null space of $\mathcal{O}$.

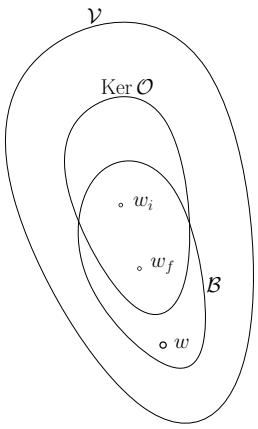

Figure 48: The dynamic Gluskabi raccordation

The dynamic Gluskabi raccordation based on the direct method is the following optimization problem:

$$\inf_{w\in\mathcal{B}} \int_{-\infty}^{\infty} \| \left(\mathcal{O}w\right)(t)\|_{\mathcal{W}}^2 \, dt \tag{209}$$

subject to

$$w_i(t) = w(t),\, t \leq 0 \text{ and } w_f(t) = w(t),\, t \geq 1,\ w_i, w_f \in \ker \mathcal{O} \cap \mathcal{B}. \tag{210}$$

The raccordation is thus the trajectory satisfying the dynamical system that minimizes the 'deviation' from $\ker \mathcal{O}$. Observe from the signal raccordation in (206) and the dynamical raccordation in (209) that the only additional 'ingredient' is the behavior $\mathcal{B}$.

Remark 7.1.1. *The optimal value in* (210) *is infinite if there does not exist a trajectory* $w \in \mathcal{B}$ *such that* (210) *is satisfied. Clearly, this relates to the controllability property of the dynamical system. In the behavioral framework a dynamical system is reachable if for any two trajectories* $w_0,\, w_1 \in \mathcal{B}$*, there exits a trajectory* $w \in \mathcal{B}$

such that $w(t) = w_0(t)$, $t \leq 0$ *and* $w(t) = w_1(t + t')$, $t \geq 0$. *Even if the system is controllable, for the optimal value to be finite, it is necessary that* $(\mathcal{O}w)(t) < \infty$, $t \in \mathcal{T}$. *Thus, drastic (impulsive) changes in the trajectory are forbidden.*

7.1.1 State Space Representation

The Gluskabi problem in the previous sections is quite general because the behavior $\mathcal{B}$ may be modeled or represented in many different ways [44, 61]. The classical input-output model describing $w = (y, u)$ via a differential equation is one way to represent $\mathcal{B}$ while the input/state/output model via an additional state variable x is another. It is further argued in [44, 61] that the notion of controllability is intrinsic to a dynamical system while observability depends on the representation of the behavior. Therefore, in order to be concrete and to avoid a discussion of issues related to observability, we choose the input/state/output model with the partition of behavior $w = (y, u) \in \mathcal{V}$, where the output map is $y = x$ and the input/state equation is

$$\frac{dx}{dt} = f(x, u). \tag{211}$$

In fact the observability property is not important to the Gluskabi raccordation problem since the raccordation interval $\mathcal{T}$ is always finite.

With this partition we obtain the more familiar form of(209):

$$\inf_{w=(x,u)\in\mathcal{B}} \int_{-\infty}^{\infty} \|\mathcal{O}_x x\|_Q^2 + \|\mathcal{O}_u u\|_R^2 \, dt, \tag{212}$$

where $\|\cdot\|_{\mathcal{V}}^2 = \|\cdot\|_Q^2 + \|\cdot\|_R^2$. There are a few issues that need to be addressed for the optimization problem in (209) to be well-posed. Firstly, as discussed in Remark 7.1.1, we need to ensure that the dynamical system (207) is reachable. Secondly, in

(209) and (210) it is implicitly assumed that the vector field is complete. In other words, $w(t) = (x(t), u(t))$ exits for all $t \in \mathbb{R}$ and, finally, the set $\ker \mathcal{O} \cap \mathcal{B}$ should be nonempty for the raccordation to be meaningful. With regard to the last two points, the notion of steady states is paramount in the sequel. As intuitive as this notion might seem in *linear* system theory, it is surprisingly hard to define for nonlinear systems in general [30, 14, 13].

To address the previous issues, we restrict the dynamics in (211) to be uniformly convergent [42]. Roughly speaking, if a system is uniformly convergent in a subset of the state space, then the dynamics is defined for all $t \in \mathbb{R}$, and furthermore, there exits a subset that qualifies as the steady state of the nonlinear system. This allows us to talk meaningfully about the stationary behaviors for the semi-intervals $(-\infty, 0]$ and $[1, \infty)$. Specifically, uniformly convergent systems posses the property that if the input $u(t)$ is constant (periodic with period T), then $x_u(t)$ is also a constant (periodic with period T). This state response x_u may be defined as the steady state response due to the input u. In fact, an example of a uniformly convergent system is the LTI system $\dot{x} = Ax + bu$, where A is Hurwitz. The steady state solution induced by the input u is

$$\overline{x}_u(t) = \int_{-\infty}^{t} e^{A(t-\tau)} bu(\tau)\, d\tau,\ t \in \mathbb{R}.$$

We refer the reader to Appendix D for a review of convergent systems. The uniform convergence property guarantees that $\ker \mathcal{O} \cap \mathcal{B}$ is non-empty and the reachability assumption ensures that the infimum is attained by a $w \in \mathcal{B}$, hence, we may replace it with a minimum.

7.2 Applications of the direct method

In this section we consider various applications of the Gluskabi raccordation.

7.2.1 Quasi-stationary raccordation

Let $\mathcal{O}w = (\mathbf{D}x, \mathbf{D}u)$, then the null space of $\mathcal{O}$ consists of all constant behaviors of the form $w_c = (x_c, u_c)$. Since the dynamics in (211) is assumed to be uniformly convergent, from Theorem $(D.1)$ for any constant input $u(t)$, $t \in \mathbb{R}$ there exists a constant steady state $x_c(t)$, $t \in \mathbb{R}$. This implies that $\ker \mathcal{O} \cap \mathcal{B} \neq \emptyset$. Thus

$$\ker \mathcal{O} \cap \mathcal{B} = \{w_c = (x_c, u_c) | 0 = f(x_c, u_c)\},$$

where $x_c \in \mathbb{R}^n$ and $u_c \in R_m$ are constants.

The Gluskabi raccordation in (212) is

$$\min \frac{1}{2} \int_{-\infty}^{\infty} \|\dot{x}\|_{\mathcal{Q}}^2 + \|\dot{u}\|_R^2 dt \tag{213}$$

$$= \min_v \frac{1}{2} \int_{-\infty}^{\infty} \|f(x,u)\|_{\mathcal{Q}}^2 + \|v\|_R^2 dt \tag{214}$$

subject to

$$\dot{x} = f(x,u), \tag{215}$$

$$\dot{u} = v, \tag{216}$$

$$f(x_0(t), u_0(t)) = 0,\ t \leq 0, \qquad f(x_1(t), u_1(t)) = 0,\ t \geq 1. \tag{217}$$

It is obvious that (214) is finite if and only if the system in (215) and (216) is reachable. Furthermore, impulsive behaviors at $t = 1$ are not allowed as this will cause (214) to be infinite.

If we specialize the previous dynamics to the LTI system $\dot{x} = Ax + bu$, where A is Hurwitz and (A, b) is reachable, then the raccordation constructs a quasi-stationary path between the stationary solutions $w(t) = (x(t), u(t)) = (A^{-1}bu_0, u_0)\,,\ t \leq 0$ and $w(t) = (x(t), u(t)) = (A^{-1}bu_1, u_1)\,,\ t \geq 1$ belonging to $\ker \mathcal{O} \cap \mathcal{B}$. This is solved in Section 4.1.8.2.

7.2.2 Gluskabi with harmonic inputs

For nonlinear systems, if the input is periodic, the state response may have none, one or multiple periodic solutions. Even if a periodic solution exits, the period of the state response is, in general, different from the period of the input. However, Theorem $(D.1)$ guarantees that for uniformly convergent systems $T-$periodic u produces $T-$periodic x. This allows us to construct a nonempty $\ker \mathcal{O} \cap \mathcal{B}$ in (208).

7.2.2.1 Harmonic Gluskabi: the LTI case

For simplicity we first consider the raccordation for a stable linear system. Recall that a stable linear system $\dot{x} = Ax + bu$ is global uniformly convergent and a harmonic function of the form $z(t) = Me^{j\omega t}$ satisfies $\mathcal{O}z = (\mathbf{D} - j\omega\mathbf{I})z = 0$. Thus, $z \in \ker \mathcal{O}$. A harmonic input $u(t) = Me^{j\omega t}, \omega = \frac{2\pi}{T}$ induces the steady state response $(j\omega I - A)^{-1}bu(t)$. Thus, the set of harmonic behaviors is the null space of the operator $\mathcal{O}w = [(\mathbf{D} - j\omega)x, (\mathbf{D} - j\omega)u]$. The quasi-harmonic raccordation in (212) is the solution to the following optimization problem:

$$\min_u \frac{1}{2}\int_{-\infty}^{\infty} \|(\mathbf{D} - j\omega)x\|_Q^2 + \|(\mathbf{D} - j\omega)u\|_R^2\, dt, \tag{218}$$

$$= \min_u \frac{1}{2}\int_{-\infty}^{\infty} \|(A - j\omega)x + bu\|_Q^2 + \|v - j\omega u\|_R^2\, dt. \tag{219}$$

subject to the dynamics

$$\begin{aligned}\frac{dx}{dt} &= Ax + bu,\\ \frac{du}{dt} &= v.\end{aligned}$$

The initial and final orbits induced by the initial and final phasor $u_i(t)$, $u_f(t)$, respectively, are $w_i(t) = (x_i(t), u_i(t)) = ((j\omega I - A)^{-1}bu_i(t), u_i(t))$, $t \leq 0$, and $w_f(t) = (x_f(t), u_f(t)) = ((j\omega I - A)^{-1}bu_f(t), u_f(t))$, $t \geq 1$. This is a complexified LQ problem where the necessary conditions of optimality is derived in Appendix C.

7.2.2.2 When $\ker \mathcal{O} \cap \mathcal{B}$ *can be explicitly computed*

Unlike the linear case in the previous section, for nonlinear systems the situation is somewhat more difficult. For a nonlinear system $\dot{x} = f(x, u)$ with a harmonic input

$$u(t) = A\sin(\omega t),\ \omega = \frac{2\pi}{T}, \tag{220}$$

even if a periodic steady solution exists, the period is, in general, different from T. For the subclass of uniformly convergent systems, however, the periodic steady state solution $x_u(t)$, $t \in \mathbb{R}$ induced by $u(t)$ will have a period T(cf. theorem $(D.1)$). Thus, the steady state solution contains harmonics with periods that are integer multiple of T. However, this solution cannot be explicitly solved for in general; this in turn prevents us from constructing the operator $\mathcal{O}$. For a subclass of convergent systems it is possible to find the steady state response induced by a harmonic input [42, 15] explicitly.

Indeed, let

$$\begin{aligned}
\dot{x}_1 &= A_1 x_1 + q_1(x_2, \ldots, x_k, u),\ x_1 \in \mathbb{R}^{d_1}, \\
\dot{x}_2 &= A_2 x_2 + q_2(x_3, \ldots, x_k, u),\ x_2 \in \mathbb{R}^{d_2}, \\
&\ldots \\
\dot{x}_k &= A_k x_k + q_k(u),\ x_k \in \mathbb{R}^{d_2},
\end{aligned} \tag{221}$$

where A_i, $i = 1, \ldots, k$ are Hurwitz and q_i, $i = 1, \ldots, k$ are polynomials. This system is globally uniformly convergent [42, p51]. For this system the steady state solution may found explicitly [15, 42]. The details may be found in [15, p.13] and [42, p.51]. Once the steady state solution is known, we may construct the operator $\mathcal{O}_x$ such that the steady state solution $x_u \in \ker \mathcal{O}_x$. Let $k_i \subseteq \mathbb{Z}^+$, $i = 1, \ldots, m$ denote the set of all harmonics present in x_u, then the x_u is in the kernel of the operator

$$\mathcal{O}_x x = (\mathbf{D}^2 + (k_1 \omega \mathbf{I})^2)(\mathbf{D}^2 + (k_2 \omega \mathbf{I})^2) \ldots (\mathbf{D}^2 + (k_m \omega \mathbf{I})^2) x.$$

Hence, the operator $\mathcal{O}w$, $w = (x, u)$ in (212) is

$$\mathcal{O}w = \begin{bmatrix} \mathcal{O}_x x \\ \mathcal{O}_u u \end{bmatrix} = \begin{bmatrix} \mathcal{O}_x x \\ (\mathbf{D}^2 + \omega^2) u \end{bmatrix}$$

With this operator $\ker \mathcal{O} \cap \mathcal{B}$ in (208) is nonempty, and the Gluskabi problem is well posed.

Example 7.2.1. *Consider the following bilinear system*

$$\begin{aligned}
\dot{x}_1 &= -a x_1 + u x_2, \\
\dot{x}_2 &= -a x_2 + u, a > 0,
\end{aligned} \tag{222}$$

which has the form in (221). *With*

$$f = \begin{bmatrix} -ax_1 \\ \\ -ax_2 \end{bmatrix}, \; g = \begin{bmatrix} x_2 \\ \\ 1 \end{bmatrix}$$

the Lie brackets are

$$[f,g] \;\; = \;\; \begin{bmatrix} 0 \\ \\ a \end{bmatrix}, \; [f,[f,g]] = - \begin{bmatrix} a \\ \\ 0 \end{bmatrix}.$$

The dimension of the distribution is two everywhere so the system is reachable. Furthermore, if the input u is periodic, then there exists a periodic steady state. Let $\{\langle u \rangle_k\}_{k=-\infty}^{k=\infty}$ be the Fourier coefficients of the input, then Fourier coefficients of the periodic steady states are

$$\begin{aligned} \langle x_1 \rangle_k &= (a + j\omega k)^{-1} \sum_l \langle x_2 \rangle_{k-l} \langle u \rangle_l \\ \langle x_2 \rangle_k &= (a + j\omega k)^{-1} \langle u \rangle_k, \; k \in \mathbb{Z}. \end{aligned}$$

For a sinusoidal input $u(t) = M\cos(\omega t)$, the Fourier coefficients are $\langle x_2 \rangle_1 = \frac{M}{2}(a + j\omega)^{-1} = \langle x_2 \rangle_{-1}^*$ and

$$\langle x_1 \rangle_k = \begin{cases} (a + 2j\omega)^{-1} \langle x_2 \rangle_1 \langle u \rangle_1, & k = 2, \\ \frac{1}{a}\left(\langle x_2 \rangle_{-1} \langle u \rangle_1 + \langle x_2 \rangle_1 \langle u \rangle_{-1} \right), & k = 0, \\ (a - 2j\omega)^{-1} \langle x_2 \rangle_{-1} \langle u \rangle_{-1}, & k = -2, \\ 0, & \textit{else}. \end{cases}$$

It is clear that $x_2(t)$ contains harmonics with frequency ω, while x_1 contains a DC component and a harmonic with frequency 2ω. The operator $\mathcal{O}_x x$ is

$$\mathcal{O}_x x = \begin{bmatrix} (\mathbf{D}^2 + (2\omega)^2)\, \mathbf{D} x_1 \\ \\ (\mathbf{D}^2 + \omega^2)\, x_2 \end{bmatrix}$$

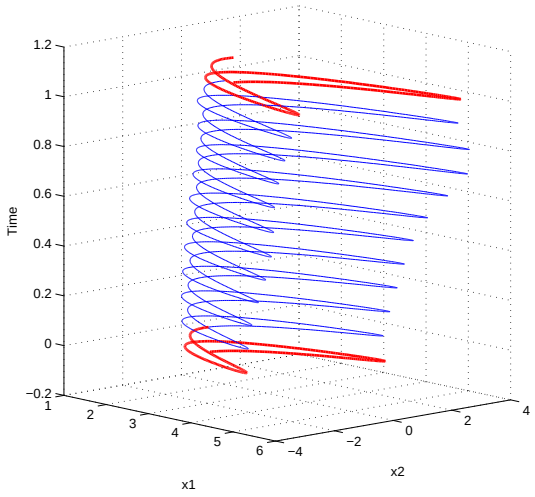

Figure 49: The Gluskabi raccoration: $\ker \mathcal{O} \cap \mathcal{B}$ explicitly computable

while $\mathcal{O}_u u = (\mathbf{D}^2 + \omega^2)u$. *We now seek a Gluskabi raccordation of two orbits in* $\ker \mathcal{O} \cap \mathcal{B}$ *induced by the sinusoids* $u_i(t) = M_i \cos(\omega t)$ *and* $u_f(t) = M_f \cos(\omega t)$.

The raccordation may be cast into the standard terminal controller by introducing a new variable $\dot{u} = \dot{x}_3 = x_4$, $\ddot{u} = \dot{x}_4 = v$ *and hence the operators are*

$$\mathcal{O}_x x = \begin{bmatrix} (a^2 + (2\omega)^2)(-ax_1 + x_2 x_3) + (-2ax_3 + 3x_4)(-ax_2 + x_3) + x_2 v \\ (a^2 + \omega^2)x_2 - ax_3 + x_4 \end{bmatrix}$$

and

$$\mathcal{O}_u u = v + \omega^2 x_3.$$

For $M_i = 150$ *and* $M_f = 175$ *the Gluskabi raccordation is shown in Figure (49)*

7.2.2.3 When $\ker \mathcal{O} \cap \mathcal{B}$ *cannot be explicitly computed*

Unlike the special case in the previous section it is in general impossible to compute the steady state solution x_u explicitly. From Theorem $D.1$ we conclude that the response to a harmonic input with period T is also $T-$periodic; it is unique as well.

Therefore, we may define

$$\mathcal{O}w = \begin{bmatrix} (\mathcal{T}_T - \mathbf{I})x \\ (\mathbf{D}^2 - \omega^2)u \end{bmatrix},$$

where $(\mathcal{T}_T x)(t) = x(t-T)$, to characterize $\ker \mathcal{O} \cap \mathcal{B}$.

The raccordation in (212) may be reformulated as follows:

$$\frac{1}{2}\int_{-\infty}^{\infty} \|(\mathcal{T}_T - \mathbf{I})x\|_Q^2 + \|(\mathbf{D}^2 - \omega^2)u\|_R^2 \, dt, \text{ subject to} \tag{223}$$

$$w_0(t) = (x_0(t), u_0(t)), 1 - T \leq t \leq 1, \tag{224}$$

$$w_1(t) = (x_1(t), u_1(t)),\ 1 \leq t \leq 1 + T,\ T << 1, \tag{225}$$

since both behaviors are $T-$periodic. In order to solve the previous problem the orbits $x_i(t)$, $i = 0, 1$, induced by $u_i(t)$, $i = 0, 1$ need to be explicitly known. Since the steady state response $x_1(t)$ induced by a fixed $T-$periodic input $u_1(t)$, $t \in [1, 1+T]$ is also $T-$periodic, the target orbit may be found by knowing either $x_1(1)$ or $x_1(1+T)$ as we can integrate the dynamics either forward or backward. The periodicity requires that $x_1(1) = x_1(1+T)$, and the $T-$periodic $x_1(t)$, $t \in [1, 1+T]$ may be obtained by solving the optimal control problem

$$\begin{aligned} &\min_{x(1)} J_f = \frac{1}{2}\|x_1(1) - x_1(1+T)\|^2 \, dt \\ &\text{subject to } \dot{x}(t)_1 = f(x_1(t), u_1(t)),\ t \in [1, 1+T]. \end{aligned} \tag{226}$$

A slight modification of the previous arguments allows us to compute the initial orbit $x_0(t)$, $t < 0$ as well. Once these solutions are known, they may used in (223) to generate the raccordation.

Proposition 7.2.1. *A global optimal solution to* (226) *exits; the optimal* $x(t)$ *is unique and periodic.*

Proof. The existence of a candidate solution follows from the existence of $T-$periodic solutions in Theorem $D.1$ for a given $T-$periodic input $u(t)$. Assume there exists two solutions defined over $[1-T, 1]$ that minimize (226). Then by periodically extending these solutions we obtain two solution defined over $(-\infty, \infty)$. This contradicts the uniqueness of the steady state solution in Theorem $D.1$. ∎

The following proposition suggests one way to compute the orbit x_1 for a $T-$periodic input u_1. Since the input is known we will denote the control system $\dot{x} = f(x, u)$ by the autonomous vector field $\dot{x} = f(x)$.

Proposition 7.2.2. *If $x(t)$ is the optimal solution to* (226)*, then it satisfies the stationary condition*

$$x(1) = x(1+T) + \lambda(1),$$

where the costate equation is

$$\dot{\lambda}(t) = \frac{\partial f}{\partial x}'(x(t))\lambda(t),\ t \in [1, 1+T), \tag{227}$$

with the boundary condition

$$\lambda(1+T) = -(x(1) - x(1+T)). \tag{228}$$

Proof. Rewrite the performance index (226) $J_f = \frac{1}{2T}\int_1^{1+T} \|x_1(1) - x_1(1+T)\|^2\, dt$ and adjoin the dynamics via λ to the performance index

$$J_0 = \int_1^{1+T} \frac{1}{2T}\|x(1) - x(1+T)\|^2 + \lambda'(t)(f(x(t)) - \dot{x}(t))\, dt. \tag{229}$$

We perturb $x \to x + \epsilon\eta$ and up to the first order in ϵ

$$\begin{aligned} J_\epsilon &= \int_1^{1+T} L(x(1), x(1+T)) + \lambda'(f(x(t)) - \dot{x}(t)) + \frac{\partial L(x(1), x(1+T))}{\partial x(1)}\eta(1) + \\ &+ \frac{\partial L(x(1), x(1+T))}{\partial x(1+T)}\eta(1+T) + \left(\lambda' \frac{\partial f}{\partial x} + \dot{\lambda}\right)\eta\, dt - \lambda'\eta\big|_1^{1+T}, \end{aligned}$$

where $L(x(1), x(1+T)) = \frac{1}{2T}\|x(1) - x(1+T)\|^2$. The Fréchet derivative is

$$\begin{aligned} \delta J &= \int_1^{1+T} \left(\lambda' \frac{\partial f}{\partial x} + \dot{\lambda}'\right)\eta\, dt + \left(T\frac{\partial L(x(1), x(1+T))}{\partial x(1)} + \lambda'(1)\right)\eta(1) + \\ &+ \left(T\frac{\partial L(x(1), x(1+T))}{\partial x(1+T)} - \lambda'(1+T)\right)\eta(1+T). \end{aligned}$$

We *choose*

$$\dot{\lambda}(t) = \frac{\partial f'}{\partial x}\lambda(t),\ t \in [1, 1+T),$$

with the boundary condition

$$-(x(1) - x(1+T)) = \lambda(1+T) \tag{230}$$

imposed to avoid computing η. Hence,

$$\delta J = \left(T\frac{\partial L(x(1), x(1+T)}{\partial x(1)} + \lambda'(1)\right)\eta(1).$$

The stationary condition implies that

$$x(1) - x(1+T) + \lambda(1) = 0 \tag{231}$$

or $x(1) = x(1+T) + \lambda(1)$. ∎

Clearly, the optimal solution is such that $\lambda(t) \equiv 0$, $t \in [1, 1+T]$; the previous derivation of the necessary condition of optimality allows us to compute the orbits in $\ker \mathcal{O} \cap \mathcal{B}$. Indeed, the following gradient descent algorithm may be easily extracted from the previous proposition.

Algorithm 7.2.1. *1. Guess an initial condition* $x(1)$.

2. *Integrate* $\dot{x}_1(t) = f(x_1(t), u_1(t))$, $t \in [1, 1+T]$ *forward for a fixed* $u_1(t)$, $t \in [1, 1+T]$. *Record* $x(1+T)$.

3. *Compute the boundary condition* $\lambda(1+T) = -(x(1) - x(1+T))$ *and integrate the costate*

$$\dot{\lambda}(t) = \frac{\partial f'}{\partial x}(x_1(t), u_1(t))\lambda(t),\ t \in [1, 1+T)$$

backwards.

4. *Compute* $\delta x(1) = \frac{\partial H'}{\partial x(1)} = x(1) - x(1+T) + \lambda(1)$.

5. *Update the initial condition:* $x_{new}(1) = x(1) - k\delta x(1)$, *where* $0 < k \leq 1$ *is a small time step.*

6. *Repeat step 2 until a desired accuracy is reached.*

With a slight modification the previous algorithm may also be used to generate the initial orbit $w_0(t) = (u_0(t), x_0(t))$, $t < 0$.

7.2.3 Quasi-periodic raccordation I

We turn our attention to the raccordation of any two $T-$periodic behaviors. Recall from Theorem $D.1$ that a $T-$periodic steady state exits if u is $T-$periodic. Hence,

$$\ker \mathcal{O} \cap \mathcal{B} = \{w = (x, u) \,|\mathcal{O}w = ((\mathbf{I} - \mathcal{T}_T)x, (\mathbf{I} - \mathcal{T}_T)u) = 0\}$$

is well defined and nonempty.

Given two $T-$periodic orbits $\dot{x}_i = f(x_i, u_i)$, $t \in [-T, 0]$ and $\dot{x}_f = f(x_f, u_f)$, $t \in [1, 1+T]$, the raccordation in (212) is the optimization problem

$$\min_u J = \int_{0^-}^{1+T} \|x(t) - x(t-T)\|_P^2 + \|u(t) - u(t-T)\|_R^2 \, dt. \tag{232}$$

Since a integral curve is determined by its initial condition and input, the final orbit $x(t) = x_f(t)$, $t \in [1, 1+T]$ is parameterized by $x_f(1^+)$ and $u(t) = u_f(t)$, $t \in [1, 1+T]$. (232) may be reformulated as follows:

$$\min_w J_0 = \int_0^{1+T} \|x(t) - x(t-T)\|_P^2 + \|w(t)\|_R^2 \, dt, \tag{233}$$

subject to the dynamics

$$\begin{aligned} \dot{x}(t) &= f(x(t), u(t)), \\ u(t) &= u(t-T) + w(t),\ t \in [0, 1+T] \end{aligned} \tag{234}$$

with the boundary conditions

$$\begin{aligned} x(1^-) &= x_f(1^+), \\ u(t) &= u_f(t),\ t \in [1, 1+T]. \end{aligned} \tag{235}$$

Proposition 7.2.3. *The gradient of* J_0 *in* (233) *is*

$$\delta J = \int_0^{1+T} \left(w'(t)R - \lambda_u'(t)\right) \delta w(t) dt, \tag{236}$$

from which the optimality condition is

$$w(t) = R^{-1}\lambda_u(t),\ t \in [0, 1+T], \tag{237}$$

where

$$
\begin{aligned}
-\dot{\lambda}_x(t) &= P\left(2x(t) - x(t-T) - x(t+T)\right) + \frac{\partial f'}{\partial x}\lambda_x(t),\ t \in [0,1), \\
-\dot{\lambda}_x(t) &= P\left(x(t) - x(t-T)\right) + \frac{\partial f'}{\partial x}\lambda_x(t),\ t \in (1,1+T], \\
-\lambda_u(t) &= \frac{\partial f'}{\partial u}\lambda_x(t) - \lambda_u(t+T),\ t \in [0,1], \\
-\lambda_u(t) &= \frac{\partial f'}{\partial u}\lambda_x(t) + \nu_u(t),\ t \in (1,1+T], \\
\lambda_x(1^-) &= \lambda_x(1^+) + \nu_x, \\
\lambda_x(1+T) &= 0.
\end{aligned}
\tag{238}
$$

ν_x and $\nu_u(t)$need to be chosen such that the boundary conditions (235) *are satisfied.*

Proof. See Proof F.1 in Appendix F. ∎

7.2.3.1 Gradient descent algorithm

From the problem formulation in the previous section, it is clear that the optimal program consists of two terminal controllers. One is the classical terminal controller that drives $x(t)$ from $x(0) = x_0$ to $x(1^-) = x(1^+)$, while the other is the terminal controller that drives the *function* $u(t) = u_i(t), t \in [-T, 0]$ to $u(t) = u_f(t),\ t \in [1, 1+T]$. An algorithm to compute the former is well known [12], and an algorithm for the latter is presented in Section 6.1.2. We now combine these two to compute the optimal control u in the previous section.

To devise a gradient descent algorithm, we follow the general procedure in Section 6.1.3. We first compute the variation of the final state constraints induced by the variations in the inputs. Thus, we let $J_{x_k} = x_k(1^-) = e_k' x(1^-)$ and seek $\delta J_{x_k} = e_k' \delta x(1^-)$, $k = 1, \ldots n$, $n = \dim x$.

Proposition 7.2.4. *The Fréchet derivative of* $J_{x_k} = x_k(1^-) = e_k' x(1^-)$ *is*

$$\begin{aligned} \delta J_{x_k} &= \delta x_k(1^-) \\ &= -\int_0^{1+T} \lambda_{u,k}'(t)\delta w(t)dt,\ k = 1, \ldots, n, \end{aligned} \tag{239}$$

where

$$\begin{aligned} -\dot{\lambda}_{x,k}(t) &= \frac{\partial f'}{\partial x}\lambda_{x,k}(t),\ t \in [0,1), \\ -\dot{\lambda}_{x,k}(t) &= \frac{\partial f'}{\partial x}\lambda_{x,k}(t),\ t \in (1,1+T], \\ -\lambda_{u,k}(t) &= \frac{\partial f'}{\partial u}\lambda_{x,k}(t) - \lambda_{u,k}(t+T),\ t \in [0,1], \\ -\lambda_{u,k}(t) &= \frac{\partial f'}{\partial u}\lambda_{x,k}(t),\ t \in (1,1+T], \\ \lambda_{x,k}(1^-) &= \lambda_{x,k}(1^+) + e_k, \\ \lambda_{x,k}(1+T) &= 0, \end{aligned} \tag{240}$$

for $k = 1, \ldots n$, $dim x = n$.

Proof. See Proof F.2 in Appendix F. ∎

From the last boundary condition and the second equation we conclude that

$$\lambda_{x,k}(t) \equiv 0,\ t \in (1, 1+T],$$

and $\lambda_{x,k}(1^+) = 0$. Thus, the fourth equation becomes

$$\lambda_{u,k}(t) \equiv 0,\ t \in [1, 1+T].$$

The previous set of costate equations reduces to

$$\begin{aligned} -\dot{\lambda}_{x,k}(t) &= \frac{\partial f'}{\partial x}\lambda_{x,k}(t),\ t \in [0,1), \\ -\lambda_{u,k}(t) &= \frac{\partial f'}{\partial u}\lambda_{x,k}(t) - \lambda_{u,k}(t+T),\ t \in [0,1], \\ \lambda_{x,k}(1^-) &= e_k \end{aligned} \tag{241}$$

for $k = 1, \ldots, n$. This shows that $\delta x_k(1^-)$ has no influence from u and x in $[1, 1+T]$. This is, of course, completely obvious as $x(1^-)$ only depends on the input in the interval $[0, 1]$.

We now turn our attention to the variation of $u_k(t)$, $t \in [1, 1+T]$, $k = 1, \ldots, m$, dim $u = m$. As in (147) we first consider the average variation in a small section $[s_i, s_i + \Delta) \subset [1, 1+T]$:

$$\begin{aligned} J_k^{s_i} &= \frac{1}{\Delta} \int_{s_i}^{s_i+\Delta} e_k' u(t) dt, \\ &= \int_1^{1+T} e_k' u(t) \Pi^\Delta(t - s_i) dt. \end{aligned} \tag{242}$$

Proposition 7.2.5. *The Fréchet derivative of $J_k^{s_i}$ is*

$$\delta J_k^{s_i} = -\int_0^{1+T} {\mu_{u,k}^{s_i}}'(t) \delta w(t) dt, \; k = 1, \ldots, m, \tag{243}$$

where

$$\begin{aligned} -\dot{\mu}_{x,k}^{s_i}(t) &= \frac{\partial f'}{\partial x} \mu_{x,k}^{s_i}(t), \; t \in [0, 1+T] \\ \mu_{x,k}^{s_i}(1+T) &= 0, \\ \mu_{u,k}^{s_i}(t) &= \mu_{u,k}^{s_i}(t+T) - \frac{\partial f'}{\partial u} \mu_{x,k}^{s_i}(t), \; t \in [0, 1] \\ \mu_{u,k}^{s_i}(t) &= -e_k \Pi^\Delta(t - s_i) - \frac{\partial f'}{\partial u} \mu_{x,k}^{s_i}(t), \; t \in (1, 1+T], \end{aligned}$$

for $k = 1, \ldots, m$.

Proof. The Fréchet derivative is easily obtained via the substitutions in (236): $P = 0$, $R = 0$, $x_f(t) = 0$, $\nu_u(t) = e_k \Pi^\Delta(t - s_i)$, $\nu_x \equiv 0$, $\lambda_x \to \mu_{x,k}^{s_i}$, $\lambda_u \to \mu_{u,k}^{s_i}$. ∎

The first two equations imply that $\mu_{i,x}^{s_i}(t) \equiv 0$, $t \in [0, 1+T]$ and, therefore, the

previous set reduces to

$$\begin{aligned}\mu_{u,k}^{s_i}(t) &= \mu_{u,k}^{s_i}(t+T),\ t \in [0,1] \\ \mu_{u,k}^{s_i}(t) &= -e_k \Pi^{\Delta}(t-s_i),\ t \in (1,1+T].\end{aligned} \tag{244}$$

Observe that the costate equations in (244) are independent of $\mu_{i,x}$ and x.

Lastly, we compute the gradient (233) in the absence of all boundary conditions.

Proposition 7.2.6. *The Fréchet derivative of* (233) *in the* absence *of the boundary conditions is*

$$\delta J = \int_0^{1+T} \left(w'(t)R - (\lambda_u^J)'(t) \right) \delta w(t) dt, \tag{245}$$

where

$$\begin{aligned}-\dot{\lambda}_x^J(t) &= P\left(2x(t) - x(t-T) - x(t+T)\right) + \frac{\partial f}{\partial x}' \lambda_x^J(t),\ t \in [0,1), \\ -\dot{\lambda}_x^J(t) &= P\left(x(t) - x(t-T)\right) + \frac{\partial f}{\partial x}' \lambda_x^J(t),\ t \in (1,1+T], \\ -\lambda_u^J(t) &= \frac{\partial f}{\partial u}' \lambda_x^J(t) - \lambda_u^J(t+T),\ t \in [0,1], \\ -\lambda_u^J(t) &= \frac{\partial f}{\partial u}' \lambda_x^J(t),\ t \in (1,1+T], \\ \lambda_x^J(1^-) &= \lambda_x^J(1^+), \\ \lambda_x^J(1+T) &= 0,\end{aligned} \tag{246}$$

Proof. By substituting $\nu_x = 0$ and $\nu_u \equiv 0$, $t \in [1, 1+T]$, in (236) and (238), we immediately obtain the desired result. The continuity of λ_x^J at $t = 1$ follows from the one before last condition. ∎

We now have all the ingredients to construct a gradient descent algorithm. The derivation is provided in Appendix F.

Algorithm 7.2.2. *Let $I = [0, 1+T]$ be the simulation interval, dt the discretization time step, $u(t) = u_0(t), t \in [-T, 0]$, $x(0) = x_0$, $u(t) = u_f(t), t \in [1, 1+T]$ and $x(1^-) = x_f$. Denote $s_0 = 1$, $s_i = s_0 + idt$, $i = 0, \ldots, N$, the discretization of the interval $[1, 1+T]$.*

1. *Guess a input $w(t)$, $t \in [0, 1+T]$ in (234).*

2. *Compute the dynamics (234) forward for $t \in [0, 1+T]$.*

3. *Compute the costate equations (241), (244) and (246).*

4. *Compute the boundary mismatch: $\Delta u(s_l) = u(s_l) - u_f(s_l)$, $l = 0, \ldots, N$, and $\Delta x(1^-) = x(1^-) - x_f(1^-)$. Set $\delta \boldsymbol{J}_l = -k_2 \Delta u(s_l)$, $l = 0, \ldots, N$, and $\delta \boldsymbol{x}(1^-) = -k_3 \Delta \boldsymbol{x}(1^-)$, $0 < k_i \leq 1, i = 2, 3$.*

5. *Compute*

$$\delta w(t) \;=\; -k_1 \boldsymbol{C}(t) - \boldsymbol{D}(t), \tag{247}$$

   where $0 < k_1 \leq 1$. The matrices $\boldsymbol{C}(t)$ and $\boldsymbol{D}(t)$ are provided in (315).

6. *Update w by $w_{new}(t) = w(t) + \delta w(t)$.*

7. *Repeat step 2 with the new input $w_{new}(t)$ until a desired accuracy is reached.*

Example 7.2.2. *Consider the system*

$$\begin{aligned} \dot{x}_1 &= -a x_1 + u x_2, \\ \dot{x}_2 &= -a x_2 + u, \end{aligned}$$

where $a = 15$. We apply the previous algorithm, and Figure (52) shows the raccordation. The thick lines are the initial and final orbits, respectively.

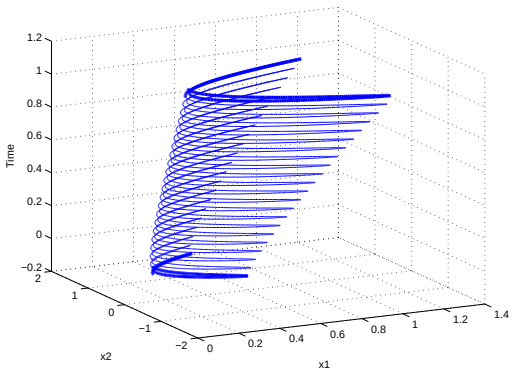

Figure 50: Amplitude raccordation

7.2.4 Quasi-periodic raccordation II

In this section we consider the Gluskabi raccordation between two periodic behaviors of different periods. Motivated from Section 6.2.1, the signal raccordation may be easily extended to the dynamical case:

$$\min_u \int_0^{1+T_1} \|x(t) - x(t - T(t))\|_P^2 + \|u(t) - u(t - T(t))\|_R^2 \, dt$$

subject to

$$\begin{aligned} \dot{x} &= f(x,u),\ t \in [0, 1+T_1] \\ (x(t),u(t)) &= (x_0(t),u_0(t)) = w_0(t),\ t \in [-\infty, 0] \\ (x(t),u(t)) &= (x_1(t),u_1(t)) = w_1(t),\ t \in [1, +\infty]. \end{aligned}$$

The orbits $w_i(t)$, $i = 0, 1$ have periods T_i, $i = 0, 1$, respectively. As before the discretization of the delay term will have a detrimental effect on the numerical computation. Therefore, we regularize the problem by adding the term $\left\| \frac{d}{dt} \left(u(t) - u(t - T(t)) \right) \right\|^2$ to the integrand. Reformulate the problem into the form used throughout this chapter

we obtain the optimization problem:

$$\min_{w} \frac{1}{2} \int_0^{1+T_1} \|x(t) - x(t - T(t))\|_P^2 + \|u(t) - u(t - T(t))\|_Q^2 + \|w(t)\|_R^2 \, dt \quad (248)$$

subject to

$$\dot{x}(t) = f(x(t), u(t)), \quad (249)$$

$$\dot{u}(t) = \begin{cases} (1 - \dot{T})\dot{u}(t - T(t)) + w(t), \, t \in [0, 1^-], \\ \dot{u}(t - T_1) + w(t), \, t \in [1^+, 1 + T_1] \end{cases} \quad (250)$$

$$u(t) = u_1(t), \, t \in [1, 1 + T_1], \quad (251)$$

$$x(1^-) = x_1, \quad (252)$$

where $T(t)$ is the straight line in (185) connecting T_0 and T_1.

7.2.4.1 Gradient descent algorithm

A gradient descent algorithm for the optimal control problem (248) may be derived using the same technique as in Section (6.2.1). In hindsight, however, a different approach yields a more compact algorithm, and this is presented instead. It is based on a reparameterization of (248).

Since the initial and final orbits are known, i.e., (u_i, x_i), $i = 0, 1$ in $\dot{x}_i = f(x_i, u_i)$, $i = 0, 1$, we may first steer x and u such that $x(1^-) = x_1(1^+), u(1^-) = u_1(1^+)$ and then switch the input to $u(t) = u_1(t)$, $t \in [1, 1 + T_1)$. Instead of (248) we simulate the following:

$$\begin{aligned} \min_{v} J_0 = \frac{1}{2} \int_0^{1+T_1} & \|x(t) - x(t - T(t))\|_P^2 + \|u(t) - u(t - T(t))\|_Q^2 \\ & + \left\| v(t) - (1 - \dot{T})v(t - T(t)) \right\|_R^2 dt \end{aligned}$$

subject to the dynamics

$$\begin{aligned} \dot{x}(t) &= f(x(t), u(t)), \\ \dot{u}(t) &= v(t),\ t \in [0,1]. \end{aligned} \tag{253}$$

For convenience we introduce a new state variable $z' = (x', u')$ and rewrite (253) as $\dot{z} = F(z, v)$. With this notation the previous performance index is

$$\min_v J_0 = \frac{1}{2}\int_0^{1+T_1} \|z(t) - z(t - T(t))\|_S^2 + \left\|v(t) - (1 - \dot{T})v(t - T(t))\right\|_R^2 \, dt. \tag{254}$$

The following is well-known [12].

Proposition 7.2.7. *The Frèchet derivative of the boundary condition* $J_i = z_i(1) = e_i' z(1)$ *is*

$$\delta z_i(1) = \int_0^1 (\lambda^i)'(t)\frac{\partial F}{\partial v}\delta v(t)dt, \tag{255}$$

where

$$\begin{aligned} \dot{\lambda}^i(t) &= -\frac{\partial F'}{\partial z}\lambda^i(t), \\ \lambda^i(1) &= \begin{cases} 0; & i \neq j, \\ 1; & i = j,\ j = 1, \ldots, n + m = N, \end{cases} \end{aligned} \tag{256}$$

and $dim\ x = n$, $dim\ u = m$.

We now proceed to compute the Fréchet derivative of (254) in the *absence* of the boundary conditions; we denote this performance index by J_v.

Proposition 7.2.8. *The Fréchet derivative in the* absence *of the boundary conditions is*

$$\delta J_v = \int_0^1 c'(t)\delta v(t)dt,$$

where

$$c(t) = \begin{cases} R\left((2-\dot{T})v(t) - (1-\dot{T})v(t-T(t)) - v\left(\frac{t+T_0}{1-\dot{T}}\right)\right) + \frac{\partial F'}{\partial v}\mu(t), & t \in [0, 1-T_1), \\ R\left(2v(t) - (1-\dot{T})v(t-T(t)) - v(t+T_1)\right) + \frac{\partial F'}{\partial v}\mu(t), & t \in [1-T_1, 1]. \end{cases}$$

The costate satisfies

$$-\dot{\mu}(t) = \begin{cases} S\left(\left(\frac{2-\dot{T}}{1-\dot{T}}\right)z(t) - z(t-T(t)) - \frac{1}{1-\dot{T}}z\left(\frac{t+T_0}{1-\dot{T}}\right)\right) + \frac{\partial F'}{\partial z}\mu(t), & t \in [0, 1-T_1), \\ S\left(2z(t) - z(t-T(t)) - z(t+T_1)\right) + \frac{\partial F'}{\partial z}\mu(t), & t \in [1-T_1, 1], \end{cases} \tag{257}$$

with the final condition $\mu(1) = 0$.

Proof. See Proof F.4 in Appendix F. ∎

We have all the ingredients for a gradient descent algorithm. The derivation is provided in F.5 in Appendix F.

Algorithm 7.2.3. *1. Guess an input* $v(t)$.

2. Compute the dynamics (253) forward.

3. Compute the costate equations (256) and (257) backward.

4. Compute $\Delta z(1) = z(1) - z_1$ *and set* $\delta z(1) = -k_2 \Delta z(1),\ 0 \leq k_2 \leq 1$.

5. Compute

$$\delta v(t) \;=\; -k_1\left(c(t) - \frac{\partial F'}{\partial v}\Lambda(t)\Lambda_g^{-1}D\right) + \frac{\partial F'}{\partial v}\Lambda(t)\Lambda_g^{-1}\delta z(1),\ 0 \leq k_1 \leq 1,$$

where $\Lambda(t)$, Λ_g *and* D *are defined in (317).*

6. Update the input $v_{new}(t) = v_{old}(t) + \delta v(t)$ *and repeat step 2 until the input gradient is sufficiently small.*

In order to illustrate this algorithm, we apply it to the system in (222); we will connect two orbits of different periods induced from sinusoidal inputs. The final orbit has a period $T_1 = 0.05$ and the magnitude of the input sinusoid is $A_1 = 20$. The initial orbit, on the other hand, has a period $T_0 = 0.95T_1$ while the magnitude of the input is $A_0 = 0.5A_1$. The Gluskabi raccordation is shown in Figure 51 for $a = 20$ while the magnitude of the gradient vs. the number of iterations is shown in Figure 52.

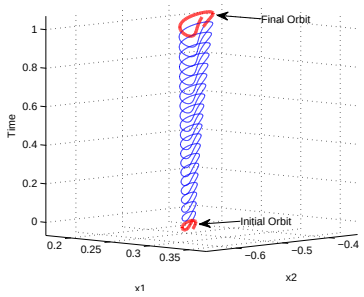

Figure 51: Trajectory of smooth transition

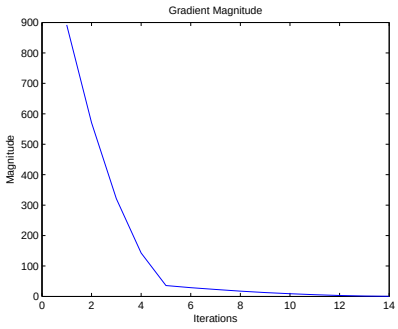

Figure 52: Magnitude of the gradient δv vs. number of iterations

7.3 Indirect method

The dynamic extension of the indirect method in Section (5.1.2) follows readily; the only additional ingredient is the dynamical constraint. As we will see shortly, this

in turn will impose a dynamic constraint on the parameter space Θ. From the problem formulation of both the signal and dynamic raccordation, it is clear that the direct method is a *trajectory* optimization problem; we seek to shape the trajectories directly. On the other hand, the indirect method involves both 'space' and 'time', which is similar to the field concept in physics. Indeed, if it is nonempty, we may parameterize $\ker \mathcal{O} \cap \mathcal{B}$ in (208) via the *global* map and obtain a parameterization $\tilde{w}(\tau, t) = (\tilde{x}(\tau, t), \tilde{u}(\tau, t))$ as a function of two independent variables. τ refers to a specific trajectory in the set $\ker \mathcal{O} \cap \mathcal{B}$ while t is the 'time' variable. In contrast to the signal Gluskabi raccordation in Section 5.1.2, the *local* map needs to satisfy the dynamics $\dot{x} = f(x, u)$ as well. This is the aforementioned constraint on the parameter space Θ.

7.3.1 Harmonic raccordation

As a simple example we consider the quasi-harmonic raccordation for the stable linear system $\dot{x} = Ax + bu$. The harmonic behavior may be parameterized by $(X(\tau)e^{j\omega t}, U(\tau)e^{j\omega t})$, where $X(\tau) = (j\omega I - A)^{-1}bU(\tau)$. For the harmonic input $u(t) = Ue^{j\omega t}$, $\omega = \frac{2\pi}{T}$, $t \in \mathbb{R}$, we have $U(\tau) \equiv U$ and, hence, $X(\tau) = (j\omega I - A)^{-1}bU$. For this example the phasors $(X(\tau), U(\tau))$ are the parameters. In order to construct the raccordation, we need to see how the parameters evolve in the parameter space. Indeed, during the raccordation the dynamics has to be satisfied. Thus,

$$\left(\frac{dX(\tau)}{d\tau} + j\omega X(\tau)\right) e^{j\omega t} = AX(\tau)e^{j\omega\tau} + bU(\tau)e^{j\omega\tau},\ \tau \in \mathcal{T} = [0, 1],$$

whence the dynamics in the parameter space

$$\frac{dX}{d\tau} = (A - j\omega \mathbf{I})\, X(\tau) + bU(\tau),\ \tau \in \mathcal{T}. \tag{258}$$

Denote the initial and final harmonic steady state by the phasor pair $(X_{i,f}e^{j\omega t}, U_{i,f}e^{j\omega t})$, respectively. The Gluskabi raccordation based on the indirect method (cf. Section 5.1.2) is constructed by minimizing the energy in the parameter space $\mathbb{C}$:

$$\int_0^1 \left\| \frac{dX(\alpha)}{d\alpha} \right\|_{\mathcal{X}}^2 + \left\| \frac{dU(\alpha)}{d\alpha} \right\|_{\mathcal{U}}^2 d\alpha \tag{259}$$

subject to (258) with the boundary conditions (X_i, U_i), $\tau < 0$ and (X_f, U_f), $\tau > 1$. Once the optimal solution is found, the quasi-harmonic behavior is reconstituted via the local map

$$\left(X(\tau)e^{j\omega t}, U(\tau)e^{j\omega t}\right)\big|_{\tau=t}, \; t \in [0,1]. \tag{260}$$

Observe that this raccordation is actually an amplitude modulation.

The previous analysis reveals a connection between the indirect and the direct method in (218). Recall (258) was obtained via the change of variable $x(t) \to X(t)e^{j\omega t}$ and $u(t) \to U(t)e^{j\omega t}$ applied to $\dot{x} = Ax + bu$. With the same substitution in (218):

$$\frac{1}{2}\int_{\mathcal{T}} \|(\mathbf{D} - j\omega)x\|_Q^2 + \|(\mathbf{D} - j\omega)u\|_R^2 \, dt \;\; = \;\; \frac{1}{2}\int_{\mathcal{T}} \left\| \frac{dX(t)}{dt} \right\|_Q^2 + \left\| \frac{dU(t)}{dt} \right\|_R^2 dt.$$

Thus, we have the following:

Proposition 7.3.1. *If the norms in* (259) *and* (218) *coincide and* $(\overline{X}(t), \overline{U}(t))$ *is the optimal solution to* (259)*, then* $x(t) = \overline{X}(t)e^{j\omega t}$ *and* $u(t) = \overline{U}(t)e^{j\omega t}$ *minimizes* (218)*.*

7.3.2 Quasi-periodic raccordation I

We now turn our attention to the dynamic analogue of the signal raccordation in Section (6.1.4). Consider the nonlinear dynamical system (211), which is assumed to be uniformly convergent. The uniformly convergence property ensures that for

any T periodic input u the state response x_u is T periodic, hence, the set $\ker \mathcal{O} \cap \mathcal{B}$ consisting of all T periodic behaviors $w = (x, u)$ is nonempty. We parameterize this set via the Fourier coefficients

$$\left(\langle x\rangle_k(\tau), \langle u\rangle_k(\tau)\right) = \left(\frac{1}{T}\int_{\tau-T}^{\tau} x(s)e^{jk\omega s}ds, \frac{1}{T}\int_{\tau-T}^{\tau} u(s)e^{jk\omega s}ds\right),\ k \in \mathbb{Z}. \tag{261}$$

From Section 6.1.4.1 the derivative of these Fourier coefficients is identically zero since both x and u are T periodic. This is the invariance in the axioms in Section (5.1.2).

The quasi-periodic Gluskabi raccordation based on the indirect method (cf. (181)) is

$$\min_{\left\{\langle u\rangle_k\right\}_{k\in\mathbb{Z}}} \int_{\mathcal{T}} \sum_{k\in\mathbb{Z}} \left\| \frac{d\langle x\rangle_k(\tau)}{d\tau} \right\|_{P_k}^2 + \left\| \frac{d\langle u\rangle_k(\tau)}{d\tau} \right\|_{R_k}^2 d\tau,\ P_k \succeq 0,\ R_k \succ 0, \tag{262}$$

subject to the infinite dimensional dynamics (cf. (175))

$$\frac{d\langle x\rangle_k(\tau)}{d\tau} = \langle f(x,u)\rangle_k(\tau) - j\omega k\langle x\rangle_k(\tau),\ \tau \in \mathcal{T} = [0,1],\ k \in \mathbb{Z}, \tag{263}$$

and boundary conditions $\langle w\rangle_k(t) = \left(\langle x\rangle_k(t), \langle u\rangle_k(t)\right) \equiv \left(\langle x_i\rangle_k, \langle u_i\rangle_k\right),\ t \in (-\infty, 0]$ and $\langle w\rangle_k(t) = \left(\langle x\rangle_k(t), \langle u\rangle_k(t)\right) \equiv \left(\langle x_f\rangle_k, \langle u_f\rangle_k\right),\ t \in [1, \infty)$.

This is a terminal controller problem [12], albeit in infinite dimensions. As in the classical terminal controller problem, the notion of controllability is of importance here since this ensures the existence of the optimal solution. As is well known, for a *finite* dimensional nonlinear system, controllability (connecting any two points in the state space) or strong accessibility (transfer from one state to another in $[0, t_f]$ for *every* $t_f > 0$ [40]) are, in general, too restrictive. Instead, we will assume that it is merely accessible which implies that every states in a neighborhood of the initial state $x(0)$ will be reached for *some* $t_f > 0$. This allows us to use standard Lie bracket

conditions. This condition will be satisfied by the Gluskabi raccordation in general as the raccordation interval is much lager than the period of the orbits.

The system in (263) is nonlinear and infinite dimensional. The notion of controllability for these systems requires a whole different set of ideas [20]. In any case we have the following for the infinite dimensional system (263).

Let $w_i = (x_i, u_i)$, $w_f = (x_f, u_f) \in \mathcal{O} \cap \mathcal{B}$ be two periodic behaviors.

Proposition 7.3.2. *If* (211) *is accessible, then there exits a* $\{\langle w \rangle_k\}_k(t)$, $t \in \mathcal{T}$, *that steers the infinite dimensional system* (263) *from* $\{\langle w_i \rangle_k\}_{k=-\infty}^{\infty}(t)$ *to* $\left\{\langle w_f \rangle_k\right\}_{k=-\infty}^{\infty}$.

Proof. Since the system is accessible, there exits a w that connects w_i to w_f. After taking the dynamic phasor representation of w, we obtain the desired trajectory that connects $\left\{\langle w_i \rangle_k\right\}_k$ to $\left\{\langle w_f \rangle_k\right\}_k$. ∎

In light of (178) the steady states of (263) consists of all functions that are continuous on the circle $C = \mathbb{R}/\mathbb{Z}T$, i.e., $\lim_{\epsilon \to 0} x(t+\epsilon) = \lim_{\epsilon \to 0} x(t+T-\epsilon)$, $t \in C$. With this observation the Gluskabi raccordation is a control problem where one steers from one equilibrium to another via a 'quasi-stationary' path, albeit in infinite dimensions. This is a generalization of the quasi-static LQ problem in Section (4.2), which treats the finite dimensional case.

7.3.2.1 Reconstitution

Once the optimal solution in (262) is found, the dynamic phasors synthesize the behavior $\hat{w}_t(\tau) = (\hat{x}_t(\tau), \hat{u}_t(\tau)) = \left(\sum_k \langle x \rangle (t)_k e^{j\omega k \tau}, \sum_k \langle u \rangle_k (t)_k e^{j\omega k \tau}\right)$, $\tau \in (t-T, t]$. Observe that this is a function of two variables t and τ, respectively. In light of the

discussion of the mid point evaluation (cf. Section 6.1.4.2) the raccordation is defined by

$$w(t) = \hat{w}_t(\tau)|_{\tau=t-\frac{T}{2}}\,,\; t \in \mathcal{T} = [0,1]. \tag{264}$$

7.3.2.2 The LTI case

The dynamics in(263) is general quite complicated because of the nonlinearity in the dynamics (211). For a stable LTI system $\dot{x} = Ax + bu$ (263) is a set of decoupled LTI systems. Indeed,

$$\frac{d\left\langle x\right\rangle_k(\tau)}{d\tau} = (A - jk\omega\mathbf{I})\left\langle x\right\rangle_k(\tau) + b\left\langle u\right\rangle_k(\tau),\; \tau \in \mathcal{T},\; k \in \mathbb{Z}. \tag{265}$$

Hence, in order to find the quasi-periodic raccordation (262) we minimize for each $k \in \mathbb{Z}$,

$$\int_0^1 \left\| \frac{d\left\langle x\right\rangle_k}{d\tau} \right\|_{P_k}^2 + \left\| \frac{d\left\langle u\right\rangle_k}{d\tau} \right\|_{R_k}^2 d\tau, \tag{266}$$

subject to the dynamics in (265). We reformulate the problem into the standard terminal controller by introducing the extended state $z_k = \begin{bmatrix} \left\langle x\right\rangle_k' & \left\langle u\right\rangle_k' \end{bmatrix}'$ and $\frac{d\left\langle u\right\rangle_k}{d\tau} = v_k$. The performance index (266) is

$$\int_{\mathcal{T}} z_k^* Q_k z_k + v_k^* R_k v_k \, d\tau,\; k \in \mathbb{Z}, \tag{267}$$

where

$$Q_k = \begin{bmatrix} A'P_kA + \omega^2k^2P_k & (A' + j\omega k\mathbf{I})P_kb \\ b'P_k(A - j\omega k\mathbf{I}) & b'P_kb \end{bmatrix},$$

subject to the dynamics

$$\frac{d}{dt}z_k = F_kz_k + Gv_k.$$

Here $F_k = \tilde{A} - j\omega k\tilde{\mathbf{I}}$, $\tilde{A} = \begin{bmatrix} A & b \\ 0 & 0 \end{bmatrix}$, $\tilde{\mathbf{I}} = \begin{bmatrix} \mathbf{I} & 0 \\ 0 & 0 \end{bmatrix}$ and $G = \begin{bmatrix} 0 \\ 1 \end{bmatrix}$.

The optimal control (cf. Section (4.1)) is

$$v_k(\tau) \;=\; -R_k^{-1}G'\left(S_k z_k + H_k\left(\Lambda_k^{-1}(0)[z_k^f - H_k(0)z_k^i]\right)\right),\ k \in \mathbb{Z},$$

where the Riccati equation is

$$\begin{aligned} 0 &= \dot{S}_k + S_k\tilde{F}_k + \tilde{F}_k^* S_k + P_k - S_k G R_k^{-1} G^* S_k \\ &= \dot{S}_k + S_k(\tilde{A} - j\omega k\mathbf{I}) + (\tilde{A}' + j\omega k\mathbf{I})S_k + P_k - S_k G R_k^{-1} G^* S_k, \\ &= \dot{S}_k + S_k\tilde{A} + \tilde{A}'S_k + P_k - S_k G R_k^{-1} G^* S_k, \quad S_k(T) = 0, \end{aligned}$$

and

$$\dot{H}_k + \left[F_k - G R_k^{-1} G^* S_k\right]^* H_k = 0, \quad H_k(T) = I.$$

Finally, the reachability Grammian is

$$\Lambda_k(t) = -\int_t^T H_k(\tau) G R_k^{-1} G^* H_k^*(\tau)\, d\tau.$$

7.3.3 Relationship between direct and indirect method

As noted before, the raccordations resulting from the direct and indirect method are in general different. However, for the quasi-periodic raccordation they are closely related. Indeed, if $\sum_k P_k = P \succeq 0, P_k \succeq 0$ and $\sum_k R_k = R \succ 0, R_k \succ 0$, $k \in \mathbb{Z}$, then it follows from (177) that

$$\begin{aligned} &\int_{\mathcal{T}} \sum_k \left\| \frac{d\,\langle x\rangle_k}{d\tau} \right\|_{P_k}^2 + \left\| \frac{d\,\langle u\rangle_k}{d\tau} \right\|_{R_k}^2 d\tau \\ &= \frac{1}{T^2}\int_{\mathcal{T}} \|x(\tau) - x(\tau - T)\|_P^2 + \|u(\tau) - u(\tau - T)\|_R^2\, d\tau. \end{aligned} \tag{268}$$

Hence, we have the following proposition.

Proposition 7.3.3. *Assume* $\sum_k P_k = P \succeq 0, P_k \succeq 0$ *and* $\sum_k R_k = R \succ 0, R_k \succ 0$, $k \in \mathbb{Z}$. *If* $w = (x, u)$ *minimizes the direct method in* (232)*, then* $\{\langle w \rangle_k\}_{k=-\infty}^{\infty} = \left(\{\langle x \rangle_k\}_{k=-\infty}^{\infty}, \{\langle u \rangle_k\}_{k=-\infty}^{\infty}\right)$ *minimizes the indirect method in* (262).

Proof. Let $w = (x, u)$ be the minimizer of (232), then (268) shows that the dynamic phasor of w also minimizes (262). ∎

This proposition does not imply that the raccordations of the direct and indirect method are the same. This actually depends on the global map used to synthesize the time domain behavior.

7.3.4 Quasi-periodic raccordation II

As in Section 6.2.3 we may extend the raccordation in the previous section to orbits with two different periods. The remarks in Section 6.2.3 are still applicable here; the only additional ingredient is the the infinite dimensional dynamics (263).

Specifically, denote the initial and final orbit by $w_0 = (u_0, x_0)$ and $w_1 = (u_1, x_1)$ with period T_0 and T_1, respectively. After writing $\frac{T_0}{T_1} = \frac{p}{q} + r$ for some $p, q \in \mathbb{N}$, $q \neq 0$, $r \in \mathbb{R}$ where p and q are coprime, we set $T = qT_0$ as the fundamental period T in the Fourier expansion (173). The dynamic counterpart of the indirect method in (205) is the optimization problem

$$\min_{\{\langle u \rangle_k\}_{k \in \mathbb{Z}}} J_{\mathcal{T}} = \int_0^1 \sum_{k=-\infty}^{\infty} \left\| \frac{d}{dt} \langle x \rangle_k (t) \right\|_{S_k}^2 + \left\| \frac{d}{dt} \langle u \rangle_k (t) \right\|_{R_k}^2 dt, \tag{269}$$

subject to the dynamics (263).The boundary conditions are

$$\langle w \rangle_k (t) = \langle w_0 \rangle_k (t), \ \frac{d}{dt} \langle w \rangle_k (t) = \frac{d}{dt} \langle w_0 \rangle_k (t), \ t \in [-\infty, 0],$$
$$\langle w \rangle_k (t) = \langle w_1 \rangle_k (t), \ \frac{d}{dt} \langle w \rangle_k (t) = \frac{d}{dt} \langle w_1 \rangle_k (t), \ t \in [1, \infty], \ k \in \mathbb{Z}.$$

The remark following (205) is still applicable here.

7.3.5 An alternative method

The indirect method in the previous section suffers from several shortcomings. The choice of the fundamental period T seems somewhat ad-hoc. Ideally, a Fourier analysis with a *time-varying* window would be tailor-made for the problem, however, such a technique is non-existent to the best of the author's knowledge.

In practice many orbits are generated by an input u that may be parameterized by a finite number of parameters, $\theta \in \mathbb{R}^d$. Denote the input explicitly by $u(t, \theta)$ and the resulting trajectory $x(t, \theta)$. In the present context it is desired to connect the orbits $w_i(t) = (x(t, \theta_i), u(t, \theta_i))$, $i = 0, 1$ in a 'smooth' manner. Recall that if the vector field is Lipshitz, then small changes in θ lead to small changes in x. This motivates us to rephrase the Gluskabi raccordation as follows:

$$\min_{\theta} \int_0^{t_f} \left\| \frac{d\theta}{dt} \right\|_{\Theta}^2 dt, \tag{270}$$

subject to the dynamics $\dot{x} = f(x, u)$ and the boundary conditions

$$\begin{aligned} \theta(t) &= \theta_0,\ x(t) = x(t, \theta_0),\ t \leq 0, \\ \theta(t) &= \theta_1,\ x(t) = x(t, \theta_1),\ t \geq t_f. \end{aligned} \tag{271}$$

Without loss of generality we will work with the interval $[0, t_f]$ instead of the unit interval in the previous chapters.

In order to facilitate the discussion we decompose the periodic inputs that generate the periodic orbits into $u(t, \theta_i) = u_p(t, \theta_{p,i}) + \theta_{d,i}$, $i = 0, 1$, where $\theta_{d,i}$ is the DC component, and u_p is the periodic part in the absence of the DC component. Thus,

the parameters in (271) are $\theta_i = (\theta_{p,i}, \theta_{d,i})$, $i = 0, 1$, respectively. We further assume throughout that the periods of $u_p(t, \theta_{p,i})$, $i = 0, 1$ are much smaller than t_f.

A suboptimal solution to (270) may be obtained as follows. We first connect $\theta_{p,i}$, $i = 0, 1$ via $\theta_p(t) = \theta_{p,0}(1 - \frac{t}{t_f}) + \theta_{p,1}\frac{t}{t_f}$, $t \in [0, t_f]$. If t_f is large, then the change in θ_p will be small. Subsequently, we solve the optimization problem

$$\min_{\theta_d} \int_0^{t_f} \left\| \frac{d\theta_d}{dt} \right\|_{\Theta_d}^2 dt, \tag{272}$$

subject to $\dot{x} = f(x, u)$ and the boundary conditions in (271).

As an example we apply the previous setup to the nonlinear system (222). For simplicity we consider two orbits generated by the inputs $u(t) = A_i \cos(\omega_i t) + c_i$, $i = 0, 1$. Therefore, the parameters are $\theta_{p,i} = (A_i, \omega_i)$ and $\theta_{d,i} = c_i$, $i = 0, 1$, respectively. Specifically, (272) reduces to

$$\min_{\theta_d} \int_0^{t_f} \left\| \frac{d\theta_d}{dt} \right\|_{R}^2 dt, \tag{273}$$

subject to the dynamics (222) with $u(t) = A(t)\cos(\omega(t)t) + \theta_d(t)$, $t \in [0, t_f]$, where $A(t) = A_0(1 - \frac{t}{t_f}) + A_1\frac{t}{t_f}$ and $\omega(t) = \omega_0(1 - \frac{t}{t_f}) + \omega_1\frac{t}{t_f}$, $t \in [0, t_f]$. The boundary conditions are $\theta_d(t) = c_0$, $x(t) = x_0(t)$, $t \leq 0$, and $\theta_d(t) = c_1$, $x(t) = x_1(t)$, $t \geq t_f$,

For the results in Figure 53 and Figure 54 we choose $t_f = 1$, $A_0 = 150$, $T_0 = 0.95T_1$ and $A_1 = 175$, $T_1 = 0.05$. We apply the gradient descent algorithm as expounded in [12].

7.4 Conclusion

In this chapter we have extended the signal Gluskabi raccordation in Chapter 6 to the dynamic case. The behavioral approach to dynamical modeling is a natural starting

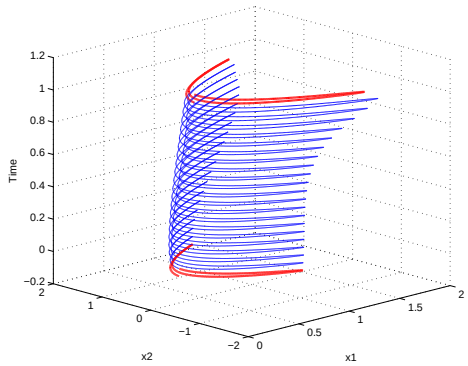

Figure 53: Trajectory of smooth transition

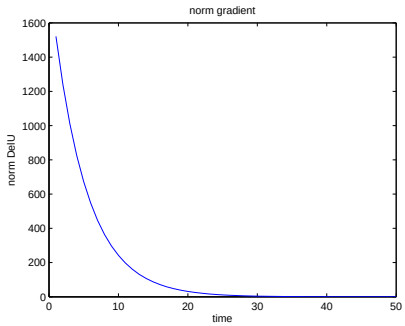

Figure 54: Magnitude of the input gradient vs. number of iterations

point for the framework. Indeed, the dynamics is simply a *hard* constraint on $\mathcal{V}$, the set of all possible trajectories.

As in Chapter 6 we have discussed both the direct and indirect method. The direct method has the advantage that the trajectory is shaped immediately while the indirect method involves a two-step procedure. Specifically, it first maps the behavior into a parameter space Θ, and the raccordation is subsequently constructed by mapping the 'smoothest' transition in Θ back to the behavior.

We applied both the direct and indirect method to the quasi-periodic raccordation. Indeed, by following the general procedure in Section 6.1.3 all algorithms for the direct method in Chapter 6 have been modified to incorporate the dynamical constraints. Subsequently, we applied the dynamic phasors to study the indirect method; the dynamics in the frequency domain is infinite dimensional. Finally, we explored the relationship between the direct and indirect method.

The indirect method for the quasi-periodic raccordation of two orbits of different periods suffers from several shortcomings. One particular shortcoming is the fixed length of the sliding window $[t - T, t)$ needed to obtain the dynamic phasors. We presented one way of choosing T for the quasi-periodic raccordation. Therefore, an alternative method is presented in Section 7.3.5. This method has a flavor of both the direct and indirect method.

CHAPTER VIII

CONCLUSIONS AND FUTURE WORK

We now briefly summarize the essential developments of each chapter and indicate possible directions for future research.

Inspired by the many varieties of legless locomotion, we studied in Chapter 2 the self-propulsion of a few legless, toy creatures based on differential friction. This friction model is based on viscous friction which is predominant in wet environment. The main goal was to consider the effects of periodic control on locomotion. Specifically, we first studied both the harmonic and optimal periodic control of the so-called flapper. Finally, we studied a simple prototype of a snake: the two-piece snake. The dynamical equations were obtained by using the Lagrangian technique, and we investigated the optimal periodic control of this system.

As indicated earlier, we may cascade two flappers serially to obtain a model of a tortoise. We could further investigate the effects of periodic control on this system. Along a similar line we may extend the two-piece snake by cascading many pieces together. Unfortunately, the resulting set of equations will be large, coupled and very complicated. In order to avoid this difficulty we may instead obtain a *continuous* model of the snake by cascading infinitesimal small two-piece snakes. The resulting equation will be a partial differential equations (PDE), and this could be more amenable to study. An immediate problem that needs to be explored is the

controllability of this PDE.

In Chapter 3 we solved a control problem for a stochastic system, under the basic constraint that the feedback control signal and the observations from the system cannot use the communication channel simultaneously. Hence, two modes of operation result: 1) an observation mode where outputs from the system are transmitted to the controller, and no inputs are sent back to the plant, 2) a control mode where the output of the plant is decoupled from the controller, but control signals are transmitted back to the plant. We looked for an optimal periodic regime in a statistical steady state by switching between the observation and the control mode. In addition to the duty cycle, the optimal gains for both the controller and the observer in either mode are determined. This is solved by considering the deterministic model for the second order information state (the covariances). In addition, we showed that the observation mode can be reduced to a lower order model, which leads to a multi-mode multi-dimensional (M^3D) problem.

In Chapter 4 we analyzed the terminal LQ controller in the limit as $T \to \infty$. Such a problem gives a good example where the limiting operation and integration do not commute. Such a misinterpretation can lead to an apparent paradox. In this chapter we used symmetrical components (the parity operator) to shed light on the correct solution. Along the way we gave a *constructive* proof of the necessary conditions of optimality, which shows that there is a decomposition of the problem into two subproblems. Furthermore, for the quasi-stationary optimal control problem we showed that the performance index approaches zero as $T \to \infty$.

In Chapter 5 we used several simple examples to introduce the main theme of

this thesis, the Gluskabi raccordation. We then considered the Gluskabi raccordation *without* a dynamics in Chapter 6. Furthermore, we presented two methods, the direct and indirect method, to construct these maximally 'smooth' transitions connecting any two behaviors with a specific property. The direct method involves the nullspace of an operator, and the Gluskabi raccordation is obtained by minimizing the deviation from this nullspace. This may be considered a 'time domain' approach. On the other hand, the indirect method first maps this nullspace to a parameter space and subsequently reconstitute the actual raccordation from the 'smoothest' path in the parameter space. This is a 'frequency domain' approach. We applied the two approaches to the quasi-periodic and the frequency raccordation, and all algorithms for generating the Gluskabi raccordation based on the direct method for these cases are presented. The indirect method for these two instances involves the dynamic phasors; we also pointed out the connection between the direct and indirect method.

In Chapter 7 we extended the theory of the signal raccordation in Chapter 6 to include a dynamical system. By viewing the dynamics as a *hard* constraint on the behavior, we saw that the generalization could be readily made; all developments in Chapter 6 were modified accordingly.

As mentioned earlier in Chapter 6 and 7 the dynamic phasors or the sliding Fourier series have several shortcomings when applied to the frequency raccordation. This is mainly caused by the fixed window length needed in the Fourier expansion. It is of interest to find a technique to resolve this issue. Another direction worth pursuing is to apply the framework to some physical systems. A good starting point may be to consider first some bilinear systems since they model many physical systems [**?**, **?**],

and they are the simplest nonlinear control systems to deal with. In [**?**] the author presents various open problems in the field of quantum control, and the resulting model is obtained via an averaging argument. The system is inherently bilinear, and the control applied is essentially a demodulation. Since the Fourier integral is also an averaging, and the indirect method involves an amplitude modulation, it is fruitful to investigate whether the indirect method based on the dynamic phasors can be applied here. In [**?**] the author studies the relationship between the control of the nonholonomic integrator and the generation of cyclic processes. In addition, a kinematic model of a biped locomotion is given. This model might serve as a starting point for applying the Gluskabi raccordation to locomotion. Finally, one could study the Gluskabi raccordation of delay systems. All the algorithms presented so far are easily modified for these systems.

APPENDIX A

COMPONENTS OF A IN (21)

The components of the matrix $A(\dot{x}, \dot{y}, q)$ in (20) and (21) are as follows:

$$
\begin{aligned}
A_{x1} &= -g_u \cos(\theta(t)+\gamma(t))^2 - g_l \cos(-\gamma(t)+\theta(t))^2 - \mu_T \sin(\theta(t)+\gamma(t))^2 \\
&\quad -\mu_T \sin(-\gamma(t)+\theta(t))^2, \\
A_{y1} &= -g_u \sin(\theta(t)+\gamma(t)) \cos(\theta(t)+\gamma(t)) + g_l \sin(-\gamma(t)+\theta(t)) \cos(-\gamma(t)+\theta(t)) \\
&\quad +\mu_T \cos(\theta(t)+\gamma(t)) \sin(\theta(t)+\gamma(t)) - \mu_T \cos(-\gamma(t)+\theta(t)) \sin(-\gamma(t)+\theta(t)), \\
A_{\theta 1} &= \frac{1}{2}\mu_T \left(\sin(\theta(t)+\gamma(t))^2 + \cos(\theta(t)+\gamma(t))^2\right) \sin(\theta(t)+\gamma(t)) \\
&\quad -\frac{1}{2}\mu_T (\sin(-\gamma(t)+\theta(t))^2 + \cos(-\gamma(t)+\theta(t))^2) \sin(-\gamma(t)+\theta(t)), \\
A_{\gamma 1} &= \frac{1}{2}\mu_T (\sin(\theta(t)+\gamma(t))^2 + \cos(\theta(t)+\gamma(t))^2) \sin(\theta(t)+\gamma(t)) \\
&\quad -\frac{1}{2}\mu_T (-\sin(-\gamma(t)+\theta(t))^2 - \cos(-\gamma(t)+\theta(t))^2) \sin(-\gamma(t)+\theta(t)), \\
A_{x2} &= -g_u \cos(\theta(t)+\gamma(t)) \sin(\theta(t)+\gamma(t)) + g_l \cos(-\gamma(t)+\theta(t)) \sin(-\gamma(t)+\theta(t)) \\
&\quad +\mu_T \sin(\theta(t)+\gamma(t)) \cos(\theta(t)+\gamma(t)) - \mu_T \sin(-\gamma(t)+\theta(t)) \cos(-\gamma(t)+\theta(t)), \\
A_{y2} &= -g_u \sin(\theta(t)+\gamma(t))^2 - g_l \sin(-\gamma(t)+\theta(t))^2 \\
&\quad -\mu_T \cos(\theta(t)+\gamma(t))^2 - \mu_T \cos(-\gamma(t)+\theta(t))^2, \\
A_{\theta 2} &= -\frac{1}{2}\mu_T (\sin(\theta(t)+\gamma(t))^2 + \cos(\theta(t)+\gamma(t))^2) \cos(\theta(t)+\gamma(t)) \\
&\quad -\frac{1}{2}\mu_T (\sin(-\gamma(t)+\theta(t))^2 + \cos(-\gamma(t)+\theta(t))^2) \cos(-\gamma(t)+\theta(t)),
\end{aligned}
$$

$$
\begin{aligned}
A_{\gamma 2} &= -\frac{1}{2}\mu_T(\sin(\theta(t)+\gamma(t))^2+\cos(\theta(t)+\gamma(t))^2)\cos(\theta(t)+\gamma(t)) \\
&\quad -\frac{1}{2}\mu_T(-\sin(-\gamma(t)+\theta(t))^2-\cos(-\gamma(t)+\theta(t))^2)\cos(-\gamma(t)+\theta(t)), \\
A_{x3} &= \mu_T \sin(\gamma(t))\cos(\theta(t)), \\
A_{y3} &= -\mu_T \cos(\gamma(t))\cos(\theta(t)), \\
A_{\theta 3} &= -\frac{2}{3}\mu_T, \\
A_{\gamma 3} &= 0, \\
A_{x4} &= \mu_T \sin(\theta(t))\cos(\gamma(t)), \\
A_{y4} &= \mu_T \sin(\theta(t))\sin(\gamma(t)), \\
A_{\theta 4} &= 0, \\
A_{\gamma 4} &= -\frac{2}{3}\mu_T,
\end{aligned}
$$

where

$$
\begin{aligned}
g_u &= \mu_a(\langle \dot{r}^u, B_x^u \rangle) = \mu_a(\dot{x}\cos(\theta+\gamma)+\dot{y}\sin(\theta+\gamma)), \qquad (274) \\
g_l &= \mu_a(\langle \dot{r}^l, B_x^l \rangle) = \mu_a(\dot{x}\cos(-\theta+\gamma)-\dot{y}\sin(-\theta+\gamma)).
\end{aligned}
$$

APPENDIX B

PROOF OF THEOREM 4.1.3

Recall that the weight matrices obtained in the even and odd decomposition are

$$\mathbf{CH}\left(\frac{T}{2}\right) = \left[\cosh\left(\mathbf{H}'\frac{T}{2}\right)\right]^{-1}\mathbf{Ch}(T)\left[\cosh\left(\mathbf{H}\frac{T}{2}\right)\right]^{-1}, \tag{275}$$

$$\mathbf{SH}\left(\frac{T}{2}\right) = \left[\sinh\left(\mathbf{H}'\frac{T}{2}\right)\right]^{-1}\mathbf{Sh}(T)\left[\sinh\left(\mathbf{H}\frac{T}{2}\right)\right]^{-1}, \tag{276}$$

where, after a change of variable, the sinh- and cosh- integrals are

$$\mathbf{Sh}(T) = \frac{1}{2}\int_0^T \sinh\left(\mathbf{H}'\frac{t}{2}\right) Q \sinh\left(\mathbf{H}\frac{t}{2}\right) dt, \tag{277}$$

$$\mathbf{Ch}(T) = \frac{1}{2}\int_0^T \cosh\left(\mathbf{H}'\frac{t}{2}\right) Q \cosh\left(\mathbf{H}\frac{t}{2}\right) dt. \tag{278}$$

We will prove that the weight matrices $\mathbf{CH}(\frac{T}{2})$ and $\mathbf{SH}(\frac{T}{2})$ are bounded as $T \to \infty$. Taking derivative of (275) and (276) with respect to T, we obtain the Lyapunov equation

$$\dot{\mathbf{CH}}\left(\frac{T}{2}\right) = -2A_c'\left(\frac{T}{2}\right)\mathbf{CH}\left(\frac{T}{2}\right) - \mathbf{CH}\left(\frac{T}{2}\right)\left(2A_c\left(\frac{T}{2}\right)\right) + Q, \tag{279}$$

$$\dot{\mathbf{SH}}\left(\frac{T}{2}\right) = -2A_s'\left(\frac{T}{2}\right)\mathbf{SH}\left(\frac{T}{2}\right) - \mathbf{SH}\left(\frac{T}{2}\right)\left(2A_s\left(\frac{T}{2}\right)\right) + Q, \tag{280}$$

where

$$A_c\left(\frac{T}{2}\right) = \frac{1}{2}\mathbf{H}\sinh\left(\mathbf{H}\frac{T}{2}\right)\cosh^{-1}\left(\mathbf{H}\frac{T}{2}\right), \tag{281}$$

$$A_s\left(\frac{T}{2}\right) = \frac{1}{2}\mathbf{H}\cosh\left(\mathbf{H}\frac{T}{2}\right)\sinh^{-1}\left(\mathbf{H}\frac{T}{2}\right). \tag{282}$$

Letting

$$\Phi_c(t,\tau) = \cosh\left(\mathbf{H}\frac{t}{2}\right)\cosh^{-1}\left(\mathbf{H}\frac{\tau}{2}\right), \tag{283}$$

$$\Phi_s(t,\tau) = \sinh\left(\mathbf{H}\frac{t}{2}\right)\sinh^{-1}\left(\mathbf{H}\frac{\tau}{2}\right), \tag{284}$$

we see that

$$\frac{d}{d\tau}\Phi_c(t,\tau) = -\Phi_c(t,\tau)A_c\left(\tau/2\right), \tag{285}$$

$$\frac{d}{d\tau}\Phi_s(t,\tau) = -\Phi_s(t,\tau)A_s\left(\tau/2\right). \tag{286}$$

Thus, if $\Phi_c(t,\tau)$ and $\Phi_s(t,\tau)$ are asymptotically stable as $\tau \to \infty$, then the boundedness of the Lyapunov equations (279) and (280) easily follows. This further implies that (275) and (276) are bounded.

Since $\mathbf{H}$ has only simplectic eigenvalues with nonzero real parts by our assumption of minimality, the convergence of (283) and (284) depends only on the eigenvalues on the open right half plane. Indeed, the evenness of the cosh function allows us to assume that $\mathbf{H}$ contains only the unstable part of $\mathbf{H}$. Then

$$\cosh^{-1}\left(\mathbf{H}\frac{\tau}{2}\right) = \frac{1}{2}\exp\left(-\mathbf{H}\frac{\tau}{2}\right)\left(I + \exp\left(-\mathbf{H}\tau\right)\right)^{-1},$$

which implies that (283) is exponentially stable. Similarly, the odd function $\sinh\mathbf{H}\frac{\tau}{2}$ may be written as

$$\sinh\mathbf{H}\frac{\tau}{2} = \sinh\mathbf{H}_+\frac{\tau}{2}S, \tag{287}$$

where $\mathbf{H}_+$ contains the unstable part of $\mathbf{H}$, and S is a sign-matrix

$$S = \begin{bmatrix} \sigma_1 I_1 & & \\ & \sigma_2 I_2 & \\ & & \ddots \end{bmatrix}.$$

σ_i is either 1 or -1 depending on whether an arrangement is needed in (287). Since $\sinh(\mathbf{H}_+\tau/2)$ is exponentially stable by similar argument as the previous case, we see that the Lyapunov equations (279) and (280) have a steady state solution. Hence, (275) and (276) are bounded as $T \to \infty$.

APPENDIX C

COMPLEXIFIED TERMINAL CONTROLLER

In this section we derive the necessary conditions of optimality for the terminal controller for LTI systems with complex parameters.

Consider the optimization problem

$$\frac{1}{2}\int_0^T x^*Px + u^*Ru\ dt$$

subject to

$$\dot{x} = Ax + bu,\ x(0) = x_i,\ x(T) = x_f.$$

where all parameters are complex, P and R are Hermitian and $P \geq 0, R > 0$.

We first form the Hamiltonian

$$H = x^*Px + u^*Ru + \lambda_x^*(Ax + bu) + (Ax + bu)^*\lambda_x$$

to preserve the realness of the Hamiltonian and the P.I. Adjoin the final state constraints to the P.I

$$\begin{aligned} J_0 &= \nu^*(x(T) - x_f) + (x(T) - x_f)^*\nu + \int_0^T x^*Px + u^*Ru \\ &\quad +\lambda_x^*(Ax + bu - \dot{x}) + (Ax + bu - \dot{x})^*\lambda_x\ dt \end{aligned}$$

We compute the variation

$$\delta J = \lim_{\epsilon \to 0} \frac{J_\epsilon - J_0}{\epsilon}$$

we obtain

$$\begin{aligned}\delta J &= (\nu - \lambda(T))^*\eta(T) + \eta^*(T)(\nu - \lambda(T)) + \lambda^*(0)\eta(0) + \eta^*(0)\lambda(0) + \\ &+ \int_0^T (Px + A^* + \dot{\lambda}) + (x^*P + \lambda^*A + \dot{\lambda}^*)\eta + \nu^*(Ru + b^*\lambda) + (Ru^* + \lambda^* b)\nu \; dt\end{aligned}$$

We choose

$$-\dot{\lambda} = Px + A^*\lambda, \text{ and } \nu = \lambda(T).$$

and the optimality condition is

$$u = -R^{-1}b^*\lambda.$$

Thus, the complex Hamiltonian system is

$$\begin{bmatrix} \dot{x} \\ \dot{\lambda} \end{bmatrix} = \begin{bmatrix} A & -bR^{-1}b^* \\ -P & -A^* \end{bmatrix} \begin{bmatrix} x \\ \lambda \end{bmatrix} \tag{288}$$

with $\lambda(T) = \nu$ chosen such that the boundary conditions are met.

APPENDIX D

CONVERGENT SYSTEMS

We first review some stability notions related to autonomous system. Consider the autonomous system

$$\dot{x} = f(x,t) \tag{289}$$

$x \in \mathbb{R}^n$, $t \in \mathbb{R}$ where $f(x,t)$is locally Lipshitz in x and piecewise continuous in t.

Definition D.1. *[43] A solution* $\overline{x}, t \in (t^*, \infty)$ *of* (289) *is*

- stable *if for any* $t_0 \in (t^*, \infty)$ *and* $\epsilon > 0$ *there exits a* $\delta > 0$ *such that* $\|x(t_0) - \overline{x}(t_0)\| < \delta$ *implies* $\|x(t) - \overline{x}(t)\| < \epsilon$ *for all* $t \geq t_0$.
- uniformly stable *if it is stable and the number* δ *is independent of* t_0.
- asymptotically stable *if it is stable and for any* $t_0 \in (t^*, \infty)$ *there exits a* $\delta = \delta(t_0) > 0$ *such that* $\|x(t_0) - \overline{x}(t_0)\| < \delta$ *implies that* $\lim_{t\to\infty} \|x(t) - \overline{x}(t)\| = 0$.
- uniformly asymptotically stable *if it is uniformly stable and there exits a* $\delta > 0$*, independent of* t_0*, such that for any* $\epsilon > 0$ *there exists* $T = T(\epsilon) > 0$ *so that* $\|x(t_0) - \overline{x}(t_0)\| < \delta$ *for* $t_0 \in (t^*, \infty)$ *implies that* $\|x(t) - \overline{x}(t)\| < \epsilon$ *for all* $t \geq t_0 + T$.

We now define stability of a solution in a pre-defined subset of the state space, instead of a neighborhood of a solution.

Definition D.2. *[43] A solution* $\overline{x}(t)$, $t \in (t^*, \infty)$ *of* (289) *is*

- asymptotically stable in a set $\mathcal{X} \in R^n$ *if it is asymptotically stable and a solution of* (289) *starting at* $x(t_0) \in \mathcal{X}$, $t_0 \in (t^*, \infty)$ *implies that* $\|x(t) - \overline{x}(t)\| \to 0$ *as* $t \to \infty$.

- uniformly asymptotically stable in a set $\mathcal{X} \in R^n$ *if it is uniformly stable and it attracts solutions of system* (289) *starting at* $x(t_0) \in \mathcal{X}$, $t_0 \in (t^*, \infty)$ *uniformly over* t_0. *In other words, for any compact set* $K \subset \mathcal{X}$ *and any* $\epsilon > 0$ *there exits* $T(\epsilon, K) > 0$ *such that if* $x(t_0) \in K$, $t_0 \in (t^*, \infty)$, *then* $\|x(t) - \overline{x}(t)\| < \epsilon$ *for all* $t \geq t_0 + T(\epsilon, K)$.

We now turn our attention to convergent systems.

Definition D.3. *[43] The system* (289) *is*

- convergent in a set $\mathcal{X} \in \mathbb{R}^n$ *if there exists a solution* $\overline{x}(t)$ *with the following properties:*

  (i) $\overline{x}(t)$ *is defined and bounded for all* $t \in \mathbb{R}$. *(ii)* $\overline{x}(t)$ *is asymptotically stable in* $\mathcal{X}$.

- uniformly convergent in $\mathcal{X}$ *if it is convergent in* $\mathcal{X}$ *and* $\overline{x}(t)$ *is uniformly asymptotically stable in* $\mathcal{X}$.

If system (289) *is (uniformly) convergent in* $\mathcal{X} = \mathbb{R}^n$, *then it is called globally (uniformly) convergent.*

$\overline{x}(t)$ is a steady state solution defined for all $t \in \mathbb{R}$.

Finally, we define the convergence properties for the controlled vector field

$$\dot{x} = f(x, u) \tag{290}$$

with state $x \in \mathbb{R}^n$ and input $w \in \mathbb{R}^m$. Let PC_m denote a class of piecewise continuous function.

Definition D.4. *[43] System* (290) *is* (uniformly) convergent in a subset $\mathcal{X} \subset \mathbb{R}^n$ *for a class of input* $\mathcal{N} \subset PC_m$ *if it is (uniformly) convergent in* $\mathcal{X}$ *for every input* $u \in \mathcal{N}$.

Thus, for any $u(t)$, $t \in \mathbb{R}$ we may define a steady state solution $x_u(t)$, $t \in \mathbb{R}$ parameterized by u. Notice that these functions are defined over the whole real line and not just the semi infinite interval (t_0, ∞) as in definitions $(D.1)$ and $(D.2)$.

The following theorem is important for the Gluscabi raccordation.

Theorem D.1. *[43] Suppose system* (290) *with a given input* $u(t)$ *is uniformly convergent in* $\mathcal{X}$*, If the input* $u(t)$ *is constant (periodic with period* T*), then the corresponding steady state solution* $\overline{x}_u(t)$ *is also constant (periodic with period* T*).*

APPENDIX E

PROOFS OF CHAPTER 6

In this appendix we collect several results left out in Chapter 6.

Proof E.1 (Proof of Proposition (6.2.2)). *Let $s_i \in (1, 1+T_1)$ and $J_k^{s_i} = e_k' x(s_i)$. After adjoining the dynamics to $J_k^{s_i}$ and letting $u \to u + \epsilon v$ and $x \to x + \epsilon\eta$ the Fréchet derivative is*

$$
\begin{aligned}
\delta J_k^{s_i} &= e_k'\eta(s_i) + \int_0^{1^-} \lambda_k^{s_i\prime}(t)\left((1-\dot T)\dot\eta(t-T(t)) + v(t) - \dot\eta(t)\right)dt \\
&\quad + \int_{1^+}^{1+T_1} \lambda_k^{s_i\prime}(t)\left(\dot\eta(t-T_1) + v(t) - \dot\eta(t)\right)dt, \\
&= e_k'\eta(s_i) - \lambda_k^{s_i\prime}(t)\eta(t)\big|_0^{1^--T_1} - \lambda_k^{s_i\prime}(t)\eta(t)\big|_{1^+-T_1}^{1^-} - \lambda_k^{s_i\prime}(t)\eta(t)\big|_{1^+}^{s_i^-} \\
&\quad - \lambda_k^{s_i\prime}(t)\eta(t)\big|_{s_i^+}^{1+T_1} + \int_0^{1+T_1} \dot\lambda_k^{s_i\prime}(t)\eta(t)dt \\
&\quad + (1-\dot T)\int_0^{1^-} \lambda_k^{s_i\prime}(t)\frac{d\eta(t-T(t))}{dt}dt + \\
&\quad + \int_{1^+}^{1+T_1} \lambda_k^{s_i\prime}(t)\frac{d\eta(t-T_1)}{dt}dt + \int_0^{1+T_1} \lambda_k^{s_i\prime}(t)v(t)dt, \\
&= \left(-\lambda_k^{s_i\prime}(1^- - T_1) + \lambda_k^{s_i\prime}(1^+ - T_1)\right)\eta(1-T_1) \\
&\quad + \left(e_k' - \lambda_k^{s_i\prime}(s_i^-) + \lambda_k^{s_i\prime}(s_i^+)\right)\eta(s_i) + \\
&\quad \left(-\lambda_k^{s_i\prime}(1^-) + \lambda_k^{s_i\prime}(1^+)\right)\eta(1) - \lambda_k^{s_i\prime}(1+T_1)\eta(1+T_1) + \\
&\quad + \int_0^{1+T_1} \frac{d\lambda_k^{s_i\prime}(t)}{dt}\eta(t)dt + (1-\dot T)\int_{-T_0}^{1^--T_1} \lambda_k^{s_i\prime}\left(\frac{\tau+T_0}{1-\dot T}\right)\frac{d\eta(\tau)}{d\tau}d\tau \\
&\quad + \int_{1^+-T_1}^{1} \lambda_k^{s_i\prime}(\tau+T_1)\frac{d\eta(\tau)}{d\tau}d\tau + \int_0^{1+T_1} \lambda_k^{s_i\prime}(t)v(t)dt,
\end{aligned}
$$

$$
\begin{aligned}
= \quad & \left(-\lambda_k^{s_i\prime}(1^- - T_1) + \lambda_k^{s_i\prime}(1^+ - T_1)\right)\eta(1-T_1) + \left(e_k' - \lambda_k^{s_i\prime}(s_i^-) + \lambda_k^{s_i\prime}(s_i^+)\right)\eta(s_i) + \\
& \left(-\lambda_k^{s_i\prime}(1^-) + \lambda_k^{s_i\prime}(1^+)\right)\eta(1) - \lambda_k^{s_i\prime}(1+T_1)\eta(1+T_1) + \\
& + \int_0^{1+T_1} \dot{\lambda_k^{s_i}}'(t)\eta(t)dt + \\
& + (1-\dot{T})\ \lambda_k^{s_i\prime}\left(\frac{\tau+T_0}{1-\dot{T}}\right)\eta(\tau)\Big|_{-T_0}^{1^- - T_1} - \int_{-T_0}^{1^- - T_1} \frac{d\lambda_k^{s_i\prime}}{d\tau}\left(\frac{\tau+T_0}{1-\dot{T}}\right)\eta(\tau)d\tau \\
& + \lambda_k^{s_i\prime}(\tau+T_1)\eta(\tau)\big|_{1^+ - T_1}^{1} - \int_{1^+ - T_1}^{1} \frac{d\lambda_k^{s_i\prime}}{d\tau}(\tau+T_1)\eta(\tau)d\tau \\
& + \int_0^{1+T_1} \lambda_k^{s_i\prime}(t)v(t)dt, \\
= & \Big(-\lambda_k^{s_i\prime}(1^- - T_1) + \lambda_k^{s_i\prime}(1^+ - T_1) + (1-\dot{T})\lambda_k^{s_i\prime}(1^-) - \lambda_k^{s_i\prime}(1^+)\Big)\eta(1-T_1) \qquad (291) \\
& + \left(e_k' - \lambda_k^{s_i\prime}(s_i^-) + \lambda_k^{s_i\prime}(s_i^+)\right)\eta(s_i) + \\
& \left(-\lambda_k^{s_i\prime}(1^-) + \lambda_k^{s_i\prime}(1^+) + \lambda_k^{s_i\prime}(1+T_1)\right)\eta(1) - \lambda_k^{s_i\prime}(1+T_1)\eta(1+T_1) + \\
& \int_0^{1-T_1}\left(\frac{d\lambda_k^{s_i}(t)}{dt}' - \frac{d\lambda_k^{s_i}}{dt}'\left(\frac{t+T_0}{1-\dot{T}}\right)\right)\eta(t)dt + \\
& \int_{1-T_1}^{1}\left(\frac{d\lambda_k^{s_i}(t)}{dt}' - \frac{d\lambda_k^{s_i}}{dt}'(t+T_1)\right)\eta(t)dt + \int_1^{1+T_1}\frac{d\lambda_k^{s_i}(t)}{dt}'\eta(t)dt \\
& + \int_0^{1+T_1}\lambda_k^{s_i\prime}(t)v(t)dt,
\end{aligned}
$$

where we have used the change of variable $t = \frac{\tau+T_0}{1-\dot{T}}, t \in [0, 1^-)$ *and* $t = \tau + T_1$, $t \in [1^+, 1+T_1]$ *and continuity of* $\eta(t)$ *at* $t = 1-T_1, 1, s_i$. *We choose*

$$
\begin{aligned}
\lambda_k^{s_i\prime}(1^- - T_1) &= \lambda_k^{s_i\prime}(1^+ - T_1) + (1-\dot{T})\lambda_k^{s_i\prime}(1^-) - \lambda_k^{s_i\prime}(1^+), \\
\lambda_k^{s_i}(s_i^-) &= e_k + \lambda_k^{s_i}(s_i^+), \qquad (292) \\
\lambda_k^{s_i}(1^-) &= \lambda_k^{s_i}(1+T_1) + \lambda_k^{s_i}(1^+), \\
\lambda_k^{s_i}(1+T_1) &= 0, \\
\lambda_k^{s_i}(1^-) &= \lambda_k^{s_i}(1^+),
\end{aligned}
$$

$$
\begin{aligned}
\dot{\lambda_k^{s_i}}(t) &= \dot{\lambda_k^{s_i}}\left(\frac{t+T_0}{1-\dot{T}}\right),\ t\in[0,1-T_1),\\
\dot{\lambda_k^{s_i}}(t) &= \dot{\lambda_k^{s_i}}(t+T_1),\ t\in[1-T_1,1),\\
\dot{\lambda_k^{s_i}}(t) &= 0,\ t\in[1,1+T_1),\ t\neq s_i.
\end{aligned}
$$

For $s_i = 1$ and $s_i = 1+T_1$ only the boundary conditions need to modified. Indeed, for $s_i = 1$ in (291) we have

$$
\begin{aligned}
& e_k'\eta(1) - \lambda_k^{s_i\prime}(t)\eta(t)\big|_0^{1^--T_1} - \lambda_k^{s_i\prime}(t)\eta(t)\big|_{1^+-T_1}^{1^-} - \lambda_k^{s_i\prime}(t)\eta(t)\big|_{1^+}^{1+T_1} +\\
& (1-\dot{T})\,\lambda_k^{s_i\prime}\left(\frac{\tau+T_0}{1-\dot{T}}\right)\eta(\tau)\Big|_{-T_0}^{1^--T_1} + \lambda_k^{s_i\prime}(\tau+T_1)\eta(\tau)\big|_{1^+-T_1}^{1}\\
= \;& \left(e_k' - \lambda_k^{s_i\prime}(1^-) + \lambda_k^{s_i\prime}(1^+) + \lambda_k^{s_i\prime}(1+T_1)\right)\eta(1) - \lambda_k^{s_i\prime}(1+T_1)\eta(1+T_1)\\
& + \left(-\lambda_k^{s_i\prime}(1^--T_1) + \lambda_k^{s_i\prime}(1^+-T_1) + (1-\dot{T})\lambda_k^{s_i\prime}(1^-) - \lambda_k^{s_i\prime}(1^+)\right)\eta(1-T_1).
\end{aligned}
$$

Hence, the boundary conditions of the corresponding costates are

$$
\begin{aligned}
\lambda_k^{s_i}(1^-) &= e_k + \lambda_k^{s_i}(1^+) + \lambda_k^{s_i}(1+T_1),\\
\lambda_k^{s_i}(1+T_1) &= 0,\\
\lambda_k^{s_i\prime}(1^--T_1) &= \lambda_k^{s_i\prime}(1^+-T_1) + (1-\dot{T})\lambda_k^{s_i\prime}(1^-) - \lambda_k^{s_i\prime}(1^+),\\
\dot{\lambda_k^{s_i}}(t) &= \dot{\lambda_k^{s_i}}\left(\frac{t+T_0}{1-\dot{T}}\right),\ t\in[0,1-T_1),\\
\dot{\lambda_k^{s_i}}(t) &= \dot{\lambda_k^{s_i}}(t+T_1),\ t\in[1-T_1,1),\\
\dot{\lambda_k^{s_i}}(t) &= 0,\ t\in[1,1+T_1),
\end{aligned}
$$

from which we conclude that $\lambda_k^{s_i}(1^+) = 0$. This set can be further simplified to

$$
\begin{aligned}
\lambda_k^{s_i}(1^-) &= e_k, \qquad (293)\\
\lambda_k^{s_i}(1+T_1) &= 0,\\
\lambda_k^{s_i}(1^--T_1) &= \lambda_k^{s_i}(1^+-T_1) + (1-\dot{T})e_k,
\end{aligned}
$$

$$
\begin{aligned}
\dot{\lambda_k^{s_i}}(t) &= \dot{\lambda_k^{s_i}}\left(\frac{t+T_0}{1-\dot{T}}\right), t \in [0, 1-T_1), \\
\dot{\lambda_k^{s_i}}(t) &= \dot{\lambda_k^{s_i}}(t+T_1), t \in [1-T_1, 1), \\
\dot{\lambda_k^{s_i}}(t) &= 0, t \in [1, 1+T_1).
\end{aligned}
$$

A careful inspection of the previous two sets of costate equations reveals that $\dot{\lambda}_k^{s_i}(t)$ *contains a impulses at* $t = 1 - T_1$ *and* $t = 1$*, respectively; these are also propagated towards* $t = 0$*. For* $s_i = 1 + T_1$ *the boundary conditions are*

$$
\begin{aligned}
& e_k'\eta(1+T_1) - \lambda_k^{s_i\prime}(t)\eta(t)\big|_0^{1^- - T_1} - \lambda_k^{s_i\prime}(t)\eta(t)\big|_{1^+-T_1}^{1^-} - \lambda_k^{s_i\prime}(t)\eta(t)\big|_{1^+}^{1+T_1} + \\
& (1-\dot{T})\,\lambda_k^{s_i\prime}\left(\frac{\tau+T_0}{1-\dot{T}}\right)\eta(\tau)\Big|_{-T_0}^{1^- - T_1} + \lambda_k^{s_i\prime}(\tau+T_1)\eta(\tau)\big|_{1^+-T_1}^{1} \\
= \; & \left(-\lambda_k^{s_i\prime}(1^-) + \lambda_k^{s_i\prime}(1^+) + \lambda_k^{s_i\prime}(1+T_1)\right)\eta(1) + \left(e_k' - \lambda_k^{s_i\prime}(1+T_1)\right)\eta(1+T_1) \\
& + \left(-\lambda_k^{s_i\prime}(1^- - T_1) + \lambda_k^{s_i\prime}(1^+ - T_1) + (1-\dot{T})\lambda_k^{s_i\prime}(1^-) - \lambda_k^{s_i\prime}(1^+)\right)\eta(1-T_1).
\end{aligned}
$$

The costates are now

$$
\begin{aligned}
\lambda_k^{s_i}(1^-) &= \lambda_k^{s_i}(1^+) + \lambda_k^{s_i}(1+T_1), \\
\lambda_k^{s_i}(1+T_1) &= e_k, \\
\lambda_k^{s_i\prime}(1^- - T_1) &= \lambda_k^{s_i\prime}(1^+ - T_1) + (1-\dot{T})\lambda_k^{s_i\prime}(1^-) - \lambda_k^{s_i\prime}(1^+), \\
\dot{\lambda_k^{s_i}}(t) &= \dot{\lambda_k^{s_i}}\left(\frac{t+T_0}{1-\dot{T}}\right), t \in [0, 1-T_1), \\
\dot{\lambda_k^{s_i}}(t) &= \dot{\lambda_k^{s_i}}(t+T_1), t \in [1-T_1, 1), \\
\dot{\lambda_k^{s_i}}(t) &= 0, t \in [1, 1+T_1).
\end{aligned}
$$

This can be further simplified to

$$\begin{aligned}
\lambda_k^{s_i}(1^-) &= 2e_k, \qquad (294)\\
\lambda_k^{s_i}(1+T_1) &= e_k,\\
\lambda_k^{s_i}(1^- - T_1) &= \lambda_k^{s_i}(1^+ - T_1) + (1-2\dot{T})e_k,\\
\dot{\lambda_k^{s_i}}(t) &= \dot{\lambda_k^{s_i}}\left(\frac{t+T_0}{1-\dot{T}}\right),\ t\in[0,1-T_1),\\
\dot{\lambda_k^{s_i}}(t) &= \dot{\lambda_k^{s_i}}(t+T_1),\ t\in[1-T_1,1),\\
\dot{\lambda_k^{s_i}}(t) &= 0,\ t\in[1,1+T_1).
\end{aligned}$$

For all $s_i \in [1, 1+T_1]$

$$\delta J_k^{s_i} = \int_0^{1+T_1} \lambda_k^{s_i\prime}(t)\delta u(t)dt. \qquad (295)$$

Proof E.2 (Proof of Proposition (6.2.3))**.** *After adjoining the dynamics and perturbing* $x(t) \to x(t) + \epsilon\eta(t)$ *and* $u(t) \to u(t) + \epsilon v(t)$*, the Fréchet derivative is*

$$\begin{aligned}
\delta J_v &= \int_0^{1^-} (x(t) - x(t-T(t)))'P(\eta(t) - \eta(t-T(t))) + u'(t)Rv(t)\\
&\quad +\lambda_v{}'(t)\left((1-\dot{T})\dot{\eta}(t-T(t)) + v(t) - \dot{\eta}(t)\right)dt\\
&\quad + \int_{1^+}^{1+T_1} (x(t) - x(t-T_1))'P(\eta(t) - \eta(t-T_1)) + u'(t)Rv(t)\\
&\quad +\lambda_v{}'(t)\left(\dot{\eta}(t-T_1) + v(t) - \dot{\eta}(t)\right)dt\\
&= \int_0^{1^-} (x(t) - x(t-T(t)))'P(\eta(t) - \eta(t-T(t)))dt\\
&\quad + \int_{1^+}^{1+T_1} (x(t) - x(t-T_1))'P(\eta(t) - \eta(t-T_1))dt\\
&\quad - \lambda_v{}'(t)\eta(t)|_0^{1^- - T_1} - \lambda_v{}'(t)\eta(t)|_{1^+-T_1}^{1^-} - \lambda_v{}'(t)\eta(t)|_{1^+}^{1+T_1} + \int_0^{1+T_1} \dot{\lambda}_v'(t)\eta(t)dt\\
&\quad +(1-\dot{T})\int_0^{1^-} \lambda_v{}'(t)\frac{d\eta(t-T(t))}{dt}dt + \int_{1^+}^{1+T_1} \lambda_v{}'(t)\dot{\eta}(t-T_1)dt +
\end{aligned}$$

$$
\begin{aligned}
&\int_0^{1+T_1} \left(u'(t)R + {\lambda_v}'(t)\right) v(t)dt \\
= &\int_0^{1^-} (x(t) - x(t-T(t)))' P\eta(t)dt - \frac{1}{1-\dot{T}} \int_{-T_0}^{1-T_1} \left(x\left(\frac{\tau+T_0}{1-\dot{T}}\right) - x(\tau)\right)' P\eta(\tau)d\tau \\
&+ \int_{1^+}^{1+T_1} (x(t) - x(t-T_1))' P\eta(t)dt - \int_{1-T_1}^{1} (x(t+T_1) - x(t))' P\eta(t)dt \\
&- {\lambda_v}'(t)\eta(t)|_0^{1^--T_1} - {\lambda_v}'(t)\eta(t)|_{1^+-T_1}^{1^-} - {\lambda_v}'(t)\eta(t)|_{1^+}^{1+T_1} + \int_0^{1+T_1} \dot{\lambda}_v'(t)\eta(t)dt \\
&+(1-\dot{T}) \int_{-T_0}^{1^--T_1} {\lambda_v}'\left(\frac{\tau+T_0}{1-\dot{T}}\right) \frac{d\eta(\tau)}{d\tau} d\tau + \int_{1^+-T_1}^{1} {\lambda_v}'(\tau+T_1)\dot{\eta}(\tau)d\tau \\
&\int_0^{1+T_1} \left(u'(t)R + {\lambda_v}'(t)\right) v(t)dt \\
= &\int_0^{1^-} (x(t) - x(t-T(t)))' P\eta(t)dt - \frac{1}{1-\dot{T}} \int_{-T_0}^{1-T_1} \left(x\left(\frac{\tau+T_0}{1-\dot{T}}\right) - x(\tau)\right)' P\eta(\tau)d\tau \\
&+ \int_{1^+}^{1+T_1} (x(t) - x(t-T_1))' P\eta(t)dt - \int_{1-T_1}^{1} (x(t+T_1) - x(t))' P\eta(t)dt \\
&- {\lambda_v}'(t)\eta(t)|_0^{1^--T_1} - {\lambda_v}'(t)\eta(t)|_{1^+-T_1}^{1^-} - {\lambda_v}'(t)\eta(t)|_{1^+}^{1+T_1} + \int_0^{1+T_1} \dot{\lambda}_v'(t)\eta(t)dt \\
&+(1-\dot{T})\, {\lambda_v}'\left(\frac{\tau+T_0}{1-\dot{T}}\right) \eta(\tau)\Big|_{-T_0}^{1^--T_1} - \int_{-T_0}^{1^--T_1} \dot{\lambda}_v'\left(\frac{\tau+T_0}{1-\dot{T}}\right) \eta(\tau)d\tau + \\
&{\lambda_v}'(\tau+T_1)\eta(\tau)|_{1^+-T_1}^{1} - \int_{1^+-T_1}^{1} \dot{\lambda}_v'(\tau+T_1)\eta(\tau)d\tau + \\
&\int_0^{1+T_1} \left(u'(t)R + {\lambda_v}'(t)\right) v(t)dt \\
= &\left(-{\lambda_v}'(1^-) + {\lambda_v}'(1^+) + {\lambda_v}'(1+T_1)\right)\eta(1) - {\lambda_v}'(1+T_1)\eta(1+T_1) \\
&+ \left(-\lambda_v'(1^- - T_1) + \lambda_v'(1^+ - T_1) + (1-\dot{T}){\lambda_v}'(1^-) - {\lambda_v}'(1^+)\right)\eta(1-T_1) \\
&+ \int_0^{1-T_1} \left(\left(x(t) - x(t-T(t)) - \frac{1}{1-\dot{T}} \left(x\left(\frac{t+T_0}{1-\dot{T}}\right) - x(t)\right)\right)' P + \dot{\lambda}_v'(t) \right. \\
&\left. -\dot{\lambda_v}'\left(\frac{t+T_0}{1-\dot{T}}\right)\right)\eta(t)dt \\
&+ \int_{1-T_1}^{1} \left((2x(t) - x(t-T(t)) - x(t+T_1))' P + \dot{\lambda}_v'(t) - \dot{\lambda}_v'(t+T_1)\right)\eta(t)dt \\
&+ \int_1^{1+T_1} \left((x(t) - x(t-T_1))' P + \dot{\lambda}_v'(t)\right)\eta(t)dt \\
&+ \int_0^{1+T_1} \left(u'(t)R + {\lambda_v}'(t)\right) v(t)dt. \qquad (296)
\end{aligned}
$$

We choose

$$\begin{aligned}
-\dot{\lambda}_v'(t) &= \left(x(t) - x(t - T(t)) - \frac{1}{1-\dot{T}}\left(x\left(\frac{t+T_0}{1-\dot{T}}\right) - x(t)\right)\right)' P \\
&- \dot{\lambda_v}'\left(\frac{t+T_0}{1-\dot{T}}\right),\ t \in [0, 1-T_1), \\
-\dot{\lambda}_v'(t) &= (2x(t) - x(t-T(t)) - x(t+T_1))' P - \dot{\lambda}_v'(t+T_1),\ t \in [1-T_1, 1), \\
-\dot{\lambda}_v'(t) &= (x(t) - x(t-T_1))' P,\ t \in [1, 1+T_1),
\end{aligned}$$

with the boundary conditions $\lambda_v(1+T_1) = 0$, $\lambda_v(1^-) = \lambda_v(1^+) + \lambda_v(1+T_1)$ *and* $-\lambda_v(1^- - T_1) + \lambda_v(1^+ - T_1) + (1-\dot{T})\lambda_v(1^-) - \lambda_v(1^+) = 0$. *With this choice the Frechet derivative* without *the boundary constraints is*

$$\delta J_v = \int_0^{1+T_1} \left(u'(t)R + \lambda_v'(t)\right) v(t) dt. \tag{297}$$

Proof E.3 (Derivation of Algorithm (6.2.1)). *Proposition (6.2.2) and Proposition (6.2.3) provide the main ingredients to construct a gradient descent algorithm.*

Indeed, we pose the following optimization problem as in (161) *and following the general procedure in Algorithm (6.1.2):*

$$\begin{aligned}\min_{\delta u} \delta\overline{J} &= \int_0^{1+T} \left(Ru(t) + \lambda_v(t)\right)' \delta u(t) + \frac{\|\delta u(t)\|^2}{2k_1}\, dt \\ &\quad + \sum_{i=0}^{N}\sum_{k=1}^{n} \nu_k^{s_i} \left(\int_0^{1+T} \lambda_k^{s_i\prime}(t)\delta u(t)dt - \delta J_k^{s_i} \right).\end{aligned}$$

After neglecting the changes in the coefficients

$$\delta^2\overline{J} = \int_0^{1+T} \left(\left(Ru(t) + \lambda_v(t)\right)' + \frac{\delta' u}{k_1} + \sum_{i=0}^{N}\sum_{k=1}^{n} \nu_k^{s_i}\lambda_k^{s_i\prime}(t) \right) dt\, \delta(\delta u).$$

The minimum is attained if

$$\delta u(t) = -k_1 \left(\left(Ru(t) + \lambda_v(t)\right) + \sum_{i=0}^{N}\sum_{k=1}^{n} \nu_k^{s_i}\lambda_k^{s_i}(t) \right). \tag{298}$$

Substituting this into (295) *we obtain*

$$\begin{aligned}\delta J_j^{s_l} &= -k_1 \left(\int_0^{1+T} \lambda_j^{s_l\prime}(t) \left(Ru(t) + \lambda_v(t)\right) dt + \sum_{i=0}^{N}\sum_{k=1}^{n} \nu_k^{s_i} \int_0^{1+T} \lambda_j^{s_l\prime}(t)\lambda_k^{s_i}(t)dt \right), \\ &= -k_1 \left(\int_0^{1+T} \lambda_j^{s_l\prime}(t) \left(Ru(t) + \lambda_v(t)\right) dt + \sum_{i=0}^{N} \nu_k^{s_i} \int_0^{1+T} \lambda_j^{s_l\prime}(t)\lambda_j^{s_i}(t)dt \right),\end{aligned}$$

where the last equality follows from the linearity of the costate equations $\lambda_j^{s_l}$ and that only the k^{th} component of $\lambda_k^{s_i}$ is excited by the unit vector e_k.

Define now

$$\begin{aligned}
\delta \boldsymbol{J}_j &= \left[\begin{array}{cccc} \delta J_j^{s_0}, & \delta J_j^{s_1}, & \ldots, & \delta J_j^{s_N} \end{array} \right]', \qquad (299)\\
\boldsymbol{U}_j &= \left[\begin{array}{cccc} \int_0^{1+T} \lambda_j^{s_0\prime}(t) \left(Ru(t) + \lambda_v(t)\right) dt, & \ldots, & \int_0^{1+T} \lambda_j^{s_N\prime}(t) \left(Ru(t) + \lambda_v(t)\right) dt \end{array} \right]',\\
\boldsymbol{\nu}_j &= \left[\begin{array}{cccc} \nu_j^{s_0}, & \nu_j^{s_1}, & \ldots, & \nu_j^{s_N} \end{array} \right]'\\
\boldsymbol{\Lambda}_j &= \left[\begin{array}{ccc} \lambda_j^{00}, & \lambda_j^{10}, & \ldots, \quad \lambda_j^{N0} \\ \lambda_j^{01}, & \lambda_j^{11}, & \ldots, \quad \lambda_j^{N1} \\ \vdots & & \ddots \\ \lambda_j^{0N}, & \lambda_j^{1N}, & \ldots, \quad \lambda_j^{NN}, \end{array} \right], \lambda_j^{li} = \int_0^{1+T} \lambda_j^{s_l\prime}(t) \lambda_j^{s_i}(t) dt
\end{aligned}$$

for $j = 1, \ldots, n$ *and rewrite the previous*

$$\frac{-1}{k_1} \delta \boldsymbol{J}_j = \boldsymbol{U}_j + \boldsymbol{\Lambda}_j \boldsymbol{\nu}_j. \qquad (300)$$

Hence, controllability implies that

$$\boldsymbol{\nu}_j = -\boldsymbol{\Lambda}_j^{-1} \left(\boldsymbol{U}_j + \frac{1}{k_1} \delta \boldsymbol{J}_j \right)$$

Substitute this into (298)

$$\begin{aligned}
\delta u(t) &= -k_1 \left(\left(Ru(t) + \lambda_v(t)\right) + \sum_{k=1}^{n} \boldsymbol{\nu}_k' \boldsymbol{\lambda}_k(t) \right)\\
&= -k_1 \left(\left(Ru(t) + \lambda_v(t)\right) - \sum_{k=1}^{n} \left(\boldsymbol{U}_k + \frac{1}{k_1} \delta \boldsymbol{J}_k \right)' \boldsymbol{\Lambda}_k^{-1} \boldsymbol{\lambda}_k(t) \right)\\
&= -k_1 \left(\left(Ru(t) + \lambda_v(t)\right) - \sum_{k=1}^{n} \boldsymbol{U}_k' \boldsymbol{\Lambda}_k^{-1} \boldsymbol{\lambda}_k(t) \right) + \sum_{k=1}^{n} \delta \boldsymbol{J}_k' \boldsymbol{\Lambda}_k^{-1} \boldsymbol{\lambda}_k(t), \qquad (301)
\end{aligned}$$

where

$$\boldsymbol{\lambda}_k(t) = \left[\begin{array}{cccc} \lambda_k^{s_0}(t), & \lambda_k^{s_1}(t), & \ldots, & \lambda_k^{s_N}(t) \end{array} \right]'.$$

This is the desired gradient of the input in the algorithm.

APPENDIX F

PROOFS OF CHAPTER 7

Proof F.1 (Proof of Proposition 7.2.3)**.** *To obtain the necessary conditions of optimality, we first adjoin the constraints to* J_0*:*

$$\begin{aligned} J_0 &= \int_0^{1+T} \|x(t)-x(t-T)\|_P^2 + \|w(t)\|_R^2 + \lambda_x'(t)\left(f(x(t),u(t))-\dot{x}(t)\right) + \\ &\quad \lambda_u'(t)\left(u(t)-u(t-T)-w(t)\right)dt + \nu_x'(x(1^-)+x_f(1^+)) + \\ &\quad + \int_{1^-}^{1+T} \nu_u'(t)(u(t)-u_f(t))dt. \end{aligned} \tag{302}$$

After letting $x \to x+\epsilon\eta$,$u \to u+\epsilon v$, $w \to w+\epsilon r$ *and keeping the first order terms,*

$$\begin{aligned} J_\epsilon &= \int_0^{1+T} \|x(t)-x(t-T)+\epsilon(\eta(t)-\eta(t-T))\|_P^2 + \|w(t)+\epsilon r(t)\|_R^2 + \\ &\quad +\lambda_x'(t)\left(f(x(t)+\epsilon\eta(t),u(t)+\epsilon v(t))-\dot{x}(t)-\epsilon\dot{\eta}(t)\right) + \\ &\quad \lambda_u'(t)\left(u(t)-u(t-T)-w(t)+\epsilon\left(v(t)-v(t-T)-r(t)\right)\right)dt + \\ &\quad +\nu_x'(x(1^-)+x_f(1^+)+\epsilon\eta(1^-)) + \int_{1^-}^{1+T} \nu_u'(t)(u(t)-u_f(t)+\epsilon v(t))dt \\ &= J_0 + \epsilon\left(\int_0^{1+T} \left(x(t)-x(t-T)\right)' P(\eta(t)-\eta(t-T)) + w'(t)Rr(t)\right. \\ &\quad +\lambda_x'(t)\left(\frac{\partial f}{\partial x}\eta(t)+\frac{\partial f}{\partial u}v(t)-\dot{\eta}(t)\right) + \lambda_u'(t)\left(v(t)-v(t-T)-r(t)\right)dt + \\ &\quad \left.+\nu_x'(\eta(1^-)) + \int_{1^-}^{1+T} \nu_u'(t)v(t)\,dt\right). \end{aligned}$$

Hence,

$$
\begin{aligned}
\delta J &= \int_0^{1+T} (x(t)-x(t-T))' P(\eta(t)-\eta(t-T)) + w'(t)Rr(t) \\
&\quad +\lambda_x'(t)\left(\frac{\partial f}{\partial x}\eta(t)+\frac{\partial f}{\partial u}v(t)-\dot\eta\right)+\lambda_u'(t)\left(v(t)-v(t-T)-r(t)\right)dt + \\
&\quad +\nu_x'(\eta(1^-))+\int_{1^-}^{1+T}\nu_u'(t)v(t)\,dt \\
&= \int_0^{1+T}(x(t)-x(t-T))'P\eta(t)\,dt-\int_{-T}^{1}(x(t+T)-x(t))'P\eta(t)\,dt \\
&\quad +\int_0^{1+T}\left(w'(t)R-\lambda_u'(t)\right)r(t)dt + \\
&\quad +\int_0^{1+T}\left(\lambda_x'(t)\frac{\partial f}{\partial x}+\dot\lambda_x'\right)\eta(t)dt-\lambda_x'(t)\eta(t)|_0^{1^-}-\lambda_x'(t)\eta(t)|_{1^+}^{1+T}+\nu_x'\eta(1^-) \\
&\quad +\int_0^{1+T}\left(\lambda_x'(t)\frac{\partial f}{\partial u}+\lambda_u'(t)\right)v(t)dt-\int_{-T}^{1}\lambda_u'(t+T)v(t)dt+\int_{1^-}^{1+T}\nu_u'(t)v(t)\,dt \\
&= \int_0^1\left(P\left(2x(t)-x(t-T)-x(t+T)\right)+\frac{\partial f'}{\partial x}\lambda_x(t)+\dot\lambda_x\right)'\eta(t)\,dt + \\
&\quad +\int_1^{1+T}\left(P\left(x(t)-x(t-T)\right)+\frac{\partial f'}{\partial x}\lambda_x(t)+\dot\lambda_x\right)'\eta(t)\,dt + \\
&\quad +\int_0^1\left(\lambda_x'(t)\frac{\partial f}{\partial u}+\lambda_u'(t)-\lambda_u'(t+T)\right)v(t)dt + \\
&\quad \int_1^{1+T}\left(\lambda_x'(t)\frac{\partial f}{\partial u}+\lambda_u'(t)+\nu_u'(t)\right)v(t)dt+\int_0^{1+T}\left(w'(t)R-\lambda_u'(t)\right)r(t)dt + \\
&\quad +\left(\lambda_x(1^+)-\lambda_x(1^-)+\nu_x\right)'\eta(1)-\lambda_x'(1+T)\eta(1+T),
\end{aligned}
$$

where we have used the fact that $\eta(1^-)=\eta(1^+)=\eta(1)$ *since* $x(t)$ *is continuous at* $t=1$,*i.e.,* $x(1^-)=x(1^+)$.

To avoid evaluating $\eta(t)$ *and* $v(t)$ *we choose*

$$
\begin{aligned}
-\dot\lambda_x(t) &= P\left(2x(t)-x(t-T)-x(t+T)\right)+\frac{\partial f'}{\partial x}\lambda_x(t),\ t\in[0,1), \\
-\dot\lambda_x(t) &= P\left(x(t)-x(t-T)\right)+\frac{\partial f'}{\partial x}\lambda_x(t),\ t\in(1,1+T], \\
-\lambda_u(t) &= \frac{\partial f'}{\partial u}\lambda_x(t)-\lambda_u(t+T),\ t\in[0,1], \qquad (303)
\end{aligned}
$$

$$
\begin{aligned}
-\lambda_u(t) &= \frac{\partial f'}{\partial u}\lambda_x(t) + \nu_u(t),\ t \in (1, 1+T], \\
\lambda_x(1^-) &= \lambda_x(1^+) + \nu_x, \\
\lambda_x(1+T) &= 0,
\end{aligned}
$$

where the last choice is due to the fact that $x(1+T)$ is free. ν_x and $\nu_u$need to be chosen such that the boundary conditions (235) *are satisfied. Observe further that λ_x is decoupled from λ_u. With the previous choice*

$$
\delta J = \int_0^{1+T} \left(w'(t)R - \lambda_u'(t)\right) r(t) dt, \tag{304}
$$

from which we conclude that the optimality condition implies that

$$
w(t) = R^{-1}\lambda_u(t),\ t \in [0, 1+T]. \tag{305}
$$

Proof F.2 (Proof of Proposition 7.2.4)**.** *Observe that the Fréchet derivative may be obtained by the following substitution in (302) and (303): $P = 0$, $R = 0$, $x_f = 0$, $\nu_u \equiv 0$, $\nu_x \to e_k$, $\lambda_x \to \lambda_{x,k}$, $\lambda_u \to \lambda_{u,k}$. Then*

$$
\begin{aligned}
\delta J_{x_k} &= \int_0^1 \left(\frac{\partial f'}{\partial x}\lambda_{x,k}(t) + \dot{\lambda}_{x,k}\right)' \eta(t)\, dt + \int_1^{1+T} \left(\frac{\partial f'}{\partial x}\lambda_{x,k}(t) + \dot{\lambda}_{x,k}\right)' \eta(t)\, dt + \\
&+ \int_0^1 \left(\lambda_{x,k}'(t)\frac{\partial f}{\partial u} + \lambda_{u,k}'(t) - \lambda_{u,k}'(t+T)\right) v(t) dt + \\
&\int_1^{1+T} \left(\lambda_{x,k}'(t)\frac{\partial f}{\partial u} + \lambda_{u,k}'(t)\right) v(t) dt - \int_0^{1+T} \lambda_{u,k}'(t) r(t) dt \\
&+ \left(\lambda_{x,k}(1^+) - \lambda_{x,k}(1^-) + e_k\right)' \eta(1) - \lambda_{x,k}'(1+T)\eta(1+T).
\end{aligned}
$$

Again, to avoid evaluating $\eta(t)$ and $v(t)$ we choose

$$
\begin{aligned}
-\dot{\lambda}_{x,k}(t) &= \frac{\partial f'}{\partial x}\lambda_{x,k}(t),\ t \in [0, 1), \\
-\dot{\lambda}_{x,k}(t) &= \frac{\partial f'}{\partial x}\lambda_{x,k}(t),\ t \in (1, 1+T], \\
-\lambda_{u,k}(t) &= \frac{\partial f'}{\partial u}\lambda_{x,k}(t) - \lambda_{u,k}(t+T),\ t \in [0, 1],
\end{aligned}
$$

$$
\begin{aligned}
-\lambda_{u,k}(t) &= \frac{\partial f'}{\partial u}\,\lambda_{x,k}(t),\ t \in (1, 1+T], \\
\lambda_{x,k}(1^-) &= \lambda_{x,k}(1^+) + e_k, \\
\lambda_{x,k}(1+T) &= 0,
\end{aligned}
$$

for $k = 1, \ldots n$, $dim\, x = n$. *The variation of* $x_k(1^-)$ *is*

$$
\begin{aligned}
\delta J_{x_k} &= \delta x_k(1^-) \\
&= -\int_0^{1+T} \lambda'_{u,k}(t)\delta w(t)dt,\ k = 1, \ldots, n.
\end{aligned}
$$

Proof F.3 (Derivation of Algorithm 7.2.2)**.** (245) *is linear in the variation of the input and has, therefore, no minimum. Hence, we solve a modified problem:*

$$
\min_{\delta w} \delta\overline{J} = \delta J + \int_0^{1+T} \frac{\|\delta w\|^2}{2k_1}
$$

We adjoin (239) *and* (243) *to the previous performance index:*

$$
\begin{aligned}
\delta\overline{J} &= \delta J + \int_0^{1+T} \frac{\|\delta w\|^2}{2k_1} + \sum_{k=0}^{n} \nu_{x,k} \left(e'_k \delta x(1^-) + \int_0^{1+T} \lambda'_{u,k}(t)\delta w(t)dt \right) + \\
&\quad + \sum_{i=1}^{N}\sum_{k=1}^{m} \nu_{u,k}^{s_i} \left(-\delta J_k^{s_i} - \int_0^{1+T} {\mu_{u,k}^{s_i}}'(t)\delta w(t)dt \right).
\end{aligned}
$$

Neglecting the changes in the coefficients

$$
\delta^2\overline{J} = \int_0^{1+T} \left(\left(w'(t)R - (\lambda_u^J)'(t)\right) + \frac{\delta w'}{k_1} + \sum_{k=0}^{n} \nu_{x,k}\lambda'_{u,k}(t) - \sum_{i=1}^{N}\sum_{k=1}^{m} \nu_{u,k}^{s_i}{\mu_{u,k}^{s_i}}'(t) \right) \delta(\delta w)\, dt.
$$

This second variation is minimal if

$$
\delta w = -k_1 \left(\left(Rw(t) - \lambda_u^J(t)\right) + \sum_{k=0}^{n} \nu_{x,k}\lambda_{u,k}(t) - \sum_{i=1}^{N}\sum_{k=1}^{m} \nu_{u,k}^{s_i}\mu_{u,k}^{s_i}(t) \right), t \in [0, 1+T]. \quad (306)
$$

Substituting this into (239) *and* (243) *we obtain the variations of the final state constrains:*

$$\begin{aligned}
\delta x_l(1^-) &= k_1 \left(\int_0^{1+T} \lambda'_{u,l}(t) \left(Rw(t) - \lambda_u^J(t) \right) \, dt + \sum_{k=0}^{n} \nu_{x,k} \int_0^{1+T} \lambda'_{u,l}(t) \lambda_{u,k}(t) dt + \right. \\
&\left. - \sum_{i=1}^{N} \sum_{k=1}^{m} \nu_{u,k}^{s_i} \int_0^{1+T} \lambda'_{u,l}(t) \mu_{u,k}^{s_i}(t) dt \right), \; l = 1, \ldots, n, \qquad (307) \\
\delta J_l^{s_r} &= k_1 \left(\int_0^{1+T} \mu_{u,l}^{s_r\prime}(t) \left(Rw(t) - \lambda_u^J(t) \right) \, dt + \sum_{k=0}^{n} \nu_{x,k} \int_0^{1+T} \mu_{u,l}^{s_r\prime}(t) \lambda_{u,k}(t) dt + \right. \\
&\left. - \sum_{i=1}^{N} \sum_{k=1}^{m} \nu_{u,k}^{s_i} \int_0^{1+T} \mu_{u,l}^{s_r\prime}(t) \mu_{u,k}^{s_i}(t) dt \right), l = 1, \ldots, m, \; r = 1, \ldots, N. \qquad (308)
\end{aligned}$$

(307) *may be written in matrix notation*

$$\delta \boldsymbol{x}(1^-) = k_1 \left(\boldsymbol{G}_u + \boldsymbol{\Lambda} \boldsymbol{\nu}_x - \sum_{i=1}^{N} \boldsymbol{\Gamma}^{s_i} \boldsymbol{\nu}_u^{s_i} \right), \qquad (309)$$

where

$$\begin{aligned}
\left[\delta \boldsymbol{x}(1^-) \right]_l &= \delta x_l(1^-), \;\; dim \; \delta \boldsymbol{x}(1^-) = n \times 1, \\
\boldsymbol{G}_u &= \int_0^{1+T} \boldsymbol{\Lambda}'_u(t) \left(Rw(t) - \lambda_u^J(t) \right) \, dt, \;\; dim \; \boldsymbol{G}_u = n \times 1, \\
\boldsymbol{\Lambda}_u(t) &= \begin{bmatrix} | & | & \ldots & | \\ \lambda_{u,1}(t) & \lambda_{u,2}(t) & \ldots & \lambda_{u,n}(t) \\ | & | & \ldots & | \end{bmatrix}, \;\; dim \;\; \boldsymbol{\Lambda}_u = m \times n, \\
[\boldsymbol{\Lambda}]_{ij} &= \int_0^{1+T} [\boldsymbol{\Lambda}'_u(t) \boldsymbol{\Lambda}_u(t)]_{ij} \, dt, \\
[\boldsymbol{\nu}_x]_i &= \nu_{x,i}, \\
[\boldsymbol{\Gamma}^{s_i}]_{lk} &= \int_0^{1+T} \lambda'_{u,l}(t) \mu_{u,k}^{s_i}(t) dt = \int_0^{1+T} [\boldsymbol{\Lambda}'_u(t) \boldsymbol{U}_u^{s_i}(t)]_{lk} \, dt, \;\; dim \; \boldsymbol{\Gamma}^{s_i} = n \times m,
\end{aligned}$$

$$
\begin{aligned}
\boldsymbol{U}_u^{s_i}(t) &= \begin{bmatrix} | & | & \cdots & | \\ \mu_{u,1}^{s_i}(t) & \mu_{u,2}^{s_i}(t) & \cdots & \mu_{u,m}^{s_i}(t) \\ | & | & \cdots & | \end{bmatrix}, \quad dim\, \boldsymbol{U}_u^{s_i} = m \times m, \\
[\boldsymbol{\nu}_u^{s_i}]_k &= \nu_{u,k}^{s_i}.
\end{aligned}
$$

In light of (244)

$$
\int_0^{1+T} \mu_{u,l}^{s_r\prime}(t)\mu_{u,k}^{s_i}(t)dt = \begin{cases} \frac{m_r+1}{\Delta} & i=r,\ k=l, \\ 0, & else, \end{cases}
$$

if $\lfloor \frac{s_i}{T} \rfloor = m_i$.

(308) *in matrix notation is*

$$
\begin{aligned}
\delta \boldsymbol{J}^{s_r} &= k_1 \left(\boldsymbol{F}_u^{s_r} + \boldsymbol{\Gamma}^{s_r\prime}\boldsymbol{\nu}_x - \frac{m_r+1}{\Delta}\boldsymbol{\nu}_u^{s_r} \right), \qquad (310) \\
\boldsymbol{F}_u^{s_r} &= \int_0^{1+T} \boldsymbol{U}_u^{s_r\prime} \left(Rw(t) - \lambda_u^J(t) \right) dt.
\end{aligned}
$$

Therefore,

$$
\boldsymbol{\nu}_u^{s_r} = \frac{\Delta}{m_r+1} \left(\boldsymbol{F}_u^{s_r} + \boldsymbol{\Gamma}^{s_r\prime}\boldsymbol{\nu}_x - \frac{1}{k_1}\delta \boldsymbol{J}^{s_r} \right). \qquad (311)
$$

Substitute this into (309)

$$
\begin{aligned}
\delta \boldsymbol{x}(1^-) &= k_1 \left(\boldsymbol{G}_u + \boldsymbol{\Lambda}\boldsymbol{\nu}_x - \sum_{i=1}^N \boldsymbol{\Gamma}^{s_i}\boldsymbol{\nu}_u^{s_i} \right), \\
&= k_1 \left(\boldsymbol{G}_u + \boldsymbol{\Lambda}\boldsymbol{\nu}_x - \sum_{i=1}^N \frac{\Delta}{m_i+1}\boldsymbol{\Gamma}^{s_i} \left(\boldsymbol{F}_u^{s_i} + \boldsymbol{\Gamma}^{s_i\prime}\boldsymbol{\nu}_x - \frac{1}{k_1}\delta \boldsymbol{J}^{s_i} \right) \right), \\
&= k_1 \left(\boldsymbol{G}_u - \sum_{i=1}^N \frac{\Delta}{m_i+1}\boldsymbol{\Gamma}^{s_i}\boldsymbol{F}_u^{s_i} + \underbrace{\left(\boldsymbol{\Lambda} - \sum_{i=1}^N \frac{\Delta}{m_i+1}\boldsymbol{\Gamma}^{s_i}\boldsymbol{\Gamma}^{s_i\prime} \right)}_{\Omega} \boldsymbol{\nu}_x \right) + \\
&+ \sum_{i=1}^N \frac{\Delta}{m_i+1}\boldsymbol{\Gamma}^{s_i}\delta \boldsymbol{J}^{s_i},
\end{aligned}
$$

from which we obtain

$$\begin{aligned}
\boldsymbol{\nu}_x &= \Omega^{-1}\left[\frac{1}{k_1}\left(\delta\boldsymbol{x}(1^-) - \sum_{i=1}^{N}\frac{\Delta}{m_i+1}\boldsymbol{\Gamma}^{s_i}\delta\boldsymbol{J}^{s_i}\right) - \boldsymbol{G}_u + \sum_{i=1}^{N}\frac{\Delta}{m_i+1}\boldsymbol{\Gamma}^{s_i}\boldsymbol{F}_u^{s_i}\right], \\
&= \frac{1}{k_1}\Omega^{-1}\left(\delta\boldsymbol{x}(1^-) - \sum_{i=1}^{N}\frac{\Delta}{m_i+1}\boldsymbol{\Gamma}^{s_i}\delta\boldsymbol{J}^{s_i}\right) + \Omega^{-1}\left(-\boldsymbol{G}_u + \sum_{i=1}^{N}\frac{\Delta}{m_i+1}\boldsymbol{\Gamma}^{s_i}\boldsymbol{F}_u^{s_i}\right), \\
&= \frac{1}{k_1}\boldsymbol{A} + \boldsymbol{B}, \qquad (312)
\end{aligned}$$

where

$$\begin{aligned}
\boldsymbol{A} &= \Omega^{-1}\left(\delta\boldsymbol{x}(1^-) - \sum_{i=1}^{N}\frac{\Delta}{m_i+1}\boldsymbol{\Gamma}^{s_i}\delta\boldsymbol{J}^{s_i}\right), \quad dim\ \boldsymbol{A} = n\times 1, \\
\boldsymbol{B} &= \Omega^{-1}\left(-\boldsymbol{G}_u + \sum_{i=1}^{N}\frac{\Delta}{m_i+1}\boldsymbol{\Gamma}^{s_i}\boldsymbol{F}_u^{s_i}\right), \quad dim\ \boldsymbol{B} = n\times 1.
\end{aligned}$$

From (311)

$$\begin{aligned}
\boldsymbol{\nu}_u^{s_r} &= \frac{\Delta}{m_r+1}\left(\boldsymbol{F}_u^{s_r} + \boldsymbol{\Gamma}^{s_r\prime}\left(\frac{1}{k_1}\boldsymbol{A} + \boldsymbol{B}\right) - \frac{1}{k_1}\delta\boldsymbol{J}^{s_r}\right), \\
&= \frac{\Delta}{m_r+1}\left(\boldsymbol{F}_u^{s_r} + \boldsymbol{\Gamma}^{s_r\prime}\boldsymbol{B} + \frac{1}{k_1}\left(\boldsymbol{\Gamma}^{s_r\prime}\boldsymbol{A} - \delta\boldsymbol{J}^{s_r}\right)\right). \qquad (313)
\end{aligned}$$

Substitute (312) *and* (313) *into the gradient* (306)

$$\begin{aligned}
\delta w(t) &= -k_1\left(\left(Rw(t) - \lambda_u^J(t)\right) + \boldsymbol{\Lambda}_u(t)\boldsymbol{\nu}_x - \sum_{i=1}^{N}\boldsymbol{U}_u^{s_i}(t)\boldsymbol{\nu}_u^{s_i}\right), \\
&= -k_1\left(\left(Rw(t) - \lambda_u^J(t)\right) + \boldsymbol{\Lambda}_u(t)\left(\frac{1}{k_1}\boldsymbol{A} + \boldsymbol{B}\right)\right. \\
&\quad \left. - \sum_{i=1}^{N}\boldsymbol{U}_u^{s_i}(t)\left(\frac{\Delta}{m_i+1}\left(\boldsymbol{F}_u^{s_i} + \boldsymbol{\Gamma}^{s_i\prime}\boldsymbol{B} + \frac{1}{k_1}\left(\boldsymbol{\Gamma}^{s_i\prime}\boldsymbol{A} - \delta\boldsymbol{J}^{s_i}\right)\right)\right)\right), \\
&= -k_1\,\boldsymbol{C}(t) - \boldsymbol{D}(t), \qquad (314)
\end{aligned}$$

where

$$
\begin{aligned}
\boldsymbol{C}(t) &= \left(Rw(t) - \lambda_u^J(t)\right) + \boldsymbol{\Lambda}_u(t)\boldsymbol{B} - \sum_{i=1}^{N} \frac{\Delta}{m_i+1} \boldsymbol{U}_u^{s_i}(t) \left(\boldsymbol{F}_u^{s_i} + \boldsymbol{\Gamma}^{s_i\prime}\boldsymbol{B}\right), \\
&= \left(Rw(t) - \lambda_u^J(t)\right) + \left(\boldsymbol{\Lambda}_u(t) - \sum_{i=1}^{N} \frac{\Delta}{m_i+1} \boldsymbol{U}_u^{s_i}(t)\boldsymbol{\Gamma}^{s_i\prime}\right)\boldsymbol{B} - \sum_{i=1}^{N} \frac{\Delta}{m_i+1} \boldsymbol{U}_u^{s_i}(t)\boldsymbol{F}_u^{s_i}, \\
\boldsymbol{D}(t) &= \boldsymbol{\Lambda}_u(t)\boldsymbol{A} - \sum_{i=1}^{N} \frac{\Delta}{m_i+1} \boldsymbol{U}_u^{s_i}(t) \left(\boldsymbol{\Gamma}^{s_i\prime}\boldsymbol{A} - \delta\boldsymbol{J}^{s_i}\right), \\
&= \left(\boldsymbol{\Lambda}_u(t) - \sum_{i=1}^{N} \frac{\Delta}{m_i+1} \boldsymbol{U}_u^{s_i}(t)\boldsymbol{\Gamma}^{s_i\prime}\right)\boldsymbol{A} + \sum_{i=1}^{N} \frac{\Delta}{m_i+1} \boldsymbol{U}_u^{s_i}(t)\delta\boldsymbol{J}^{s_i}. \qquad (315)
\end{aligned}
$$

Proof F.4 (Proof of Proposition 7.2.8)**.** *We first adjoin the dynamics to the performance index;*

$$
\begin{aligned}
J_0 &= \int_0^1 \frac{1}{2}\left\|z(t) - z(t-T(t))\right\|_S^2 + \frac{1}{2}\left\|v(t) - (1-\dot{T})v(t-T(t))\right\|_R^2 dt \\
&\quad + \int_1^{1+T_1} \frac{1}{2}\left\|z_1(t) - z(t-T_1)\right\|_S^2 + \frac{1}{2}\left\|v_1(t) - v(t-T_1)\right\|_R^2 dt \\
&\quad + \int_0^1 \mu'(t)\left(F(z(t),v(t)) - \dot{z}(t)\right) dt.
\end{aligned}
$$

After letting $z(t) \to z(t) + \epsilon\eta(t)$, $v(t) \to v(t) + \epsilon w(t)$, we obtain

$$
\begin{aligned}
\delta J_v = &\int_0^1 \left(z(t) - z(t-T(t))\right)' S \left(\eta(t) - \eta(t-T(t))\right) \\
&+ \left(v(t) - (1-\dot{T})v(t-T(t))\right)' R \left(w(t) - (1-\dot{T})w(t-T(t))\right) \\
&+ \left(\mu'(t)\frac{\partial F}{\partial z} + \dot{\mu}'(t)\right)\eta(t) + \mu'(t)\frac{\partial F}{\partial v} w(t)\, dt - \mu(t)\eta(t)\Big|_0^1 \\
&+ \int_1^{1+T_1} \left(z_1(t) - z(t-T_1)\right)' S \left(-\eta(t-T_1)\right) + \left(v_1(t) - v(t-T_1)\right)' R \left(-w(t-T_1)\right) dt \\
= &\int_0^{1-T_1} \left(\left(\left(\frac{2-\dot{T}}{1-\dot{T}}\right) z(t) - z(t-T(t)) - \frac{1}{1-\dot{T}} z\left(\frac{t+T_0}{1-\dot{T}}\right)\right)' S + \mu'(t)\frac{\partial F}{\partial z} + \dot{\mu}'(t)\right)\eta(t) \\
&+ \left(\left((2-\dot{T})v(t) - (1-\dot{T})v(t-T(t)) - v\left(\frac{t+T_0}{1-\dot{T}}\right)\right)' R + \mu'(t)\frac{\partial F}{\partial v}\right) w(t) dt \\
&+ \int_{1-T_1}^1 \left(\left(2z(t) - z(t-T(t)) - z(t+T_1)\right)' S + \mu'(t)\frac{\partial F}{\partial z} + \dot{\mu}'(t)\right)\eta(t) +
\end{aligned}
$$

$$
\begin{aligned}
&+ \quad \left(\left(2v(t) - (1-\dot{T})v(t-T(t)) - v(t+T_1) \right)' R + \mu'(t) \frac{\partial F}{\partial v} \right) w(t) dt \\
&- \quad \mu' \eta(t) |_0^1 .
\end{aligned}
$$

Since the boundary conditions are free, $\mu(1) = 0$. *For* $t \in [0, 1-T_1)$ *we choose*

$$
-\dot{\mu}(t) \;=\; S \left(\left(\frac{2-\dot{T}}{1-\dot{T}} \right) z(t) - z(t-T(t)) - \frac{1}{1-\dot{T}} z \left(\frac{t+T_0}{1-\dot{T}} \right) \right) + \frac{\partial F'}{\partial z} \mu(t),
$$

and for $t \in [1-T_1, 1]$

$$
-\dot{\mu}(t) \;=\; S \left(2z(t) - z(t-T(t)) - z(t+T_1) \right) + \frac{\partial F'}{\partial z} \mu(t).
$$

Hence,

$$
\delta J_v \;=\; \int_0^1 c'(t) \delta v(t) dt,
$$

where

$$
c(t) = \begin{cases} R \left((2-\dot{T})v(t) - (1-\dot{T})v(t-T(t)) - v\left(\frac{t+T_0}{1-\dot{T}} \right) \right) + \frac{\partial F'}{\partial v} \mu(t), & t \in [0, 1-T_1), \\ R \left(2v(t) - (1-\dot{T})v(t-T(t)) - v(t+T_1) \right) + \frac{\partial F'}{\partial v} \mu(t), & t \in [1-T_1, 1]. \end{cases}
$$

Proof F.5 (Derivation of Algorithm (7.2.3))**.** *As usual we post the optimization problem*

$$
\delta \overline{J} \;=\; \delta J_v + \int_0^1 \frac{\|\delta v\|^2}{2k_1} + \sum_{k=1}^{N} \nu_k \left(e_k' \delta z(1^-) + \int_0^1 \lambda^{k'}(t) \frac{\partial F}{\partial v} \delta v(t) dt \right). \quad (316)
$$

Neglecting the changes in the coefficients, the second variation is

$$
\delta^2 \overline{J} = \int_0^1 \left(c'(t) + \frac{1}{k_1} \delta v'(t) + \sum_{k=1}^{N} \nu_k \lambda^{k'}(t) \frac{\partial F}{\partial v} \right) dt.
$$

(316) is minimal if

$$
\delta v(t) = -k_1 \left(c(t) + \sum_{k=1}^{N} \nu_k \frac{\partial F'}{\partial v} \lambda^k(t) \right).
$$

After substituting this into (255), we obtain

$$\begin{aligned}\delta z_i(1) &= -k_1 \int_0^1 (\lambda^i)'(t) \frac{\partial F}{\partial v} \left(c(t) + \sum_{k=1}^{N} \nu_k \frac{\partial F'}{\partial v} \lambda^k(t) \right) dt, \\ &= -k_1 \left(\int_0^1 (\lambda^i)'(t) \frac{\partial F}{\partial v} c(t) dt + \sum_{k=1}^{N} \nu_k \int_0^1 (\lambda^i)'(t) \frac{\partial F}{\partial v} \frac{\partial F'}{\partial v} \lambda^k(t) dt \right),\end{aligned}$$

which in matrix notation is

$$\begin{aligned}\delta z(1) &= -k_1 \left(D + \int_0^1 \Lambda'(t) \frac{\partial F}{\partial v} \frac{\partial F'}{\partial v} \Lambda(t) dt \nu \right), \\ &= -k_1 \left(D + \Lambda_g \nu \right),\end{aligned}$$

where

$$\begin{aligned}\Lambda(t) &= \begin{bmatrix} | & | & \dots & | \\ \lambda^1(t) & \lambda^2(t) & \dots & \lambda^N(t) \\ | & | & \dots & | \end{bmatrix}, \qquad (317) \\ D &= \int_0^1 (\lambda^i)'(t) \frac{\partial F}{\partial v} c(t) dt, \\ \Lambda_g &= \int_0^1 \Lambda'(t) \frac{\partial F}{\partial v} \frac{\partial F'}{\partial v} \Lambda(t) dt.\end{aligned}$$

Under the reachability assumption we may solve for ν:

$$\nu = -\Lambda_g^{-1} \left(D + \frac{\delta z(1)}{k_1} \right).$$

Hence,

$$\begin{aligned}\delta v(t) &= -k_1 \left(c(t) + \frac{\partial F'}{\partial v} \Lambda(t) \nu \right), \\ &= -k_1 \left(c(t) - \frac{\partial F'}{\partial v} \Lambda(t) \Lambda_g^{-1} \left(D + \frac{\delta z(1)}{k_1} \right) \right), \\ &= -k_1 \left(c(t) - \frac{\partial F'}{\partial v} \Lambda(t) \Lambda_g^{-1} D \right) + \frac{\partial F'}{\partial v} \Lambda(t) \Lambda_g^{-1} \delta z(1).\end{aligned}$$

REFERENCES

[1] B. Andresen, R. S. Berry, A. Nitzan, and P. Salamon. Thermodynamics in finite time. i. the step-carnot cycle. *Phys. Rev. A*, 15:2086–2093, 1977.

[2] L. Armijo. Minimization of functions having Lipschitz continuous first-partial derivatives. *Pacific Journal of Mathematics*, 16:1–3, 1966.

[3] J. Bailey. Periodic operation of chemical reactor: A review. *Chem. Eng. Commun.*, 1:111–124, 1973.

[4] S. Bittanti. *Time Series and Linear Systems*, volume 86 of *Lecture Notes in Control and Information Science*, chapter Deterministic and stochastic periodic systems, pages 141–182. Berlin: Springer-Verlag, 1986.

[5] S. Bittanti and P. Colaneri. *Periodic Systems: Filtering and Control*. Springer Verlag, 2009.

[6] S. Bittanti and G. O. Guardabassi. Optimal periodic control and periodic system analysis: An overview. In *Proceedings of the 25th IEEE Conference on Decision and Control*, pages 1417–1423, Athens, Greece, December 1986.

[7] E. Bizzi, N. Hogan, F. Mussa-Ivaldi, and S. Giszter. Does the nervous system use equilibrium-point control to guide single and multiple joint movements? *Behavioral and Brain Sciences*, 15:808–815, 1992.

[8] M. S. Branicky, V. S. Borkar, and S. K. Mitter. A unified framework for hybrid control: Model and optimal control theory. *IEEE Transactions on Automatric Control*, 43(1):32–45, 1998.

[9] R. W. Brockett. *Perspectives in Control*, chapter Hybrid Models for Motion Control Systems, pages 29–54. Birkhäuser, 1993.

[10] D. D. Bruns and J. E. Bailey. Process operation near an unstable steady state using nonlinear feedback control. *Chem. Eng. Commun.*, 32:755–264, 1975.

[11] A. E. Bryson, Jr. *Dynamic Optimization*. Addison-Wesley, 1999.

[12] A. E. Bryson, Jr and Y. Ho. *Applied Optimal Control*. Hemisphere, 1975.

[13] C. I. Byrnes. Book review: Uniform output regulation of nonlinear systems: A convergent dynamics approach. *IEEE Transcaction on Automatic Control*, 52: 2013–2015, 2007.

[14] C. I. Byrnes and D. S. Gilliam. Analysis and design of nonlinear control systems. chapter The Steady-state response of a nonlinear control system, Lyapunov stable attractors, and forced oscillations, pages 415–427. Springer Verlag, 2008.

[15] C. I. Byrnes, F. D. Priscoli, and A. Isidori. *Output Regulation of Uncertain Nonlinear Systems*. Birkhäuser, 1997.

[16] V. Caliskan, G. Verghese, and A. Stankovic. Multifrequency averaging of dc/dc converters. *IEEE Transactions on Power Electronics*, 14(1):124–133, 1999.

[17] S. Childress. *Mechanics of Swimming and Flying*. Cambridge University Press, 1981.

[18] F. Colonius. *Optimal Periodic Control*. Springer Verlag, 1988.

[19] J. R. Couper, W. R. Penney, J. R.Fair, and S. M. Walas. *Chemical Process Equipment*. Elsevier, 2005.

[20] R. F. Curtain and H. Zwart. *An Introduction to Infinite-Dimensional Linear Systems Theory*. Springer-Verlag, 1995.

[21] G. Earhart and P. Stein. Step, swim and scratch motor patterns in the turtle. *J. Neurophysiol*, 84:2181–2190, 2000.

[22] M. Egerstedt, T. Murphey, and J. Ludwig. *Motion Programs for Puppet Choreography and Control*. Springer-Verlag, Pisa, Italy, April 2007. 190-202 pp.

[23] M. Fjeld. Optimal control of multivariate periodic processes. *Automatica*, 5: 497–506, 1969.

[24] M. Golubitsky and I. Stewart. *The Symmetry Perspective: From Equilibrium to Chaos in Phase Space and Physical Space*. Birkhäuser Basel, 2004.

[25] D. J. Griffiths. *Introduction to Quantum Mechanics*. Prentice Hall, 1995.

[26] S. Hedlund and A. Rantzer. Optimal control of hybrid system. In *Proceedings of the 38th IEEE Conference on Decision and Control*, pages 3972–3977, Phoenix, Arizona, December 1999.

[27] S. Hirose. *Biologically Inspired Robots*. Oxford Science Publications, 1993.

[28] D. K. Holmes, R.J. Full and J. Guckenheimer. The dynamics of legged locomotion: Models, analyses, and challenges. *SIAM Review*, 48(2):207–304, 2006.

[29] P. Holmes, R. Full, D. Koditschek, and J. Guckenheimer. The dynamics of legged locomation: Model, analyses, and challenges. *SIAM Review*, 48(2):207–304.

[30] A. Isidori and C. Byrnes. Steady-state behaviors in nonlinear systems with an application to robust disturbance rejection. *Annual Reviews in Control*, 32:1–16, 2008.

[31] M. Ji, A. Muhammad, and M. Egerstedt. Leader-based multi-agent coordination: Controllability and optimal control. In *Proceedings of the American Control Conference*, pages 1358–1363, Minneapolis, MN, 2006.

[32] E. Lee and D. Spyker. On linear periodic control problems. *IEEE Transactions on Automatic Control*, 18(1):39–40, 1973.

[33] A. Locatelli. *Optimal Control*. Birkhäuser, 2001.

[34] J. H. Long Jr, J. Schumacher, N. Livingston, and M. Kemp. Four flippers or two? tetrapedal swimming with an aquatic robot. *Bioinspiration & Biommimetics*, 1: 20–29, 2006.

[35] M. Matsubara and K. Onogi. Stabilized suboptimal periodic control of chemical reactor. *IEEE Transactions on Automatic Control*, 23(6):1005–1008, 1978.

[36] K. A. McIsaac and J. Ostrowski. Motion planning for anguilliform locomotion. *IEEE Transactions on Robotics and Automation*, 19(4):637–652, August 2003.

[37] T. Mehta, D. Yeung, E. Verriest, and M. Egerstedt. Optimal control of multi-dimensional, hybrid ice-skater model. In *Proceedings of the American Control Conference*, pages 2787 – 2792, New York, NY, July 2007.

[38] J. Milnor. *Morse Theory*. Princeton University Press, Princeton, New Jersey, 1963.

[39] S. Nakaoka, S. Kajita, and K. Yokoi. Intuitive and flexible user interface for creating whole body motions of biped humanoid robots. In *The 2010 IEEE/RSJ International Conference on Intelligent Robots and Systems*, pages 1675–1682, Taipay, Taiwan, October 2010.

[40] H. Nijmeijer and A. J. van der Schaft. *Nonlinear Dynamical Control Systems*. Springer Verlag, 1990.

[41] J. Ostrowski, J. Burdick, A. Lewis, and R. Murray. The mechanics of undulatory locomotion: The mixed kinematic and dynamics case. In *Proc. IEEE Int. Conf. Robotics and Automation*, pages 1945–1951, Nagoya, Japan, May 1995.

[42] A. Pavlov, N. van de Wouw, and H. Nijmeijer. *Uniform Output Regulation of Nonlinear Systems: A Convergent Dynamics Approach*. Birkhäuser, 2006.

[43] A. Pavlov, N. van de Wouw, and H. Nijmeijer. Frequency response functions for nonlinear convergent systems. *IEEE Transactions on Automatic Control*, 52: 1159–1165, 2007.

[44] J. Polderman and J. Willems. *Introduction to Mathematical Systems Theory: A Behavioral Approach*. Springer Verlag, New York, 1998.

[45] T. I. Seidman. How violent are fast control ? *Mathematics of Control, Signals and Systems*, 1:89–95, 1998.

[46] A. Shapere and F. Wilczek. Self-propulsion at low Reynolds number. *Physical Review Letters*, 58(20):2051–2054, May 1987.

[47] S. T. Spicer. *Glooscap legends*. Down East Books, 2007.

[48] C. Sultan. Nonlinear systems control using equilibrium paths. In *Proceedings of the 46th IEEE Conf. Decision Control*, pages 50–55, New Orleans, LA, December 2007.

[49] G. Tadmor. On approximate phasor models in dissipative bilinear systems. *IEEE Transaction On Circuits And Systems-I: Fundamental Theory and Applications*, 49(8):1167–1179, August 2002.

[50] E. I. Verriest. Regularization method for optimally switched and impulsive systems with biomedical applications. In *Proceedings of the 42nd IEEE Conference on Decision and Control*, pages 2156–2161, Maui, Hawaii, December 2003.

[51] E. I. Verriest. Multi-Mode Multi-Dimensional systems. In *International Symposium on the Mathematical Theory of Networks and Systems*, pages 1268–1274, Kyoto, Japan, July 24-28 2006.

[52] E. I. Verriest. Locomotion of friction coupled systems. In *the IFAC Workshop on Periodic Systems Control (PSYCO-07)*, St-Petersburg, Russia, August 2007.

[53] E. I. Verriest. Causal behavior of switch delay systems as multi-mode multi-dimensional systems. In *Proceedings of the 8th IFAC Workshop on Time-Delay Systems*, Sinaia, Romania, September 2009.

[54] E. I. Verriest. Multi-Mode Multi-Dimensional systems with Poissonian sequencing. *Communications in Information and Systems*, 9(1):77–102, 2009.

[55] E. I. Verriest. Inconsistencies in systems with time varying delays and their resolution. *In print, IMA Journal of Mathematical Control and Information*, 2011.

[56] E. I. Verriest and W. S. Gray. Geometry and topology of the state space via balancing. In *International Symposium on the Mathematical Theory of Networks and Systems*, pages 840–848, Kyoto, Japan, July 2006.

[57] E. I. Verriest and D. Yeung. Parity in LQ control: the infinite time limit for terminal control. In *Proceedings of the American Control Conference*, pages 1706–1711, 2006.

[58] E. I. Verriest and D. Yeung. Locomotion based on differential friction. In *Proceedings of the American Control Conference*, pages 862–867, Seattle, WA, July 2008.

[59] E. I. Verriest and D. Yeung. Maximally smooth transfers: Gluskabi raccordation. In *International Symposium on Mathematical Theory of Networks and Systems*, Blacksburg, VA, July 2008.

[60] K. R. Westerterp, v. S. W. P. M, and A. A. C. M. Benackers. *Chemical Reactor Design and Operation*. John Wiley & Sons, 1984.

[61] J. C. Willems. The behavioral approach to open and interconnected systems. *IEEE Control Systems Magazine*, 27(6):46–99, 2007.

[62] H. S. Witsenhausen. A class of hybrid-state continuous-time dynamic systems. *IEEE Transactions on Automatic Control*, 11:161–167, 1966.

[63] X. Xu and P. Antsaklis. An approach for solving general switched linear quadratic optimal control problems. In *Proceedings of the 40th IEEE Conf. Decision Control*, pages 2478–2483, 2001.

[64] X. Xu and P. Antsaklis. Optimal control of switched systems based on parameterization of the switching instants. *IEEE Transactions on Automatic Control*, 49(1):2–16, January 2004.

[65] D. Yeung and E. I. Verriest. A stochastic approach to optimal switching between control and observation. In *Proceedings of the 45th IEEE Conference on Decision and Control*, pages 2655–2660, San Diego, CA, December 2006.

[66] D. Yeung and E. I. Verriest. On connecting trajectories maximum persistence of behavior. In *Proceedings of the joint 48th IEEE Conference on Decision and Control and 28th Chinese Control Conference*, Shanghai, P.R. China, December 2009.

[67] D. Yeung and E. I. Verriest. On connecting periodic trajectories with quasi-periodic paths. In *Proceedings of the 49th IEEE Conf. Decision and Control*, pages 4825–4830, Atlanta, GA, December 2010.

[68] D. Yeung and E. I. Verriest. Smooth transitions via quasi-periodic paths. In *18th World Congress of the IFAC*, Milano, Italy, 2011.

[69] Y. Zhang, B. Fidan, and P. A. Ioannou. Backstepping control of linear time-varying systems with known and unknown parameters. *IEEE Transaction on Automatic Control*, 48:1908–1925, 2003.

[70] Y. Zhu. Animating sand as a fluid. Master's thesis, University of Britisch Columbia, 2005.

VITA

Deryck Yeung was born in Paramaribo, Suriname. He received the B.S. and M.S. degree in the Electrical and Computer Engineering from the Georgia Institute of Technology. His research interests include optimal control theory, hybrid systems, stochastic control and signal processing.